Non-Abelian quasi-particles in electronic systems

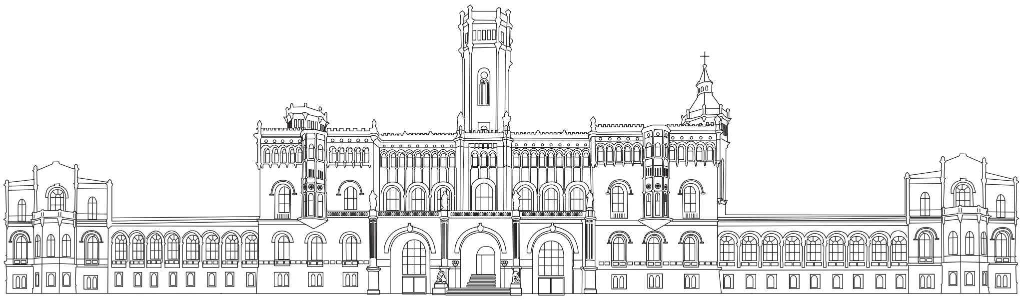

Von der Fakultät für Mathematik und Physik
der Gottfried Wilhelm Leibniz Universität Hannover

zur Erlangung des akademischen Grades
Doktor der Naturwissenschaften
Dr. rer. nat.

genehmigte Dissertation von

M.Sc. Daniel Borcherding

2018

Referent:	Prof. Dr. Holger Frahm, Leibniz Universität Hannover
Korreferenten:	Prof. Dr. Patrik Recher, Technische Universität Braunschweig
	Prof. Dr. Andreas Klümper, Bergische Universität Wuppertal
Tag der Promotion:	12.12.2018

Abstract

Ever since the proposal of Kitaev for decoherence-free quantum computing based on non-Abelian anyons physical realizations of these exotic particles have been investigated extensively. Starting from one-dimensional models of interacting fermions with different symmetries the emergence and condensation of $\mathfrak{su}(2)_{N_f}$, $\mathfrak{su}(3)_{N_f}$ and $\mathfrak{so}(5)_{N_f}$ anyons is studied in the framework of integrable perturbed WZNW models. For sufficiently small temperatures and fields non-Abelian anyons residing on massive solitonic excitations are identified by their quantum dimension. By tuning the external fields the density of anyons can be increased continuously to study the effect of interactions between them. For each model the conformal field theories describing the various collective states of the interacting anyons are determined and a phase diagram for the anyonic modes is proposed.

Keywords: Bethe ansatz, anyons, WZNW models, anyon condensation

Zusammenfassung

Seit dem Vorschlag von Kitaev zu dekohärenzfreien Quantencomputern basierend auf nicht-abelschen Anyonen wurden physikalische Realisierungen dieser exotischen Teilchen ausgiebig erforscht. Ausgehend von eindimensionalen Modellen für wechselwirkende Fermionen mit unterschiedlichen Symmetrien wird die Entstehung und Kondensation von $\mathfrak{su}(2)_{N_f}$, $\mathfrak{su}(3)_{N_f}$ und $\mathfrak{so}(5)_{N_f}$-Anyonen im Rahmen von integrablen gestörten WZNW-Modellen untersucht. Für hinreichend kleine Temperaturen und Felder werden nicht-abelsche Anyonen, die an massive solitonische Anregungen gebunden sind, über ihre Quantendimension identifiziert. Durch Einstellen der externen Felder kann die Dichte der Anyonen erhöht werden, um den Effekt von Wechselwirkungen zwischen ihnen zu untersuchen. Für jedes Modell werden die konformen Feldtheorien, welche die verschiedenen kollektiven Zustände der wechselwirkenden Anyonen beschreiben, bestimmt und ein Phasendiagramm für die anyonischen Moden vorgeschlagen.

Schlagwörter: Bethe-Ansatz, Anyonen, WZNW-Modelle, Anyonen-Kondensation

Contents

Introduction

The standard model of particle physics teaches us that the main building blocks of our universe consist only of particles with integer spin, called bosons, and half-integer spin, called fermions. Directly related to the spin of these particles are their exchange statistics: bosons satisfy the Bose-Einstein statistics while fermions satisfy the Fermi-Dirac statistics [1, 2]. In other words, a wave function describing bosons is unchanged when two particles are exchanged while the wave function describing fermions picks up a minus sign. These simple properties of bosons and fermions lie at the heart of many interesting phenomena ranging from condensed matter physics to high-energy physics.

However, this understanding turned out to be incomplete. In 1977 it was found by Leinaas and Myrheim that the allowed exchange statistics of bosons and fermions are in fact a restriction appearing only in a world with at least three spatial dimensions [3]. Hence, the wave function describing particles in less than three spatial dimensions can in principle pick up *any* phase factor when two particles are exchanged. Due to this observation Wilzcek named particles whose statistics differ from bosonic and fermionic statistics *anyons* in 1982 [4].

The first evidence that anyons are not just a mathematical curiosity came with the study of the integer and fractional quantum Hall effect. These effects are based on a setup where electrons are confined to a two-dimensional plane while a strong magnetic field is applied perpendicular to it. For sufficiently small temperatures von Klitzing observed in 1980 that the resistivity of the sample with respect to the magnetic field shows plateaus of value $1/\nu$ times the constant $2\pi\hbar/e^2$ with ν being an integer [5]. The measurement of the integer ν, called filling factor, to an astonishing accuracy of approximately one part in 10^9 brought von Klitzing the Nobel prize in 1985.

Two years after von Klitzings measurement Tsui and Störmer repeated the experiment with a sample with less disorder. Interestingly, they observed that new plateaus emerge at fractional values of the filling factor ν [6]. Later Laughlin gave a theoretical explanation for the appearance of fractional plateaus in terms of quasi-particles with anyonic exchange statistics [7] by which means Laughlin, Tsui and Störmer received the Nobel prize in 1998. This was the first evidence that anyons may exist as quasi-particle excitations in a sample of electrons confined to two spatial dimensions. On top of that, it was realized that the appearance of anyonic quasi-particles is due to the emergence of a new phase of matter in the two-dimensional sample, called *topological order* [8, 9].

Almost at the same time as the fractional quantum Hall effect was observed, Richard Feynman proposed the idea of a quantum mechanical computer, which could efficiently simulate a quantum system [10]. This idea was pursued by Deutsch, who defined the quantum Turing machines and quantum circuits in 1985 [11]. Later in 1997 the first concrete evidence that quantum computers can outperform classical computers in certain tasks was given by Shor [12]. His proposed quantum algorithm, if implemented on a functioning quantum computer, can factor integers in polynomial time which is currently impossible on a classical computer.

From the practical point of view Preskill called the era of quantum computing we are entering in the near future “noisy intermediate-scale quantum” (NISQ) [13]. Intermediate-scale refers to quantum computers working on 50 to a few hundred quantum bits (qubits), where 50 qubits is approximately the threshold needed to overcome to demonstrate quantum supremacy over classical computers [13].[1] However, Preskill also pointed out that the NISQ technologies are highly limited by noise occurring during computation. This is mainly due to great challenges of storing and manipulating the fragile quantum states that are easily corrupted by decoherence, i.e. their coupling with the environment.

To overcome these difficulties Kitaev proposed the usage of topologically ordered systems for quantum memories as well as quantum computers in 2003 [14]. This idea was based on the observation that classical information stored on a magnetic media is intrinsically protected from thermal fluctuations. In other words, physics itself protects the classical information and no fault-tolerant algorithm is necessary.

For topologically ordered systems Kitaev found that their degenerate ground space is suitable for storing quantum information similar to the classical case. This is based on the fact that the ground space can only be corrupted by a non-local operation caused by anyonic excitations that are created and annihilated after moving around the entire system. Due to an energy gap separating the ground space from the excitation spectrum this can be exponentially suppressed for sufficiently small temperatures. See for example [15–17] for further developments on so-called topological quantum memories.

For quantum computing Kitaev proposed the usage of a certain kind of anyonic quasi-particle excitation called *non-Abelian* quasi-particle or simply *non-Abelian anyon*. In contrast to *Abelian anyons*, whose exchange statistics are determined solely by phase factors distinct from the bosonic and fermionic cases, non-Abelian anyons are described by a degenerate state that undergoes a unitary transformation when two non-Abelian anyons are exchanged. Kitaev proposed to use this degeneracy for storing quantum information as it is intrinsically protected from local errors caused by decoherence. Only the non-local operation of exchanging non-Abelian anyons (also called *braiding*) manipulates the stored information, i.e. a so-called *topological* quantum computation is performed. Furthermore, it was found that for certain models of non-Abelian anyons any quantum computation can be approximated with arbitrary precision by braiding of the non-Abelian anyons [18, 19].

A challenge of topological quantum computing is to suppress possible interactions between the non-Abelian anyons. As soon as anyonic quasi-particles approach each other their interactions lift the necessary degeneracy of their states. However, suitable interactions between anyons may also be useful to realize topological quantum memories that automatically correct errors caused by decoherence [17]. To obtain a better understanding of the collective behavior of interacting anyons in general, effective lattice models with interactions based on the anyonic fusion rules have been studied since 2007 [20–24]. These developments are also significant to further understand the boundaries between different topological phases of two-dimensional matter. Here, the anyonic excitations become interacting at the boundaries resulting in a collective state described by conformal field theory [25–28]. Despite this progress the rich structure of interacting anyons or anyonic condensation has not been fully understood for general anyonic models.

Besides the theoretical study of non-Abelian anyons, Kitaev's proposal on topological quantum computing has driven the search for physical realizations of these particles. This includes further developments to make use of the fractional quantum Hall effect: for the filling factor of $\nu = 5/2$ non-Abelian anyons (more precisely $\mathfrak{su}(2)_2$ spin-1/2 anyons) described by

[1] Google and IBM have recently announced 49-qubit and 50-qubit quantum computers, respectively [13].

the Moore-Read state are expected to emerge [29]. This conjecture has been strengthened by recent experiments unveiling the non-Abelian nature of the $\nu = 5/2$ quantum Hall state [30–32]. Another model of non-Abelian anyons ($\mathfrak{su}(2)_3$ spin-1 anyons), which is universal for quantum computing, is expected to emerge at filling factor $\nu = 12/5$ described by the Read-Rezayi state [33]. On top of that, the $\mathfrak{su}(3)_2$ anyonic model is a potential candidate for describing the quasi-particle excitations of the non-Abelian spin-singlet state at filling factor $\nu = 4/7$ [34]. Notice that these developments are not only important for demonstrating the existence of non-Abelian anyons, but also are steps towards a topological quantum computer based on the fractional quantum Hall effect [35].

Beyond exploiting the fractional quantum Hall effect for realizing non-Abelian anyons, the usage of $p + \mathrm{i}p$ superconductors [36] as well as various one-dimensional systems have been proposed [37–39]. In the one-dimensional case non-Abelian anyons were shown to emerge as localized, topologically protected zero-energy modes bound to quasi-particles or defects. For the simplest one-dimensional system Kitaev showed in 2001 that Majorana anyons occur as zero-energy modes localized at the boundaries of the wire [37]. Experimentally, realizations of Kitaev's setup in fact showed signatures of Majorana anyons in 2012 [40, 41]. See also [42] for a current perspective of Majorana anyons as well as [43] for a proposal of topological quantum computing with Majorana anyons using networks of quantum wires.

However, the usage of Majorana anyons requires additional quantum error correction as they are not universal for quantum computing. Consequently, extensions of Kitaev's chain based on n-state generalizations of the Ising model have been studied. In the presence of chiral interactions $Z_{n>2}$ parafermions were shown to emerge as zero-energy modes [44–49]. In contrast to the free Majorana anyons appearing in Kitaev's chain the generalized $Z_{n>2}$ parafermions were found to be interacting objects, which is manifested in the fact that their correlators do not satisfy Wick's theorem.

A different approach based on interacting fermions with spin and orbital degrees of freedom was proposed by Tsvelik in 2014 [39, 50]. The considered model is an integrable model of fermions consisting of a $\mathfrak{su}(2)_{N_f}$ Wess-Zumino-Novikov-Witten (WZNW) model with a marginally relevant $SU(2)$ current-current interaction. We refer to this model as the perturbed $\mathfrak{su}(2)_{N_f}$ WZNW model. From its exact solution Tsvelik concludes that non-Abelian anyons reside on solitonic 'kink' excitations with finite mass. For sufficiently small temperatures the kinks, and therefore also the non-Abelian anyons, form a dilute gas whose Hilbert space scales as the quantum dimension of $\mathfrak{su}(2)_{N_f}$ spin-1/2 anyons to the power of the number of kinks. In other words, the degeneracy of the kink excitations corresponds to the fractionalized quantum dimension of $\mathfrak{su}(2)_{N_f}$ spin-1/2 anyons. For $N_f = 3$ this includes the so-called Fibonacci anyons, which are universal for quantum computing.

Additionally, it is possible to control the density of the kink excitations by applying an external magnetic field in this setup. Using this fact Tsvelik showed that the degeneracy of the kink excitations is lifted as soon as they become interacting, while the effective integral equations describing the thermodynamics in this regime coincide with the ones of critical RSOS models. Therefore, perturbed WZNW models in general could be suitable to study the transition from free to interacting anyons by changing a control parameter.

Based on this idea the motivation for studying integrable perturbed WZNW models can be boiled down to Baxter's reason for studying integrable models in general [51]:

> Basically, I suppose the justification for studying these models is very simple: they are relevant and they can be solved, so why not do so and see what they tell us?

In this spirit we have studied integrable perturbed WZNW models with different symmetry groups finding new insights about the rich structure of non-Abelian quasi-particles in electronic systems. More precisely, this thesis contains extensions of Tsvelik's approach [39] based on our publications about the low-temperature phases of the integrable perturbed $\mathfrak{su}(2)_{N_f}$ and $\mathfrak{su}(3)_{N_f}$ WZNW model [52, 53]. Furthermore, an outlook is presented for the study of low-temperature phases for the perturbed $\mathfrak{so}(5)_{N_f}$ WZNW model.

In the case of the perturbed $\mathfrak{su}(2)_{N_f}$ WZNW model so-called breather excitations are found to dominate the contribution to the free energy for sufficiently small magnetic fields. From the computation of their quantum dimension it follows that breathers consist of two $\mathfrak{su}(2)_{N_f}$ spin-1/2 anyons. Furthermore, the transition from a low-density phase of free anyons to a phase with a finite density of anyons that are interacting is analyzed in more detail. Above a critical value of the magnetic field the kink excitations become massless and are described by a bosonic mode, while the collective state of the interacting anyonic degrees of freedom is described by a Z_{N_f} parafermion conformal field theory. To summarize the results a phase diagram for the low-temperature phases is proposed.

The generalization of Tsvelik's approach to the $SU(3)$ and $SO(5)$ symmetry group of the perturbed WZNW model enables the study of emerging $\mathfrak{su}(3)_{N_f}$ and $\mathfrak{so}(5)_{N_f}$ anyons respectively as well as their transition to a phase of interacting anyons. For the perturbed $\mathfrak{su}(3)_{N_f}$ WZNW model it is found that the anyons corresponding to the fundamental representation and the adjoint representation dominate the free energy for sufficiently small external fields. In the case when both particle types form a condensate, its collective state is described by two bosonic modes as well as a $Z_{\mathfrak{su}(3)_{N_f}}$ parafermion conformal field theory (see [54] for generalized parafermion CFT's). By a different choice of the external fields only one anyonic particle type forms a condensate leading to a collective state described by one bosonic mode and a coset of parafermion conformal field theories, $Z_{\mathfrak{su}(3)_{N_f}}/Z_{\mathfrak{su}(2)_{N_f}}$. Notice that the study of one-dimensional models of interacting $\mathfrak{su}(3)_{N_f}$ anyons is also relevant to the fractional quantum Hall effect, where $\mathfrak{su}(3)_2$ anyons described by a non-Abelian spin-singlet state at filling fraction $\nu = 4/7$ form a one-dimensional chain of interacting anyons at the boundary [34].

Similarly, the formation of a condensate of $\mathfrak{so}(5)_{N_f}$ anyons is studied in the perturbed $\mathfrak{so}(5)_{N_f}$ WZNW model. It is found that the collective states of interacting anyons depending on the external fields can be described in terms of Gepner's generalized parafermion CFT's [54] for the $\mathfrak{so}(5)$ Lie algebra. Our results are summarized in a phase diagram and are found to be consistent with the results [55] from a study of interacting $\mathfrak{so}(5)_2$ anyons in an effective model.

Thesis overview

By trying to keep this thesis self-contained it is split into two parts, where the first part is dedicated to the preliminaries needed to follow the computations and the interpretation of the results for the perturbed WZNW models. In the second part the results for the perturbed $\mathfrak{su}(2)_{N_f}$ and $\mathfrak{su}(3)_{N_f}$ WZNW models are presented following our publications [52, 53], while an outlook is given for the perturbed $\mathfrak{so}(5)_{N_f}$ WZNW model.

In the first section of the preliminaries a short review of the quantum inverse scattering method, which is the mathematical basis of most integrable models, is given and the thermodynamic Bethe ansatz based on the XXZ spin-S model is introduced. Especially, the discussion of the thermodynamics of the XXZ spin-S model is relevant for studying signatures of non-Abelian anyons in the perturbed $\mathfrak{su}(2)_{N_f}$ WZNW model.

The second section deals with a review of Lie algebras, which determine the underlying structure of the anyonic models, the WZNW models as well as the generalized parafermion conformal field theories. It is focused on establishing an understanding of how to extract weights and roots given a Cartan matrix of a Lie algebra.

The algebraic language of anyonic models based on category theory is discussed in Sec. I 3. It is shown that a list of particle types, rules for fusing and rules for braiding are sufficient to describe an anyonic model mathematically. Furthermore, the construction of local Hamiltonians that describe short-range interactions between anyons based on their *fusion rules* is demonstrated. These concepts will turn out to be essential for interpreting the different low-temperature phases appearing in the perturbed WZNW models of Part II.

The low-temperature phases for interacting anyons appearing in the perturbed WZNW models will be described in terms of generalized parafermion conformal field theories. Hence, a short introduction to conformal field theory is given in Sec. I 4. This chapter is aimed at introducing the main CFT aspects needed to define the WZNW models as well as their related parafermion conformal field theories. An extensive discussion of these topics, which is beyond the scope of this thesis, can for e.g. be found in [56].

In the last part of the preliminaries, Sec. I 5, Abelian and non-Abelian bosonization are discussed based on [57]. These methods are useful for reducing suitable fermionic models into simpler bosonic theories and will therefore be used as a starting point for the discussion of fermionic models with spin and orbital degrees of freedom in Part II.

More precisely, non-Abelian bosonization is used in Sec. II 1.1, to demonstrate that perturbed WZNW models appear naturally in the low-energy limit of interacting fermions with spin and orbital degrees. Furthermore, modifications of the quantum inverse scattering method of Sec. I 1 for studying the integrable perturbed WZNW models are discussed. In the remaining sections of Part II the thermodynamic Bethe ansatz is applied directly to the perturbed $\mathfrak{su}(2)_{N_f}$, $\mathfrak{su}(3)_{N_f}$ and $\mathfrak{so}(5)_{N_f}$ WZNW model, while the resulting low-temperature phases are summarized in a phase diagram, respectively.

Part I

Preliminaries

1. Integrable models

The term *integrable* exists in various physical and mathematical contexts. For example a Hamiltonian mechanical system with n degrees of freedom is called *completely integrable* if it has n independent integrals of motion, in which case it is completely solvable. Here the focus is on a class of quantum field-theoretical models in $1+1$-dimensional spacetime, which are solvable by means of the *quantum inverse scattering method* (QISM). Those models were termed by Faddeev in the early 1980s as *integrable models* [58]. Later it was shown by Izergin and Korepin that also their lattice counterparts, which can be interpreted as quantum spin chains, are integrable, i.e. solvable by the QISM [59]. This relationship will be used extensively in this thesis as many results of the perturbed WZNW models of Part II are rooted in the mathematical description of related quantum spin chains.

The main aspects of the QISM as well as the algebraic Bethe ansatz are discussed in Sec. I 1.1 in the framework of quantum spin chains. The latter is a method used to determine eigenvalues and eigenstates of the Hamiltonian given the operators and commutation relations of the QISM. Sec. I 1.2 is dedicated to the integrable XXZ spin-S model including a discussion of its quasi-particles and their relation to solutions of its Bethe equations. Based on these solutions the thermodynamic Bethe ansatz for the XXZ spin S model is given in Sec. I 1.3 enabling the computation of thermodynamic quantities of integrable models.

1.1. Quantum inverse scattering method

Following [60, 61] it is described how the solution of the Yang-Baxter equation leads to a Hamiltonian description of the corresponding model, where its solutions are given in terms of consistency equations called Bethe equations. The essence of this procedure is the introduction of an auxiliary space $\mathcal{V}_a$, which encodes the interactions of the model and enables a systematic strategy to solve the model at hand.

Instead of starting with a Hamiltonian describing an integrable quantum field-theory or a quantum spin chain, the quantum *inverse* scattering method starts with the Yang-Baxter equation, whose solutions describe integrable models. The corresponding Hamiltonian description can be obtained later from the solutions of the Yang-Baxter equation.

Auxilliary spaces are denoted by $\mathcal{V}_a$ ($a = 1, 2, 3$) and the R-matrices are denoted by $R_{a,b}(\lambda)$ defining mappings from $\mathcal{V}_a \otimes \mathcal{V}_b$ to itself

$$\mathcal{R}_{a,b}(\lambda) : \mathcal{V}_a \otimes \mathcal{V}_b \to \mathcal{V}_a \otimes \mathcal{V}_b \,,$$

where λ denotes the *spectral parameter.* In terms of this notation the R-matrices are specified by the *Yang-Baxter equation* (YBE) given by

$$\mathcal{R}_{1,2}(\lambda-\mu)\mathcal{R}_{1,3}(\lambda-\nu)\mathcal{R}_{2,3}(\mu-\nu) = \mathcal{R}_{2,3}(\mu-\nu)\mathcal{R}_{1,3}(\lambda-\nu)\mathcal{R}_{1,2}(\lambda-\mu), \tag{I.1}$$

where the products are defined in the tensor product space $\mathcal{V}_1 \otimes \mathcal{V}_2 \otimes \mathcal{V}_3$. The YBE is the central building block of the quantum inverse scattering method as each solution defines an R-matrix and thereby an integrable model.[2] To relate this solution to the physical Hilbert space the *Lax-operator* $\mathcal{L}_{j,a}(\lambda)$ is constructed as a map

$$\mathcal{L}_{j,a} : \mathcal{H}_j \otimes \mathcal{V}_a \to \mathcal{H}_j \otimes \mathcal{V}_a \,,$$

[2] Notice that models described by the QISM method are just one class of quantum integrable models. A discussion of more general definitions of quantum integrability can be found in [62].

where $\mathcal{H}_j$ denotes the one-particle Hilbert space of site j with the complete N-particle Hilbert space given by $\mathcal{H} = \otimes_{j=1}^{N} \mathcal{H}_j$. Moreover, the Lax-operator is assumed to be determined by the fundamental commutation relations (FCR)

$$\mathcal{L}_{j,a}(\lambda)\mathcal{L}_{j,b}(\mu)\mathcal{R}_{a,b}(\mu-\lambda) = \mathcal{R}_{a,b}(\mu-\lambda)\mathcal{L}_{j,b}(\mu)\mathcal{L}_{j,a}(\lambda)\,. \tag{I.2}$$

In fact, the existence and uniqueness of the Lax-operator turns out to be guaranteed as long as the R-matrices satisfy the YBE (I.1) [63, 64].

The Lax-operator can be expanded to the *monodromy operator* acting on the complete Hilbert space by taking the ordered product of Lax operators over all N sites

$$\mathcal{T}_a(\lambda) \equiv \mathcal{L}_{N,a}(\lambda)\mathcal{L}_{N-1,a}(\lambda)\cdots\mathcal{L}_{1,a}(\lambda)\,. \tag{I.3}$$

Due to the fact that the monodromy operator is constructed from the Lax operators it also satisfies the FCR

$$\mathcal{T}_a(\lambda)\mathcal{T}_b(\mu)\mathcal{R}_{a,b}(\mu-\lambda) = \mathcal{R}_{a,b}(\mu-\lambda)\mathcal{T}_b(\mu)\mathcal{T}_a(\lambda)\,.$$

In the following discussion we assume that the auxiliary space $\mathcal{V}_a$ is two-dimensional for simplicity. In this case the monodromy can be written as a 2×2 matrix

$$\mathcal{T}_a = \begin{pmatrix} A(\lambda) & B(\lambda) \\ C(\lambda) & D(\lambda) \end{pmatrix}\,,$$

whose entries act in $\mathcal{H}$. Its trace over the auxiliary space defines the *transfer matrix*

$$\mathbf{T}(\lambda) \equiv \mathrm{tr}_a \mathcal{T}_a(\lambda) = A(\lambda) + D(\lambda)\,,$$

which is independent of the auxiliary space and serves as a generating object for physical observables. Given the special spectral parameter η for which the Lax operator becomes proportional to a permutation operator, called *shift-point*, the Hamiltonian H and the momentum operator P are generated as

$$H \propto \frac{\mathrm{d}}{\mathrm{d}\lambda} \ln \mathbf{T}(\lambda)\bigg|_{\lambda=\eta}\,, \qquad P \propto \ln \mathbf{T}(\lambda)|_{\lambda=\eta}\,. \tag{I.4}$$

Hence, given a solution of the YBE describing an integrable model, the corresponding integrable Hamiltonian is specified by the transfer matrix.

The *algebraic Bethe ansatz* (ABA) goes one step further and allows for a systematic construction of the eigenvalues and eigenstates of (I.4), which leads to a set of consistency equations known as the Bethe equations. The starting point of the ABA is a reference state $|0\rangle$ also called *pseudo-vacuum*, which is defined by

$$C(\lambda)|0\rangle = 0\,,$$

i.e. it is annihilated by $C(\lambda)$. On the other hand, the $B(\lambda)$ operator acts as a quasi-particle creation operator so that a state with M quasi-particles becomes

$$|\lambda_1,\ldots,\lambda_M\rangle = \prod_{j=1}^{M} B(\lambda_j)|0\rangle\,. \tag{I.5}$$

This state depends on particular spectral parameters λ_j for which the eigenstate equation

$$\mathbf{T}(\lambda)|\lambda_1,\ldots,\lambda_M\rangle = (A(\lambda)+D(\lambda))|\lambda_1,\ldots,\lambda_M\rangle = \Lambda(\lambda)|\lambda_1,\ldots,\lambda_M\rangle \tag{I.6}$$

is satisfied. Using the FCR for the monodromy, commutation relations for the A, B, C and D operators can be derived and applied to (I.6) resulting in consistency equations for the spectral parameters λ_j called *Bethe equations*.

To give an explicit example of the QISM operators let us consider the XXX spin-1/2 model. It is the isotropic version of the spin-1/2 Heisenberg model given by

$$H_{\mathrm{XXX}} = \sum_{n=1}^{N}\left(S_n^x S_{n+1}^x + S_n^y S_{n+1}^y + S_n^z S_{n+1}^z - \frac{1}{4}\right), \tag{I.7}$$

where S_n^α $(\alpha = x, y, z)$ denote the Pauli matrices at site n. In this case the one-particle space $\mathcal{H}_n$ as well as the auxiliary space $\mathcal{V}_a$ are given by $\mathbb{C}^2$. The R-matrix leading to (I.7) was found to be

$$\mathcal{R}_{a,b}(\lambda) = \lambda I_{a,b} + \mathrm{i}P_{a,b}, \tag{I.8}$$

where $P_{a,b}$ denotes a permutation

$$P_{a,b} : \mathcal{V}_a \otimes \mathcal{V}_b \to \mathcal{V}_b \otimes \mathcal{V}_a, \quad a\otimes b \mapsto b \otimes a$$

and $I_{a,b}$ is the unit matrix in $\mathcal{V}_a \otimes \mathcal{V}_b$. It can easily be shown that the Lax operator

$$\mathcal{L}_{n,a}(\lambda) = \left(\lambda - \frac{\mathrm{i}}{2}\right) I_{n,a} + \mathrm{i}P_{n,a}$$

satisfies the fundamental commutation relation (I.2). Following the procedure explained above one can derive the transfer matrix $\mathbf{T}(\lambda)$ and show that the Hamiltonian and the momentum operator (I.7) can equivalently be written as

$$H_{\mathrm{XXX}} = \frac{\mathrm{i}}{2}\frac{\mathrm{d}}{\mathrm{d}\lambda}\ln \mathbf{T}(\lambda)\Big|_{\lambda=\mathrm{i}/2} - \frac{N}{2}, \qquad P_{\mathrm{XXX}} = -\mathrm{i}\ln \mathrm{i}^{-N}\mathbf{T}(\lambda)\Big|_{\lambda=\mathrm{i}/2}$$

Furthermore, the eigenstate equation (I.6) results in the Bethe equations for the M spectral parameters λ_j

$$\left(\frac{\lambda_j+\mathrm{i}}{\lambda_j-\mathrm{i}}\right)^N = \prod_{k\neq j}^{M}\frac{\lambda_j-\lambda_k+2\mathrm{i}}{\lambda_j-\lambda_k-2\mathrm{i}}. \tag{I.9}$$

This equation was first derived by Hans Bethe in 1931 using the *coordinate Bethe ansatz*, i.e. an ansatz for the eigenstates of the Hamiltonian (I.7) based on superpositions of plane waves [65]. The spectral parameters λ_j are also called *Bethe roots*. Also notice that a set of Bethe roots $\{\lambda_j\}$ $(j = 1,\ldots,M)$ solving (I.9) describes a particular eigenstate $|\psi\rangle$ by (I.5), which satisfies

$$\begin{aligned} H_{\mathrm{XXX}}|\lambda_1,\ldots,\lambda_M\rangle &= \sum_{j=1}^{M}\epsilon(\lambda_j)|\lambda_1,\ldots,\lambda_M\rangle, \\ P_{\mathrm{XXX}}|\lambda_1,\ldots,\lambda_M\rangle &= \sum_{j=1}^{M}p(\lambda_j)|\lambda_1,\ldots,\lambda_M\rangle \end{aligned} \tag{I.10}$$

with

$$\epsilon(\lambda) = -\frac{1}{2}\frac{1}{\lambda^2 + 1/4}\,, \quad p(\lambda) = \frac{1}{\mathrm{i}}\ln\frac{\lambda + \mathrm{i}/2}{\lambda - \mathrm{i}/2}\,.$$

Due to (I.10) one can interpret $B(\lambda_j)$ as a creation operator for a quasi-particle with energy $\epsilon(\lambda_j)$ and momentum $p(\lambda_j)$. This quasi-particle interpretation of solutions λ_j of Bethe equations will be used extensively in this thesis.

1.2. The XXZ spin-S model

In the last section we considered the XXX spin-1/2 model (I.7). The anisotropic generalization of this model is given by

$$H_{\mathrm{XXZ}} = \sum_{n=1}^{N} \left(S_n^x S_{n+1}^x + S_n^y S_{n+1}^y + \Delta S_n^z S_{n+1}^z\right),$$

where we focus on $\Delta \equiv \cos\gamma \leq 1$ denoted as the easy plane XXZ system, which was originally solved by Bethe [65]. In this case the energy gap above the total spin $S = 0$ ground state vanishes.

The generalization of this model to higher spins cannot simply be done by replacing the Pauli matrices S^α with different representations, since this results in non-integrable models. However, using the QISM Babujian and Takhtajan succeeded in finding the integrable XXX spin-S model [66–68] and later Sogo, Kirillov, Reshetikhin and Kulish studied the integrable XXZ spin-S model [69–73]. The solution of the Yang-Baxter equation (I.1) leading to the Hamiltonian $H_{\mathrm{XXZ}}^{(S)}$ of the integrable XXZ spin-S model will not be discussed here. Instead the Bethe equations are taken as a starting point to show how its solutions lead to thermodynamic quantities.

The Bethe equations for the integrable XXZ spin-S model are given by

$$\left(\frac{\sinh\frac{\gamma}{2}(\lambda_j + \mathrm{i}2S)}{\sinh\frac{\gamma}{2}(\lambda_j - \mathrm{i}2S)}\right)^N = \prod_{k\neq j}^{M} \frac{\sinh\frac{\gamma}{2}(\lambda_j - \lambda_k + 2\mathrm{i})}{\sinh\frac{\gamma}{2}(\lambda_j - \lambda_k - 2\mathrm{i})}. \tag{I.11}$$

Notice that these equations become the XXX spin-1/2 Bethe equations (I.9) for $S = 1/2$ and $\gamma \to 0$. A set of Bethe roots $\{\lambda_j\}$ solving (I.11) describe a state $|\lambda_1, \ldots, \lambda_M\rangle$, which satisfies

$$H_{\mathrm{XXZ}}^{(S)}|\lambda_1, \ldots, \lambda_M\rangle = \sum_{j=1}^{M} \epsilon(\lambda_j)|\lambda_1, \ldots, \lambda_M\rangle\,, \tag{I.12}$$

$$\mathbf{p}|\lambda_1, \ldots, \lambda_M\rangle = \sum_{j=1}^{M} p(\lambda_j)|\lambda_1, \ldots, \lambda_M\rangle \tag{I.13}$$

with

$$\epsilon(\lambda) = \frac{-\sin(2S\gamma)}{\sinh\frac{\gamma}{2}(\lambda + 2S\mathrm{i})\sinh\frac{\gamma}{2}(\lambda - 2S\mathrm{i})}\,,$$

$$p(\lambda) = 2\arctan\left(\tanh(\gamma\lambda/2)\cot(\gamma S)\right)\,. \tag{I.14}$$

The eigenvalue of the spin projection $S^z = \sum_{n=1}^{N} S_n^z$ of this state is found to be

$$S^z|\lambda_1, \ldots, \lambda_M\rangle = (SN - M)|\lambda_1, \ldots, \lambda_M\rangle \tag{I.15}$$

showing that each $B(\lambda_j)$ reduces the spin projection SN of the pseudo-vacuum by one, while the states $|\lambda_1, \dots, \lambda_M\rangle$ are still highest-weight states:

$$S^+|\lambda_1, \dots, \lambda_M\rangle = \sum_{j=1}^{N} S_j^+|\lambda_1, \dots, \lambda_M\rangle = 0\,.$$

In order to compute thermodynamic quantities it is necessary to study the solutions of (I.11) in the thermodynamic limit $N \to \infty$. It is well known that in this limit the Bethe roots can be described in so-called *strings*, which denote sets of roots that are evenly spaced by 2i in the complex plane. A heuristic reason for the forming of strings can be seen from the Bethe equations (I.11): if the left side vanishes or diverges for $N \to \infty$, then there has to exist a λ_k on the right side with $\lambda_j - \lambda_k \approx \pm 2\mathrm{i}$ to account for this.

For the Bethe equations of the XXX spin-1/2 model (I.9) this argument holds as well. In the limit of large N with fixed M/N all Bethe roots are formed by strings $\{\lambda_{\alpha,j}^n\}_{j=1}^n$ of length n

$$\lambda_{\alpha,j}^n = \lambda_\alpha^n + \mathrm{i}(n + 1 - 2j), \quad \text{with } j = 1, \dots, n\,,$$

where $\lambda_\alpha^n \in \mathbb{R}$ denotes the center of the string. In fact, all string lengths n appear as solutions of (I.9) and need to be considered to compute thermodynamic quantities of the XXX model.

For the XXZ spin-S model, on the other hand, it was shown that the allowed string lengths depend on the anisotropy parameter γ [70, 74]. In the thermodynamic limit $N \to \infty$ with fixed M/N and $0 \le M/N < S$ the Bethe roots are arranged as strings of length n and *parity* $v_n = \pm 1$ of the form

$$\lambda_{\alpha,j}^n = \lambda_\alpha^n + \mathrm{i}\left(n + 1 - 2j + \frac{1}{2}(1 - v_{2S} v_n)\frac{\pi}{\gamma}\right) \quad \text{with } j = 1, \dots, n\,. \tag{I.16}$$

Following [52, 70] the admissible strings and parities of the XXZ spin-S model are described by the numbers p_i, b_i, y_i and m_i with $i \le \ell - 1$:

$$\begin{array}{lllll}
p_0 = \pi/\gamma & p_1 = 1 & b_i = [p_i/p_{i+1}] & p_{i+1} = p_{i-1} - b_{i-1}p_i & \\
y_{-1} = 0 & y_0 = 1 & y_1 = b_0 & y_{i+1} = y_{i-1} + b_i y_i & i \ge 0 \\
m_0 = 0 & m_1 = b_0 & m_{i+1} = m_i + b_i & i \ge 0\,, &
\end{array}$$

where ℓ is the length of the continued fraction expansion of the rational number p_0

$$\begin{aligned}
p_0 &= [b_0, b_1, b_2, \dots, b_{\ell-1}] = b_0 + \cfrac{1}{b_1 + \frac{1}{b_2 + \dots}}\,, \\
p_i/p_{i+1} &= [b_i, b_{i+1}, \dots, b_{\ell-1}]
\end{aligned}$$

and $[x]$ denotes the integer part of x. In terms of these numbers the strings (I.16) appearing in the solution of the Bethe equations for the XXZ chain with $S = 1/2$ have been classified by Takahashi and Suzuki [74]: their lengths and parities are

$$\begin{aligned}
n_j &= y_{i-1} + (j - m_i)y_i \quad \text{for } m_i \le j < m_{i+1}\,, \\
v_j \equiv v_{n_j} &= \exp\left(\mathrm{i}\left[\frac{n_j - 1}{p_0}\right]\right) \qquad j \ne m_1\,, \\
v_{m_\ell} &= (-1)^\ell\,,
\end{aligned} \tag{I.17}$$

for $1 \leq j < m_\ell$ and $n_{m_\ell} = y_{\ell-1}$, $v_{m_\ell} = (-1)^\ell$. Provided that $2S+1$ appears in the sequence of *Takahashi numbers* n_j, i.e.

$$n_\sigma = 2S+1\,, \quad m_r \leq \sigma < m_{r+1}\,, \tag{I.18}$$

the same classification holds for the integrable XXZ spin-S chain. The condition that $2S+1$ needs to be a Takahashi number is always satisfied if the Hamiltonian $H^{(S)}_{\mathrm{XXZ}}$ generated by the QISM is Hermitian [75]. For $S > 1/2$ this restricts the admissible anisotropy parameter by $2S < p_0 = \frac{\pi}{\gamma}$.

Considering a root configuration consisting of ν_j strings of type (n_j, v_{n_j}) and using (I.16), the Bethe equations (I.11) can be rewritten in terms of the real string-centers $\lambda^{(j)}_\alpha \equiv \lambda^{n_j}_\alpha$. In their logarithmic form they read

$$N t_{j,2S}(\lambda^{(j)}_\alpha) = 2\pi I^{(j)}_\alpha + \sum_{k\geq 1}\sum_{\beta=1}^{\nu_k} \theta_{jk}(\lambda^{(j)}_\alpha - \lambda^{(k)}_\beta)\,, \tag{I.19}$$

where $I^{(j)}_\alpha$ are integers (or half-integers) and we have introduced functions

$$\begin{aligned} t_{j,2S}(\lambda) =& \sum_{l=1}^{\min(n_j,2S)} f(\lambda, |n_j - 2S| + 2l - 1, v_j v_{2S}) \\ \theta_{jk}(\lambda) =& f(\lambda, |n_j - n_k|, v_j v_k) + f(\lambda, n_j + n_k, v_j v_k) \\ &+ 2\sum_{\ell=1}^{\min(n_j,n_k)-1} f(\lambda, |n_j - n_k| + 2\ell, v_j v_k) \end{aligned} \tag{I.20}$$

with

$$f(\lambda, n, v) = \begin{cases} 2\arctan\left(\tan((\frac{1+v}{4} - \frac{n}{2p_0})\pi)\tanh(\frac{\pi\lambda}{2p_0})\right) & \text{if } \frac{n}{p_0} \neq \text{integer} \\ 0 & \text{if } \frac{n}{p_0} = \text{integer} \end{cases}.$$

Hence, it was shown how the Bethe equations of the integrable XXZ spin-S model (I.11) can be rewritten in terms of equations for the real parts of the strings (I.19) as long as the admissible string solutions are known. In the next section the equations for the string-centers (I.19) in the thermodynamic limit $N \to \infty$ are studied leading to a continuous distribution of the centers.

1.3. Thermodynamic Bethe ansatz

The thermodynamic Bethe ansatz (TBA) developed by Yang and Yang in 1969 [76] enables the computation of thermodynamic quantities of integrable models. The main idea of the thermodynamic Bethe ansatz is to introduce densities for the string-centers $\lambda^{(j)}_\alpha$ of equation (I.19), which are distributed continuously for $N \to \infty$. Using an expression of the entropy in terms of these densities, the free energy can be minimized to derive integral equations describing the thermodynamics. To give an example, this procedure is applied to the XXZ spin-S model in this section.

The starting point is the definition of the *counting function*

$$c_j(\lambda) \equiv \frac{(-1)^{r(j)}}{2\pi}\left(t_{j,2S}(\lambda) - \frac{1}{N}\sum_{k\geq 1}\sum_{\beta=1}^{\nu_k}\theta_{jk}(\lambda - \lambda^{(k)}_\beta)\right)\,, \tag{I.21}$$

where $r(j)$ is chosen such that $c_j(\lambda)$ is monotonically increasing:

$$(-1)^{r(j)} = \operatorname{sign}\left(\frac{\mathrm{d}}{\mathrm{d}\lambda} t_{j,2S}(\lambda)\right),$$

see [75] for more details. From (I.19) it is apparent that $c_j(\lambda_\alpha^{(j)}) = I_\alpha^{(j)}/N$. Hence, each set of centers $\{\lambda_\alpha^{(j)}\}$ can alternatively be described by a set of integers (or half-integers) $\{I_\alpha^{(j)}\}$, i.e. the $I_\alpha^{(j)}$ are admissible quantum numbers for the states.

In the thermodynamic limit $N \to \infty$ the centers are distributed continuously with density $\rho_j(\lambda)$, while the λ's not appearing in (I.19), called *holes*, are distributed with the hole density $\rho_j^h(\lambda)$. Due to Yang and Yang [76] the densities are defined by

$$\begin{aligned} N\rho_j(\lambda)\mathrm{d}\lambda &= \text{number of } \lambda_\alpha^{(j)}\text{'s in } [\lambda, \lambda + \mathrm{d}\lambda]\,, \\ N\rho_j^h(\lambda)\mathrm{d}\lambda &= \text{number of holes in } [\lambda, \lambda + \mathrm{d}\lambda]\,. \end{aligned} \tag{I.22}$$

Furthermore, the counting function (I.21) uniquely maps λ's solving (I.19) as well as holes to integers (or half-integers) so that it satisfies

$$N\mathrm{d}c_j(\lambda) = N\frac{\mathrm{d}c_j}{\mathrm{d}\lambda}\mathrm{d}\lambda = \text{number of } \lambda\text{'s and holes in } [\lambda, \lambda + \mathrm{d}\lambda]\,. \tag{I.23}$$

From (I.22) and (I.23) one can conclude

$$\frac{\mathrm{d}}{\mathrm{d}\lambda} c_j(\lambda) = \rho_j(\lambda) + \rho_j^h(\lambda)\,,$$

which using (I.21) for $N \to \infty$ results in a set of integral equations for the densities

$$\rho_j^h(\lambda) = \rho_j^{(0)}(\lambda) - \sum_{k\geq 1}(-1)^{r(j)} A_{jk} * \rho_k(\lambda)\,, \tag{I.24}$$

where $a * b$ denotes a convolution. The bare densities $\rho_j^{(0)}(\lambda)$ and the kernels $A_{jk}(\lambda)$ of the integral equations are given by

$$\begin{aligned} \rho_j^{(0)}(\lambda) &= (-1)^{r(j)} a_{j,2S}(\lambda)\,, \quad a_{j,2S}(\lambda) = \frac{1}{2\pi}\frac{d}{d\lambda} t_{j,2S}(\lambda)\,, \\ A_{jk}(\lambda) &= \frac{1}{2\pi}\frac{d}{d\lambda}\theta_{jk}(\lambda) + (-1)^{r(j)}\delta_{jk}\delta(\lambda)\,. \end{aligned}$$

Each solution of (I.24) describes a particular state of the integrable XXZ spin-S model for $N \to \infty$. However, to derive the equilibrium state of the model for a given temperature one has to minimize the free energy. To approach this in full generality a magnetic field H is introduced that couples to the eigenvalue of the spin projection S_z, i.e. the Hamiltonian is replaced by

$$H_{\mathrm{XXZ}}^{(S)} \to H_{\mathrm{XXZ}}^{(S)} - HS^z.$$

Consequently, the energy density of a given solution of the integral equations (I.24) follows from (I.12) and (I.15)

$$\begin{aligned} \mathcal{E} = \frac{E}{N} &= \frac{1}{N}\sum_j \sum_{\alpha=1}^{\nu_j}(-4p_0 a_{j,2S}(\lambda_\alpha^{(j)}) + n_j H) - SH \\ &\overset{N\to\infty}{=} \sum_j \int_{-\infty}^{\infty} \mathrm{d}\lambda \epsilon_{0,j}(\lambda)\rho_j(\lambda) - SH\,, \end{aligned} \tag{I.25}$$

where the bare energy

$$\epsilon_{0,j}(\lambda) = -4p_0 a_{j,2S}(\lambda) + n_j H$$

is introduced. The entropy $\mathrm{d}S$ in the interval $[\lambda, \lambda + \mathrm{d}\lambda]$ is defined as the logarithm of the number of possible states in this interval, which follows from (I.22)

$$\mathrm{d}S = \ln \prod_k \frac{[N(\rho_k(\lambda) + \rho_k^h(\lambda))\mathrm{d}\lambda]!}{[N\rho_k(\lambda)\mathrm{d}\lambda]!\,[N\rho_k^h(\lambda)\mathrm{d}\lambda]!}\,.$$

Hence, using Stirling's formula $\ln n! = n \ln n - n + \mathcal{O}(\ln n)$ the total entropy density $\mathcal{S}$ becomes

$$\mathcal{S} = \frac{1}{N}\int \mathrm{d}S = \sum_{j\geq 1}\int_{-\infty}^{+\infty} \mathrm{d}\lambda \,\left[(\rho_j + \rho_j^h)\ln(\rho_j + \rho_j^h) - \rho_j \ln \rho_j - \rho_j^h \ln \rho_j^h\right]$$

in the thermodynamic limit. The equilibrium state at finite temperature is found by minimizing the free energy density $\mathcal{F}$ with temperature T

$$\mathcal{F} = \mathcal{E} - T\mathcal{S}\,.$$

This results in a set of integral equations

$$T\ln(1 + e^{\epsilon_j/T}) = \epsilon_{0,j}(\lambda) + \sum_{j\geq 1}(-1)^{r(k)} A_{jk} * T\ln(1 + e^{-\epsilon_j/T}) \tag{I.26}$$

for the dressed energies $\epsilon_j(\lambda)$ defined by $e^{-\epsilon_j/T} = \rho_j/\rho_j^h$. Given a solution of the integral equations (I.26) for a temperature T and magnetic field H one can compute the corresponding densities describing the equilibrium state from (I.24). In terms of the dressed energies $\epsilon_j(\lambda)$ the free energy density becomes

$$\mathcal{F} = -\sum_j \int_{\infty}^{\infty} \rho_{0,j}(\lambda) T \ln(1 + e^{-\epsilon_j(\lambda)/T})\,. \tag{I.27}$$

The equations (I.26) and (I.27) are sufficient to compute thermodynamic quantities of the integrable XXZ spin-S model for different fields H and temperatures T. In fact, many results for the perturbed $\mathfrak{su}(2)_{N_f}$ WZNW model discussed in Part II of this thesis will be based on the thermodynamic Bethe ansatz for its lattice counterpart, i.e. the integrable XXZ spin-$N_f/2$ chain.

2. Simple Lie algebras

The goal of this section is to introduce the main concepts of simple Lie algebras needed to discuss the anyonic models, the Wess-Zumino-Novikov-Witten (WZNW) models as well as the parafermion conformal field theories of the subsequent sections. WZNW models turn out to be uniquely determined by a Lie algebra and a level k, while their action is invariant under transformations of the corresponding Lie group. The spectrum, however, is generated by conserved currents defining an affine Lie algebra, which is an extension of a simple Lie algebra. For the purpose of this thesis it is sufficient to focus on the representation theory of simple Lie algebras, while mentioning the differences in the representation theory of affine Lie algebras whenever necessary. Similarly, the $\mathfrak{su}(2)_k$, $\mathfrak{su}(3)_k$ and $\mathfrak{so}(5)_k$ anyonic models are defined using the representation theory of simple Lie algebras while applying simple modifications to it coming from their affine Lie algebraic structure. A complete introduction to simple Lie algebras and affine Lie algebras can be found in [56].

Following [56] roots, weights, Cartan matrices as well as the Weyl group for simple Lie algebras are discussed. The section is ended by showing how the representation theory is encoded in a Cartan matrix and can be reproduced from it, giving explicit examples for the $\mathfrak{su}(2)$ and $\mathfrak{su}(3)$ Lie algebra.

2.1. The Cartan-Weyl basis

A *Lie algebra* $\mathfrak{g}$ is a vector space over a field F with a binary operation $[.,.] : \mathfrak{g} \times \mathfrak{g} \to \mathfrak{g}$ called a *commutator* that satisfies

- bilinearity:

$$[aX + bY, Z] = a[X, Z] + b[Y, Z]\,, \quad [Z, aX + bY] = a[Z, X] + b[Z, Y]\,,$$

- anticommutativity:

$$[X, Y] = -[Y, X]\,,$$

- Jacobi identity:

$$[X, [Y, Z]] + [Z, [X, Y]] + [Y, [Z, X]] = 0$$

for scalars $a, b \in F$ and $X, Y, Z \in \mathfrak{g}$. The relationship to the corresponding *Lie group* G is given by the exponential: elements $X \in \mathfrak{g}$ are mapped to the connected component of G containing its unit element by $e^{\mathrm{i}aX}$, where $a \in F$.

Instead of working with the abstract algebraic structure of a Lie algebra, one can study *representations* of it, which are mappings that make the elements of a Lie algebra more concrete by associating them with matrices. More precisely, a *representation* ϕ is a linear map $\phi : \mathfrak{g} \to \mathfrak{gl}(V)$ that satisfies

$$\phi([X, Y]) = \phi(X)\phi(Y) - \phi(Y)\phi(X)\,,$$

where $\mathfrak{gl}(V)$, defined as the space of linear maps $V \to V$, is a Lie algebra with the commutator $[X, Y] = XY - YX$ for $X, Y \in \mathfrak{gl}(V)$. The *dimension* of a representation is defined as the dimension of the vector space V. Furthermore, a subspace $W \subseteq V$ is called *invariant* if $\phi(X)w \in W$ for all $w \in W$ and $X \in \mathfrak{g}$. If an invariant subspace $W \neq V, \{0\}$ exists, the representation ϕ is called *reducible*, otherwise it is termed *irreducible*.

Given these definitions it is possible to define simple Lie algebras as well as describe them in terms of the Cartan-Weyl basis. The generators of a Lie algebra $\mathfrak{g}$ are denoted by $\{J^a\}$ and satisfy the commutation relations

$$[J^a, J^b] = \mathrm{i} \sum_c f_c^{ab} J^c ,$$

where the constants f_c^{ab} are called *structure constants. Simple Lie algebras* are Lie algebras whose only ideals are $\{0\}$ and itself, i.e. no subset of generators $\{L^a\} \neq \{J^a\}, \{0\}$ exists such that $[L^a, J^b] \in \{L^a\}$ for all $J^b \in \{J^a\}$.

An elegant way of describing a Lie algebra is obtained by writing the generators in terms of the *Cartan-Weyl basis.* It is constructed by first finding a maximal set of Hermitian generators $\{H^i\}$ that are commuting, i.e. satisfy

$$[H^i, H^j] = 0 . \tag{I.28}$$

The set $\{H^i\}$ with $i = 1, \dots, r$ generates the *Cartan subalgebra* h, while r denotes the *rank* of the Lie algebra. Due to (I.28) one can diagonalize elements of the Cartan subalgebra simultaneously and describe states of a representation in terms of its eigenvalues, see Sec. I 2.3. The missing generators needed to form the complete Lie algebra $\mathfrak{g}$ are constructed from $\{J^a\}$ to satisfy the relation

$$[H^i, E^\alpha] = \alpha^i E^\alpha , \tag{I.29}$$

where $\alpha = (\alpha^1, \dots, \alpha^r)$ denotes a *root* and Δ denotes the set of all roots satisfying (I.29). Notice that the relation (I.29) can also be reinterpreted in the adjoint representation: an element $X \in \mathfrak{g}$ is represented as $\mathrm{ad}(X) \in \mathfrak{gl}(\mathfrak{g})$, whose action is defined by

$$\mathrm{ad}(X)Y = [X, Y] .$$

Consequently, (I.29) becomes

$$\mathrm{ad}(H^i)E^\alpha = \alpha^i E^\alpha , \tag{I.30}$$

which leads to the interpretation of roots as linear maps $\alpha(H^i) \to \alpha^i$, i.e. elements of the dual space h^*. The action of the generators $\{E^\alpha\}$ in terms of *ladder operators* is discussed in Sec. I 2.3.

The last commutator $[E^\alpha, E^\beta]$ needed to obtain the full set of commutation relations follows from a relation implied by the Jacobi identity and (I.29):

$$[H^i, [E^\alpha, E^\beta]] = (\alpha^i + \beta^i)[E^\alpha, E^\beta] .$$

By evaluating this equation for the cases $\alpha + \beta \in \Delta$, $\alpha + \beta \notin \Delta$ and $\alpha = -\beta$ the full set of commutation relations specifying the Cartan-Weyl basis becomes

$$\begin{aligned}
&[H^i, H^j] = 0 , \\
&[H^i, E^\alpha] = \alpha^i E^\alpha , \\
&[E^\alpha, E^\beta] = \begin{cases} N_{\alpha,\beta} E^{\alpha+\beta} & \text{if } \alpha + \beta \in \Delta \\ \frac{2}{|\alpha|^2} \alpha \cdot H & \text{if } \alpha = -\beta \\ 0 & \text{otherwise} \end{cases} ,
\end{aligned} \tag{I.31}$$

where $N_{\alpha,\beta}$ is a constant and

$$[E^\alpha, E^{-\alpha}] = \frac{2}{|\alpha|^2} \alpha \cdot H = \frac{2}{|\alpha|^2} \sum_{i=1}^r \alpha^i H^i$$

was chosen to fix the normalization of the ladder operators.

2.2. Simple roots

In this section the roots that appeared in the Cartan-Weyl basis are discussed in more detail and the notion of simple roots is introduced, which leads to the Cartan matrix.

The roots introduced in the previous section label the ladder operators E^α, which are the missing generators needed to form the complete Lie algebra $\mathfrak{g}$. This results in the following relation

$$|\Delta| = \dim(\mathfrak{g}) - r\,,$$

where $\dim(\mathfrak{g})$ is defined as the number of generators of $\mathfrak{g}$. It is sufficient to focus on a linearly independent subset of Δ to describe the roots. To obtain this subset a basis $\{\beta_1, \beta_2, \ldots, \beta_r\}$ in the space dual to the Cartan subalgebra h is fixed and an arbitrary root $\alpha \in \Delta$ is written as

$$\alpha = \sum_{i=1}^{r} n_i \beta_i\,.$$

The set of roots Δ can now be divided into two classes: the set of positive roots Δ_+ and the set of negative roots Δ_-. Let n_i be the first nonzero element of the coefficients $(n_1, n_2, \ldots, n_r)$ of a root α. If $n_i > 0$, the root α is positive and belongs to Δ_+. Similarly, if $n_i < 0$, $\alpha \in \Delta_-$ is called negative.

It turns out that there are r *simple roots* α_i, which are positive roots that cannot be further decomposed into sums of positive roots. The set of simple roots $\{\alpha_1, \ldots, \alpha_r\}$ will from now on be used as a convenient basis for the space of roots. In Sec. I 2.4 it is shown how the complete set of roots Δ can be reconstructed from the set of simple roots using the Weyl group.

An elegant way of encoding the information of simple roots is given by the *Cartan matrix* A_{ij}. It is defined as

$$A_{ij} = \left(\alpha_i, \frac{2\alpha_j}{|\alpha_j|^2}\right).$$

Equivalently, it can be expressed as

$$A_{ij} = (\alpha_i, \alpha_j^\vee)\,, \tag{I.32}$$

where $\alpha_j^\vee = 2\alpha_j/|\alpha_j|^2$ denotes the *coroot* of α_j.

In order to fix the normalization of the simple roots it is convenient to define another quantity called the *highest root* θ and fix its length by $|\theta|^2 = 2$. It is defined as the root $\theta = \sum_i m_i \alpha_i \in \Delta$ for which the sum of the coefficients $\sum_i m_i$ is maximized. The expansion of the highest root in terms of simple roots or coroots is given by

$$\theta = \sum_{i=1}^{r} a_i \alpha_i = \sum_{i=1}^{r} a_i^\vee \alpha_i^\vee\,, \tag{I.33}$$

where a_i, $a_i^\vee$ are called marks, comarks.

The comarks also define the *dual Coexter number*

$$g = \sum_{i=1}^{r} a_i^\vee + 1\,, \tag{I.34}$$

which is used to define the Killing form (I.39) later.

2.3. Weights

The Cartan subalgebra consists of the maximal number of commuting generators of a Lie algebra. Consequently, its elements $\{H^i\}$ can be diagonalized simultaneously and the states of a vectors space V corresponding to a finite-dimensional representation ϕ can be specified by the eigenvalues of $\{H^i\}$. An eigenstate of H^i is a state $|\lambda\rangle$ satisfying

$$H^i|\lambda\rangle = \lambda^i|\lambda\rangle \, ,$$

where $\lambda = (\lambda^1, \dots, \lambda^r)$ is called a *weight*. Hence, weights can be interpreted as elements of the dual space h^*, while roots are elements of h^* in the adjoint representation.

The reason E^α is called *ladder operator* is based on the fact that it changes the weight λ of a state $|\lambda\rangle$ by α:

$$H^i E^\alpha|\lambda\rangle = ([H^i, E^\alpha] + E^\alpha H^i)|\lambda\rangle = (\lambda^i + \alpha^i)E^\alpha|\lambda\rangle \, ,$$

$$\Rightarrow \; E^\alpha|\lambda\rangle \propto |\lambda + \alpha\rangle \, .$$

Notice that, just as for the $\mathfrak{su}(2)$ Lie algebra[3], the action of E^α on a state $|\alpha\rangle$ can vanish for certain roots α and weights λ. This can be further specified by looking at the commutators of $\{E^\alpha, E^{-\alpha}, \alpha\cdot H/|\alpha|^2\}$ following (I.31)

$$[E^\alpha, E^{-\alpha}] = 2\frac{\alpha\cdot H}{|\alpha|^2} \, , \quad \left[\frac{\alpha\cdot H}{|\alpha|^2}, E^{\pm\alpha}\right] = \pm E^{\pm\alpha} \, .$$

These are the same commutation relations as satisfied by the generators $\{J^+, J^-, J^3\}$ of $\mathfrak{su}(2)$ and therefore define a $\mathfrak{su}(2)$ subalgebra of $\mathfrak{g}$. Hence, for an arbitrary root α there must be positive integers p, q such that

$$\begin{aligned}(E^\alpha)^{p+1}|\lambda\rangle &\propto E^\alpha|\lambda + p\alpha\rangle = 0 \, , \\ (E^{-\alpha})^{q+1}|\lambda\rangle &\propto E^{-\alpha}|\lambda - q\alpha\rangle = 0 \, .\end{aligned}$$

The states $|\lambda + p\alpha\rangle$ and $|\lambda - q\alpha\rangle$ satisfy the following eigenvalue equation

$$\begin{aligned}\frac{\alpha\cdot H}{|\alpha|^2}|\lambda + p\alpha\rangle &= \frac{(\alpha, \lambda + p\alpha)}{|\alpha|^2}|\lambda + p\alpha\rangle \\ \frac{\alpha\cdot H}{|\alpha|^2}|\lambda - q\alpha\rangle &= \frac{(\alpha, \lambda - q\alpha)}{|\alpha|^2}|\lambda - q\alpha\rangle \, .\end{aligned} \tag{I.35}$$

Just as for $\mathfrak{su}(2)$ the eigenvalues appearing in (I.35) have to differ by a sign which results in the *master formula*

$$2\frac{(\alpha, \lambda)}{|\alpha|^2} = q - p \, . \tag{I.36}$$

This relation can be used to compute all the weights of a given representation by starting for example with the *highest weight*, i.e. a weight λ with $p = 0$, and apply ladder operators E^α to it that are consistent with the $q - p$ values of the master formula.

[3] $\mathfrak{su}(n)$ ($n \geq 1$) denotes the Lie algebra of the Lie group $SU(n)$ consisting of $n \times n$ unitary matrices with determinant equal to 1. The definition of $\mathfrak{su}(\mathfrak{n})$ for $n = 2, 3$ in terms of Cartan matrices is given in Sec. I 2.6.

Up to this point, we have not fixed a basis for the weights. However, it turns out that a convenient basis for the weights is given by the set of *fundamental weights* $\{\omega_i\}$, which are dual to the simple coroot basis $\{\alpha_j^\vee\}$, i.e. they are defined by

$$(\omega_i, \alpha_j^\vee) = \delta_{ij} \,.$$

In terms of the fundamental weight basis an arbitrary weight λ is written as

$$\lambda = \sum_{i=1}^{r} \lambda_i \omega_i \,, \tag{I.37}$$

where the coefficients $\lambda_i = (\lambda, \alpha_i^\vee)$ are called *Dynkin labels.* From the master formula (I.36) it follows that Dynkin labels are always integers. Furthermore, the Dynkin labels $(\lambda_1, \ldots, \lambda_r)$ are often used to specify a particular representation by fixing the state λ of (I.37) as the highest weight state of that representation. Equivalently, Young diagrams can be used to label a representation: a Young diagram $[x_1, x_2, \ldots, x_r]$ consists of x_i nodes in the i-th row. The relation between the number of nodes x_i and the Dynkin labels λ_i is given by

$$x_i - x_{i+1} = \lambda_i \quad \text{for } i = 1, 2, \ldots, r \,,$$

where $x_{r+1} \equiv 0$.

From the definition of the Cartan matrix in terms of the coroots (I.32) it becomes apparent that the elements of the Cartan matrix A_{ij} are the coefficients of the simple root expanded in the fundamental weight basis:

$$\alpha_i = \sum_j A_{ij} \omega_j . \tag{I.38}$$

Another important operator whose eigenvalues are often used to label a weight or a representation is called the quadratic *Casimir operator* $\mathcal{Q}$. Given a basis of generators $\{\mathcal{L}^a\}$ it is defined by

$$\mathcal{Q} = \sum_{a,b} [K(\mathcal{L}^a, \mathcal{L}^b)]^{-1} \mathcal{L}^a \mathcal{L}^b \,,$$

where K denotes the *Killing form.* For arbitrary $X, Y \in \mathfrak{g}$ the Killing form given by

$$K(X,Y) \equiv \frac{1}{2g} \mathrm{Tr}(\mathrm{ad}X \mathrm{ad}Y) \,, \tag{I.39}$$

defines a symmetric bilinear form for the Lie algebra, where g denotes the dual Coexter number (I.34). Hence, given an orthonormal basis $\{J^a\}$ with respect to K, i.e. a basis that satisfies $K(J^a, J^b) = \delta_{ab}$, the quadratic Casimir operator becomes

$$\mathcal{Q} = \sum_a J^a J^a \,.$$

In the Cartan-Weyl basis it reads

$$\mathcal{Q} = \sum_i H^i H^i + \sum_{\alpha \in \Delta_+} \frac{|\alpha|^2}{2} (E^\alpha E^{-\alpha} + E^{-\alpha} E^\alpha) \,. \tag{I.40}$$

The eigenvalue of $\mathcal{Q}$ for a state with weight λ can be shown to result in

$$\mathcal{Q}|\lambda\rangle = (\lambda, \lambda + 2\rho)|\lambda\rangle \,,$$

where ρ denotes the *Weyl vector*

$$\rho = \sum_i \omega_i \,. \tag{I.41}$$

2.4. The Weyl group

As mentioned in Sec. I 2.2 the Weyl group provides a tool to reconstruct the complete set of roots Δ from the set of simple roots. This can be understood by studying the $\mathfrak{su}(2)$ subalgebra generated by $\{E^{\alpha}, E^{-\alpha}, \alpha \cdot H/|\alpha|^2\}$ in the adjoint representation. In this case a ladder operator E^{β} can be interpreted as a state $|\beta\rangle$, which is an eigenstate of $\mathrm{ad}(\alpha \cdot H/|\alpha|^2)$:

$$\mathrm{ad}\left(\frac{\alpha}{|\alpha|^2} \cdot H\right)|\beta\rangle = \frac{1}{2}(\alpha^{\vee}, \beta)|\beta\rangle \,.$$

If $(\alpha^{\vee}, \beta) \neq 0$, there has to exist another eigenstate $|\beta + l\alpha\rangle$ of $\mathrm{ad}(\alpha \cdot H/|\alpha|^2)$ whose eigenvalue satisfies

$$(\alpha^{\vee}, \beta + l\alpha) \stackrel{!}{=} -(\alpha^{\vee}, \beta) \quad \Leftrightarrow \quad l = -(\alpha^{\vee}, \beta) \,.$$

Hence, $\beta - (\alpha^{\vee}, \beta)\alpha$ is a root whenever β is a root.

The mapping from β to $\beta - (\alpha^{\vee}, \beta)\alpha$ can also be written in terms of the operation s_{α} defined by

$$s_{\alpha}\beta = \beta - (\alpha^{\vee}, \beta)\alpha \,.$$

The set of all operations s_{α} defines a group, called the *Weyl group* W. As roots are generated by simple roots the Weyl group is generated by r *simple Weyl reflections* s_i

$$s_i \equiv s_{\alpha_i} \,.$$

The action of the simple Weyl reflections on the simple roots can be written in terms of the Cartan matrix

$$s_i\alpha_j = \alpha_j - A_{ji}\alpha_i \,.$$

It turns out that the simple Weyl reflections satisfy the following relations

$$(s_i s_j)^{m_{ij}} = 1, \quad \text{with} \quad m_{ij} = \begin{cases} 2 & \text{if } i = j \\ \frac{\pi}{\pi - \theta_{ij}} & \text{if } i \neq j \end{cases} , \tag{I.42}$$

where θ_{ij} denotes the angle between the simple roots α_i and α_j

$$\theta_{ij} = \arccos \frac{(\alpha_i, \alpha_j)}{|\alpha_i||\alpha_j|} \,.$$

In fact, the relations (I.42) are sufficient to construct every element of the Weyl group, as will be demonstrated for $\mathfrak{su}(2)$ and $\mathfrak{su}(3)$ in Sec. I 2.6.

Given the Weyl group W it can be shown that the complete set of roots Δ can be generated from a set of simple roots as

$$\Delta = \{w\alpha |\, \alpha \in \{\alpha_1, \dots, \alpha_r\},\, w \in W\} \,.$$

2.5. The Chevalley basis

In the last sections it was discussed how the roots and weights can be reconstructed from the Cartan matrix: starting with equation (I.38) one can express the simple roots in the fundamental weight basis given the Cartan matrix. Consequently, the scalar products of the simple roots, which are encoded in the Cartan matrix by (I.32), also determine the scalar products of the fundamental weights. The normalization of the lengths of roots and weights is fixed by the condition that the highest root (I.33) satisfies $|\theta|^2 = 2$. Using the Weyl group the complete set of roots Δ can be constructed. At last, by applying the master formula (I.36) for different roots of Δ, the complete set of weights of a representation, labeled by Dynkin labels, can be constructed from the highest weight (I.37).

The Cartan matrix also determines the commutation relations of the generators (I.31). This turns out to be more apparent in the *Chevalley basis*, which is based on the following generators defined for the simple roots

$$e^i = E^{\alpha_i}, \quad f^i = E^{-\alpha_i}, \quad h^i = \alpha_i^\vee \cdot H \,. \tag{I.43}$$

Its commutators are given by

$$\begin{aligned} &[h^i, h^j] = 0\,, & &[e^i, f^j] = \delta_{ij} h^j\,, \\ &[h^i, e^j] = A_{ji} e^j\,, & &[h^i, f^j] = -A_{ji} f^j\,, \end{aligned} \tag{I.44}$$

while the commutators of the remaining ladder operators are determined by (I.31).

2.6. Examples

Starting from the Cartan matrix it is discussed how to obtain roots, weights as well as the generators and their commutation relations for the $\mathfrak{su}(2)$ and $\mathfrak{su}(3)$ Lie algebra.

2.6.1. The $\mathfrak{su}(2)$ Lie algebra

The Cartan matrix for the $\mathfrak{su}(2)$ Lie algebra is given by $A = (2)$. $\mathfrak{su}(2)$ has rank one and its only simple root α_1 in the fundamental weight basis follows from (I.38)

$$\alpha_1 = 2\omega_1\,.$$

If all the lengths of the simple roots are equal, the remaining roots have the same length and the Lie algebra is called *simply laced*. Consequently, the lengths of α_1 and ω_1 are fixed by the length of the highest root θ:

$$|\alpha_1|^2 = |\theta|^2 = 2 \quad \Rightarrow \quad |\omega_1|^2 = \frac{1}{2}\,.$$

From (I.42) one can conclude that the simple Weyl reflection s_1 satisfies

$$s_1^2 = 1\,.$$

Hence, the complete Weyl group is given by $W = \{1, s_1\}$ and the complete set of roots is found to be

$$\Delta = \{\alpha_1, s_1\alpha_1\} = \{\alpha_1, -\alpha_1\}\,.$$

An arbitrary representation can be labeled by a Dynkin label l. The highest weight of this representation (I.37) is given by $\Lambda = l\omega_1$. Using the master formula (I.36) it is found that the admissible weights are constructed by applying $E^{-\alpha_1}$ l times to the state $|\Lambda\rangle$:

$$2\frac{(\alpha_1, l\omega_1)}{|\alpha_1|^2} = l \quad \Rightarrow \quad (q,p) = (l, 0)\,.$$

The weights of a representation with Dynkin label l generated hereby become

$$\lambda_{l,m} = m\omega_1 \quad \text{with } m = -l, -l+2, \ldots, l\,.$$

The generators of $\mathfrak{su}(2)$ in the Chevalley basis are determined by its commutation relations (I.44)

$$[h,e] = 2e\,, \quad [h,f] = -2f \quad [e,f] = h\,.$$

Furthermore, the action of h on a state $|\lambda_{l,m}\rangle$ becomes

$$h|\lambda_{l,m}\rangle = m|\lambda_{l,m}\rangle\,.$$

We finish the discussion of $\mathfrak{su}(2)$ by giving the generators in the Cartan-Weyl basis

$$H = h/\sqrt{2}\,, \quad E^+ = e\,, \quad E^- = f$$

and the *spin basis* known from quantum mechanics

$$J^3 = h/2\,, \quad J^+ = e\,, \quad J^- = f\,.$$

2.6.2. The $\mathfrak{su}(3)$ Lie algebra

The Cartan matrix for the $\mathfrak{su}(3)$ Lie algebra is given by

$$A_{ij} = \begin{pmatrix} 2 & -1 \\ -1 & 2 \end{pmatrix}\,.$$

$\mathfrak{su}(3)$ has rank 2 and the simple roots α_1, α_2 in the fundamental weight basis follow from (I.38)

$$\begin{aligned} \alpha_1 &= 2\omega_1 - \omega_2 \\ \alpha_2 &= -\omega_1 + 2\omega_2\,. \end{aligned} \tag{I.45}$$

Due to the fact that the Cartan matrix is symmetric one can conclude from its definition (I.32) that the lengths of the simple roots are equal, i.e. the Lie algebra is simply laced. Hence, the scalar products of the simple roots and the fundamental weights follow from the Cartan matrix and the condition $|\theta|^2 = 2$:

$$(\alpha_1, \alpha_1) = (\alpha_2, \alpha_2) = |\theta|^2 = 2 \quad \Rightarrow \quad (\alpha_1, \alpha_2) = -1$$

$$\Rightarrow \quad (\omega_1, \omega_1) = (\omega_2, \omega_2) = 2/3\,, \quad (\omega_1, \omega_2) = 1/3\,.$$

The angle θ_{12} between the simple roots α_1 and α_2 is given by

$$\theta_{12} = \arccos\left(\frac{(\alpha_1, \alpha_2)}{|\alpha_1||\alpha_2|}\right) = \frac{2\pi}{3}\,,$$

which results in a condition for the simple Weyl reflections s_1, s_2:

$$(s_1 s_2)^3 = 1 \quad \Rightarrow \quad s_1 s_2 s_1 = s_2 s_1 s_2\,.$$

Consequently, the Weyl group can only consist of the following elements

$$W = \{1, s_1, s_2, s_1 s_2, s_2 s_1, s_1 s_2 s_1\}\,,$$

which are used to generate the complete set of roots Δ:

$$\begin{aligned}\Delta &= \{w\alpha \,|\, \alpha \in \{\alpha_1, \alpha_2\}\,,\, w \in W\} \\ &= \{\alpha_1, \alpha_2, \alpha_1 + \alpha_2, -\alpha_1, -\alpha_2, -\alpha_1 - \alpha_2\}\,. \end{aligned} \tag{I.46}$$

The representations for the $\mathfrak{su}(3)$ Lie algebra can be labeled by Dynkin labels (l_1, l_2). To explicitly construct all the weights of a given representation we focus on the case $(1, 0)$. The highest weight in this representation is given by

$$\Lambda_{(1,0)} = \omega_1\,.$$

By repeatedly applying the master formula it can easily be shown that the multiplet of weights corresponding to the $(1, 0)$ representation becomes

$$\{\omega_1, -\omega_1 + \omega_2, -\omega_2\}\,.$$

Just as for $\mathfrak{su}(2)$ the generators of $\mathfrak{su}(3)$ in the Chevalley basis are determined by its commutation relations (I.44). The action of the elements of the Cartan-subalgebra $\{h^1, h^2\}$ is defined by

$$h^i|\lambda\rangle = \lambda_i|\lambda\rangle \quad \text{with} \quad \lambda = \lambda_1\omega_1 + \lambda_2\omega_2\,.$$

3. Anyons

This section deals with the algebraic theory of anyonic models based on category theory. It has been developed with the aim to describe general anyonic models using a simple unified language. Furthermore, it naturally leads to new anyonic models and allows a simple description of their braiding properties. In this section we follow [77] to discuss the main aspects of anyonic models using the algebraic language. More details on this can be found for e.g. in the appendix of [78].

Sec. I 3.1 deals with the fusion behavior as well as the Hilbert space of several anyons, while the braiding or exchange statistics of anyons are discussed in Sec. I 3.2. Both braiding and fusion processes have to satisfy consistency equations called pentagon and hexagon equations that are discussed in Sec. I 3.3. Furthermore, differences between free and interacting anyons, which are relevant to interpret the low-temperature phases of the perturbed WZNW models in Part II, are pointed out in Sec. I 3.4. Explicitly, this is demonstrated by reference to the $\mathfrak{su}(2)_{N_f}$ anyons in Sec. I 3.5.

3.1. Fusion

Following [77] the abstract definition of an anyonic model consists of rules for particle types, rules for fusing and splitting and rules for braiding. This section deals with particle types and their fusion and splitting rules.

To label the different anyonic particle types Latin letters $\{a, b, c, \dots\}$ are used. A label is also called *superselection sector* of the theory or *topological charge*. These terms emphasize that a label is a physical property of a localized object, which is invariant under any local physical process. Hence, the topological charges are immune to local interactions with the environment, namely decoherence.

The special label $\mathbf{1}$ is reserved for the vacuum and exists in any anyonic model. An anyon a and its antiparticle labeled by $\bar{a}$ can be created out of the vacuum. In this case the combined topological charge of a and $\bar{a}$ is the vacuum labeled by $\mathbf{1}$.

The process of combining two anyons is also called *fusion* while the rules describing the allowed fusion outcomes of two anyons are called *fusion rules*. In general two anyons a and b can fuse to an anyon c in N_{ab}^c distinguishable ways, where N_{ab}^c are non-negative integers. A convenient way of writing the fusion rules is given by

$$a \times b = \sum_c N_{ab}^c \, c \, , \tag{I.47}$$

where the sum goes over all labels and a, b can fuse into c as long as $N_{ab}^c > 0$.

Similar relations are known from the fusion of two spin-1/2 particles. Their fusion rule is given by

$$\frac{1}{2} \times \frac{1}{2} = 0 + 1 \, ,$$

since they can either fuse to a spin-1 particle or a spin-0 particle. However, in this case the labels specify vector spaces and the fusion rule describes how the tensor product of two vector spaces is split into a direct sum of vector spaces. For anyons there does not exist a one-particle Hilbert space corresponding to a label so that the interpretation of fusion rules in terms of the decomposition of tensor products is not possible. In the anyonic case the fusion rules are simply understood as abstract relations defining the fusion outcomes of an anyonic model.

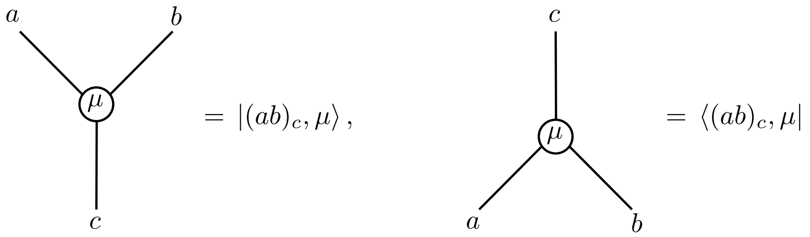

Figure 1: Graphical notation for the fusion states of V_{ab}^{c} showing the fusion of a and b into c (left). The graphical notation for the basis states of the dual space V_{c}^{ab} emphasizes the splitting of c into a and b (right). Notice that the time axis is going vertically downward in these diagrams.

Nevertheless, it is possible to associate a Hilbert space to the fusion of two anyons a and b into an anyon c. More precisely, we denote by V_{ab}^{c} a Hilbert space called *fusion space* whose orthonormal basis is given by the N_{ab}^{c} distinguishable ways the anyons a, b can fuse into c. The states of V_{ab}^{c} are called *fusion states* and its orthonormal basis is denoted by

$$\{|(ab)_c,\, \mu\rangle \,|\, \mu = 1,\, 2,\, \dots,\, N_{ab}^{c}\}\,.$$

The dual space of V_{ab}^{c} is denoted by V_{c}^{ab} and its dual basis is given by

$$\{\langle(ab)_c,\, \mu| \,|\, \mu = 1,\, 2,\, \dots,\, N_{ab}^{c}\}\,.$$

A graphical notation for the basis states of V_{ab}^{c} and its dual basis is given in Figure 1.

The full Hilbert space for the fusion of the anyons a, b is given by $\oplus_c V_{ab}^{c}$. Its basis states are orthogonal to the corresponding dual basis states

$$\langle(ab)_{c'}, \mu'|(ab)_c, \mu\rangle = \delta_c^{c'}\delta_\mu^{\mu'}$$

and the completeness relation of the basis is expressed as

$$\sum_{c,\mu} |(ab)_c, \mu\rangle\langle(ab)_c, \mu| = I_{ab}\,,$$

where I_{ab} is the projector onto the full Hilbert space $\oplus_c V_{ab}^{c}$.

It turns out that there is a useful distinction between *Abelian anyons* and *non-Abelian anyons*. An anyonic model consists of Abelian anyons, or is called Abelian, if exchanging two anyons only results in a phase factor. In terms of the abstract language introduced above an anyonic model is Abelian as long as

$$\dim\left(\bigoplus_c V_{ab}^{c}\right) = \sum_c N_{ab}^{c} = 1 \tag{I.48}$$

for any pair a, b of the anyonic model. As the fusion space of a, b is one-dimensional if the condition (I.48) is satisfied, only phase factors can be obtained when exchanging a and b. Non-Abelian anyons on the other hand have the property that their exchange can generate non-Abelian unitary transformations of the fusion space. It was shown in [79] that this occurs in an anyonic model if and only if the dimension of the fusion space for at least some pair a, b is larger than two:

$$\dim\left(\bigoplus_c V_{ab}^{c}\right) = \sum_c N_{ab}^{c} \geq 2\,. \tag{I.49}$$

Hence, an anyonic model is called non-Abelian if the condition (I.49) is satisfied for at least one pair of anyons a, b. An important consequence is the fact that quantum information is encoded non-locally in a pair of non-Abelian anyons that are far apart. This information is protected from decoherence and can only be corrupted by a non-local process, i.e. exchanging the anyons of the pair.

Rules for fusing and splitting needed to define an anyonic model also comprise rules for fusing three anyons. Physically, the overall topological charge of three anyons is independent of their fusion order. Hence, fusion of three anyons is associative:

$$(a \times b) \times c = a \times (b \times c).$$

The two different ways of fusing three anyons however results in two distinct decompositions of the the Hilbert space V^d_{abc}:

$$V^d_{abc} \cong \bigoplus_e V^e_{ab} \otimes V^d_{ec} \cong \bigoplus_{e'} V^d_{ae'} \otimes V^{e'}_{bc} \,.$$

Therefore, there are two different sets of basis states for V^d_{abc}. The first one is given by the basis of $\oplus_e V^e_{ab} \otimes V^d_{ec}$

$$|((ab)_e c)_d, \mu\nu\rangle \equiv |(ab)_e, \mu\rangle \otimes |(ec)_d, \nu\rangle$$

and the second one is the basis of $\oplus_{e'} V^d_{ae'} \otimes V^{e'}_{bc}$

$$|(a(bc)_{e'})_d, \mu'\nu'\rangle \equiv |(ae')_d, \nu'\rangle \otimes |(bc)_{e'}, \mu'\rangle \,.$$

These basis states must be related by a unitary transformation F called *F-matrix*:

$$|((ab)_e c)_d, \mu\nu\rangle = \sum_{e',\mu',\nu'} \left(F^d_{abc}\right)^{e'\mu'\nu'}_{e\mu\nu} |(a(bc)_{e'})_d, \mu'\nu'\rangle \,. \tag{I.50}$$

In terms of the graphical notation equation (I.50) is written as

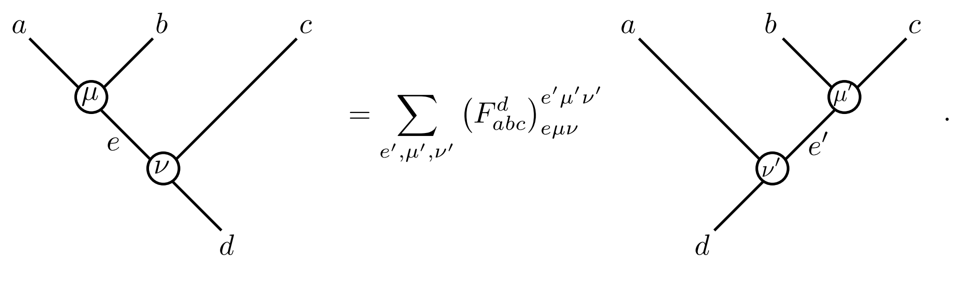

Additionally to the particle types and fusion rules also the F-matrices are necessary to define an anyonic model. However, in some cases it is possible to uniquely derive the F-matrices from consistency equations, see Sec. I 3.3.

3.2. Braiding

The remaining part needed to define an anyonic model are its rules for braiding. Due to the symmetry $(a \times b = b \times a)$ of the fusion rules (I.47) there exists an isomorphism between the Hilbert spaces V^c_{ab} and V^c_{ba}. The mapping between them is given by the braid operator R. In terms of the basis states $\{|(ba)_c, \mu\rangle\}$ and $\{|(ab)_c, \mu'\rangle\}$ the braid operator R transforms as a unitary matrix called R-matrix:

$$R|(ba)_c, \mu\rangle = \sum_{\mu'} (R^c_{ab})^{\mu'}_{\mu} \, |(ab)_c, \mu'\rangle \, . \tag{I.51}$$

Notice that for Abelian anyons the R-matrix is always a phase factor.

In terms of the graphical notation the R-matrix is expressed by braiding the incoming lines of a and b counterclockwise:

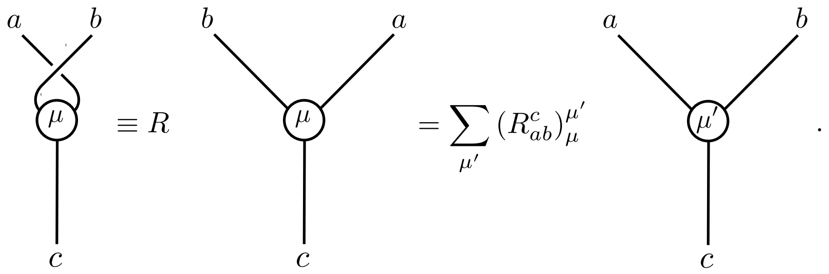

Often the braiding of two anyons of a chain of anyons is needed. For this a chain of n anyons with total topological charge c is labeled by a_1, a_2, $\dots$, a_n and its Hilbert space $V^c_{a_1 a_2 \dots a_n}$ is decomposed by fusing the anyons from the left to the right:

$$V^c_{a_1 a_2 \dots a_n} \cong \bigoplus_{b_1, b_2, \dots, b_{n-2}} V^{b_1}_{a_1 a_2} \otimes V^{b_2}_{b_1 a_3} \otimes \dots \otimes V^c_{b_{n-2} a_n} \, .$$

The dimension of this Hilbert space results in

$$N^c_{a_1 a_2 \dots a_n} \equiv \dim(V^c_{a_1 a_2 \dots a_n}) = \sum_{b_1, b_2, \dots, b_{n-2}} N^{b_1}_{a_1 a_2} N^{b_2}_{b_1 a_3} \dots N^c_{b_{n-2} a_n} \, . \tag{I.52}$$

A basis for $V^c_{a_1 a_2 \dots a_n}$ is again given by the tensor products of basis states of the decomposed parts $V^{b_j}_{b_{j-1} a_{j+1}}$

$$\{|(a_1 a_2)_{b_1}, \mu_1\rangle |(b_1 a_3)_{b_2}, \mu_2\rangle \dots |(b_{n-2} a_n)_c, \mu_{n-1}\rangle\} \, ,$$

which can also be expressed using the graphical notation

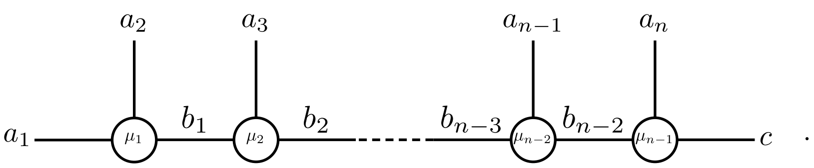

In order to apply the braid operator to two neighboring anyons a_j, a_{j+1} one only needs to consider the part of the Hilbert space $V^c_{a_1 a_2 \dots a_n}$ that is affected by the braid operator. Using the simpler notation $b_{j-2} = b$, $b_{j-1} = c$ and $b_j = d$ this part reads

$$V^d_{b a_j a_{j+1}} \cong \bigoplus_c V^c_{b a_j} \otimes V^d_{c a_{j+1}} \, .$$

The exchange of a_j and a_{j+1} can be performed by transforming the states of $V^d_{b a_j a_{j+1}}$ with the F-matrix such that the R-matrix can be applied and then transforming them back with

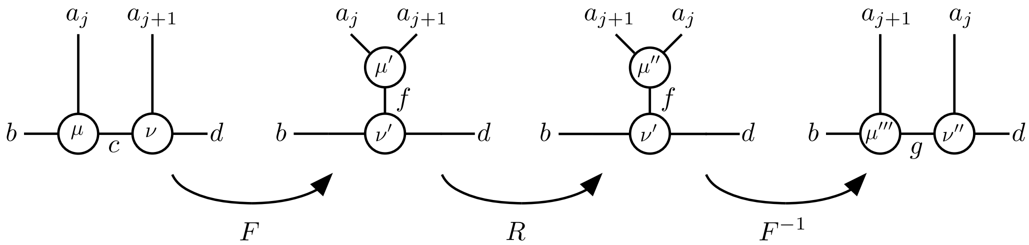

Figure 2: Sequence of F- and R-matrices defining the braid operator for a chain of anyons. The first F-move changes the basis such that the R-matrix can be applied to a_j and a_{j+1}, while the inverse F-move transforms back to the original basis.

the inverse F-matrix. See Figure 2 for an illustration of this process. Hence, one can define a braid operator B as a mapping between $V^d_{ba_ja_{j+1}}$ and $V^d_{ba_ja_{j+1}}$

$$B : V^d_{ba_ja_{j+1}} \to V^d_{ba_{j+1}a_j} ,$$

where B is defined as

$$\begin{aligned} B|((ba_j)_c a_{j+1})_d, \mu\nu\rangle &\equiv F^{-1}RF|((ba_j)_c a_{j+1})_d, \mu\nu\rangle , \\ &= \sum_{g,\mu''',\nu''} \left(B^d_{ba_{j+1}a_j}\right)^{g\mu'''\mu''}_{c\mu\nu} |((ba_{j+1})_g a_j)_d, \mu''', \nu''\rangle \end{aligned}$$

$$\left(B^d_{ba_{j+1}a_j}\right)^{g\mu'''\mu''}_{c\mu\nu} = \sum_{f,\mu',\mu'',\nu'} \left((F^{-1})^d_{ba_{j+1}a_j}\right)^{g\mu'''\nu''}_{f\mu''\nu'} \left(R^f_{a_ja_{j+1}}\right)^{\mu''}_{\mu'} \left(F^d_{ba_ja_{j+1}}\right)^{f\mu'\nu'}_{c\mu\nu} .$$

Using the graphical notation this definition becomes

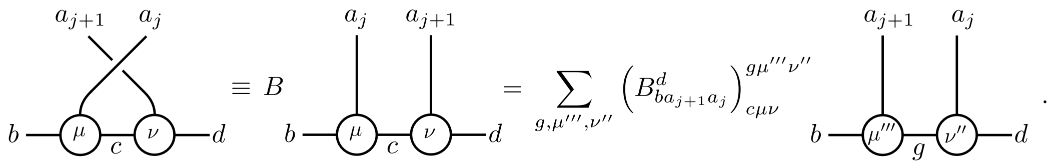

Consequently, the exchange of two anyons of an anyon chain can always be expressed in terms of F- and R-matrices. Moreover, this shows that an anyonic model is completely specified by the following objects:

1. a set of labels $\{a, b, \dots\}$
2. the fusion rules $a \times b = \sum_c N^c_{ab}\, c$
3. the F-matrices
4. the R-matrices

Mathematically, this set of objects defines a unitary braided fusion category [78].

3.3. Pentagon and hexagon equations

From the last section one might get the impression that any fusion rule together with a F-matrix and a R-matrix defines an admissible anyonic model. However, as will be shown,

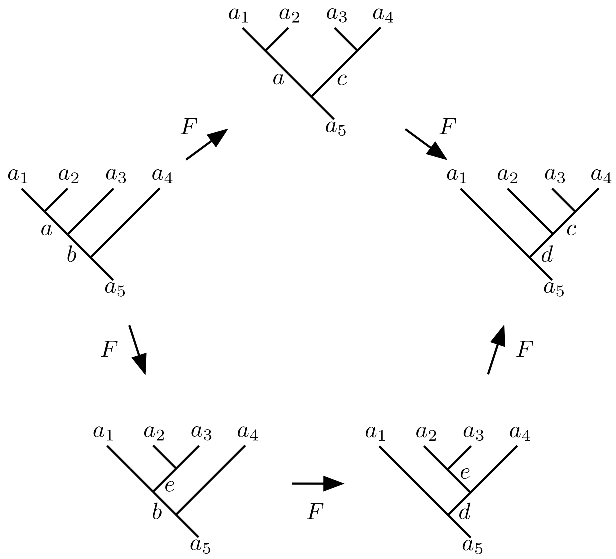

Figure 3: The figure shows the five different decompositions of $V^{a_5}_{a_1a_2a_3a_4}$ and their relation in terms of F-moves. Starting from the top left the two sequences of F-moves define the pentagon equations.

the F- and R-matrices have to satisfy consistency conditions called pentagon and hexagon equations so that only fusion rules with suitable F- and R-matrices define an admissible anyonic model.

The first set of consistency conditions are obtained by considering the five different possibilities four anyons of a specified order can be fused. Each possibility corresponds to a distinct decomposition of the Hilbert space $V^{a_5}_{a_1a_2a_3a_4}$. As shown in Figure 3 all the decompositions of $V^{a_5}_{a_1a_2a_3a_4}$ are isomorphic to each other since they are related by a series of F-moves. Notice that for simplicity the fusion indices are neglected in Figure 3 and the following discussion. The shape of the diagrams in Figure 3 motivates the name *pentagon equations* for the corresponding consistency equations.

If written out explicitly, the top part of Figure 3 results in

$$|(((a_1a_2)_a a_3)_b a_4)_{a_5}\rangle = \sum_{c,d} \left(F^{a_5}_{a_1a_2c}\right)^d_a \left(F^{a_5}_{aa_3a_4}\right)^c_b |(a_1(a_2(a_3a_4)_c)_d)_{a_5}\rangle$$

while the bottom part becomes

$$|(((a_1a_2)_a a_3)_b a_4)_{a_5}\rangle = \sum_{c,d,e} \left(F^{a_5}_{a_2a_3a_4}\right)^c_e \left(F^{a_5}_{a_1ea_4}\right)^d_b \left(F^{b}_{a_1a_2a_3}\right)^e_a |(a_1(a_2(a_3a_4)_c)_d)_{a_5}\rangle \,.$$

Hence, the consistency equations of the F-matrices called pentagon equations result in

$$\left(F^{a_5}_{a_1a_2c}\right)^d_a \left(F^{a_5}_{aa_3a_4}\right)^c_b = \sum_{e} \left(F^{a_5}_{a_2a_3a_4}\right)^c_e \left(F^{a_5}_{a_1ea_4}\right)^d_b \left(F^{b}_{a_1a_2a_3}\right)^e_a \,. \tag{I.53}$$

The second set of consistency conditions are obtained by considering the six different possibilities of fusing three anyons with arbitrary order. Figure 4 shows the combinations of F- and R-matrices that relate the different decompositions of the Hilbert space. The set of consistency equations corresponding to Figure 4 are called *hexagon equations*.

If written out explicitly, the top part of Figure 4 results in

$$|((a_1a_2)_a a_3)_{a_4}\rangle = \sum_{b,c} \left(F^{a_4}_{a_2a_3a_1}\right)^c_b R^{a_4}_{a_1b} \left(F^{a_4}_{a_1a_2a_3}\right)^b_a |(a_2(a_3a_1)_c)_{a_4}\rangle$$

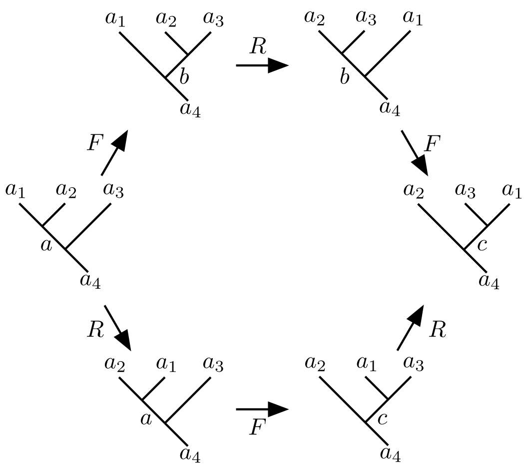

Figure 4: The figure shows the six different fusion possibilities of three anyons with arbitrary order and their relation in terms of F- and R-moves. Starting from the left the two sequences of F- and R-moves define the hexagon equations.

while the bottom part becomes

$$|((a_1a_2)_a a_3)_{a_4}\rangle = \sum_c R^c_{a_1a_3} \left(F^{a_4}_{a_2a_1a_3}\right)^c_a R^a_{a_1a_2} |(a_2(a_3a_1)_c)_{a_4}\rangle \,.$$

Hence, the hexagon equations become

$$R^c_{a_1a_3} \left(F^{a_4}_{a_2a_1a_3}\right)^c_a R^a_{a_1a_2} = \sum_b \left(F^{a_4}_{a_2a_3a_1}\right)^c_b R^{a_4}_{a_1b} \left(F^{a_4}_{a_1a_2a_3}\right)^b_a \,.$$

In category theory the *MacLane coherence theorem* states that there are no further consistency conditions that need to be satisfied by the F- and R-matrices [80]. In other words, any two sequences of F- and R-matrices that map one basis of n anyons to another basis describe the same isomorphism if the pentagon and hexagon equations are satisfied.

Moreover, solving the pentagon and hexagon equations provides a way to compute the F- and R-matrices given a set of labels and its fusion rules. In fact, each solution of the pentagon and hexagon equations, if it exists, defines a unique anyonic model.

3.4. Free vs. interacting anyons

So far it was mentioned that quantum information can be encoded non-locally in a pair of non-Abelian anyons that are far apart. Here far apart meant that the anyons are separated enough to be considered as free particles. Only in this case there exists a ground space degeneracy in which quantum information can be encoded non-locally. As soon as the particles are brought close to each other this degeneracy is lifted, because interactions of the particles may cause some of the fusion outcomes to be preferred. In the case of spin chains such interactions can be modeled by local Hamiltonians that prefer ferromagnetic or antiferromagnetic coupling of the spins. Below this construction is generalized to chains of anyons.

The degeneracy of a non-interacting chain of n anyons of type a with overall topological charge b is given by the dimension of the Hilbert space $V^b_{aa\ldots a}$ (I.52):

$$N^b_{aa\ldots a} = \sum_{b_1,b_2,\ldots,b_{n-2}} N^{b_1}_{aa} N^{b_2}_{ab_1} N^{b_3}_{ab_2} \ldots N^b_{ab_{n-2}}$$

As mentioned before it is not possible to express the Hilbert space $V^b_{aa\ldots a}$ into tensor products of single particle Hilbert spaces. However, for large n it can be shown that the main contribution to the dimension of $V^b_{aa\ldots a}$ is given by

$$N^b_{aa\ldots a} = \frac{d_b}{\mathcal{D}^2} d_a^n + \ldots\,,$$

where d_a denotes the *quantum dimension* of anyon a derived from

$$d_a d_b = \sum_c N^c_{ab} d_c \tag{I.54}$$

and $\mathcal{D}$ is the total quantum dimension

$$\mathcal{D} = \sqrt{\sum_c d_c^2}\,.$$

Hence, even though there is no single particle Hilbert space of anyon a one can define a quantum dimension d_a corresponding to it that describes the rate of growth of $V^b_{aa\ldots a}$ for large n. Notice that it is another characteristic of anyonic models to possess non-integer quantum dimensions. An example of this will be given in the next section.

In order to define a Hamiltonian modelling short-range interactions of an anyon chain a procedure similar to the definition of the braid operator is applied. Suppose that we have a chain of n anyons a with overall topological charge a. The corresponding Hilbert space is decomposed as before

$$V^a_{aa\ldots a} \cong \bigoplus_{b_1,b_2,\ldots,b_{n-2}} V^{b_1}_{aa} \otimes V^{b_2}_{b_1 a} \otimes \ldots \otimes V^a_{b_{n-2}a}\,.$$

A local Hamiltonian $H = \sum_j \sum_b J_b H_j^{(b)}$ acting on this Hilbert space can be defined by assigning different energies to the fusion outcomes of neighboring anyons a. For example, if the fusion rule of a with itself is given by

$$a \times a = b + \ldots\,,$$

we can assign an energy $E = -1$ for the fusion outcome b and the energy $E = 0$ for the other fusion outcomes. In this case the modelled interactions favor the fusion of a with itself to anyon b. More precisely, $H_j^{(b)}$ acts on the j-th part of Hilbert space given by

$$V^{b_{j+1}}_{b_{j-1}aa} = \bigoplus_{b_j} V^{b_j}_{b_{j-1}a} \otimes V^{b_{j+1}}_{b_j a}$$

and the energies are assigned to the fusion outcome of a with itself by applying F-moves as shown in Figure 5. Written out explicitly the action of $H_j^{(b)}$ turns out to be

$$\begin{aligned} H_j^{(b)} |((b_{j-1}a)_{b_j} a)_{b_{j+1}}\rangle &= \sum_c \left(H_j^{(b)}\right)^c_{b_j} |((b_{j-1}a)_c a)_{b_{j+1}}\rangle \\ \left(H_j^{(b)}\right)^c_{b_j} &\equiv -\left((F^{-1})^{b_{j+1}}_{b_{j-1}aa}\right)^c_b \left(F^{b_{j+1}}_{b_{j-1}aa}\right)^b_{b_j}\,. \end{aligned} \tag{I.55}$$

An example of this construction for $\mathfrak{su}(2)_k$ anyons is given in the next section.

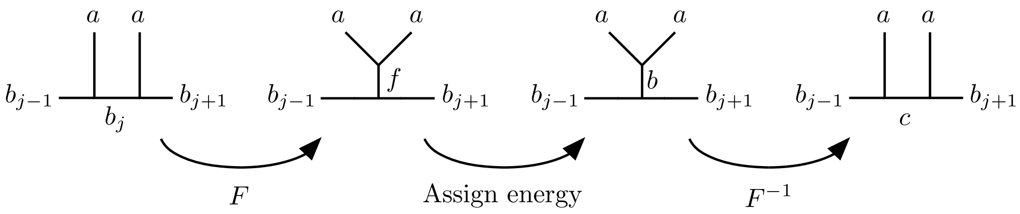

Figure 5: Sequence of F-moves defining a local Hamiltonian with nearest neighbor interactions for a chain of anyons. After applying the first F-move it is projected onto a state with fusion outcome of a with itself given by b while assigning the energy $E = -1$ to this state. Applying F^{-1} the resulting state is transformed back to the original basis.

3.5. $\mathfrak{su}(2)_k$ anyons

In this section an important class of anyonic models called $\mathfrak{su}(2)_k$ anyons is defined. For each integer k, called level, the different anyon types are labeled by the allowed irreducible representations of the corresponding affine Lie algebra, i.e. $\mathfrak{su}(2)_k$. In general this coincides with the irreducible representations of the corresponding Lie algebra, whose highest weights Λ satisfy the condition

$$(\Lambda, \theta) \leq k\,, \tag{I.56}$$

where θ is the highest root (see Sec. I 2.2). For $\mathfrak{su}(2)_k$ the highest weights are $\Lambda = l\omega_1$ with integer l and the highest root is $\theta = 2\omega_1$ such that the condition (I.56) results in

$$l \leq k\,.$$

However, instead of using the Dynkin labels satisfying $l \leq k$ to label the anyon types we use the 'spin' $s = l/2$:

$$\text{labels} = \left\{0,\, \frac{1}{2},\, 1,\, \dots,\, \frac{k}{2}\right\}\,,$$

where 0 denotes the vacuum and not $\mathbf{1}$. The corresponding fusion rules are the tensor product decompositions of the $\mathfrak{su}(2)$ representations

$$j_1 \times j_2 = \sum_{j=|j_1-j_2|}^{j_1+j_2} j$$

with the restriction that the fusion outcome j has to satisfy (I.56), i.e. $j \leq k/2$. An example of this is given for the fusion rules defining the $\mathfrak{su}(2)_3$ anyons

$$\begin{aligned} &\frac{1}{2} \times \frac{1}{2} = 0 + 1\,, \qquad \frac{1}{2} \times 1 = \frac{1}{2} + \frac{3}{2}\,, \qquad \frac{1}{2} \times \frac{3}{2} = 1\,,\\ &1 \times 1 = 0 + 1\,, \qquad 1 \times \frac{3}{2} = \frac{1}{2}\,,\\ &\frac{3}{2} \times \frac{3}{2} = 0\,. \end{aligned}$$

The subset of the $\mathfrak{su}(2)_3$ anyons with labels $0, 1$ and fusion rule $1 \times 1 = 0 + 1$ defines an important model called the Fibonacci anyons. Its quantum dimension, following from (I.54), is given by the golden mean:

$$d_1^2 = 1 + d_1 \quad \Leftrightarrow \quad d_1 = \frac{1}{2}(1 + \sqrt{5})\,.$$

By deriving the F- and R-matrices for the Fibonacci anyons from the pentagon and hexagon equations it can be shown that Fibonacci anyons are *universal* for quantum computing. More precisely, given a chain of n Fibonacci anyons a qubit can be encoded into each set of three anyons and every gate necessary for quantum computation can be approximated with arbitrary precision by applying braid operations. See for example [81] for the implementation of gates using F- and R-matrices of the Fibonacci anyons. Furthermore, it can be shown that the $\mathfrak{su}(2)_k$ anyons with $k \geq 3$ and $k \neq 4$ are computationally universal [18, 19].

For future reference we also give a general formula for the quantum dimension of a $\mathfrak{su}(2)_k$ anyon with label j [78, 82]

$$d_j = \frac{\sin\left(\frac{(2j+1)\pi}{k+2}\right)}{\sin\left(\frac{\pi}{k+2}\right)} \,. \tag{I.57}$$

Interacting $\mathfrak{su}(2)_k$ anyons can be modelled by considering a chain of 1/2 anyons with local Hamiltonian $H = J\sum_j H_j^{(1)}$ defined by (I.55). For $J > 0$ this describes an anyonic chain with ferromagnetic coupling as the spin-1/2 anyons favor fusing to the spin-1 anyon. Interestingly, this model is described by a $Z_{\mathfrak{su}(2)_k}$ parafermion conformal field theory (defined in Sec. I 4.7) with central charge

$$c = 2\frac{k-1}{k+2} \,.$$

For $J < 0$ the coupling is antiferromagnetic as the anyons 1/2 favor fusing to the 0 anyon. This model defines a unitary minimal conformal field theory with central charge

$$c = 1 - \frac{6}{(k+1)(k+2)} \,,$$

see for e.g. [20] for more details on the relationship to conformal field theory.

The quantum dimension and the central charge describing the behavior of free and interacting anyons will turn out to be the essential quantities that we compute for the perturbed WZNW models in Part II. The anyons will appear in these models as quasi-particle excitations for sufficiently small temperatures.

4. Conformal field theory

The purpose of this section is to define the WZNW models as well as their related parafermion conformal field theories. This however requires many aspects from conformal field theory, whose detailed introduction is beyond the scope of this thesis. Therefore, only the main features of conformal field theory that are relevant for a discussion of WZNW models are briefly reviewed. A complete introduction to conformal field theory and WZNW models can be found for e.g. in [56].

To give an idea of the main application of conformal field theory the relationship between critical points of condensed matter systems and conformal symmetry is given in Sec. I 4.1. In Sec. I 4.2 a CFT is defined as a quantum field theory, whose metric is invariant under conformal transformations, i.e. transformations of spacetime that preserve the angle. This invariance of quantum field theories under conformal transformations results in restrictions of correlation functions, that are discussed in Sec. I 4.3. Other important aspects of CFT like the operator formalism and the notion of a Hilbert space are introduced in Sec. I 4.4 and Sec. I 4.5. All of this is sufficient to define WZNW models (Sec. I 4.6) and Gepner's generalized parafermion CFT's (Sec. I 4.7).

4.1. Conformal symmetry at the critical point

In condensed matter physics a first- or second-order *phase transition* appears at a point in parameter space for which the first or second derivative of the free energy becomes discontinuous. The parameter used to characterize the different phases is called *order parameter* (e.g. the magnetization for the Ising model). A physical example of first-order phase transitions are the transitions between the solid, liquid and gas phase of water. The second-order phase transition for water appears at the end point of the pressure-temperature curve separating the liquid and the gas phase. This point is also called *critical point* and always goes along with a diverging *correlation length* ξ, which denotes the maximal length of a system at which degrees of freedom are correlated.

A condensed matter system at the critical point is therefore not changing its behavior when zooming in or out in spacetime, i.e. it is scale-invariant. Mathematically, this scale invariance can be studied using the *renormalization group*: in a lattice system the renormalization group maps each block of spins into one block spin and thereby rewrites the corresponding Hamiltonian in terms of the block spins. For a scale-invariant theory this procedure does not affect the overall form of the Hamiltonian and only maps the coupling constants to a new set of coupling constants. Hence, by applying the renormalization group several times the *relevant* coupling constants for the system at larger length scales become apparent.

Furthermore, the renormalization group motivates the *scaling hypothesis* of a scale-invariant theory. Given a temperature T_c at which a second-order phase transition occurs, the scaling hypothesis states that the free energy density F is a homogeneous function of the reduced temperature $t = T/T_c - 1$ and the magnetic field H:

$$F(\lambda^a t, \lambda^b H) = \lambda F(t, H)\,,$$

where a, b are exponents depending on the described theory. From this one can conclude that $t^{-1/a}F(t,H)$ is invariant under the scale transformations $t \to \lambda^a t$, $H \to \lambda^b H$ and can therefore only be given by some function $g(y)$ depending on the scale-invariant variable $y = H/t^{b/a}$:

$$t^{-1/a}F(t,H) \overset{!}{=} g(y) \quad \Rightarrow \quad F(t,H) = t^{1/a} g(y)\,. \tag{I.58}$$

The behavior of thermodynamic quantities near the critical point is determined solely by (I.58) following from the scaling hypothesis. For example the magnetization near criticality becomes

$$M = -\left.\frac{\partial F}{\partial H}\right|_{H=0} = t^{(1-b)/a} g'(0)\,,$$

where $(1-b)/a$ is the *critical exponent* of the magnetization.

Conformal field theories come into play whenever a scale-invariant theory is also invariant under more general *conformal* transformations. These are transformations of spacetime that preserve the angle, but allow scale transformations. In fact, in [83] it is proven, under some technical assumptions, that scale-invariant quantum field theories in 2D also possess the enhanced conformal symmetry. Hence, critical points of condensed matter systems seem to be naturally described by $1+1$-dimensional conformal field theories.

In the language of conformal field theories the critical exponents turn out to be the *conformal dimensions* of certain fields. Consequently, the main physical aspects describing a second order phase transition can be extracted from a conformal field theory describing the condensed matter system.

4.2. Conformal transformations

A quantum field theory is called *conformally invariant* if and only if its action is invariant under *conformal transformations*. Conformal transformations consist of any coordinate transformation that leaves the metric invariant up to a scale factor $\Lambda(x)$

$$g'_{\mu\nu}(\mathbf{x}') = \Lambda(\mathbf{x}) g_{\mu\nu}(\mathbf{x})\,, \tag{I.59}$$

where $\mathbf{x} \to \mathbf{x}'$ denotes an invertible mapping. It can be shown that the admissible conformal transformations are given by translations, dilations, rigid rotations and *special conformal transformations* (SCT):

$$\begin{aligned} \text{Translation:} \qquad & x'^{\mu} = x^{\mu} + a^{\mu} \\ \text{Dilation:} \qquad & x'^{\mu} = \alpha x^{\mu} \\ \text{Rigid rotation:} \qquad & x'^{\mu} = M^{\mu}{}_{\nu} x^{\nu} \\ \text{SCT:} \qquad & x'^{\mu} = \frac{x^{\mu} - b^{\mu}\mathbf{x}^2}{1 - 2\mathbf{b}\cdot\mathbf{x} + \mathbf{b}^2\mathbf{x}^2}\,, \end{aligned} \tag{I.60}$$

where a^{μ}, α, $M^{\mu}{}_{\nu}$, $b^{\mu} \in \mathbb{R}$.

The effect of conformal transformations on fields $\phi(\mathbf{x})$ is found by studying representations of the infinitesimal generators of (I.60). In general a transformation of a field is given by a coordinate transformation $\mathbf{x}' \to \mathbf{x}$ and a functional change $\phi \to \phi'$, which can be written in terms of a mapping $\mathcal{F}$ on $\phi(\mathbf{x})$:

$$\begin{aligned} &\mathbf{x} \to \mathbf{x}' \\ &\phi(\mathbf{x}) \to \phi'(\mathbf{x}') = \phi'(\mathbf{x}'(\mathbf{x})) \equiv \mathcal{F}(\phi(\mathbf{x}))\,. \end{aligned}$$

Let us consider a *spinless* field ϕ, i.e. a field ϕ for which the matrix representation of the infinitesimal Lorentz transformation vanishes. In d-dimensional spacetime such a field transforms under a conformal transformation as

$$\phi(\mathbf{x}) \to \phi'(\mathbf{x}') = \left|\frac{\partial \mathbf{x}'}{\partial \mathbf{x}}\right|^{-\Delta/d} \phi(\mathbf{x}) = \Lambda(\mathbf{x})^{\Delta/2}\phi(\mathbf{x})\,, \tag{I.61}$$

where $|\partial \mathbf{x}'/\partial \mathbf{x}|$ denotes the Jacobian of the coordinate transformation and Δ is called the *scaling dimension* of the field ϕ. In general fields ϕ that transform under any conformal transformation as (I.61) are called *quasi-primary.*

From now on we will focus on a two-dimensional spacetime. This case requires special attention as there exists an infinite number of coordinate transformations that are *locally conformal* instead of the transformations (I.60), which are defined globally. Furthermore, it will be shown how local invariance of a two-dimensional quantum field theory leads to exact solutions.

In two-dimensions we denote the coordinates by (z^0, z^1). From (I.59) one can conclude that a coordinate transformation $z^\mu \to w^\mu(z^0, z^1)$ has to satisfy either the condition of a *holomorphic* function

$$\frac{\partial w^1}{\partial z^0} = -\frac{\partial w^0}{\partial z^1} \quad \text{and} \quad \frac{\partial w^0}{\partial z^0} = \frac{\partial w^1}{\partial z^1}$$

or the condition of an *antiholomorphic* function

$$\frac{\partial w^1}{\partial z^0} = \frac{\partial w^0}{\partial z^1} \quad \text{and} \quad \frac{\partial w^0}{\partial z^0} = -\frac{\partial w^1}{\partial z^1} \,.$$

Consequently, it is convenient to work with complex coordinates z and $\bar{z}$ defined by

$$\begin{aligned} z &= z^0 + \mathrm{i} z^1 \,, & z^0 &= \frac{1}{2}(z+\bar{z}) \,, \\ \bar{z} &= z^0 - \mathrm{i} z^1 \,, & z^1 &= \frac{1}{2\mathrm{i}}(z-\bar{z}) \,, \\ \partial_z &= \frac{1}{2}(\partial_0 - \mathrm{i}\partial_1) \,, & \partial_0 &= \partial_z + \partial_{\bar{z}} \,, \\ \partial_{\bar{z}} &= \frac{1}{2}(\partial_0 + \mathrm{i}\partial_1) \,, & \partial_1 &= i(\partial_z - \partial_{\bar{z}}) \,. \end{aligned} \tag{I.62}$$

The generators of local conformal transformations can be found by studying an arbitrary holomorphic infinitesimal transformation of a field $\phi(z, \bar{z})$. From complex analysis it is known that such a coordinate transformation may be expressed as

$$z' = z + \epsilon(z) \,, \qquad \epsilon(z) = \sum_{n=-\infty}^{\infty} c_n z^{n+1} \,.$$

which has the following effect on the field

$$\phi'(z', \bar{z}') = \phi(z, \bar{z}) \,.$$

Hence, the infinitesimal transformation of the field $\delta\phi$ becomes

$$\begin{aligned} \delta\phi(z,\bar{z}) &\equiv \phi'(z,\bar{z}) - \phi(z,\bar{z}) \\ &= -\epsilon(z)\partial_z\phi(z,\bar{z}) - \bar{\epsilon}(\bar{z})\partial_{\bar{z}}\phi(z,\bar{z}) \\ &= \sum_n \Big(c_n l_n \phi(z,\bar{z}) + \bar{c}_n \bar{l}_n \phi(z,\bar{z}) \Big) \,, \end{aligned}$$

where l_n and $\bar{l}_n$ are the generators of the holomorphic and antiholomorphic local conformal transformations defined by

$$l_n = -z^{n+1}\partial_z \,, \qquad \bar{l}_n = -\bar{z}^{n+1}\partial_{\bar{z}} \,.$$

They satisfy the following commutation relations

$$\begin{aligned} [l_n, l_m] &= (n-m)l_{n+m} , \\ [\bar{l}_n, \bar{l}_m] &= (n-m)\bar{l}_{n+m} , \\ [l_n, \bar{l}_m] &= 0 . \end{aligned} \tag{I.63}$$

Notice that the elements l_{-1}, l_0 and l_1 as well as their counterparts generate translations, rotations or scale transformations and special conformal transformations. Hence, these elements generate a subalgebra given by the generators of the global conformal transformations.

In two dimensions the definition of quasi-primary fields can be generalized to fields with spin s by defining the *holomorphic conformal dimension* h and the *antiholomorphic conformal dimension* $\bar{h}$ as

$$h = \frac{1}{2}(\Delta + s) , \qquad \bar{h} = \frac{1}{2}(\Delta - s) ,$$

where Δ denotes the scaling dimension of $\phi(z, \bar{z})$. Hence, a quasi-primary field with conformal dimensions $(h, \bar{h})$ transforms under any global conformal transformation $z \to w(z)$, $\bar{z} \to \bar{w}(\bar{z})$ as

$$\phi'(w, \bar{w}) = \left(\frac{\mathrm{d}w}{\mathrm{d}z}\right)^{-h} \left(\frac{\mathrm{d}\bar{w}}{\mathrm{d}\bar{z}}\right)^{-\bar{h}} \phi(z, \bar{z}) . \tag{I.64}$$

Moreover, a field transforming under any local conformal transformation as (I.64) is called *primary.*

4.3. Correlation functions

Correlation functions are the main objects of interest in a quantum field theory as they can be related to physical quantities. In this chapter correlation functions are defined using the path integral formalism and its structure due to conformal invariance is discussed.

Given a bosonic field $\phi(\mathbf{x})$ in d dimensions the correlation function of $\phi(\mathbf{x}_1)$ and $\phi(\mathbf{x}_2)$ is defined as

$$\langle \phi(\mathbf{x}_1)\phi(\mathbf{x}_2)\rangle = \langle 0|\mathcal{T}(\phi(\mathbf{x}_1)\phi(\mathbf{x}_2))|0\rangle , \tag{I.65}$$

where $|0\rangle$ denotes the ground state and the *time ordering operator* $\mathcal{T}$ is defined as

$$\mathcal{T}(\phi(\mathbf{x}_1)\phi(\mathbf{x}_2))) = \begin{cases} \phi(\mathbf{x}_1)\phi(\mathbf{x}_2) , & \text{if } x_1^0 > x_2^0 \\ \phi(\mathbf{x}_2)\phi(\mathbf{x}_1) , & \text{if } x_2^0 > x_1^0 \end{cases} .$$

The time ordering of n bosonic fields is defined analogously, while for fermionic fields a minus sign is introduced every time two fields are commuted. By using the path integral formalism the correlation function (I.65) can be written as

$$\langle \phi(\mathbf{x}_1)\phi(\mathbf{x}_2)\rangle = \lim_{\epsilon\to 0} \frac{\int [\mathrm{d}\phi]\phi(\mathbf{x}_1)\phi(\mathbf{x}_2) \exp \mathrm{i}S_\epsilon(\phi)}{\int [\mathrm{d}\phi] \exp \mathrm{i}S_\epsilon(\phi)} ,$$

where S_ϵ denotes the action S with the replacement $x^0 \leftrightarrow x^0(1 - \mathrm{i}\epsilon)$.

In the *Euclidean formalism* the time component x^0 is replaced by $-\mathrm{i}\tau$ and the *Euclidean action* defined as

$$\mathrm{i}S_E(\phi(\tau, x^1, \dots, x^{n-1})) = S(\phi(-\mathrm{i}\tau, x^1, \dots, x^{n-1})) .$$

Hence, in the Euclidean formalism the correlation function (I.65) becomes

$$\langle\phi(\mathbf{x}_1)\phi(\mathbf{x}_2)\rangle = \frac{1}{Z}\int [\mathrm{d}\phi]\phi(\mathbf{x}_1)\phi(\mathbf{x}_2)\exp\left(-S_E(\phi)\right), \tag{I.66}$$

where Z denotes the partition function

$$Z = \int [\mathrm{d}\phi]\exp\left(-S_E(\phi)\right).$$

Equation (I.66) can be used as the starting point for the analysis of correlation functions in conformal field theory. The correlation function (I.66) is also called *two-point function.* More generally the correlation function of n-fields is called *n-point function.* It can be shown that global conformal invariance fixes the form of two- and three-point functions up to coefficients. For the exact computation of all n-point functions in a two-dimensional conformal field theory, the *conformal bootstrap* approach can be used, see Sec. I 4.4.

To discuss two- and three-point functions of primary fields the focus is again on two-dimensional spacetime. The transformation behavior of a general n-point function under local conformal transformations follows from (I.64) and the fact that the action as well as the integration measure of the path integral are invariant under those transformations:

$$\langle\phi_1(w_1,\bar{w}_1)\dots\phi_n(w_n,\bar{w}_n)\rangle = \prod_{i=1}^{n}\left(\frac{\mathrm{d}w}{\mathrm{d}z}\right)^{-h_i}_{w=w_i}\left(\frac{\mathrm{d}\bar{w}}{\mathrm{d}\bar{z}}\right)^{-\bar{h}_i}_{\bar{w}=\bar{w}_i}\langle\phi_1(z_1,\bar{z}_1)\dots\phi_n(z_n,\bar{z}_n)\rangle\,. \tag{I.67}$$

By studying (I.67) for global conformal transformations the form of the two-point function of primary fields is found to be

$$\langle\phi_1(z_1,\bar{z}_1)\phi_2(z_2,\bar{z}_2)\rangle = \begin{cases}\frac{C_{12}}{(z_1-z_2)^{2h_1}(\bar{z}_1-\bar{z}_2)^{2\bar{h}_1}} & \text{if } h_1 = h_2\,,\ \bar{h}_1=\bar{h}_2 \\ 0 & \text{otherwise}\end{cases}\,, \tag{I.68}$$

where $(h_i,\bar{h}_i)$ denote the conformal dimensions of ϕ_i. Similarly, the form of the three-point function of primary fields becomes

$$\begin{aligned}\langle\phi_1(z_1,\bar{z}_1)\phi_2(z_2,\bar{z}_2)\phi_2(z_3,\bar{z}_3)\rangle = C_{123}&\frac{1}{z_{12}^{h_1+h_2-h_3}z_{23}^{h_2+h_3-h_1}z_{13}^{h_3+h_1-h_2}} \\ \times&\frac{1}{\bar{z}_{12}^{\bar{h}_1+\bar{h}_2-\bar{h}_3}\bar{z}_{23}^{\bar{h}_2+\bar{h}_3-\bar{h}_1}\bar{z}_{13}^{\bar{h}_3+\bar{h}_1-\bar{h}_2}}\,,\end{aligned} \tag{I.69}$$

where $z_{ij} \equiv z_i - z_j$. In the next section the ingredients needed to compute all n-point functions with $n > 3$ as well as the coefficients for the two-point and three-point functions are discussed.

4.4. Operator product expansion

Typically, correlation functions like the two- and three-point functions (I.68), (I.69) diverge as the arguments of the operators are brought close to each other. A representation of this behavior is given by the *operator product expansion* (OPE). If an arbitrary field is labeled by ϕ_k, the OPE of two fields fields $\phi_i(z)$ and $\phi_j(w)$ is defined as

$$\phi_i(z)\phi_j(w) = \sum_k c_{ij}^k\frac{\phi_k(w)}{(z-w)^{n_{ijk}}}\,, \tag{I.70}$$

where $c_{ij}^k \in \mathbb{R}$, $n_{ijk} \in \mathbb{Z}$ are constants and $\phi_k(w)$ is nonsingular at $w = z$.

Notice that the operator product expansion (I.70) is only defined within correlation functions. However, an operator meaning can be obtained using *radial quantization* and applying a *radial ordering* to the left side of (I.70). In short, this is based on the fact that the coordinates $(t, 0)$ and (t, L) in $1+1$-dimensional Minkowski space for some length L are identified. A coordinate (t_i, x_i) is then mapped to a complex coordinate z_i by

$$z_i = \exp 2\pi(t_i + \mathrm{i}x_i)/L \tag{I.71}$$

so that time ordering $t_1 > t_2$ corresponds to radial ordering $|z_1| > |z_2|$. Consequently, operators appearing in operator product expansions are consistent with operators inside correlation function as long as they are radially ordered.

To give an example of an operator product expansion we consider the correlation function of the *energy-momentum tensor* $T_{\mu\nu}$ and a single primary field ϕ with conformal dimensions $(h, \bar{h})$. The energy-momentum tensor is defined as the conserved current associated with translation invariance by Noether's theorem. It can be shown that the correlation function of $T(z) \equiv -2\pi T_{zz}$ and $\phi(w, w')$ is given by

$$\langle T(z)\phi(w,w')\rangle \sim \frac{h}{(z-w)^2}\langle\phi(w,w')\rangle + \frac{1}{z-w}\partial_w\langle\phi(w,w')\rangle\,,$$

where "$\sim$" means equality modulo expressions that are regular as $z \to w$. This expression and its antiholomorphic counterpart with $\bar{T}(\bar{z}) \equiv -2\pi T_{\bar{z}\bar{z}}$ can be represented as OPE's by neglecting the "brackets":

$$\begin{aligned} T(z)\phi(w,w') &\sim \frac{h}{(z-w)^2}\phi(w,w') + \frac{1}{z-w}\partial_w\phi(w,w')\,, \\ \bar{T}(\bar{z})\phi(w,w') &\sim \frac{\bar{h}}{(\bar{z}-\bar{w})^2}\phi(w,w') + \frac{1}{\bar{z}-\bar{w}}\partial_{\bar{w}}\phi(w,w')\,. \end{aligned} \tag{I.72}$$

Another operator product expansion can be found by computing the correlation function of the energy-momentum tensor with itself:

$$T(z)T(w) \sim \frac{c/2}{(z-w)^4} + \frac{2T(w)}{(z-w)^2} + \frac{\partial_w T(w)}{z-w}\,, \tag{I.73}$$

where c denotes the *central charge* of the conformal field theory.

The central charge is a characteristic quantity of a conformal field theory and appears in several relations. Often it is understood as the collective degrees of freedom of the system. This understanding can be motivated from the appearance of the central charge in the low-temperature behavior of the free energy F or specific heat C per unit length given by

$$F = F_0 - \frac{\pi}{6v_F}cT^2\,, \qquad C \equiv -T\frac{\partial^2 F}{\partial T^2} = \frac{\pi}{3v_F}cT\,,$$

where v_F denotes the Fermi velocity. Important examples are the theory of free massless bosons where the central charge is given by $c = 1$ and the theory of free massless fermions with $c = 1/2$.

Similarly, as for anyons it is possible to introduce fusion rules for the fields. In a conformal field theory fusion rules can be understood as a representation of the OPE's (I.70) given by

$$\phi_i \times \phi_j = \sum_k \phi_k\,.$$

Examples of fusion rules that are also related to non-Abelian anyons will be given for parafermions in Sec. I 4.7.

At last, we discuss the essential ingredients that are necessary to solve a conformal field theory, i.e. compute all the correlation functions that in turn are related to physical quantities. It can be shown that the operator product expansions of all primary fields with each other (also called *operator algebra*) can be derived from conformal invariance given that the central charge c, all the conformal dimensions of the primary fields and the three-point function coefficients C_{pnm} are known. The operator algebra can then be used to compute n-point functions of primary fields by successively reducing the tuples of primary fields. n-point functions of nonprimary fields can be computed as well, since they can be expressed in terms of primary field n-point functions, see Sec. I 4.5. Consequently, the essential ingredients of a conformal field theory from a computational point of view can be summarized as

- the list of primary fields $\{\phi_j\}$,
- its conformal dimensions $\{(h_j, \bar{h}_j)\}$,
- the coefficients C_{pnm} of primary three-point functions,
- the central charge.

A possible approach to derive the C_{pnm} coefficients is the *conformal bootstrap*. It is based on the reduction of four-point functions to three-point functions using the operator algebra. This results in consistency conditions of the coefficients C_{pnm} called *crossing symmetry relations*. Examples in which the crossing symmetry relations can be solved completely are the important class of *minimal models*, see for e.g. [56].

4.5. The Hilbert space

In this section basic aspects about the Hilbert space structure of a conformal field theory are discussed. Similarly as for Lie algebras the states of the Hilbert space can be constructed by applying ladder operators to a highest weight state, which is given by a primary field. In fact, the fields of a conformal field theory may be grouped in families $[\phi]$ consisting of one primary field ϕ and *descendant fields* derived by applying admissible ladder operators to ϕ.

To obtain the ladder operators one can consider the Laurent series of the energy-momentum tensor:

$$\begin{aligned} T(z) &= \sum_{n\in\mathbb{Z}} z^{-n-2} L_n \,, & L_n &= \frac{1}{2\pi \mathrm{i}} \oint \mathrm{d}z\, z^{n+1} T(z)\,, \\ \bar{T}(\bar{z}) &= \sum_{n\in\mathbb{Z}} \bar{z}^{-n-2} \bar{L}_n \,, & \bar{L}_n &= \frac{1}{2\pi \mathrm{i}} \oint \mathrm{d}\bar{z}\, \bar{z}^{n+1} \bar{T}(\bar{z})\,. \end{aligned} \tag{I.74}$$

It turns out that L_n, $\bar{L}_n$ are the generators of local conformal transformations on the Hilbert space in contrast to the generators l_n, $\bar{l}_n$ which are generators of local conformal transformations on the space of functions. The commutation relations satisfied by L_n, $\bar{L}_n$ differ from the commutation relations (I.63) of l_n, $\bar{l}_n$ by a term proportional to the central charge c:

$$\begin{aligned}
[L_n, L_m] &= (n-m)L_{n+m} + \frac{c}{12}n(n^2-1)\delta_{n+m,0}\,, \\
[\bar{L}_n, \bar{L}_m] &= (n-m)\bar{L}_{n+m} + \frac{c}{12}n(n^2-1)\delta_{n+m,0}\,, \\
[L_n, \bar{L}_m] &= 0\,.
\end{aligned} \tag{I.75}$$

The algebra defined by (I.75) is called the *Virasoro algebra*.

The operator $L_0 + \bar{L}_0$ is known to generate dilations $(z, \bar{z}) \to \lambda(z, \bar{z})$, which can be interpreted as time dilations in radial quantization. Hence, the Hamiltonian H is found to be proportional to $L_0 + \bar{L}_0$:

$$H \propto L_0 + \bar{L}_0\,.$$

Furthermore, the generators L_{-1}, L_0, L_1 and their counterparts define a subalgebra generating global conformal transformations on the Hilbert space.

To start building the Hilbert space restrictions on the vacuum state $|0\rangle$ are imposed. It is assumed that $T(z)|0\rangle$ and $\bar{T}(\bar{z})|0\rangle$ are well-defined for z, $\bar{z} \to 0$, which corresponds to the limit $t \to -\infty$ in Minkowski space and results in the conditions

$$L_n|0\rangle = \bar{L}_n|0\rangle = 0 \qquad \text{for } n \geq -1\,.$$

These conditions include the global conformal invariance of the vacuum as well as a vanishing vacuum expectation value of the energy-momentum tensor

$$\langle 0|T(z)|0\rangle = \langle 0|\bar{T}(\bar{z})|0\rangle = 0\,.$$

A state of conformal dimension $(h, \bar{h})$ is obtained by applying the asymptotic primary field $\phi(0,0)$ to the vacuum:

$$|h, \bar{h}\rangle \equiv \phi(0,0)|0\rangle\,.$$

To derive the eigenvalues of the Hamiltonian for this state the commutators of L_n, $\bar{L}_n$ with $\phi(z, \bar{z})$ obtained from the OPE (I.72) are needed

$$\begin{aligned}
[L_n, \phi(z,\bar{z})] &= h(n+1)z^n\phi(z,\bar{z}) + z^{n+1}\partial_z\phi(z,\bar{z})\,, \\
[\bar{L}_n, \phi(z,\bar{z})] &= \bar{h}(n+1)\bar{z}^n\phi(z,\bar{z}) + \bar{z}^{n+1}\partial_{\bar{z}}\phi(z,\bar{z})\,.
\end{aligned}$$

Applying these relations to the state $|h, \bar{h}\rangle$ for $n = 0$ results in

$$L_0|h,\bar{h}\rangle = h|h,\bar{h}\rangle\,, \qquad \bar{L}_0|h,\bar{h}\rangle = \bar{h}|h,\bar{h}\rangle\,,$$

which shows that $|h, \bar{h}\rangle$ is an eigenstate of the Hamiltonian. Analogously, we obtain for $n > 0$

$$L_n|h,\bar{h}\rangle = \bar{L}_n|h,\bar{h}\rangle = 0\,.$$

From the Virasoro algebra the commutators

$$[L_0, L_{-m}] = mL_{-m}\,, \quad [\bar{L}_0, \bar{L}_{-m}] = m\bar{L}_{-m}\,, \qquad m > 0$$

can be derived showing that the operators L_{-m}, $\bar{L}_{-m}$ with $m > 0$ act as ladder operators and increase the holomorphic, antiholomorphic conformal dimension by m. Hence, a general descendant state is obtained by successively applying the ladder operator to $|h, \bar{h}\rangle$,

$$|h', \bar{h}'\rangle = L_{-m_1}L_{-m_2}\ldots L_{-m_N}\bar{L}_{-\bar{m}_1}\bar{L}_{-\bar{m}_2}\ldots L_{-\bar{m}_{\bar{N}}}|h,\bar{h}\rangle\,,$$

where $m_i < m_{i+1}$, $\bar{m}_i < \bar{m}_{i+1}$ by convention and h', $\bar{h}'$ can be derived by applying L_0, $\bar{L}_0$:

$$h' = h + \sum_{i=1}^{N} m_i \,, \qquad \bar{h}' = \bar{h} + \sum_{i=1}^{\bar{N}} \bar{m}_i \,.$$

At last, let us mention that descendant states can also be derived by applying a *descendant field* to the vacuum. For example using (I.74) the descendant state $L_{-n}|h, \bar{h}\rangle$ can be written as

$$L_{-n}|h, \bar{h}\rangle = \frac{1}{2\pi \mathrm{i}} \oint \mathrm{d}z \, z^{1-n} T(z) \phi(0,0)|0\rangle \,.$$

Hence, this expression can be expressed as $(L_{-n}\phi)(0)|0\rangle$, where $(L_{-n}\phi)(w)$ is a descendant field defined by

$$(L_{-n}\phi)(w) = \frac{1}{2\pi \mathrm{i}} \oint_w \mathrm{d}z \, (z-w)^{1-n} T(z) \phi(w) \,.$$

Given the definition of descendant fields it is possible to express the correlation functions of descendant fields with a set of primary fields $X = \phi_1(w_1) \dots \phi_N(w_N)$ with conformal dimensions $h_1, h_2, \dots, h_N$ by

$$\langle L_{-n}\phi(w) X\rangle = \mathcal{L}_{-n} \langle \phi(w) X\rangle \,,$$

where $\mathcal{L}_{-n}$ is the differential operator defined by

$$\mathcal{L}_{-n} = \sum_i \left(\frac{(n-1)h_i}{(w_i - w)^n} - \frac{1}{(w_i - w)^{n-1}} \partial_{w_i} \right) \,.$$

Hence, as mentioned in the previous chapter, correlation functions of nonprimary fields can be related to correlation functions of primary fields.

4.6. WZNW models

The main results of this thesis are based on a low-temperature analysis of perturbed Wess-Zumino-Novikov-Witten (WZNW) models. In this section we discuss the main conformal field theoretical aspects of these models, which are based on its Lie algebraic symmetry. In contrast to the discussion before, WZNW models can be defined by an action and its algebraic properties are extracted from its conserved currents. An alternative definition is then found in terms of the energy-momentum tensor in Sugawara form, which in turn motivates the definition of a corresponding Hamiltonian. The spectrum of the Hamiltonian is found to be generated by elements of the conserved currents, which define an affine Lie algebra.

Given a Lie algebra $\mathfrak{g}$ the action of the *Wess-Zumino-Novikov-Witten model* is defined as

$$\begin{aligned} S^{\mathrm{WZNW}} &= \frac{k}{16\pi} \int \mathrm{d}^2 x \, \mathrm{Tr}'(\partial^\mu g^{-1} \partial_\mu g) + k\Gamma \,, \\ \Gamma &\equiv \frac{-\mathrm{i}}{24\pi} \int_B \mathrm{d}^3 y \, \epsilon_{\alpha\beta\gamma} \mathrm{Tr}'(\tilde{g}^{-1} \partial^\alpha \tilde{g} \tilde{g}^{-1} \partial^\beta \tilde{g} \tilde{g}^{-1} \partial^\gamma \tilde{g}) \,, \end{aligned} \tag{I.76}$$

where $g = g(z, \bar{z})$ is a field with values in the Lie group G corresponding to the Lie algebra $\mathfrak{g}$. The global symmetry of S^{WZNW} model is given by $G \times G$, while a unitary representation of G is chosen to obtain a real action. Due to the fact that the normal trace Tr for matrix representations of $\mathfrak{g}$'s generators t^a depends on a representation dependant constant x_{rep} called *Dynkin index*

$$\mathrm{Tr}(t^a t^b) = 2 x_{\mathrm{rep}} \delta_{ab} \,,$$

the trace Tr′ of the WZNW action (I.76) is defined independently of a particular representation by

$$\mathrm{Tr}' = \frac{1}{x_{\mathrm{rep}}}\mathrm{Tr} \quad \Rightarrow \quad \mathrm{Tr}'(t^a t^b) = 2\delta_{ab}\,.$$

The second term Γ of the WZNW action is also called *Wess-Zumino* term. Its integration goes over a three-dimensional manifold B, where $\tilde{g}$ denotes the extension of g to this manifold. Due to an ambiguity of this extension it is found that the coupling constant k, called *level*, can only be an integer.

By minimizing the variation of the WZNW action the equations of motion are found to be

$$\partial_z(g^{-1}\partial_{\bar{z}}g) = 0 \quad \Leftrightarrow \quad \partial_{\bar{z}}(\partial_z g g^{-1}) = 0\,.$$

This motivates the definition of two independent conserved currents

$$\begin{aligned} J_z &= \partial_z g g^{-1} \quad &\Rightarrow \quad \partial_{\bar{z}} J_z = 0\,, \\ J_{\bar{z}} &= g^{-1}\partial_{\bar{z}} g \quad &\Rightarrow \quad \partial_z J_{\bar{z}} = 0\,. \end{aligned} \tag{I.77}$$

It turns out that the energy-momentum tensor of the WZNW model can be written in terms of its conserved currents. For this we define rescaled currents by

$$\begin{aligned} J(z) &\equiv -\frac{k}{\sqrt{2}} J_z(z) = -\frac{k}{\sqrt{2}}\partial_z g g^{-1}\,, \\ \bar{J}(\bar{z}) &\equiv \frac{k}{\sqrt{2}} J_{\bar{z}}(\bar{z}) = \frac{k}{\sqrt{2}} g^{-1}\partial_{\bar{z}} g\,. \end{aligned}$$

Expanding the currents $J(z)$, $\bar{J}(\bar{z})$ in terms of the basis $\{t^a\}$ of $\mathfrak{g}$ its components $J^a(z)$, $\bar{J}^a(\bar{z})$ are obtained

$$J(z) = \sum_a J^a(z) t^a\,, \quad \bar{J}(\bar{z}) = \sum_a \bar{J}^a(\bar{z}) t^a\,,$$

which in turn can be expanded using the Laurent expansion

$$J^a(z) = \sum_{n\in\mathbb{Z}} z^{-n-1} J^a_n\,, \quad \bar{J}^a(\bar{z}) = \sum_{n\in\mathbb{Z}} \bar{z}^{-n-1} \bar{J}^a_n\,.$$

It can be shown that the modes J^a_n, $\bar{J}^a_n$ satisfy the commutation relations of a *Kac-Moody* algebra of level k:

$$\begin{aligned} [J^a_n, J^b_m] &= \sum_c \mathrm{i} f_{abc} J^c_{n+m} + \frac{kn}{2}\delta_{ab}\delta_{n+m,0}\,, \\ [\bar{J}^a_n, \bar{J}^b_m] &= \sum_c \mathrm{i} f_{abc} \bar{J}^c_{n+m} + \frac{kn}{2}\delta_{ab}\delta_{n+m,0}\,, \\ [J^a_n, \bar{J}^b_m] &= 0\,. \end{aligned}$$

Notice that these are also the commutation relations defining an affine Lie algebra of level k giving the currents an equivalent interpretation in terms of generators of an affine Lie algebra.

Moreover, the energy-momentum tensor can be written in terms of the currents, called the *Sugawara form*,

$$T(z) = \frac{1}{k+g}\sum_a :J^a J^a:\,, \quad \bar{T}(\bar{z}) = \frac{1}{k+g}\sum_a :\bar{J}^a \bar{J}^a:\,,$$

where the dots : indicate a normal ordering. From the operator product expansion of the energy-momentum tensor with itself the central charge of the WZNW model can be determined according to (I.73)

$$c = \frac{k \dim \mathfrak{g}}{k+g}\,, \tag{I.78}$$

where g is the dual Coexter number (I.34) and $\dim \mathfrak{g}$ denotes the number of generators of $\mathfrak{g}$.

In order to derive the structure of the Hilbert space the energy-momentum tensor with components $T(z)$, $\bar{T}(\bar{z})$ is expressed in terms of its modes according to (I.74) which results in an expression for the modes L_n

$$L_n = \frac{1}{k+g}\sum_a \left(\sum_{m\le -1} J^a_m J^a_{n-m} + \sum_{m\ge 0} J^a_{n-m} J^a_m \right)$$

and an analogous expression for $\bar{L}_n$. The modes L_n, $\bar{L}_n$ satisfy the usual Virasoro algebra (I.75), while the commutator with elements of the Kac-Moody algebra are given by

$$[L_n, J^a_m] = -mJ^a_{n+m}, \quad [\bar{L}_n, \bar{J}^a_m] = -m\bar{J}^a_{n+m}\,.$$

The Hamiltonian of the WZNW model $H[\mathfrak{g}_k]$, which is proportional to $L_0 + \bar{L}_0$, can be written in terms of the generators of the Kac-Moody algebra as

$$\begin{aligned} H[\mathfrak{g}_k] &= 2\pi(L_0 + \bar{L}_0) \\ &= \frac{2\pi}{k+g}\sum_a \left(J^a_0 J^a_0 + 2\sum_{m\ge 1} J^a_{-m} J^a_m + J \leftrightarrow \bar{J} \right)\,. \end{aligned}$$

Equivalently, the Hamiltonian density in terms of the currents $J^a(z)$, $\bar{J}^a(\bar{z})$ is expressed as

$$\mathcal{H}[\mathfrak{g}_k] = \frac{2\pi}{k+g}\sum_a (: J^a J^a : + : \bar{J}^a \bar{J}^a :)\,.$$

This shows that instead of using the elements of the Virasoro algebra one can use the Kac-Moody algebra as the *spectrum-generating algebra* showing the importance of affine Lie algebras for WZNW models. In fact, from now on we will refer to WZNW models with level k and Lie algebra $\mathfrak{g}$ as the $\mathfrak{g}_k$ WZNW model.

Let us denote by $g^{\Lambda,\bar{\Lambda}}$ a WZNW primary field transforming in the holomorphic sector with representation Λ and in the antiholomorphic sector with representation $\bar{\Lambda}$, where Λ, $\bar{\Lambda}$ denote the highest weight of the corresponding representation. For simplicity the label of the antiholomorphic sector is neglected and the focus is placed on the holomorphic sector. The WZNW primary field g^Λ can be defined as a field satisfying

$$\begin{aligned} J^a_0 g^\Lambda &= -t^{a,\Lambda} g^\Lambda\,, \\ J^a_n g^\Lambda &= 0 \quad \text{for } n > 0\,, \end{aligned} \tag{I.79}$$

where $t^{a,\Lambda}$ denotes the generator t^a in the Λ representation. A state $|g^\Lambda\rangle$ corresponding to the field g^Λ is defined by

$$|g^\Lambda\rangle \equiv g^\Lambda(0,0)|0\rangle\,,$$

which gives an equivalent definition of primary fields in terms of states:

$$\begin{aligned} J_0^a |g^\Lambda\rangle &= -t^{a,\Lambda}|g^\Lambda\rangle \\ J_n^a |g^\Lambda\rangle &= 0 \quad \text{for } n > 0 \end{aligned}$$

Interestingly, WZNW primary fields according to this definition are also Virasoro primary fields satisfying

$$\begin{aligned} L_0 |g^\Lambda\rangle &= h^\Lambda |g^\Lambda\rangle \,, \\ L_n |g^\Lambda\rangle &= 0 \quad \text{for } n > 0 \end{aligned}$$

with the holomorphic conformal dimension

$$h^\Lambda = \frac{(\Lambda, \Lambda + 2\rho)}{2(k+g)} \,,$$

where ρ denotes the Weyl vector (I.41). WZNW descendant fields are constructed analogously to Virasoro descendant fields using the Kac-Moody generators J_{-n}^a as ladder operators.

4.7. Parafermions

In this section some properties of the generalized parafermion conformal field theories introduced by Gepner [54] are discussed. Given a Lie algebra $\mathfrak{g}$ and a level k one can define a $Z_{\mathfrak{g}_k}$ parafermion theory from the $\mathfrak{g}_k$ WZNW model. The reason for this is the observation that the energy-momentum tensor of the WZNW model $T^{(\mathrm{WZNW})}$ can be split into two parts

$$T^{(\mathrm{WZNW})} = T^{(\mathrm{b})} + T^{(\mathrm{p})} \,,$$

where $T^{(\mathrm{b})}$ denotes the energy-momentum tensor of a bosonic system and $T^{(\mathrm{p})}$ is referred to as the parafermionic system. Gepner studied the properties of the parafermionic part for general Lie algebras $\mathfrak{g}$ and related the WZNW primary fields discussed in the last section to parafermionic primary fields.

Equivalently, the parafermionic theory can be defined using a *coset* construction. The coset can be understood as a quotient of two conformal field theories with central charges c_1, c_2, whose resulting central charge is given by their difference $c_1 - c_2$. Hence, the parafermionic theory can be defined by dividing out the bosonic degrees of freedom of the WZNW model. More precisely, given a Lie algebra $\mathfrak{g}$ with rank r a parafermionic theory may be defined as

$$Z_{\mathfrak{g}_k} = \frac{\mathfrak{g}_k}{\mathfrak{u}(1)^r} \,,$$

where $\mathfrak{u}(1)^r$ denotes the product of r bosonic theories each contributing a central charge $c = 1$. Consequently, using (I.78) the central charge of the parafermionic theory $Z_{\mathfrak{g}_k}$ becomes

$$c = \frac{k \dim \mathfrak{g}}{k+g} - r \,. \tag{I.80}$$

To relate the primary fields of the parafermionic theory to the primary fields of the WZNW model, Gepner introduced a vector ϕ consisting of r bosons $\phi = (\phi_1, \phi_2, \dots, \phi_r)$, where each boson can be split into a holomorphic and antiholomorphic part $\phi_i = \phi_i(z) + \phi_i(\bar{z})$. Let us denote by $g^{\Lambda,\bar{\Lambda}}_{\lambda,\bar{\lambda}}$ a general WZNW primary field with weights λ, $\bar{\lambda}$ according to (I.79).

A corresponding parafermionic primary field $\phi^{\Lambda,\bar{\Lambda}}_{\lambda,\bar{\lambda}}$ was found to be related to the WZNW primary field by

$$g^{\Lambda,\bar{\Lambda}}_{\lambda,\bar{\lambda}} =: e^{((\lambda,\phi)+(\bar{\lambda},\bar{\phi}))/\sqrt{k}} : \phi^{\Lambda,\bar{\Lambda}}_{\lambda,\bar{\lambda}} \,.$$

This relation enabled the computation of all the parafermion correlation functions, fusion rules and conformal dimensions from the WZNW theory. The holomorphic conformal dimension of the parafermion primary field results in

$$h^{\Lambda}_{\lambda} = \frac{\Lambda(\Lambda+2\rho)}{2(k+g)} - \frac{\lambda^2}{2k} + n^{\Lambda}_{\lambda} \,,$$

where n^{Λ}_{λ} is an integer that vanishes for weights λ of the representation Λ.

To give an example of a parafermion conformal field theory the $\mathfrak{g} = \mathfrak{su}(2)$ case following [84] is discussed. From Sec. I 2.6 we know that the weights of a representation with Dynkin label l are given by

$$\lambda_{l,m} = m\omega_1 \quad \text{with } m = -l, -l+2, \ldots, l \,,$$

where $\Lambda_l \equiv \lambda_{l,l}$ denotes the highest weight. Hence, the holomorphic conformal dimensions of the primary fields $\phi^l_m \equiv \phi^{\Lambda_l}_{\lambda_{l,m}}$ (the antiholomorphic label is neglected for simplicity) are given by

$$h_{l,m} = \frac{l(l+2)}{4(k+2)} - \frac{m^2}{4k} \,,$$

since $\rho = \omega_1$ and $g = a^\vee_1 + 1 = 2$. As mentioned before the spectrum generating algebra for WZNW models is given by an affine Lie algebra with level k. From the representation theory of the affine Lie algebra $\mathfrak{su}(2)_k$ the maximal value of the Dynkin label l is found to be bounded by the level k, i.e. its allowed values are $l = 0, 1, \ldots, k$. Following [54, 84] the sectors $\phi^l_m \equiv \phi^{k-l}_{m+k}$ are identified such that the parafermion fields and their conformal dimensions for $i = 0, 1, \ldots, k-1$ become

$$\begin{aligned}
\psi_i &= \phi^0_{2i} \equiv \phi^k_{2i-k} \,, & h_{\psi_i} &= \frac{i(k-i)}{k} \\
\sigma_i &= \phi^i_i \,, & h_{\sigma_i} &= \frac{i(k-i)}{2k(k+2)} \\
\epsilon_{l/2} &= \phi^l_0 \,, & h_{\epsilon_{l/2}} &= \frac{l(l+2)}{2(k+2)} \quad \text{(for even } l\text{)} \,.
\end{aligned}$$

The fusion rules obtained from the WZNW theory are given by

$$\phi^l_m \times \phi^{l'}_{m'} = \bigoplus_{b=|l-l'|/2}^{\min(l+l',2k-l-l')/2} \phi^{2b}_{m+m'} \,.$$

For $k = 3$ the resulting parafermion fields and their conformal dimension become

$$\begin{aligned}
\psi_1 &= \phi^0_2 \,,\ \psi_2 = \phi^0_4 \,, & h_{\psi_i} &= \frac{2}{3} \\
\sigma_1 &= \phi^1_1 \,,\ \sigma_2 = \phi^2_2 & h_{\sigma_i} &= \frac{1}{15} \\
\epsilon &= \phi^2_0 \,, & h_\epsilon &= \frac{2}{5} \,,
\end{aligned}$$

$\times$	ψ_1	ψ_2	σ_1	σ_2	ϵ
ψ_1	ψ_2	$\mathbf{1}$	ϵ	σ_1	σ_2
ψ_2	$\mathbf{1}$	ψ_1	σ_2	ϵ	σ_1
σ_1	ϵ	σ_2	$\psi_1 + \sigma_2$	$\mathbf{1} + \epsilon$	$\psi_2 + \sigma_1$
σ_2	σ_1	ϵ	$\mathbf{1} + \epsilon$	$\psi_2 + \sigma_1$	$\psi_1 + \sigma_2$
ϵ	σ_2	σ_1	$\psi_2 + \sigma_1$	$\psi_1 + \sigma_2$	$\mathbf{1} + \epsilon$

Table 1: Fusion rules of the parafermion fields from the parafermion theory $Z_{\mathfrak{su}(2)_3}$.

which satisfy the fusion rules of Table 1.

At last, the central charge of the $Z_{\mathfrak{su}(N)_k}$ parafermion theory is given for future reference. It follows from (I.80) using dim $\mathfrak{su}(N) = N^2 - 1$, $l = N - 1$ and $g = N$:

$$c = \frac{N(N-1)(k-1)}{k+N} \,. \tag{I.81}$$

For the example discussed before this implies $c = 4/5$ with $N = 2$, $k = 3$. More details about the $Z_{\mathfrak{su}(2)_3}$ parafermion CFT as well as the $Z_{\mathfrak{su}(3)_2}$ parafermion CFT can be found in [84, 85].

5. Bosonization

In physics it is often the case that the problem at hand simplifies drastically if written in the right coordinates. The same is true for fermionic systems in one dimension: it was found that particle-hole excitations near the Fermi point essentially behave as bosons. This motivated the development of a method called *bosonization*, which enables the description of one-dimensional fermionic systems at low temperatures in terms of simpler bosonic theories.

There are two types of bosonization: *Abelian* and *non-Abelian* bosonization. Abelian bosonization is often applied to fermionic theories with a $U(1)$ symmetry. For fermionic theories with non-Abelian symmetry it is more convenient to use non-Abelian bosonization as it returns a theory for bosonic fields that have simple transformation rules under the non-Abelian transformations.

To discuss bosonization we start with a non-interacting fermionic model and derive its low-energy description close to the Fermi point in Sec. I 5.1. For the Abelian bosonization case we focus on one fermion species and discuss its low-energy description in terms of current operators, which turns out to be equivalent to a bosonic theory, see Sec. I 5.2. In Sec. I 5.3 a fermionic model with non-Abelian symmetry and more than one fermion species is found to be equivalent to a bosonic theory given by a WZNW model.

5.1. Effective field theory

Let us denote by $c_k^\dagger$ and c_k the fermionic creation and annihilation operator for a fermion with wavevector k, where indices for spin and orbital degrees of freedom are neglected for the moment. The operators satisfy the following commutation relations:

$$\{c_k^\dagger, c_{k'}\} = \delta_{k,k'}\,, \quad \{c_k^\dagger, c_{k'}^\dagger\} = \{c_k, c_k^\dagger\} = 0\,,$$

where $\{A, B\} = AB + BA$ denotes the anticommutator. Given a dispersion relation ϵ_k the lattice Hamiltonian may be written as

$$H = \sum_k \epsilon_k c_k^\dagger c_k\,. \tag{I.82}$$

Figure 6 shows a typical dispersion relation in one dimension, where E_F denotes the Fermi energy and k_F the Fermi point. To obtain an effective low-energy description of (I.82) only particle hole excitations near the Fermi points are considered. The dispersion relation linearized at the Fermi points becomes

$$\begin{aligned} \epsilon_{k+k_F} &\approx \epsilon_{k_F} + v_F k + \dots \\ \epsilon_{k-k_F} &\approx \epsilon_{-k_F} - v_F k + \dots\,, \end{aligned} \tag{I.83}$$

where $v_F \equiv \mathrm{d}\epsilon_k/\mathrm{d}k|_{k=k_F}$ denotes the Fermi velocity and $\epsilon_{k_F} = \epsilon_{-k_F} = 0$. Furthermore, creation and annihilation operators are split into operators creating and annihilating left- and right-moving fermions as

$$\begin{aligned} c_k^L &= c_{-k_F+k}\,, & c_k^{L\dagger} &= c_{-k_F+k}^\dagger \\ c_k^R &= c_{k_F+k}\,, & c_k^{R\dagger} &= c_{k_F+k}^\dagger\,. \end{aligned} \tag{I.84}$$

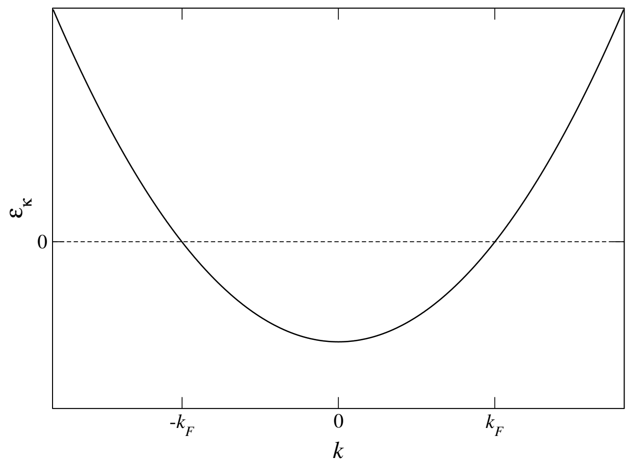

Figure 6: Form of the dispersion relation ϵ_k. The dashed line shows the Fermi energy E_F, while $-k_F$, k_F are the Fermi points.

Given (I.83), (I.84) the Hamiltonian for the low-energy behavior becomes

$$H = \sum_{k=-\Lambda}^{\Lambda} v_F k (c_k^{R\dagger} c_k^R - c_k^{L\dagger} c_k^L) \,, \tag{I.85}$$

where Λ denotes the wavevector cutoff parameter. In the continuum limit (I.85) results in

$$H = \int_{-\Lambda}^{\Lambda} \frac{\mathrm{d}k}{2\pi} v_F k (c_k^{R\dagger} c_k^R - c_k^{L\dagger} c_k^L) \,. \tag{I.86}$$

An equivalent expression for the low-energy effective Hamiltonian (I.86) can be obtained in terms of left- and right-moving fermionic fields. For this the fermionic field defined by

$$\psi(x) = \int_{\infty}^{\infty} \frac{\mathrm{d}k}{2\pi} e^{\mathrm{i}xk} c_k$$

is split into left- and right-moving fields as

$$\begin{gathered} \psi(x) = e^{ik_F x} R(x) + e^{-\mathrm{i}k_F x} L(x) \,, \\ R(x) = \int_{-\Lambda}^{\Lambda} \frac{\mathrm{d}k}{2\pi} e^{\mathrm{i}xk} c_k^R \,, \qquad L(x) = \int_{-\Lambda}^{\Lambda} \frac{\mathrm{d}k}{2\pi} e^{\mathrm{i}xk} c_k^L \,, \end{gathered} \tag{I.87}$$

which results in the Hamiltonian

$$H = -\mathrm{i} v_F \int \mathrm{d}x (R^\dagger(x) \partial_x R(x) - L^\dagger(x) \partial_x L(x)) \,.$$

Notice that this coincides with the massless Dirac equation for the Dirac spinor

$$\Psi = (L(x), R(x)) \,.$$

The more general case of fermions with spin ($\alpha = 1, \ldots, N_s$) and orbital ($j = 1, \ldots, N_f$) degrees of freedom is found analogously and results in

$$H = -\mathrm{i} v_F \sum_{j=1}^{N_f} \sum_{\alpha=1}^{N_s} \int \mathrm{d}x (R_{j\alpha}^\dagger(x) \partial_x R_{j\alpha}(x) - L_{j\alpha}^\dagger(x) \partial_x L_{j\alpha}(x)) \,, \tag{I.88}$$

where the left- and right-moving fields satisfy the usual fermionic commutation relations

$$\{L^\dagger_{j\alpha}(x), L_{j'\alpha'}(x')\} = \delta_{jj'}\delta_{\alpha\alpha'}\delta(x-x')\,,$$
$$\{R^\dagger_{j\alpha}(x), R_{j'\alpha'}(x')\} = \delta_{jj'}\delta_{\alpha\alpha'}\delta(x-x')\,,$$
$$\{L_{j\alpha}(x), R^{(\dagger)}_{j'\alpha'}(x')\} = 0\,.$$

The non-interacting Hamiltonian (I.88) will serve as a starting point for the discussion of Abelian and non-Abelian bosonization in the subsequent sections, while bosonization of interaction terms is discussed in Part II.

5.2. Abelian bosonization

Following [57] we focus on (I.88) with $N_s = 1$, $N_f = 1$ to discuss Abelian bosonization for free massless fermions with one species. In this case the Hamiltonian density is given by

$$\mathcal{H} = -\mathrm{i}v_F(R^\dagger\partial_x R - L^\dagger\partial_x L)$$

and the equations of motion result in

$$(\partial_0 + v_F\partial_x)L(x) = 0 \qquad (\partial_0 - v_F\partial_x)R(x) = 0\,.$$

To obtain an equivalent bosonic theory the Hamiltonian is rewritten in terms of the following current operators

$$J(x) =: L^\dagger(x)L(x):\,, \qquad \bar{J}(x) =: R^\dagger(x)R(x):\,,$$

which are conserved due to the equations of motion, i.e. $\partial_+ J = \partial_- \bar{J} = 0$ with $x_\pm = x_0 \pm v_F x_1$. The currents obey the commutation relations

$$[J(x), J(y)] = \frac{\mathrm{i}}{2\pi}\delta'(x-y)\,, \qquad [\bar{J}(x), \bar{J}(y)] = \frac{\mathrm{i}}{2\pi}\delta'(x-y)\,,$$

where $\delta'(x)$ denotes the derivative of the delta function.

It turns out that the Hamiltonian density in terms of the current operators results in

$$\mathcal{H} = \pi v_F(:JJ: + :\bar{J}\bar{J}:)\,. \tag{I.89}$$

In [57] it was shown that a free massless bosonic theory with Hamiltonian density

$$\mathcal{H} = \frac{v_F}{2}(\Pi^2 - (\partial_x\phi)^2)\,, \quad \Pi = \partial_t\phi \tag{I.90}$$

is equivalent to (I.89). This is due to the fact that the Hamiltonian density can be written as (I.89) using the currents

$$J = \frac{1}{\sqrt{4\pi}}\partial_-\phi\,, \qquad \bar{J} = -\frac{1}{\sqrt{4\pi}}\partial_+\phi\,,$$

which are conserved as well and satisfy the same commutation relations.

5.3. Non-Abelian bosonization

For non-Abelian bosonization a free fermion theory with arbitrary N_f and $N_s = 1$ is discussed at first. Its Hamiltonian density is given by

$$\mathcal{H} = -\mathrm{i}v_F \sum_{j=1}^{N_f} (R_j^\dagger \partial_x R_j - L_j^\dagger \partial_x L_j) \,. \tag{I.91}$$

To generalize the Abelian bosonization rules one could introduce one boson for each fermion type. However, the resulting bosonized form would have non-trivial transformation properties under the $SU(N_f)$ transformations. To reflect the $SU(N_f)$ symmetry of (I.91) in the bosonized form it is useful to introduce the following currents

$$\begin{aligned} J &= L_i^\dagger L_i \,, & \bar{J} &= R_i^\dagger R_i \,, \\ J^A &= L_i^\dagger (t^A)_{ij} L_j \,, & \bar{J}^A &= R_i^\dagger (t^A)_{ij} R_j \,, \end{aligned}$$

where t^A are the generators of the $\mathfrak{su}(N_f)$ Lie algebra normalized so that

$$\mathrm{tr}\, T^A T^B = \frac{1}{2}\delta^{ab}$$

holds. The currents can be shown to obey the commutation relations

$$\begin{aligned} [J(x), J(y)] &= \frac{\mathrm{k}}{2\pi}\delta'(x-y) \,, \\ [J^A(x), J^B(y)] &= \mathrm{i} f^{ABC} J^C(x)\delta(x-y) + \frac{\mathrm{i}}{4\pi}\delta^{AB}\delta'(x-y) \,. \end{aligned}$$

where f^{ABC} are the structure constants of $\mathfrak{su}(N_f)$ and similar relations hold for the right-moving currents. Hence, the currents J^A, $\bar{J}^A$ satisfy the Kac-Moody algebra of level one, that we encountered in Sec. I 4.6 for the components of currents of WZNW models. In fact, by writing the Hamiltonian density (I.91) in terms of the currents it decouples into a free massless bosonic theory (I.90) and a $\mathfrak{su}(N_f)_1$ WZNW model:

$$\begin{aligned} \mathcal{H} &= \mathcal{H}[\mathfrak{u}(1)] + \mathcal{H}[\mathfrak{su}(N_f)_1] \,, \\ \mathcal{H}[\mathfrak{u}(1)] &= \frac{\pi v_F}{k}(:JJ: + :\bar{J}\bar{J}:) \,, \\ \mathcal{H}[\mathfrak{su}(N_f)_1] &= \frac{2\pi v_F}{k+1}(:J^A J^A: + :\bar{J}^A \bar{J}^A:) \,. \end{aligned}$$

As before the $\mathfrak{u}(1)$ currents can be represented in terms of a massless free scalar described by (I.90)

$$J = \sqrt{\frac{k}{4\pi}}\partial_-\phi \,, \quad \bar{J} = -\sqrt{\frac{k}{4\pi}}\partial_+\phi \,.$$

The $SU(N_f)$ currents on the other hand are described in terms of a WZNW field g

$$J^A = -\frac{\mathrm{i}}{2\pi}\mathrm{tr}\,(\partial_- g) g^\dagger T^A \,, \qquad \bar{J}^A = \frac{\mathrm{i}}{2\pi}\mathrm{tr}\, g^\dagger \partial_+ g T^A \,,$$

where the matrix-valued field g is determined by the action of the WZNW model (I.76). Hence, for non-Abelian bosonization the WZNW field plays the role of a bosonic $SU(N_f)$

matrix.

At last, let us discuss non-Abelian bosonization of free fermions with arbitrary spin and orbital degrees of freedom. According to (I.88) their Hamiltonian density is given by

$$\mathcal{H} = -\mathrm{i}v_F \sum_{j=1}^{N_f} \sum_{\alpha=1}^{N_s} (R_{j\alpha}^\dagger \partial_x R_{j\alpha} - L_{j\alpha}^\dagger \partial_x L_{j\alpha}) \tag{I.92}$$

and the corresponding $U(1)$, $SU(N_f)$ and $SU(N_s)$ currents are defined by

$$\begin{aligned} J &= L_{i\alpha}^\dagger L_{i\alpha}\,, & \bar{J} &= R_{i\alpha}^\dagger R_{i\alpha}\,, \\ J^A &= L_{i\alpha}^\dagger (t^A)_{ij} L_{j\alpha}\,, & \bar{J}^A &= R_{i\alpha}^\dagger (t^A)_{ij} R_{j\alpha}\,, \\ J^a &= L_{i\alpha}^\dagger (t^a)_{ij} L_{j\alpha}\,, & \bar{J}^a &= R_{i\alpha}^\dagger (t^a)_{ij} R_{j\alpha}\,, \end{aligned} \tag{I.93}$$

where t^a are the generators of $\mathfrak{su}(N_s)$. The commutation relations of the left-moving currents result in

$$\begin{aligned} [J(x), J(y)] &= \frac{N_f N_s}{2\pi} \delta'(x-y)\,, \\ [J^A(x), J^B(y)] &= \mathrm{i} f^{ABC} J^C(x) \delta(x-y) + \frac{\mathrm{i}N_s}{4\pi} \delta^{AB} \delta'(x-y)\,, \\ [J^a(x), J^b(y)] &= \mathrm{i} f^{abc} J^c(x) \delta(x-y) + \frac{\mathrm{i}N_f}{4\pi} \delta^{ab} \delta'(x-y)\,, \end{aligned}$$

where similar relations hold for the right-moving currents. As before the $SU(N_f)$ currents satisfy the commutation relations of a Kac-Moody algebra, but this time with arbitrary level N_s. Similarly, the $SU(N_s)$ currents satisfy the Kac-Moody algebra with level N_f. By writing the Hamiltonian density (I.92) in terms of the currents it is found that the Hamiltonian density splits into a free massless bosonic theory (I.90), a $\mathfrak{su}(N_f)_{N_s}$ WZNW model and a $\mathfrak{su}(N_s)_{N_f}$ WZNW model:

$$\begin{aligned} \mathcal{H} &= \mathcal{H}[\mathfrak{u}(1)] + \mathcal{H}[\mathfrak{su}(N_f)_{N_s}] + \mathcal{H}[\mathfrak{su}(N_s)_{N_f}]\,, \\ \mathcal{H}[\mathfrak{u}(1)] &= \frac{\pi v_F}{N_f N_s} (: JJ : + : \bar{J}\bar{J} :)\,, \\ \mathcal{H}[\mathfrak{su}(N_f)_{N_s}] &= \frac{2\pi v_F}{N_f + N_s} (: J^A J^A : + : \bar{J}^A \bar{J}^A :)\,, \\ \mathcal{H}[\mathfrak{su}(N_s)_{N_f}] &= \frac{2\pi v_F}{N_f + N_s} (: J^a J^a : + : \bar{J}^a \bar{J}^a :) \end{aligned} \tag{I.94}$$

Hence, using non-Abelian bosonization the relationship between free massless fermions with spin and orbital degrees of freedom and WZNW models has been shown. Former were defined in Sec. I 4.6 as abstract conformal field theories with Lie algebraic symmetry, while non-Abelian bosonization unveils their application to fermionic models. In the next chapter the WZNW models as well as perturbations of them are discussed as integrable models. This enables the computation of thermodynamic quantities of perturbed WZNW models and simultaneously leads to signatures of non-Abelian anyons.

Part II

Perturbed WZNW models

1. Perturbed $\mathfrak{su}(2)_{N_f}$ WZNW model

In this section Tsvelik's study of the integrable $\mathfrak{su}(2)_{N_f}$ WZNW model with anisotropic current-current interaction [39] is further extended based on our publication [52]. For sufficiently small temperatures and fields Tsvelik identified spin-1/2 $\mathfrak{su}(2)_{N_f}$ anyons bound to massive solitonic *kink* excitations by their quantum dimension [39]. Here also the contribution of breather excitations is studied, that are bound states of kinks and antikinks and carry two spin-1/2 $\mathfrak{su}(2)_{N_f}$ anyons. Additionally, the entropy with respect to the magnetic field is computed analytically and numerically to investigate the transition from a dilute gas of kinks to a phase with a finite density of them in more detail.

To obtain a better understanding of the emergence of perturbed WZNW models in general non-Abelian bosonization is applied to a model of interacting fermions with spin and orbital degrees of freedom in Sec. II 1.1. The resulting sectors are integrable perturbed WZNW models that can be solved exactly by applying small modifications to the QISM discussed for lattice models in Sec. I 1.1. In Sec. II 1.1 the eigenvalues of the perturbed $\mathfrak{su}(2)_{N_f}$ WZNW model depending on the Bethe roots are discussed, which lead to a set of integral equations describing the thermodynamics for large system sizes, see Sec. II 1.3. After a detailed study of the low-temperature thermodynamics of the perturbed $\mathfrak{su}(2)_{N_f}$ WZNW model the contributions of the anyonic modes are summarized in a phase diagram in Sec. II 1.4.

1.1. Integrable relativistic fermions

Following [86, 87] the emergence of relativistic fermions in a model of one-dimensional fermions with spin and orbital degrees of freedom is discussed. These additional degrees of freedom can for example be realized using an ultracold gas of fermionic atoms trapped in a periodic potential [88, 89]. Interactions of the model involve the Hund's coupling, which supports the formation of higher spin states while the hopping terms hinders this.

An exactly solvable model taking these processes into account is given by

$$H = \int \mathrm{d}x \left(\frac{1}{2m} \sum_{f,\alpha} \psi^\dagger_{f\alpha} \left(-\frac{\mathrm{d}^2}{\mathrm{d}x^2} - k_F^2 \right) \psi_{f\alpha} + \frac{g}{2} \sum_{f,g,\alpha,\beta} \psi^\dagger_{f\alpha}\psi_{f\beta}\psi^\dagger_{g\beta}\psi_{g\alpha} \right) , \tag{II.1}$$

where k_F denotes the Fermi point, m is the mass and $\psi_{f\alpha}$ are fermionic fields with orbital degrees of freedom $f = 1, \dots, N_f$ and spin degrees of freedom $\alpha = 1, \dots, N_s$. Notice that the symmetry group of the Hamiltonian (II.1) is $SU(N_f) \times SU(N_s)$.

Using the decomposition into left- and right-moving fields (I.87) the behavior of (II.1) near the Fermi points can be obtained. The Hamiltonian density of the free part written in Einstein's summation convention results in

$$\mathcal{H}_{\text{free}} = -\mathrm{i}v_F \left(R^\dagger_{f\alpha}\partial_x R_{f\alpha} - L^\dagger_{f\alpha}\partial_x L_{f\alpha} \right) ,$$

where $v_F = k_F/m$ and terms that are oscillatory (proportional to $e^{\pm \mathrm{i}k_F x}$) as well as second derivatives of the slow fields R, L are neglected. Written in terms of the corresponding currents (I.93) the free part results in a sum of one Gaussian model and two WZNW models (I.94)

$$\mathcal{H}_{\text{free}} = \mathcal{H}[\mathfrak{u}(1)] + \mathcal{H}[\mathfrak{su}(N_f)_{N_s}] + \mathcal{H}[\mathfrak{su}(N_s)_{N_f}] \,.$$

The interacting part of (II.1) can also be rewritten using the currents. For this we first write it in terms of left- and right-moving fields

$$\begin{aligned}\mathcal{H}_{\text{int}} &= \frac{g}{2}\sum_{f,g,\alpha,\beta}\psi^\dagger_{f\alpha}\psi_{f\beta}\psi^\dagger_{g\beta}\psi_{g\alpha}\\ &= \frac{g}{2}\sum_{f,g,\alpha,\beta}\left(L^\dagger_{f\alpha}L_{f\beta}L^\dagger_{g\beta}L_{g\alpha} + L^\dagger_{f\alpha}L_{f\beta}R^\dagger_{g\beta}R_{g\alpha} + L^\dagger_{f\alpha}R_{f\beta}R^\dagger_{g\beta}L_{g\alpha} + L\leftrightarrow R\right)\,,\end{aligned}\tag{II.2}$$

where oscillatory terms are neglected. Notice that in the case of half-filling $4k_F = 2\pi/a$ (a denotes the lattice spacing) such that $e^{\pm \mathrm{i}4k_F x} = 1$, since x is an integer times the lattice spacing. In this case there are additional terms appearing in (II.2), which may result in a gap of the charge sector, see Sec. II 1.2.

The first term of (II.2) as well as the corresponding term with right-moving fields will be neglected below since they only renormalize the Fermi velocities of the WZNW models. The remaining terms can be further rewritten using the identities

$$\begin{aligned}L^\dagger_{f\alpha}L_{f\beta}R^\dagger_{g\beta}R_{g\alpha} &= \frac{1}{2}J\bar{J} + 2J^a\bar{J}^a\,,\\ L^\dagger_{f\alpha}R_{f\beta}R^\dagger_{g\beta}L_{g\alpha} &= -\frac{1}{2}J\bar{J} - 2J^A\bar{J}^A\,,\end{aligned}$$

which are derived from the definitions of the currents (I.93). Analogous identities are obtained for $L\leftrightarrow R$. Consequently, the Hamiltonian density of the interacting part results in

$$\mathcal{H}_{\text{int}} = -2gJ^A\bar{J}^A + 2gJ^a\bar{J}^a \tag{II.3}$$

showing that the low-energy behavior of (II.1) near the Fermi points is described by three independent sectors. This observation coincides with Tsvelik's exact solution of (II.1) in the relativistic limit, i.e. $0 < g \ll 1$ and $T \ll g^{1/2}\epsilon_F$ [86].

Below each sector is discussed in more detail. The *charge sector* describes the part of the Hamiltonian density given solely by $\mathcal{H}[\mathfrak{u}(1)]$:

$$\mathcal{H}_c = \frac{\pi v_c}{N_s N_f}(:JJ: + :\bar{J}\bar{J}:)\,,$$

where v_c is the renormalized Fermi velocity of the charge sector. The *orbital* and the *spin sector* result in

$$\begin{aligned}\mathcal{H}_o &= \frac{2\pi v_o}{N_s+N_f}(:J^AJ^A: + :\bar{J}^A\bar{J}^A:) - 2gJ^A\bar{J}^A\,,\\ \mathcal{H}_s &= \frac{2\pi v_s}{N_s+N_f}(:J^aJ^a: + :\bar{J}^a\bar{J}^a:) + 2gJ^a\bar{J}^a\,,\end{aligned}\tag{II.4}$$

where v_o and v_s are the renormalized Fermi velocities of the corresponding sector. Here the effect of the interaction terms depends on the sign of their coupling constant. A renormalization group analysis (see for example [87, 90]) as well as Tsvelik's exact solution [86] show that the perturbation with negative sign in the orbital sector is marginally irrelevant and can be neglected. The excitations of this sector correspond to massless excitations. For the spin sector, on the other hand, the perturbation is marginally relevant resulting in massive excitations.

Furthermore, Tsvelik's analysis unveiled that the spin sector is described by an integrable model of relativistic fermions that transform with respect to the $SU(N_s)$ irreducible representation with highest weight $\Lambda = (N_f, 0, \ldots, 0)$. In general a model of integrable relativistic fermions can be constructed from any R matrix describing a quantum spin chain [91]: its Lagrangian density is given by

$$\mathcal{L} = \mathrm{i}\bar{\Psi}_{f\alpha}\gamma^\mu\partial_\mu\Psi_{f\alpha} + (\bar{\Psi}_{f\alpha_2}\gamma_\mu\Psi_{f\alpha_1})V^{\alpha_2\beta_2}_{\alpha_1\beta_1}(\bar{\Psi}_{g\beta_2}\gamma^\mu\Psi_{g\beta_1})\,, \tag{II.5}$$

where γ^μ $(\mu = 1, 2)$ are the gamma matrices, $\bar{\Psi}_{f\alpha} = \Psi^\dagger_{f\alpha}\gamma^0$ and $\Psi_{f\alpha} = (L_{f\alpha}, R_{f\alpha})$ is the Dirac spinor with left- and right-moving fields as its components. The interaction term of (II.5) is determined by an R-matrix satisfying the Yang-Baxter equation (I.1)

$$V^{\alpha_2\beta_2}_{\alpha_1\beta_1} = -\mathrm{i}\left[\ln \mathcal{R}(\lambda)|_{\lambda=1/g}\right]^{\alpha_2\beta_2}_{\alpha_1\beta_1}\,. \tag{II.6}$$

The integrable spin sector of (II.5) is described by the transfer matrix

$$\mathbf{T}(\lambda;\{k_i\}) = \mathcal{R}^{\alpha'_1 i_1}_{\alpha_1\alpha}(\lambda - k_1)\mathcal{R}^{\alpha'_2 i_2}_{\alpha_2 i_1}(\lambda - k_2)\ldots\mathcal{R}^{\alpha'_N\alpha}_{\alpha_N i_N}(\lambda - k_N)\,,$$

where k_i are parameters. In contrast to the Hamiltonian density of the quantum spin chain derived from (I.4), the Hamiltonian density for $\mathcal{N}$ relativistic fermions in a box of length L with periodic boundary conditions reads

$$\mathcal{H} = -\mathrm{i}\frac{\mathcal{N}}{L}\left(\ln \mathbf{T}(\lambda;\{k_i\})|_{\lambda=0,k_i=1/g} + \ln \mathbf{T}(\lambda;\{k_i\})|_{\lambda=0,k_i=-1/g}\right)\,. \tag{II.7}$$

Notice that the Hamiltonian density corresponding to the spin sector of the integrable relativistic fermions (II.5) coincides with the spin sector (II.4) for $v_s = 1$. This observation will serve as the starting point for studying emerging zero-energy modes with non-Abelian statistics in the spin sector (II.4).

1.2. Integrability study of perturbed $\mathfrak{su}(2)_{N_f}$ WZNW model

As mentioned in the previous section the Hamiltonian (II.1) splits into three independent parts for low-energies with massive excitations appearing in the spin sector due to a marginal relevant perturbation. From the point of view of topological quantum computing the spin sector (II.4) has significant properties as its massive excitations obey non-Abelian statistics [86]. To demonstrate the emergence of non-Abelian anyons within the spin sector Tsvelik used its exact solution for fermions with two spin degrees of freedom ($N_s = 2$) and arbitrary flavor degrees of freedom N_f [39]. Moreover, choosing an anisotropic current-current interaction resulted in a finite number of integral equations describing the low-energy excitations. When exposing the fermions to a magnetic field H coupling to the generator of the $\mathfrak{su}(2)$ Cartan subalgebra the Hamiltonian density studied by Tsvelik may be written in terms of the $SU(2)$ currents (I.93) in the Cartan-Weyl basis:

$$\begin{aligned}
\mathcal{H} &= \mathcal{H}[\mathfrak{su}(2)_{N_f}] + \mathcal{H}_{\text{int}} + \mathcal{H}_{\text{magnetic}}\\
\mathcal{H}[\mathfrak{su}(2)_{N_f}] &= \frac{2\pi}{N_f+2}\left(:J^aJ^a: + :\bar{J}^a\bar{J}^a:\right)\\
\mathcal{H}_{\text{int}} &= \lambda_\parallel J^z\bar{J}^z + \frac{1}{2}\lambda_\perp\left(J^+\bar{J}^- + J^-\bar{J}^+\right)\\
\mathcal{H}_{\text{magnetic}} &= -H(J^z + \bar{J}^z)
\end{aligned} \tag{II.8}$$

$\lambda_\parallel$, $\lambda_\perp$ are coupling constants becoming $g = \lambda_\parallel = \lambda_\perp$ in the isotropic limit.

Notice that in order to single out the anyonic excitations of (II.8) from the excitations of the charge and orbital sectors an experiment has to be constructed where the energy scale of the spin degrees of freedom is the lowest one. The realization of such a scenario is still an open problem. In fact, in the model of the previous section (II.1) the different signs of the current-current interactions of the spin and orbital sector (II.4) resulted in massive excitations in the spin sector, but massless excitations in the orbital sector. Only for the charge sector a gap may be obtained at half-filling ($4k_F = 2\pi/a$): in this case there are two more admissible terms when writing the interacting part of (II.1) into left- and right-movers

$$\mathcal{H}_{\text{int}} = \frac{g}{2} \sum_{f,g,\alpha,\beta} (L^\dagger_{f\alpha} R_{f\beta} L^\dagger_{g\beta} R_{g\alpha} + R^\dagger_{f\alpha} L_{f\beta} R^\dagger_{g\beta} L_{g\alpha} + \dots)\,,$$

where the dots are placeholders for the terms in equation (II.2). Similarly as for the Hubbard model (see e.g. [90]) these extra terms generate a gap in the charge sector. Still the exact solution of the perturbed $\mathfrak{su}(2)_{N_f}$ WZNW model (II.8) provides significant insights into emerging anyonic zero-energy modes in fermionic systems. Especially the transition from free anyons to interacting anyons, which interferes with possible implementations of quantum gates, can be studied in great detail using the thermodynamic Bethe ansatz.

The exact spectrum of the fermion model (II.8) can be obtained by means of the Bethe ansatz using the relationship between relativistic fermions and integrability: the model (II.8) without magnetic field coincides with the spin sector of (II.5) if the R-matrix of the XXZ spin-$N_f/2$ model is used for the interaction term (II.6). Placing the system of $\mathcal{N}$ fermions into a box of length L with periodic boundary conditions the eigenvalues of (II.8) following from (II.7) become [92–95]

$$E = \sum_{j=1}^{\mathcal{N}/2} k_j^{(+)} - \sum_{j=1}^{\mathcal{N}/2} k_j^{(-)} - H\left(\frac{\mathcal{N}}{2} - N_1\right)\,,$$

where $k_j^{(\pm)}$ are the momenta of the fermions with $\pm$ chirality. In a sector with magnetization $S^z = (\mathcal{N}/2) - N_1$, the momenta (II.10) are parametrized by the complex parameters λ_α, $\alpha = 1, \dots, N_1$ (Bethe roots), solving the Bethe equations

$$e^{\mathrm{i}k_j^{(\tau)}L} = \prod_{\alpha=1}^{N_1} \frac{\sinh(\frac{\pi}{2p_0}(\lambda_\alpha - \tau/g + N_f\mathrm{i}))}{\sinh(\frac{\pi}{2p_0}(\lambda_\alpha - \tau/g - N_f\mathrm{i}))}\,,$$

$$\prod_{\tau=\pm1} \left(\frac{\sinh\left(\frac{\pi}{2p_0}(\lambda_\alpha + \tau/g + N_f\mathrm{i})\right)}{\sinh\left(\frac{\pi}{2p_0}(\lambda_\alpha + \tau/g - N_f\mathrm{i})\right)}\right)^{\mathcal{N}/2} = \prod_{\beta=1}^{N_1} \frac{\sinh(\frac{\pi}{2p_0}(\lambda_\alpha - \lambda_\beta + 2\mathrm{i}))}{\sinh(\frac{\pi}{2p_0}(\lambda_\alpha - \lambda_\beta - 2\mathrm{i}))}\,, \tag{II.9}$$

where g and p_0 are functions of the coupling constants $\lambda_\parallel$ and $\lambda_\perp$. Written in terms of the Bethe roots the eigenvalues of (II.8) result in

$$E = \frac{\mathcal{N}}{L} \sum_{\alpha=1}^{N_1} \left(\sum_{\tau=\pm1} \frac{\tau}{2\mathrm{i}} \ln\left(\frac{\sinh(\frac{\pi}{2p_0}(\lambda_\alpha + \tau/g - N_f\mathrm{i}))}{\sinh(\frac{\pi}{2p_0}(\lambda_\alpha + \tau/g + N_f\mathrm{i}))}\right) + H \right) - \frac{\mathcal{N}H}{2}\,. \tag{II.10}$$

The relativistic invariance of the low-energy spectrum is broken by the boundary conditions used. It can be restored by considering observables in the scaling limit $g \ll 1$ and $L, \mathcal{N} \to \infty$ such that the mass of the spin excitations is small compared to the particle density $\mathcal{N}/L$.

Due to the fact that the Bethe equations (II.9) coincide with the ones obtained for an integrable spin $S = N_f/2$ XXZ chain of $\mathcal{N}$ sites with staggered inhomogeneities [70, 96], the root configurations solving (II.9) in the thermodynamic limit can be classified in terms of strings, i.e. groups consisting of n Bethe roots

$$\lambda^n_{\alpha,j} = \lambda^n_\alpha + i\left(n + 1 - 2j + \frac{p_0}{2}(1 - v_{2S} v_n)\right), \qquad j = 1, \dots, n, \tag{II.11}$$

where $\lambda^n_\alpha \in \mathbb{R}$ is the center of the string and $v_n \in \{\pm 1\}$ is called its parity, $v_{2S} = v_{n=2S}$. The length and parity (n_j, v_{n_j}) of admissible strings depend on the parameter $p_0 = N_f + 1/\nu$, see Sec. I 1.2. To simplify the discussion below we assume $\nu > 2$ to be an integer.[4] Considering a root configuration consisting of ν_j strings of type (n_j, v_{n_j}) and using (II.11) the Bethe equations (II.9) can be rewritten in terms of the real string-centers $\lambda^{(j)}_\alpha \equiv \lambda^{n_j}_\alpha$. In their logarithmic form they read

$$\frac{\mathcal{N}}{2}\left(t_{j,N_f}(\lambda^{(j)}_\alpha + 1/g) + t_{j,N_f}(\lambda^{(j)}_\alpha - 1/g)\right) = 2\pi I^{(j)}_\alpha + \sum_{k\geq 1}\sum_{\beta=1}^{\nu_k} \theta_{jk}(\lambda^{(j)}_\alpha - \lambda^{(k)}_\beta), \tag{II.12}$$

where $I^{(j)}_\alpha$ are integers (or half-integers) and we have introduced functions

$$t_{j,N_f}(\lambda) = \sum_{l=1}^{\min(n_j,N_f)} f(\lambda, |n_j - N_f| + 2l - 1, v_j v_{N_f}),$$

$$\theta_{jk}(\lambda) = f(\lambda, |n_j - n_k|, v_j v_k) + f(\lambda, n_j + n_k, v_j v_k) + 2\sum_{\ell=1}^{\min(n_j,n_k)-1} f(\lambda, |n_j - n_k| + 2\ell, v_j v_k)$$

with

$$f(\lambda, n, v) = \begin{cases} 2\arctan\left(\tan\left(\left(\frac{1+v}{4} - \frac{n}{2p_0}\right)\pi\right)\tanh\left(\frac{\pi\lambda}{2p_0}\right)\right) & \text{if } \frac{n}{p_0} \neq \text{integer} \\ 0 & \text{if } \frac{n}{p_0} = \text{integer} \end{cases}.$$

In the thermodynamic limit, $N_1, \mathcal{N} \to \infty$ with $N_1/\mathcal{N}$ fixed, the centers $\lambda^{(j)}_\alpha$ are distributed continuously with densities $\rho_j(\lambda)$ and hole densities $\rho^h_j(\lambda)$. Within the root density formalism [76] the densities are defined through the following integral equations

$$\tilde{\rho}^{(0)}_j(\lambda) = (-1)^{r(j)}\rho^h_j(\lambda) + \sum_{k\geq 1} A_{jk} * \rho_k(\lambda). \tag{II.13}$$

Here $a * b$ denotes a convolution and $r(j)$ is determined by $m_{r(j)} \leq j < m_{r(j)+1}$, see Sec. I 1.2. The bare densities $\tilde{\rho}^{(0)}_j(\lambda)$ and the kernels $A_{jk}(\lambda)$ of the integral operators are given by

$$\tilde{\rho}^{(0)}_j(\lambda) = \frac{1}{2}\left(a_{j,N_f}(\lambda + 1/g) + a_{j,N_f}(\lambda - 1/g)\right), \quad a_{j,N_f}(\lambda) = \frac{1}{2\pi}\frac{d}{d\lambda} t_{j,N_f}(\lambda),$$
$$A_{jk}(\lambda) = \frac{1}{2\pi}\frac{d}{d\lambda}\theta_{jk}(\lambda) + (-1)^{r(j)}\delta_{jk}\delta(\lambda).$$

[4]This is a technical assumption which does not limit the applicability of the results given below: the properties of the model depend smoothly on the parameter p_0 in extended intervals around this value [70, 75].

In terms of the solution of (II.13) for the densities of strings the energy density $\mathcal{E} = E/\mathcal{N}$ is obtained from (II.10) as

$$\begin{aligned} \mathcal{E} &= \frac{1}{\mathcal{N}} \sum_{j\geq 1} \sum_{\alpha=1}^{\nu_j} \left(\frac{1}{2}(t_{j,N_f}(\lambda_\alpha^{(j)} + 1/g) - t_{j,N_f}(\lambda_\alpha^{(j)} - 1/g)) + n_j H \right) - \frac{H}{2} \\ &\overset{\mathcal{N}\to\infty}{=} \sum_{j\geq 1} \int_{-\infty}^{+\infty} \mathrm{d}\lambda\, \tilde{\epsilon}_j^{(0)}(\lambda) \rho_j(\lambda) - \frac{H}{2}, \end{aligned} \tag{II.14}$$

where we introduced the bare energies

$$\tilde{\epsilon}_j^{(0)}(\lambda) = \frac{1}{2} \left(t_{j,N_f}(\lambda + 1/g) - t_{j,N_f}(\lambda - 1/g) \right) + n_j H\,.$$

In the present context with $p_0 = N_f + 1/\nu$ with integer $\nu > 2$ there are $N_f + \nu$ allowed string configurations (II.11). The energy (II.14) is minimized by a configuration where only j_0-strings of length $n_{j_0} = N_f$ have a finite density. For small magnetic fields they fill the entire real axis. Inverting the kernel $A_{j_0 j_0}$ in the equation for ρ_{j_0} and inserting the result into the other equations of (II.13) the following set of integral equations arise,

$$\begin{aligned} \rho_{j_0}(\lambda) &= \rho_{j_0}^{(0)}(\lambda) - B_{j_0 j_0} * \rho_{j_0}^h(\lambda) - \sum_{k\neq j_0} B_{j_0 k} * \rho_k(\lambda), \\ \rho_j^h(\lambda) &= \rho_j^{(0)}(\lambda) - B_{j j_0} * \rho_{j_0}^h(\lambda) - \sum_{k\neq j_0} B_{jk} * \rho_k(\lambda), \quad j \in \{j_1\} \cup \{j_2\}, \end{aligned} \tag{II.15}$$

where the kernels $B_{jk}(\lambda)$ given in Appendix A are introduced. Following [96] holes in the distribution of j_0-strings with density $\rho_{j_0}^h(\lambda)$ are called kinks, the particle like excitations corresponding to the ν types of strings with $j \in \{j_1 : N_f \leq j_1 < N_f + \nu\}$ are called breathers. In addition there are $N_f - 1$ auxiliary zero-energy modes ($j \in \{j_2\} = \{1, 2, \ldots, N_f - 1\}$), see Sec. I 1.2. The bare densities of these modes entering the integral equations (II.15) are (see Appendix B for details on taking the scaling limit $g \ll 1$ for $\rho_j^{(0)}(\lambda)$)

$$\begin{aligned} \rho_{j_0}^{(0)}(\lambda) &\equiv \frac{1}{A_{j_0 j_0}} * \rho_{j_0}^{(0)}(\lambda) \overset{g\ll 1}{=} \frac{M_0}{4} \cosh(\pi\lambda/2) \\ \rho_{j_1}^{(0)}(\lambda) &\equiv \frac{A_{j_1 j_0}}{A_{j_0 j_0}} * \rho_{j_0}^{(0)}(\lambda) - \rho_{j_1}^{(0)}(\lambda) \overset{g\ll 1}{=} \frac{M_{j_1}}{4} \cosh(\pi\lambda/2) \\ \rho_{j_2}^{(0)}(\lambda) &\equiv \rho_{j_2}^{(0)}(\lambda) - \frac{A_{j_2 j_0}}{A_{j_0 j_0}} * \rho_{j_0}^{(0)}(\lambda) = 0\,, \end{aligned} \tag{II.16}$$

with masses $M_{j_0} \equiv M_0 = 2e^{-\frac{\pi}{2g}}$ and

$$M_{j_1} \equiv \begin{cases} 2M_0 \sin\left((j_1 - N_f + 1)\frac{\pi}{2\nu}\right) & \text{if } N_f \leq j_1 < N_f + \nu - 1\,, \\ M_0 & \text{if } j_1 = N_f + \nu - 1. \end{cases}$$

In terms of the kink and breather densities the energy density is given by

$$\mathcal{E} = E_0 + \int_{-\infty}^{\infty} \mathrm{d}\lambda\, \epsilon_{j_0}^{(0)}(\lambda) \rho_{j_0}^h(\lambda) + \sum_{j_1} \int_{-\infty}^{\infty} \mathrm{d}\lambda\, \epsilon_{j_1}^{(0)}(\lambda) \rho_{j_1}(\lambda)\,. \tag{II.17}$$

Here the new bare energies are

$$\begin{aligned}
\epsilon_{j_0}^{(0)}(\lambda) &\equiv \frac{1}{A_{j_0 j_0}} * \epsilon_{j_0}^{(0)}(\lambda) \overset{g\ll 1}{=} M_0 \cosh(\pi\lambda/2) - zH\,, \\
\epsilon_{j_1}^{(0)}(\lambda) &\equiv \epsilon_{j_1}^{(0)}(\lambda) - \frac{A_{j_0 j_1}}{A_{j_0 j_0}} * \epsilon_{j_0}^{(0)}(\lambda) \overset{g\ll 1}{=} M_{j_1} \cosh(\pi\lambda/2) + zH\,\delta_{j_1, j_0 - 1}\,, \\
\epsilon_{j_2}^{(0)}(\lambda) &\equiv \epsilon_{j_2}^{(0)}(\lambda) - \frac{A_{j_0 j_2}}{A_{j_0 j_0}} * \epsilon_{j_0}^{(0)}(\lambda) = 0\,,
\end{aligned} \tag{II.18}$$

with $z \equiv n_{j_0}/A_{j_0 j_0}(0) = \frac{1}{2}(1 + N_f \nu)$. E_0 is the ground state energy density

$$E_0 = \int_{-\infty}^{\infty} \mathrm{d}\lambda \epsilon_{j_0}^{(0)}(\lambda) \rho_{j_0}^{(0)}(\lambda) - \frac{H}{2}\,.$$

Note that the breather with $j_1 = N_f + \nu - 1 \equiv \tilde{j}_0$ has the same mass M_{j_0} as the kink. Its coupling to the magnetic field, however, is with the opposite sign. Therefore, following Ref. [94], we denote this breather *antikink* below.

1.3. Thermodynamics

For the physical properties of the different quasi-particles appearing in the Bethe ansatz solution of the model (II.8) its thermodynamics are studied. The equilibrium state at finite temperature is obtained by minimizing the free energy, $F/\mathcal{N} = \mathcal{E} - T\mathcal{S}$, with the combinatorial entropy [76]

$$\mathcal{S} = \sum_{j\geq 1} \int_{-\infty}^{+\infty} \mathrm{d}\lambda \left[(\rho_j + \rho_j^h) \ln(\rho_j + \rho_j^h) - \rho_j \ln \rho_j - \rho_j^h \ln \rho_j^h \right]. \tag{II.19}$$

The resulting thermodynamic Bethe ansatz (TBA) equations read

$$T \ln(1 + e^{\epsilon_k/T}) = \epsilon_k^{(0)}(\lambda) + \sum_{j\geq 1} B_{jk} * T \ln(1 + e^{-\epsilon_j/T}), \tag{II.20}$$

where the dressed energies $\epsilon_j(\lambda)$ are introduced through $e^{-\epsilon_j/T} = \rho_j/\rho_j^h$ for breathers and auxiliary modes $j \in \{j_1\} \cup \{j_2\}$ and $e^{-\epsilon_{j_0}/T} = \rho_{j_0}^h/\rho_{j_0}$ for kinks. In terms of the dressed energies the free energy per particle is

$$\begin{aligned}
\frac{F}{\mathcal{N}} &= -T \sum_{j\notin\{j_2\}} \int_{-\infty}^{\infty} \mathrm{d}\lambda\, \rho_j^{(0)}(\lambda) \ln(1 + e^{-\epsilon_j/T}) \\
&\overset{g\ll 1}{=} -\frac{T}{4} \sum_{j\notin\{j_2\}} M_j \int_{-\infty}^{\infty} \mathrm{d}\lambda\, \cosh(\pi\lambda/2) \ln(1 + e^{-\epsilon_j/T})\,.
\end{aligned} \tag{II.21}$$

Finally, the corresponding integral equations determining the dressed energies ϵ_{j_0}, $\epsilon_{\tilde{j}_0}$ of the kink and antikink, ϵ_{j_1} of the breathers ($j_1 \neq \tilde{j}_0$), and ϵ_{j_2} of the auxiliary modes are

$$\begin{aligned}
\epsilon_{j_0}(\lambda) &= M_0 \cosh(\pi\lambda/2) - zH + \sum_{k\geq 1} (B_{kj_0} - \delta_{kj_0}) * T \ln(1 + e^{-\epsilon_k/T}) \\
\epsilon_{\tilde{j}_0}(\lambda) &= M_0 \cosh(\pi\lambda/2) + zH + \sum_{k\geq 1} (B_{kj_0} - \delta_{k\tilde{j}_0}) * T \ln(1 + e^{-\epsilon_k/T}) \\
\epsilon_{j_1}(\lambda) &= M_{j_1} \cosh(\pi\lambda/2) + \sum_{k\geq 1} (B_{kj_1} - \delta_{k\in\{j_1\}}) * T \ln(1 + e^{-\epsilon_k/T}) \\
\epsilon_{j_2}(\lambda) &= \sum_{k\geq 1} (B_{kj_2} - \delta_{k\in\{j_2\}}) * T \ln(1 + e^{-\epsilon_k/T})\,.
\end{aligned} \tag{II.22}$$

Solving these equations we obtain the spectrum of the model (II.8) for a given temperature and magnetic field, see Figure 7 for $T = 0$.

For magnetic fields $zH \lesssim M_0$ the kinks, antikinks and breathers are gapped. As H is increased the kink gap closes and they condense into a phase where they form a collective state with finite density.

Now the low-temperature behavior of the free energy as function of the magnetic field can be discussed.

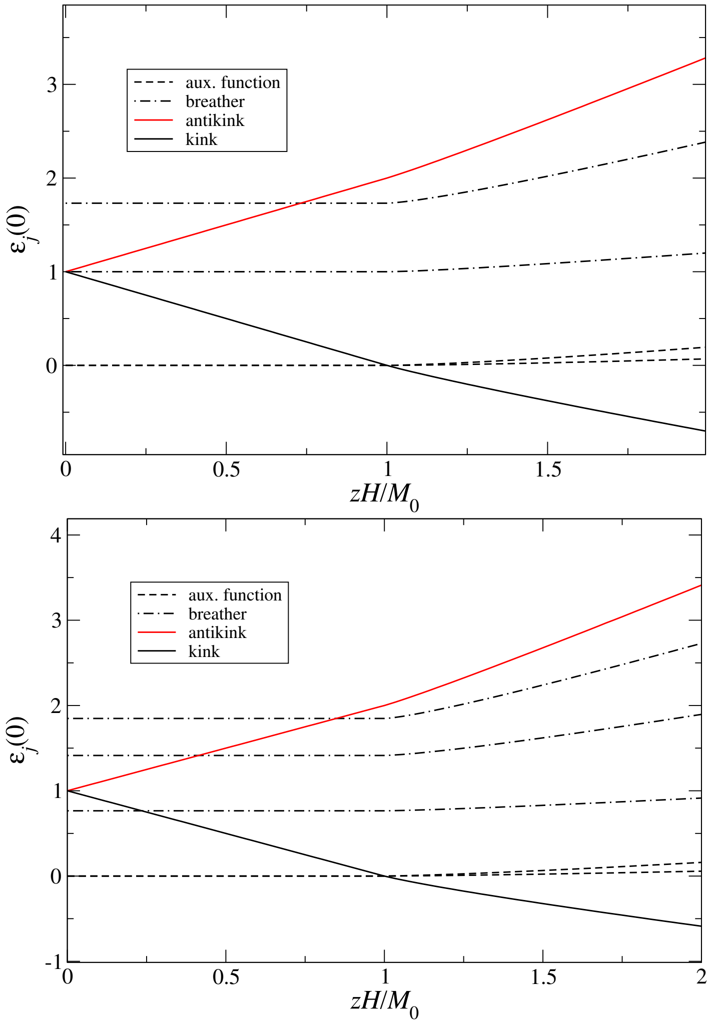

Figure 7: The zero temperature spectrum of excitations (and Fermi energy of the kinks for $zH > M_0$, respectively) $\epsilon_j(0)$ obtained from the numerical solution of (II.22) as function of the magnetic field for $N_f = 3$. The number and masses of the breather modes depend on the value of ν being 3 (top) and 4 (bottom), respectively. The low-lying modes with energies described by the auxiliary functions are clearly separated from the spectrum of kinks, antikinks and breathers. Their degeneracy is lifted as soon as the kink gap closes.

1.3.1. Non-interacting kinks

For magnetic fields $zH < M_0$ temperatures below the gaps of the kink and the lowest energy breather ($j_1 = N_f$), i.e. $T \ll \min(M_0 - zH, M_{N_f})$ are considered. In this regime the nonlinear integral equations (II.22) can be solved asymptotically analytically [39]: the energies of kinks, antikinks, and breathers, ϵ_{j_0}, $\epsilon_{\tilde{j}_0}$ and ϵ_{j_1} are well described by their first order approximation while those of the auxiliary modes can be replaced by the asymptotic solution for $|\lambda| \to \infty$

$$1 + e^{\epsilon_{j_2}/T} = \left(\frac{\sin(\frac{\pi(j_2+1)}{N_f+2})}{\sin(\frac{\pi}{N_f+2})} \right)^2 .$$

For the other modes we obtain ($Q = 2\cos(\pi/(N_f+2))$)

$$\begin{aligned} \epsilon_{j_0}(\lambda) &= M_0 \cosh(\pi\lambda/2) - zH - T \ln Q \,, \\ \epsilon_{\tilde{j}_0}(\lambda) &= M_0 \cosh(\pi\lambda/2) + zH - T \ln Q \,, \\ \epsilon_{j_1}(\lambda) &= M_{j_1} \cosh(\pi\lambda/2) - T \ln Q^2 \,, \end{aligned} \tag{II.23}$$

resulting in the free energy

$$\begin{aligned} \frac{F}{\mathcal{N}} = &- TQ \int \frac{\mathrm{d}p}{2\pi} e^{-(M_0 - zH)/T - p^2/2M_0T} - TQ \int \frac{\mathrm{d}p}{2\pi} e^{-(M_0+zH)/T - p^2/2M_0T} \\ &- TQ^2 \sum_{j \in \{j_1\} \setminus \{\tilde{j}_0\}} \int \frac{\mathrm{d}p}{2\pi} e^{-M_j/T - p^2/2M_jT} . \end{aligned} \tag{II.24}$$

As observed in Ref. [39] each of the terms appearing in this expression is the free energy of an ideal gas of particles with the corresponding mass carrying an internal degree of freedom with non-integer *quantum dimension* Q for the kinks (and antikinks) and Q^2 for the breathers. Their densities

$$\begin{aligned} n_{j_0} &= Q \sqrt{\frac{M_0 T}{2\pi}} e^{-(M_0 - zH)/T}, \quad n_{\tilde{j}_0} = Q \sqrt{\frac{M_0 T}{2\pi}} e^{-(M_0+zH)/T} \\ n_{j_1} &= Q^2 \sqrt{\frac{M_{j_1} T}{2\pi}} e^{-M_{j_1}/T}, \quad j_1 \neq \tilde{j}_0 \end{aligned}$$

can be controlled by variation of the temperature and the magnetic field, which acts as a chemical potential $\pm zH$ for kinks and antikinks, respectively.

For $zH \lesssim M_0$ the dominant contribution to F is that of the kinks. Their degeneracy Q coincides with the quantum dimension of anyons satisfying $SU(2)_{N_f}$ fusion rules with spin $j = 1/2$ (I.57) [78, 82] [5]

$$d_{N_f}(j) = \sin\left(\frac{\pi(2j+1)}{N_f+2}\right) / \sin\left(\frac{\pi}{N_f+2}\right) . \tag{II.25}$$

This has been interpreted as a signature for the presence of anyonic zero modes bound to the kinks [39]. As the field is reduced the gap of the kinks increases and for $\nu > 3$, the lowest breather, $j_1 = N_f$, dominates the free energy when $zH \lesssim M_0 - M_{N_f}$. Its degeneracy Q^2 can be understood as a consequence of the breather being a bound state of a kink and an antikink, each contributing a factor $Q = d_{N_f}(\frac{1}{2})$: from the fusion rule for $\mathfrak{su}(2)_{N_f}$ spin-$\frac{1}{2}$ anyons, $\frac{1}{2} \times \frac{1}{2} = 0 + 1$, the degeneracy of this bound state to be $Q^2 = d_{N_f}(0) + d_{N_f}(1)$ is obtained.

[5] These include Ising anyons for $N_f = 2$ and, due to the automorphism $j \to N_f/2 - j$, Fibonacci anyons for $N_f = 3$.

1.3.2. Condensate of kinks

Following [71] we observe that in this regime the dressed energies and densities can be related as

$$\begin{aligned}
\rho_j(\lambda) &= (-1)^{\delta_{j\in\{j_2\}}} \frac{1}{2\pi} \frac{\mathrm{d}\epsilon_j(\lambda)}{\mathrm{d}\lambda} f\left(\frac{\epsilon_j(\lambda)}{T}\right), \\
\rho_j^h(\lambda) &= (-1)^{\delta_{j\in\{j_2\}}} \frac{1}{2\pi} \frac{\mathrm{d}\epsilon_j(\lambda)}{\mathrm{d}\lambda} \left(1 - f\left(\frac{\epsilon_j(\lambda)}{T}\right)\right),
\end{aligned} \tag{II.26}$$

for $\lambda > \lambda_\delta$ with $\exp(\pi\lambda_\delta/2) \gg 1$, where $f(\epsilon) = (1+e^\epsilon)^{-1}$ is the Fermi function. Inserting this into (II.19) with $(\phi_j = \epsilon_j/T)$

$$\begin{aligned}
\mathcal{S} &= \sum_j \mathcal{S}_j(\lambda_\delta) - \frac{T}{\pi} \sum_j (-1)^{\delta_{j\in\{j_2\}}} \int_{\phi_j(\lambda_\delta)}^{\phi_j(\infty)} \mathrm{d}\phi_j \, \left[f(\phi_j)\ln f(\phi_j) + (1-f(\phi_j))\ln(1-f(\phi_j))\right], \\
\mathcal{S}_j(\lambda_\delta) &\equiv \int_{-\lambda_\delta}^{\lambda_\delta} \mathrm{d}\lambda \, \left[(\rho_j+\rho_j^h)\ln(\rho_j+\rho_j^h) - \rho_j\ln\rho_j - \rho_j^h \ln\rho_j^h\right]
\end{aligned} \tag{II.27}$$

is obtained. The integrals over ϕ_j can be performed giving

$$\mathcal{S} = \sum_j \mathcal{S}_j(\lambda_\delta) - \frac{2T}{\pi} \sum_j (-1)^{\delta_{j\in\{j_2\}}} [L(f(\phi_j(\infty)) - L(f(\phi_j(\lambda_\delta)))] \tag{II.28}$$

in terms of the Rogers dilogarithm $L(x)$

$$L(x) = -\frac{1}{2}\int_0^x \mathrm{d}y \left(\frac{\ln y}{1-y} + \frac{\ln(1-y)}{y}\right).$$

In the regime considered here, i.e. $T \ll zH - M_0$ and $\log(zH/M_0) > \lambda_\delta \gg 1$, from (II.22) it can be concluded that

$$\begin{aligned}
&f(\phi_{j_0}(\lambda_\delta)) = 1, \quad f(\phi_{j_1}(\lambda_\delta)) = 0, \quad f(\phi_{j_2}(\lambda_\delta)) = 0 \\
&f(\phi_{j_0}(\infty)) = 0, \quad f(\phi_{j_1}(\infty)) = 0, \quad f(\phi_{j_2}(\infty)) = \left(\frac{\sin(\frac{\pi}{N_f+2})}{\sin(\frac{\pi(j_2+1)}{N_f+2})}\right)^2,
\end{aligned} \tag{II.29}$$

and therefore

$$\rho_{j_0}(\lambda) = 0, \quad \rho_{j_1}^h(\lambda) = 0, \quad \rho_{j_2}^h(\lambda) = 0, \quad \text{for } |\lambda| < \lambda_\delta$$

giving $\mathcal{S}_j(\lambda_\delta) = 0$ for all j. Finally, using the identity

$$\sum_{k=2}^{n-2} L\left(\frac{\sin^2(\pi/n)}{\sin^2(\pi k/n)}\right) = \frac{2(n-3)}{n} L(1), \quad L(1) = \frac{\pi^2}{6}, \quad n \geq 3 \tag{II.30}$$

the expression

$$\mathcal{S} = \frac{\pi}{3}\left(1 + 2\frac{N_f-1}{N_f+2}\right) T + O(T^2) = \frac{\pi}{3}\frac{3N_f}{N_f+2} T + O(T^2) \tag{II.31}$$

is found for the universal low-T asymptotics of the entropy in the phase with finite kink density. The low-energy excitations near the Fermi points $\epsilon_{j_0}(\pm\Lambda) = 0$ of the kink dispersion propagate with velocity $v_{\text{kink}} = (\partial_\lambda \epsilon_{j_0})/(2\pi\rho_{j_0}^h)\Big|_\Lambda \to 1$ for magnetic fields $H > H_\delta$ such that

$\Lambda(H_\delta) > \lambda_\delta$. Hence the conformal field theory (CFT) describing the collective low-energy modes is the $SU(2)$ WZNW model at level N_f or, by conformal embedding [39, 56, 87], a product of a free $U(1)$ boson and a Z_{N_f}-parafermion coset $SU(2)_{N_f}/U(1)$ contributing $c = 1$ and ((I.81) with $N = 2$)

$$c(Z_{N_f}) = 2\frac{N_f - 1}{N_f + 2} \tag{II.32}$$

to the central charge, respectively. The latter is the critical theory for the $(N_f + 1)$-state restricted solid-on-solid (RSOS) model on one of its critical lines or, equivalently, a quantum chain of $SU(2)_{N_f}$ spin-$\frac{1}{2}$ anyons with ferromagnetic pair interaction favouring fusion in the $j = 1$ channel [25, 97].

To study the transition from the gas of free anyons to the condensate of kinks described by the CFT given above we have solved the TBA equations (II.22) numerically by an iterative method for a given magnetic field H, temperature T and anisotropy parameter p_0. Using (II.21) the entropy can be computed from the numerical data as

$$\begin{aligned}\mathcal{S} &= -\frac{\mathrm{d}}{\mathrm{d}T}\frac{F}{\mathcal{N}} \\ &= \sum_{j\notin\{j_2\}} \frac{M_j}{4}\int_{-\infty}^{\infty} \mathrm{d}\lambda\, \cosh\left(\frac{\pi\lambda}{2}\right)\left(\log\left(1+e^{-\epsilon_j/T}\right) + \left(\frac{\epsilon_j}{T} - \frac{\mathrm{d}}{\mathrm{d}T}\epsilon_j\right)\left(1+e^{\epsilon_j/T}\right)^{-1}\right).\end{aligned} \tag{II.33}$$

For magnetic fields large enough to suppress the contribution of breathers to the entropy, $zH \gg M_0$, the entropy is seen to be given by the term $j = j_0$ in (II.33) alone and to converge to the expected analytical value (II.31). In the intermediate regime, $M_0 < zH \lesssim zH_\delta$, and temperatures below the smallest of the breather masses $T \ll M_{N_f}$, the entropy deviates from this asymptotic expression: in this range of H the auxiliary modes propagate with a velocity (independent of j_2) differing from that of the kinks, v_{kink}, namely

$$v_{pf} = -\left.\frac{\partial_\lambda \epsilon_{j_2}(\lambda)}{2\pi\rho^h_{j_2}(\lambda)}\right|_{\lambda\to\infty}.$$

As a consequence the bosonic (spinon) and parafermionic degrees of freedom separate and the low-temperature entropy is

$$\mathcal{S} = \frac{\pi}{3}\left(\frac{1}{v_{\text{kink}}} + \frac{c(Z_{N_f})}{v_{pf}}\right)T\,. \tag{II.34}$$

Note that both Fermi velocities depend on the magnetic field and approach 1 as $H \gtrsim H_\delta$, see Figure 8, giving the entropy (II.31) of the WZNW model. In Figure 9 the computed entropy (II.33) is shown for various temperatures as a function of the magnetic field together with the $T \to 0$ behavior (II.34) expected from conformal field theory. Additionally, Figure 9 shows the decoupling into bosonic and parafermionic modes for $zH \gtrsim M_0$.[6]

[6] For low-temperatures and magnetic fields $zH > M_0$ the contribution of kinks in (II.33) develops a singularity which prevents reaching the asymptotic regime in the numerical analysis.

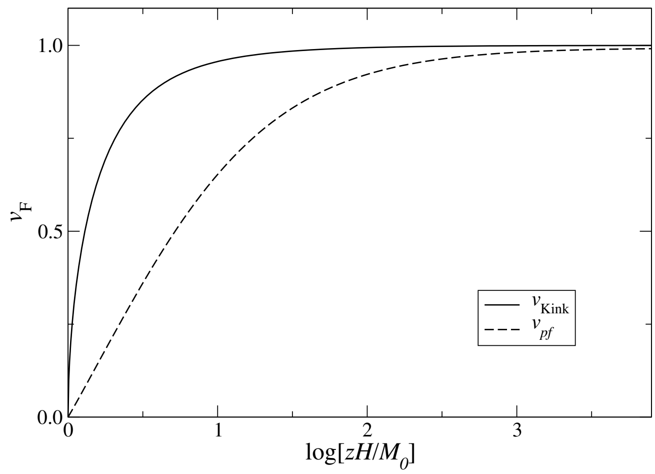

Figure 8: Fermi velocities of kinks and parafermion modes as a function of the magnetic field $zH > M_0$ for $p_0 = 2 + 1/3$ at zero temperature. For large field, $H > H_\delta$, both Fermi velocities approach 1 leading to the asymptotic result for the low-temperature entropy (II.31).

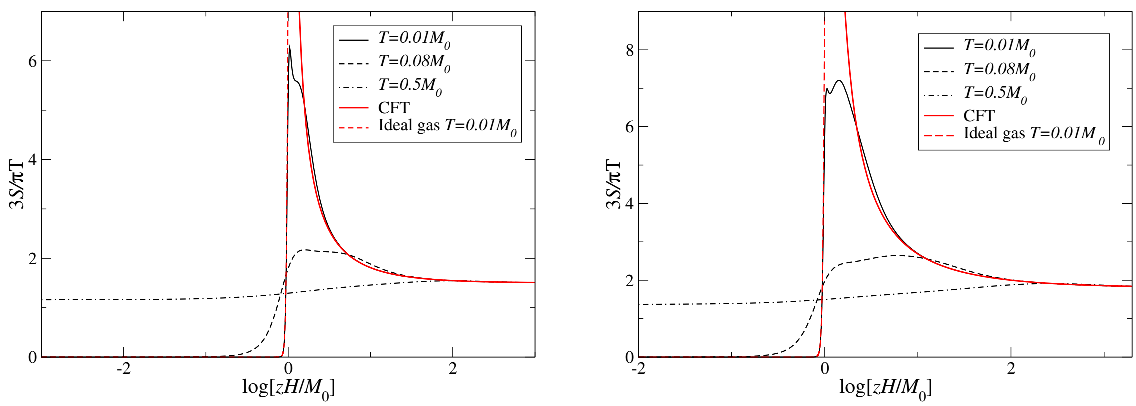

(a) **(b)**

Figure 9: Entropy obtained from numerical solution of the TBA equations (II.22) for $p_0 = 2 + 1/3$ (a), $p_0 = 3 + 1/3$ (b) as a function of the magnetic field H for different temperatures. For magnetic fields large compared to the kink mass, $zH \gg M_0$, the entropy approaches the expected analytical value (II.34) for a field theory with a free bosonic and a Z_{N_f} parafermion sector propagating with velocities v_{Kink} and v_{pf}, respectively (full red line). For magnetic fields $zH < M_0$ and temperature $T \ll M_0$ the entropy is that of a dilute gas of non-interacting quasi-particles with degenerate internal degree of freedom due to the anyons (dashed red line).

1.4. Phase diagram

The findings for the contribution of the anyonic degrees of freedom to the low-temperature thermodynamical properties of the system are summarized in Figure 10: for temperatures small compared to the smallest breather mass, $T \ll M_{N_f}$, the coupling to breathers $\{j_1\}$ can be neglected in the TBA equation (II.22) and signatures of $\mathfrak{su}(2)_{N_f}$ non-Abelian anyons are found in thermodynamic quantities. For magnetic fields $zH < M_0$ and temperatures small compared to the kink mass ($T \ll M_0 - zH$) the free energy (II.24) coincides with the free energy of a non-interacting gas of kinks and breathers. It was found that the kinks carry an internal degree of freedom given by the spin-$\frac{1}{2}$ $\mathfrak{su}(2)_{N_f}$ anyons while the breathers carry the $\frac{1}{2} \times \frac{1}{2}$ topological charge. For sufficiently small magnetic fields (region I in Figure 10) the main contribution to the free energy comes from the lowest ($j_1 = N_f$) breather. Once the magnetic field is increased such that $\epsilon_{j_0}(0) < \epsilon_{N_f}(0)$ the situation changes and kinks dominate the free energy (region II in Figure 10).

For magnetic fields $zH \lesssim M_0$ the kink gap closes and interactions between the anyonic modes lift the degeneracy (region III in Figure 10). In terms of the TBA equations this happens for temperatures $M_0 - zH \lesssim T \ll M_{N_f}$ resulting in corrections of the solutions (II.23). The formation of a collective state by the anyons with ferromagnetic pair interactions becomes apparent for magnetic fields $zH > M_0$: here the resulting effective field theory describing the interacting modes splits into a product of a bosonic theory and a Z_{N_f} parafermionic theory describing the kinks and collective modes of the anyons, respectively. By further increasing the magnetic field beyond H_δ the Fermi velocities of the bosonic and parafermionic sectors degenerate giving a central charge that coincides with that of the $\mathfrak{su}(2)_{N_f}$ WZNW model.

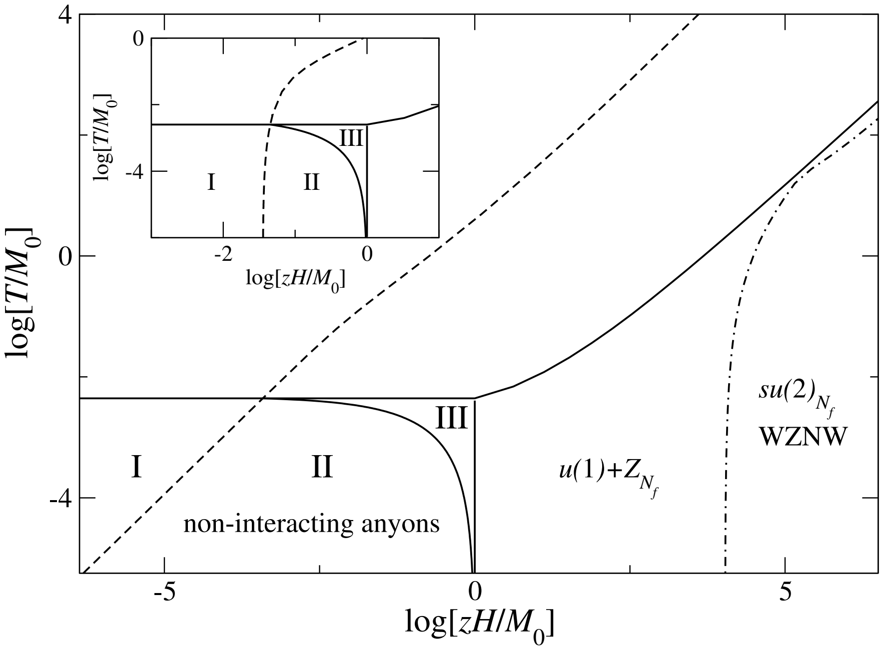

Figure 10: Phase diagram for the contribution of $\mathfrak{su}(2)_{N_f}$ anyons to the low-temperature properties of the model (II.8) for $\nu = 3$ (inset for $\nu = 4$). For small magnetic fields a gas of non-interacting quasi-particles with the anyon as an internal zero energy degree of freedom bound to them is realized. Here the dashed line indicates $\epsilon_{j_0}(0) = \epsilon_{N_f}(0)$, i.e. the location of the crossover between regions where the lowest energy breathers, $j_1 = N_f$, (region I) or kinks (region II) dominate the free energy. In region III the presence of thermally activated kinks with a small but finite density lifts the degeneracy of the zero modes. For fields $zH > M_0$ the kinks condense and the low-energy behavior of the model is determined by the corresponding $U(1)$ bosonic mode and the Z_{N_f} parafermion collective modes. For $zH \gg M_0$ the Fermi velocities of kinks and parafermions degenerate yielding a $\mathfrak{su}(2)_{N_f}$ WZNW model for the effective description of the model.

2. Perturbed $\mathfrak{su}(3)_{N_f}$ WZNW model

Tsvelik's approach to study non-Abelian anyons within a perturbed $\mathfrak{su}(2)_{N_f}$ WZNW model can be generalized to other symmetry groups. Here a system described by fermion fields with $SU(3)$ ($N_s = 3$) and $SU(N_f)$ symmetry is studied. As done before a weak anisotropic current-current interaction is chosen together with couplings of the fields h_1, h_2 to the currents of the $\mathfrak{su}(3)$ Cartan subalgebra. In the low-energy limit non-Abelian bosonization splits the Hamiltonian into a sum of three commuting parts describing the fractionalized degrees of freedom. One of these parts is a perturbed $\mathfrak{su}(3)_{N_f}$ WZNW model, whose low-temperature thermodynamics is studied extensively in this section.

In section II 2.1 string solutions of the corresponding Bethe equations are discussed in the thermodynamic limit. The excitations are found to be solitons carrying quantum numbers in the fundamental quark and antiquark representations of $\mathfrak{su}(3)$. Using the thermodynamic Bethe ansatz signatures of $\mathfrak{su}(3)_{N_f}$ anyons bound to the solitons are found, see section II 2.2. As before the fields can be varied to study the transition from free to interacting $\mathfrak{su}(3)_{N_f}$ anyons in detail. The findings, including the conformal field theories describing the interacting regimes, are summarized in a phase diagram in section II 2.3.

2.1. Integrability study of perturbed $\mathfrak{su}(3)_{N_f}$ WZNW model

The Hamiltonian density describing the perturbed $\mathfrak{su}(3)_{N_f}$ WZNW model is given by

$$\begin{aligned}
\mathcal{H} =& \mathcal{H}[\mathfrak{su}(3)_{N_f}] + \mathcal{H}_{\text{int}} + \mathcal{H}_{\text{fields}}\,, \\
\mathcal{H}[\mathfrak{su}(3)_{N_f}] =& \frac{2\pi}{N_f+3}\left(:\mathbf{J}\cdot\mathbf{J}: + :\bar{\mathbf{J}}\cdot\bar{\mathbf{J}}:\right)\,, \\
\mathcal{H}_{\text{int}} =& \lambda_\parallel \sum_{i=1}^{2} J^i \bar{J}^i + \lambda_\perp \sum_{\alpha>0} \frac{|\alpha|^2}{2}\left(J^\alpha \bar{J}^{-\alpha} + J^{-\alpha}\bar{J}^\alpha\right)\,, \\
\mathcal{H}_{\text{fields}} =& -\sum_{i=1}^{2} h_i (J^i + \bar{J}^i)\,,
\end{aligned} \tag{II.35}$$

where $\lambda_\parallel$, $\lambda_\perp$ are coupling constants. Here $\mathbf{J}$ and $\bar{\mathbf{J}}$ are the right- and left-moving $\mathfrak{su}(3)_{N_f}$ Kac-Moody currents with components

$$\begin{aligned}
J^i &= R^\dagger_{ak}(H^i_c)_{ab}R_{bk}\,, \qquad & J^\alpha &= R^\dagger_{ak}(E^\alpha)_{ab}R_{bk}\,, \\
\bar{J}^i &= L^\dagger_{ak}(H^i_c)_{ab}L_{bk}\,, \qquad & \bar{J}^\alpha &= L^\dagger_{ak}(E^\alpha)_{ab}L_{bk}\,,
\end{aligned}$$

where H^i_c ($i = 1,2$) are the generators of the $\mathfrak{su}(3)$ Cartan subalgebra and E^α denotes the ladder operator for the root α in the Cartan-Weyl basis ($1 \leq a,b \leq 3$ and $1 \leq k \leq N_f$ are color and flavor indices, respectively). Also notice that the form of $\mathcal{H}_{\text{int}}$ is directly related to the Casimir operator in the Cartan-Weyl basis (I.40).

The spectrum of (II.35) can be obtained using Bethe ansatz methods based on the observation that the underlying structures coincide with those of an integrable deformation of the $SU(3)$ magnet with Dynkin label $(N_f, 0)$ [98–103]. Specifically, placing $\mathcal{N} = \sum \mathcal{N}_\alpha$ fermions into a box of length L with periodic boundary conditions the energy eigenvalues in the sector with $\mathcal{N}_1 \geq \mathcal{N}_2 \geq \mathcal{N}_3$ are

$$E = \sum_{j=1}^{\mathcal{N}/2} k_j^{(+)} - \sum_{j=1}^{\mathcal{N}/2} k_j^{(-)} + N_1 H_1 + N_2 H_2 - \frac{\mathcal{N}}{3}(2H_1 + H_2)\,, \tag{II.36}$$

where $k_j^{(\pm)}$ are the momenta of the fermions with $\pm$ chirality and $N_1 = \mathcal{N}_2 + \mathcal{N}_3$, $N_2 = \mathcal{N}_3$. The fields H_1, H_2 are linear combinations of the previous fields $H_1 \equiv \vec{\alpha}_1 \cdot \vec{h}$, $H_2 \equiv \vec{\alpha}_2 \cdot \vec{h}$, where $\vec{\alpha}_1$, $\vec{\alpha}_2$ are the simple roots of $\mathfrak{su}(3)$ (I.45). The relativistic invariance of the fermion model is broken by the choice of boundary conditions but will be restored later by considering observables in the scaling limit $L, \mathcal{N} \to \infty$ and $g \ll 1$ such that the mass of the elementary excitations is small compared to the particle density $\mathcal{N}/L$.

The momenta of the energy eigenvalues (II.36) are parametrized by complex parameters $\lambda_\alpha^{(m)}$ with $\alpha = 1, \dots, N_m$ and $m = 1, 2$ solving the hierarchy of Bethe equations (cf. Refs. [99, 104–106] for the magnet in the fundamental representation, $N_f = 1$)

$$e^{\mathrm{i}k_j^{(\tau)} L} = \prod_{\alpha=1}^{N_1} \frac{\sinh(\frac{\pi}{2p_0}(\lambda_\alpha - \tau/g + N_f \mathrm{i}))}{\sinh(\frac{\pi}{2p_0}(\lambda_\alpha - \tau/g - N_f \mathrm{i}))}\,,$$

$$\begin{aligned}
\prod_{\tau=\pm 1} e_{N_f}(\lambda_\alpha^{(1)} + \tau/g)^{\mathcal{N}/2} &= \prod_{\beta\neq\alpha}^{N_1} e_2(\lambda_\alpha^{(1)} - \lambda_\beta^{(1)}) \prod_{\beta=1}^{N_2} e_{-1}(\lambda_\alpha^{(1)} - \lambda_\beta^{(2)})\,, \quad \alpha = 1, \dots N_1 \\
\prod_{\beta=1}^{N_1} e_1(\lambda_\alpha^{(2)} - \lambda_\beta^{(1)}) &= \prod_{\beta\neq\alpha}^{N_2} e_2(\lambda_\alpha^{(2)} - \lambda_\beta^{(2)})\,, \quad \alpha = 1, \dots, N_2
\end{aligned} \tag{II.37}$$

where $e_k(x) = \sinh\left(\frac{\pi}{2p_0}(x + \mathrm{i}k)\right) / \sinh\left(\frac{\pi}{2p_0}(x - \mathrm{i}k)\right)$ and g, p_0 are functions of the coupling constants $\lambda_\parallel$, $\lambda_\perp$. Written in terms of the Bethe roots the energy eigenvalues (II.35) become

$$E = \frac{\mathcal{N}}{L} \sum_{\alpha=1}^{N_1} \sum_{\tau=\pm 1} \frac{\tau}{2\mathrm{i}} \ln \left(\frac{\sinh(\frac{\pi}{2p_0}(\lambda_\alpha^{(1)} + \tau/g - N_f \mathrm{i}))}{\sinh(\frac{\pi}{2p_0}(\lambda_\alpha^{(1)} + \tau/g + N_f \mathrm{i}))} \right) + N_1 H_1 + N_2 H_2 - \frac{\mathcal{N}}{3}(2H_1 + H_2)\,. \tag{II.38}$$

Based on equations (II.37), (II.38) the thermodynamics of the model can be studied provided that the solutions to the Bethe equations describing the eigenstates in the limit $\mathcal{N} \to \infty$ are known. Here it is argued that the root configurations corresponding to the ground state and excitations relevant for the low-temperature behavior of (II.35) can be built based on the string hypothesis for the $U_q(sl(2))$ models [74], i.e. that in the thermodynamic limit the Bethe roots $\lambda_\alpha^{(m)}$ on both levels $m = 1, 2$ can be grouped into *j-strings* of length n_j and with parity $v_{n_j} \in \{\pm 1\}$

$$\lambda_{j,\alpha,k}^{(m)} = \lambda_{j,\alpha}^{(m)} + i\left(n_j + 1 - 2k + \frac{p_0}{2}(1 - v_{N_f} v_{n_j})\right)\,, \qquad k = 1, \dots, n_j, \quad m = 1, 2\,, \tag{II.39}$$

with real centers $\lambda_{j,\alpha}^{(m)} \in \mathbb{R}$. The allowed lengths and parities depend on the parameter p_0. Below the discussion is further simplified by assuming $p_0 = N_f + 1/\nu$ with integer $\nu > 2$ where the following $N_f + \nu$ different string configurations contribute to the low-temperature thermodynamics:

- $j_0 = N_f + \nu$ with $(n_{j_0}, v_{n_{j_0}}) = (N_f, +1)$,
- $j_1 \in \{N_f, N_f + 1, \dots N_f + \nu - 1\}$ with $(n_{j_1}, v_{n_{j_1}}) = ((j_1 - N_f)N_f + 1, (-1)^{j_1 + N_f + 1})$,

- $j_2 \in \{1, 2, \ldots, N_f - 1\}$ with $(n_{j_2}, v_{n_{j_2}}) = (j_2, +1)$.

Within the root density approach the Bethe equations are rewritten as coupled integral equations for the densities of these strings [107]. For vanishing magnetic fields one finds that the Bethe root configuration corresponding to the lowest energy state is described by finite densities of j_0-strings on both levels $m = 1, 2$. The elementary excitations above this ground state are of three types: similar as in the isotropic magnet [108] there are solitons or *quarks* and *antiquarks* corresponding to holes in the distributions of j_0-strings on level $m = 1, 2$. They carry quantum numbers in the fundamental representations $(1, 0)$ and $(0, 1)$ of $SU(3)$, respectively (independent of the representation $(N_f, 0)$ used for the construction of the spin chain). The ν different types of j_1-strings are called *breathers*. Finally, there are auxiliary modes given by j_2-strings. The densities $\rho_j^{(m)}(\lambda)$ of these excitations (and $\rho_j^{h(m)}(\lambda)$ for the corresponding vacancies) satisfy the integral equations ($a * b$ denotes the convolution of a and b)

$$\rho_k^{h(m)}(\lambda) = \rho_{0,k}^{(m)}(\lambda) - \sum_{\ell=1}^{2} \sum_j \left(B_{kj}^{(m,\ell)} * \rho_j^{(\ell)} \right)(\lambda) , \qquad m = 1, 2 , \tag{II.40}$$

see Appendix C. As mentioned above relativistic invariance is restored in the scaling limit $g \ll 1$ where the solitons are massive particles with bare densities $\rho_{0,j_0}^{(m)}(\lambda)$ and bare energies $\epsilon_{0,j_0}^{(m)}$

$$\begin{aligned} \rho_{0,j_0}^{(m)}(\lambda) &\overset{g \ll 1}{\simeq} \frac{M_0}{6} \cosh(\pi\lambda/3) , \\ \epsilon_{0,j_0}^{(m)}(\lambda) &\overset{g \ll 1}{\simeq} M_0 \cosh(\pi\lambda/3) - \begin{cases} (Z_1 H_1 + Z_2 H_2) , & m = 1, \\ (Z_2 H_1 + Z_1 H_2) , & m = 2 . \end{cases} \end{aligned} \tag{II.41}$$

Here $M_0 \equiv M_{j_0} = (2\mathcal{N}/L) \sin(\pi/3) e^{-\frac{\pi}{3g}}$ is the soliton mass and $z \equiv (1 + N_f \nu)$, $Z_1 = \frac{2}{3} z$, $Z_2 = \frac{1}{3} z$. Furthermore, the corresponding charges can be read off from (II.41): for a general excitation with mass M and bare energy $\epsilon_0(\lambda)$ its *charges* (q_1, q_2) are defined by

$$\epsilon_0(\lambda) = M \cosh\left(\frac{\pi\lambda}{3}\right) - z \begin{pmatrix} \omega_1 \\ \omega_2 \end{pmatrix} \cdot \begin{pmatrix} h_1 \\ h_2 \end{pmatrix} = M \cosh\left(\frac{\pi\lambda}{3}\right) - \begin{pmatrix} q_1 \\ q_2 \end{pmatrix} \cdot \begin{pmatrix} Z_1 H_1 \\ Z_2 H_2 \end{pmatrix} , \tag{II.42}$$

where ω_1, ω_2 are the components of a weight in a $\mathfrak{su}(3)$ representation. Consequently, quarks of type j_0 carry the charge $(q_1, q_2) = (1, 1)$, while antiquarks of type j_0 carry the charge $(q_1, q_2) = (1/2, 2)$. These charges correspond to the highest weight states of the quark and antiquark representation of $\mathfrak{su}(3)$. All possible charges corresponding to the quark and antiquark multiplet are shown in Figure 11.

Similarly, breathers have bare densities and energies

$$\begin{aligned} \rho_{0,j_1}^{(m)}(\lambda) &\overset{g \ll 1}{\simeq} \frac{M_{j_1}}{6} \cosh(\pi\lambda/3) , \\ \epsilon_{0,j_1}^{(m)}(\lambda) &\overset{g \ll 1}{\simeq} M_{j_1} \cosh(\pi\lambda/3) - \begin{cases} (-1)^m Z_2 (H_1 - H_2) , & \text{if } j_1 = N_f + \nu - 1, \\ (Z_2 H_1 + Z_1 H_2) , & \text{if } 0 \le j_1 - N_f < \nu - 1 , \, m = 1, \\ (Z_1 H_1 + Z_2 H_2) , & \text{if } 0 \le j_1 - N_f < \nu - 1 , \, m = 2 , \end{cases} \end{aligned} \tag{II.43}$$

with masses

$$M_{j_1} \equiv \begin{cases} 2M_0 \sin\left((j_1 - N_f + 1) \frac{\pi}{3\nu} + \frac{\pi}{6} \right) , & \text{if } 0 \le j_1 - N_f < \nu - 1 , \\ M_0 , & \text{if } j_1 = N_f + \nu - 1 \equiv \tilde{j}_0 . \end{cases}$$

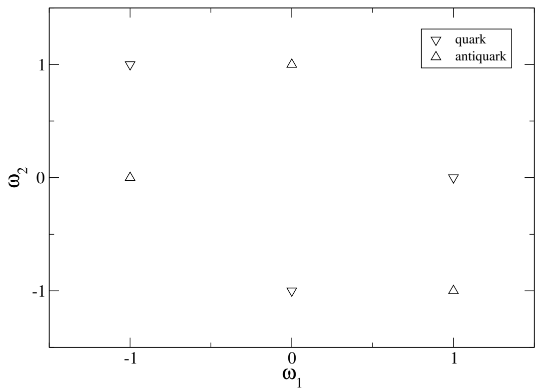

(a) weights

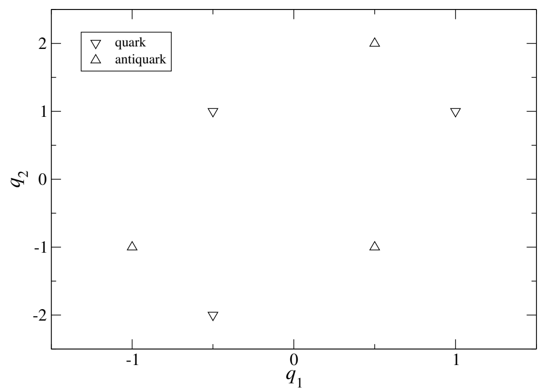

(b) charges

Figure 11: Relationship between the weights (a) of the quark and antiquark representation of $\mathfrak{su}(3)$ and the charges (b) determined by (II.42) with $H_1 = \vec{\alpha_1} \cdot \vec{h}$, $H_2 = \vec{\alpha_2} \cdot \vec{h}$.

Note that the mass of the breathers with $j_1 = \tilde{j}_0$ coincides with that of the solitons. The charges $(-1/2, 1)$, $(1/2, -1)$ of this breather for $m = 1, 2$, however, indicate that they are descendents of the $\mathfrak{su}(3)$ highest weight states in the quark and antiquark multiplet. Therefore excitations of types j_0 and $\tilde{j}_0$ will both be labelled solitons (or quarks and antiquarks for solitons on level $m = 1$ and 2, respectively) below. The masses and $\mathfrak{su}(3)$ charges of the auxiliary modes vanish, i.e. $\rho^{(m)}_{0,j_2}(\lambda) = 0 = \epsilon^{(m)}_{0,j_2}(\lambda)$.

The energy density of a macro-state with densities given by (II.40) is

$$\Delta\mathcal{E} = \sum_{m=1}^{2} \sum_{j} \int_{-\infty}^{\infty} \mathrm{d}\lambda \, \epsilon^{(m)}_{0,j}(\lambda) \rho^{(m)}_{j}(\lambda) \,. \tag{II.44}$$

2.2. Low-temperature thermodynamics

Additional insights into the physical properties of the different quasi-particles appearing in the Bethe ansatz solution of the model (II.35) can be obtained from its low-temperature thermodynamics. The equilibrium state at finite temperature is obtained by minimizing the free energy, $F/\mathcal{N} = \mathcal{E} - T\mathcal{S}$, with the combinatorial entropy density [76]

$$\mathcal{S} = \sum_{m=1}^{2} \sum_{j} \int \mathrm{d}\lambda \, \left[(\rho^{(m)}_j + \rho^{h(m)}_j) \ln(\rho^{(m)}_j + \rho^{h(m)}_j) - \rho^{(m)}_j \ln \rho^{(m)}_j - \rho^{h}_j \ln \rho^{h(m)}_j \right] \,. \tag{II.45}$$

The resulting thermodynamic Bethe ansatz (TBA) equations for the dressed energies $\epsilon^{(m)}_j(\lambda) = T \ln\left(\rho^{h(m)}_j(\lambda)/\rho^{(m)}_j(\lambda)\right)$ read

$$T \ln(1 + e^{\epsilon^{(m)}_k/T}) = \epsilon^{(m)}_{0,k}(\lambda) + \sum_{\ell=1}^{2} \sum_{j} B^{(\ell,m)}_{jk} * T \ln(1 + e^{-\epsilon^{(\ell)}_j/T}). \tag{II.46}$$

It is convenient to rewrite the equations for the auxiliary modes $j \in \{j_2\}$

$$\begin{aligned}
\epsilon_{j_2}^{(m)}(\lambda) =& s * T \ln(1 + e^{\epsilon_{j_2+1}^{(m)}/T})(1 + e^{\epsilon_{j_2-1}^{(m)}/T}) - s * T \ln(1 + e^{-\epsilon_{j_2}^{(3-m)}/T}) \,, \\
& j_2 = 1, \dots, N_f - 2 \,, \\
\epsilon_{N_f-1}^{(m)}(\lambda) =& s * T \ln(1 + e^{\epsilon_{N_f-2}^{(m)}/T}) - s * T \ln(1 + e^{-\epsilon_{N_f-1}^{(3-m)}/T}) \\
& + \sum_{j \notin \{j_2\}} C_j^{(m)} * T \ln(1 + e^{-\epsilon_j^{(m)}/T}) \,,
\end{aligned} \tag{II.47}$$

where $\epsilon_0^{(m)} = -\infty$, $s(\lambda) = \frac{1}{4 \cosh \pi\lambda/2}$ and the kernels $C_j^{(m)}$ are defined in Appendix C. The free energy per particle in terms of the solutions to the TBA equations for the solitons and breathers is

$$\begin{aligned}
\frac{F}{\mathcal{N}} &= -T \sum_{m=1}^{2} \sum_{j \notin \{j_2\}} \int_{-\infty}^{\infty} \mathrm{d}\lambda \, \rho_{0,j}^{(m)}(\lambda) \ln(1 + e^{-\epsilon_j^{(m)}/T}) \\
&\overset{g \ll 1}{=} -\frac{T}{6} \sum_{m=1}^{2} \sum_{j \notin \{j_2\}} M_j \int_{-\infty}^{\infty} \mathrm{d}\lambda \, \cosh(\pi\lambda/3) \ln(1 + e^{-\epsilon_j^{(m)}/T}) \,.
\end{aligned} \tag{II.48}$$

Solving the TBA equations (II.46) the spectrum of the model (II.35) for given temperature T and fields H_1, H_2 is obtained. Below the focus is on the regime $H_1 \geq H_2$ – exchanging $H_1 \leftrightarrow H_2$ corresponds to interchanging the two levels of the Bethe ansatz. From the expressions (II.41) and (II.43) for the bare energies of the elementary excitations the qualitative behavior of these modes can be deduced at low temperatures: As long as $Z_1 H_1 + Z_2 H_2 \lesssim M_0$ solitons and breathers remain gapped. Increasing the fields with $H_1 > H_2$ the gap of the quarks ($m = 1$ in (II.41)) closes once $Z_1 H_1 + Z_2 H_2 \simeq M_0$. For larger fields they condense into a phase with finite density $\rho_{j_0}^{(1)}$ and the degeneracy of the corresponding zero-energy auxiliary modes is lifted. At even larger fields the gap of the $\mathfrak{su}(3)$ highest weight state of the antiquark will close, too, and the systems enters a collective phase with a finite density of quarks and antiquarks. In Figure 12 the zero temperature mass spectrum for the model with $N_f = 2$, $\nu = 3$ is shown as function of H_1 for $H_2 = 0$ and $H_1 = H_2$, respectively.[7] Note that in the latter case the spectra of elementary excitations on level 1 and 2 coincide, $\epsilon_j^{(1)} \equiv \epsilon_j^{(2)}$ for all j.

Based on this picture the behavior of the free energy as function of the fields at temperatures small compared to the relevant energy scales is discussed, i.e. the masses or Fermi energies of the solitons, $0 < T \ll |Z_1 H_1 + Z_2 H_2 - M_0|$.

2.2.1. Non-interacting solitons

For fields $Z_1 H_1 + Z_2 H_2 \lesssim M_0$ solitons and breathers are gapped. At temperatures small compared to the gaps of the solitons the nonlinear integral equations (II.46) can be solved asymptotically by iteration: the energies of the massive excitations are well described by their first order approximation [39] while those of the auxiliary modes are given by the asymptotic

[7] We note that the highest energy soliton levels are not captured by the string hypothesis (II.39). However, since the gaps of these modes grow with the magnetic field they do not contribute to the low-temperature thermodynamics studied in this paper.

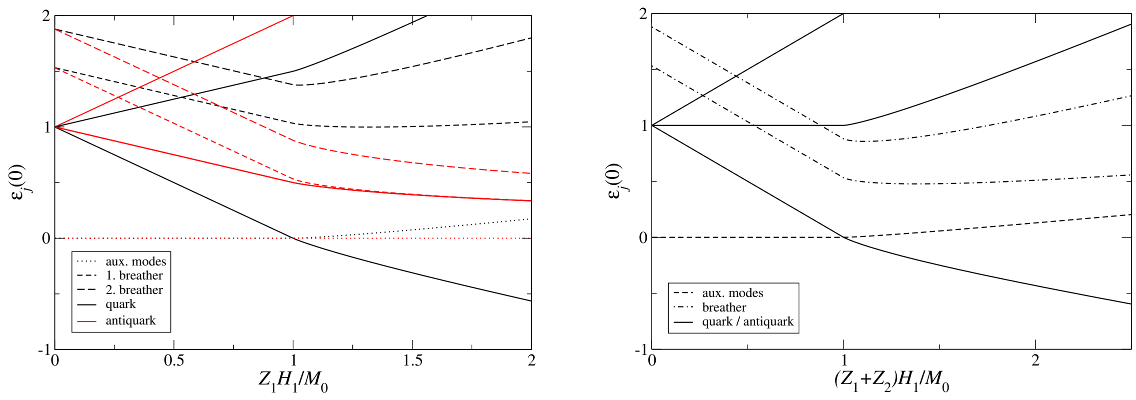

(a) **(b)**

Figure 12: The zero-temperature energy gap of the elementary excitations (and Fermi energy of quarks/antiquarks in the condensed phase, respectively) $\epsilon_j^{(m)}(0)$ obtained from the numerical solution of (II.46) for $p_0 = 2+1/3$ as a function of the field H_1 with $H_2 = 0$ (a) or $H_1 \equiv H_2$ (b) (gaps on level $m = 1$ (2) are displayed in black (red)). Note that in (a) the high-energy quark and the low-energy antiquark levels are twofold degenerate. In (b) the elementary excitations for $m = 1$ and $m = 2$ are degenerate. The gaps of quarks/antiquarks close for $Z_1H_1 = M_0$ in (a) and for $(Z_1 + Z_2) = M_0$ in (b), respectively. In this phase the degeneracy of the auxiliary modes is lifted. Increasing the field to $Z_1H_1 \gg M_0$ the gaps of the antiquarks ($\epsilon_{j_0}^{(2)}(0)$ and $\epsilon_{\tilde{j}_0}^{(2)}(0)$) close in (a). For small fields the low-lying auxiliary modes are clearly separated from the spectrum of solitons and breathers.

solution of (II.47) for $|\lambda| \to \infty$ [109]

$$1 + e^{\epsilon_{j_2}^{(m)}/T} = \frac{\sin\left(\frac{(j_2+1)\pi}{N_f+3}\right)\sin\left(\frac{(j_2+2)\pi}{N_f+3}\right)}{\sin\left(\frac{\pi}{N_f+3}\right)\sin\left(\frac{2\pi}{N_f+3}\right)}\,.$$

For solitons and breathers this implies ($Q \equiv 1 + e^{\epsilon_1^{(1)}} = \frac{\sin(3\pi/(N_f+3))}{\sin(\pi/(N_f+3))}$)

$$\epsilon_j^{(m)}(\lambda) = \begin{cases} \epsilon_{0,j}^{(m)}(\lambda) - T\ln Q & j = j_0, \tilde{j}_0 \\ \epsilon_{0,j}^{(m)}(\lambda) - T\ln Q^2 & j \in \{j_1\} \setminus \{\tilde{j}_0\} \end{cases}$$

resulting in the free energy

$$\begin{aligned} \frac{F}{\mathcal{N}} = &- \sum_{m=1}^{2} \sum_{j=j_0,\tilde{j}_0} TQ \int \frac{\mathrm{d}p}{2\pi}\, e^{-\left(\epsilon_{0,j}^{(m)}(0) - p^2/2M_0\right)/T} \\ &- \sum_{m=1}^{2} \sum_{j\in\{j_1\}\setminus\{\tilde{j}_0\}} TQ^2 \int \frac{\mathrm{d}p}{2\pi} e^{-\left(\epsilon_{0,j}^{(m)}(0) - p^2/2M_j\right)T}\,. \end{aligned} \tag{II.49}$$

As observed in Refs. [39, 52] each of the terms appearing in this expression is the free energy of an ideal gas of particles with the corresponding mass carrying an internal degree of freedom with non-integer quantum dimension Q for the solitons and Q^2 for the breathers ($j_1 \neq \tilde{j}_0$). Their densities

$$n_j = \begin{cases} Q\sqrt{\frac{M_0T}{2\pi}} e^{-\epsilon_{0,j}^{(m)}(0)/T} & j = j_0, \tilde{j}_0, \\ Q^2\sqrt{\frac{M_jT}{2\pi}} e^{-\epsilon_{0,j}^{(m)}(0)/T} & j \in \{j_1\} \setminus \{\tilde{j}_0\} \end{cases}$$

can be controlled by variation of the temperature and the fields, which act as chemical potentials.

For the interpretation of this observation, fields $H_1 > H_2$ and $Z_1 H_1 + Z_2 H_2 \lesssim M_0$ are considered where the dominant contribution to the free energy is that of the lowest energy quarks, $j = j_0$, $m = 1$. Their degeneracy Q coincides with the quantum dimension of anyons satisfying $\mathfrak{su}(3)_{N_f}$ fusion rules with topological charge $[1, 0]$

$$d_{N_f}([x_1, x_2]) = \frac{\sin\left(\frac{\pi(x_1+2)}{N_f+3}\right)\sin\left(\frac{\pi(x_2+1)}{N_f+3}\right)\sin\left(\frac{\pi(x_1-x_2+1)}{N_f+3}\right)}{\sin\left(\frac{\pi}{N_f+3}\right)\sin\left(\frac{\pi}{N_f+3}\right)\sin\left(\frac{2\pi}{N_f+3}\right)}\,,$$

see Ref. [110]. Here $[x_1, x_2]$ denotes the Young diagram with x_i nodes in the i-th row. Following the discussion in Ref. [39] this is interpreted as a signature for the presence of $\mathfrak{su}(3)_{N_f}$ anyonic zero modes bound to the quarks. The degeneracy Q^2 of the breather can be understood as a consequence of the breather being a bound state of two quarks, each contributing a factor Q to the quantum dimension: from the fusion rule for $\mathfrak{su}(3)_{N_f}$ $[1, 0]$ and $[1, 1]$ anyons,

$$[1,0] \times [1,0] = [1,1] + [2,0]\,, \quad [1,1] \times [1,1] = [1,0] + [2,2]\,,$$

for $N_f > 1$, the degeneracy of this bound state is obtained to be $Q^2 = d_{N_f}([1,1]) + d_{N_f}([2,0]) = d_{N_f}([1,0]) + d_{N_f}([2,2])$.

2.2.2. Condensate of quarks

For fields $Z_1 H_1 \gtrsim M_0 - Z_2 H_2 > \frac{2}{3} M_0$ the quarks in the $\mathfrak{su}(3)$ highest weight state form a condensate, while the contribution to the free energy of the other solitons and the breathers can be neglected. For large fields $Z_1 H_1 \gg M_0 - Z_2 H_2$ the low-temperature thermodynamics in this regime can be studied analytically: following [70] we observe that the dressed energies and densities can be related as

$$\begin{aligned}
\rho_j^{(m)}(\lambda) &= (-1)^{\delta_{j\in\{j_2\}}} \frac{1}{2\pi} \frac{\mathrm{d}\epsilon_j^{(m)}(\lambda)}{\mathrm{d}\lambda} f\left(\frac{\epsilon_j^{(m)}(\lambda)}{T}\right), \\
\rho_j^{h(m)}(\lambda) &= (-1)^{\delta_{j\in\{j_2\}}} \frac{1}{2\pi} \frac{\mathrm{d}\epsilon_j^{(m)}(\lambda)}{\mathrm{d}\lambda} \left(1 - f\left(\frac{\epsilon_j^{(m)}(\lambda)}{T}\right)\right),
\end{aligned} \tag{II.50}$$

for $\lambda > \lambda_\delta$ with a sufficiently large $\exp(\pi\lambda_\delta/2) \gg 1$. $f(\epsilon) = 1/(1 + e^\epsilon)$ is the Fermi function. Inserting this into (II.45) with ($\phi_j^{(m)} = \epsilon_j^{(m)}/T$) results in

$$\begin{aligned}
\mathcal{S} = &-\frac{T}{\pi}\sum_{m,j}(-1)^{\delta_{j\in\{j_2\}}} \int_{\phi_j^{(m)}(\lambda_\delta)}^{\phi_j^{(m)}(\infty)} \mathrm{d}\phi_j^{(m)} \left[f(\phi_j^{(m)}) \ln f(\phi_j^{(m)}) + (1 - f(\phi_j^{(m)})) \ln(1 - f(\phi_j^{(m)}))\right] \\
&+ \sum_{m,j} \mathcal{S}_j^{(m)}(\lambda_\delta)\,, \\
\mathcal{S}_j^{(m)}(\lambda_\delta) \equiv &\int_{-\lambda_\delta}^{\lambda_\delta} \mathrm{d}\lambda \left[(\rho_j^{(m)} + \rho_j^{h(m)}) \ln(\rho_j^{(m)} + \rho_j^{h(m)}) - \rho_j^{(m)} \ln \rho_j^{(m)} - \rho_j^{h(m)} \ln \rho_j^{h(m)}\right].
\end{aligned} \tag{II.51}$$

The integrals over $\phi_j^{(m)}$ can be performed giving

$$\mathcal{S} = \sum_{m,j} \mathcal{S}_j^{(m)}(\lambda_\delta) - \frac{2T}{\pi} \sum_{m,j} (-1)^{\delta_{j\in\{j_2\}}} [L(f(\phi_j^{(m)}(\infty)) - L(f(\phi_j^{(m)}(\lambda_\delta)))] \tag{II.52}$$

in terms of the Rogers dilogarithm $L(x)$

$$L(x) = -\frac{1}{2}\int_0^x \mathrm{d}y \left(\frac{\ln y}{1-y} + \frac{\ln(1-y)}{y}\right).$$

In the regime considered here, i.e. $T \ll Z_1H_1 + Z_2H_2 - M_0$ and $\log((Z_1H_1 + Z_2H_2)/M_0) > \lambda_\delta \gg 1$, it can be concluded from (II.46),(II.47) that

$$\begin{aligned}
&f(\phi_{j_0}^{(m)}(\lambda_\delta)) = \begin{cases} 1 & m=1 \\ 0 & m=2 \end{cases}, && f(\phi_{j_0}^{(m)}(\infty)) = 0, \\
&f(\phi_{j_1}^{(m)}(\lambda_\delta)) = 0, && f(\phi_{j_1}^{(m)}(\infty)) = 0, \\
&f(\phi_{j_2}^{(m)}(\lambda_\delta)) = \begin{cases} 0 & m=1 \\ \left(\frac{\sin(\frac{\pi}{N_f+2})}{\sin(\frac{\pi(j_2+1)}{N_f+2})}\right)^2 & m=2 \end{cases}, && f(\phi_{j_2}^{(m)}(\infty)) = \frac{\sin(\frac{\pi}{N_f+3})\sin(\frac{2\pi}{N_f+3})}{\sin(\frac{j_2\pi}{N_f+3})\sin(\frac{(j_2+1)\pi}{N_f+3})},
\end{aligned} \tag{II.53}$$

and therefore

$$\rho_{j_0}^{h(1)}(\lambda) = \rho_{j_0}^{(2)}(\lambda) = \rho_{j_1}^{(m)}(\lambda) = \rho_{j_2}^{(1)} = 0$$

for $|\lambda| < \lambda_\delta$. Using $\rho_{j_2}^{(2)}(\lambda) = e^{-\epsilon_{j_2}^{(2)}/T}\rho_{j_2}^{h(2)}(\lambda)$ the integral equations (II.40) for $\rho_{j_2}^{h(2)}$ simplify in this regime to

$$\rho_{j_2}^{h(2)} = -\sum_{k_2} B_{j_2k_2}^{(2,2)} * e^{-\epsilon_{k_2}^{(2)}/T}\rho_{k_2}^{h(2)} \qquad \text{for } |\lambda| < \lambda_\delta,$$

it can be concluded that $\rho_{j_2}^{h(2)} \to 0$, $\rho_{j_2}^{(2)} \to 0$ such that $\rho_{j_2}^{(2)}/\rho_{j_2}^{h(2)} = e^{-\epsilon_{j_2}^{(2)}/T} = \text{const}$ for $|\lambda| < \lambda_\delta$. Consequently, $\mathcal{S}_j^{(m)}(\lambda_\delta) = 0$ for all j, m is obtained. Using $L(1) = \pi^2/6$ and the relation with $(N, N_f \geq 2)$

$$\sum_{m=1}^{N-1}\sum_{j_2=1}^{N_f-1} L\left(\frac{\sin(\frac{(N-m)\pi}{N_f+N})\sin(\frac{m\pi}{N_f+N})}{\sin(\frac{(N+j_2-m)\pi}{N_f+N})\sin(\frac{(j_2+m)\pi}{N_f+N})}\right) = \frac{\pi^2}{6}\left(\frac{N_f(N^2-1)}{N_f+N} - (N-1)\right) \tag{II.54}$$

for $N = 2, 3$ the following low-temperature behavior of the entropy

$$\mathcal{S} = \frac{\pi}{3}\left(\frac{8N_f}{N_f+3} - \frac{3N_f}{N_f+2}\right)T \tag{II.55}$$

arises. This is consistent with an effective description of the low-energy collective modes in this regime through the coset $\mathfrak{su}(3)_{N_f}/\mathfrak{su}(2)_{N_f}$ conformal field theory with central charge

$$c = \frac{8N_f}{N_f+3} - \frac{3N_f}{N_f+2}.$$

Using the conformal embedding [111] (see also [112])

$$\frac{\mathfrak{su}(3)_{N_f}}{\mathfrak{su}(2)_{N_f}} = \mathfrak{u}(1) + \frac{Z_{\mathfrak{su}(3)_{N_f}}}{Z_{\mathfrak{su}(2)_{N_f}}}, \tag{II.56}$$

where $Z_{\mathfrak{su}(N)_{N_f}} = \mathfrak{su}(N)_{N_f}/\mathfrak{u}(1)^N$ denotes generalized parafermions [54], the collective modes can equivalently be described by a product of a free $\mathfrak{u}(1)$ boson contributing $c = 1$ to the central charge and a parafermion coset $Z_{\mathfrak{su}(3)_{N_f}}/Z_{\mathfrak{su}(2)_{N_f}}$ contributing

$$c = \frac{8N_f}{N_f+3} - \frac{3N_f}{N_f+2} - 1 = \frac{6(N_f-1)}{N_f+3} - \frac{2(N_f-1)}{N_f+2}\,.$$

To study the transition from the gas of free anyons to the condensate of quarks described by the CFT (II.56) at intermediate fields $Z_1H_1 \gtrsim M_0 - Z_2H_2$ the TBA equations (II.46) have been solved numerically. Similar as in Ref. [52] this can be done by choosing suitable initial distributions and iterating the integral equations for given fields H_1, H_2, temperature T and anisotropy parameter p_0.

Using (II.48) the entropy can be computed from the numerical data as

$$\mathcal{S} = -\frac{\mathrm{d}}{\mathrm{d}T}\frac{F}{\mathcal{N}}\,. \tag{II.57}$$

From the numerical solution of the TBA equations one finds that the low-energy behavior is determined by the quarks and the auxiliary modes on the first level which propagate with Fermi velocities

$$v^{(1)}_{\text{quark}} = \left.\frac{\partial_\lambda \epsilon^{(1)}_{j_0}}{2\pi\rho^{h(1)}_{j_0}}\right|_{\Lambda}\,, \qquad v^{(1)}_{pf} = -\left.\frac{\partial_\lambda \epsilon^{(1)}_{j_2}(\lambda)}{2\pi\rho^{h(1)}_{j_2}(\lambda)}\right|_{\lambda\to\infty}\,,$$

where Λ is defined by $\epsilon^{(1)}_{j_0}(\Lambda) = 0$. Note that $v^{(1)}_{pf}$ is the same for all auxiliary modes ($j \in \{j_2\}, m = 1$).

The resulting low-temperature entropy is the sum of contributions from a $\mathfrak{u}(1)$ boson (quark) and a $Z_{\mathfrak{su}(3)_{N_f}}/Z_{\mathfrak{su}(2)_{N_f}}$ parafermionic coset (from the auxiliary modes)

$$\mathcal{S} = \frac{\pi}{3}\left(\frac{1}{v^{(1)}_{\text{quark}}} + \frac{1}{v^{(1)}_{pf}}\left(\frac{6(N_f-1)}{N_f+3} - \frac{2(N_f-1)}{N_f+2}\right)\right)T\,. \tag{II.58}$$

This behavior is consistent with the conformal embedding (II.56). Note that both Fermi velocities depend on the field H_1 and approach 1 as $H_1 \gtrsim H_{1,\delta}$ such that $\Lambda(H_{1,\delta}) > \lambda_\delta$, see Figure 13 (a).

Therefore, in this limit the entropy (II.55) of the coset $\mathfrak{su}(3)_{N_f}/\mathfrak{su}(2)_{N_f}$ is approached. In Figure 13 (b) the computed entropy (II.57) of the model with $N_f = 2$, $\nu = 3$ is shown for $T = 0.01\,M_0$ as a function of the field H_1 together with the $T \to 0$ behavior (II.58) expected from conformal field theory.

2.2.3. Condensate of quarks and antiquarks

For fields $H_1 \geq H_2 \gtrsim M_0/(Z_1+Z_2)$ the system forms a collective state of solitons ($j = j_0$) on both levels, $m = 1, 2$. Again, the low-temperature thermodynamics can be studied analytically for $H_1 \geq H_2 \gg M_0/(Z_1+Z_2)$. Repeating the analysis of Section 2.2.2 one can

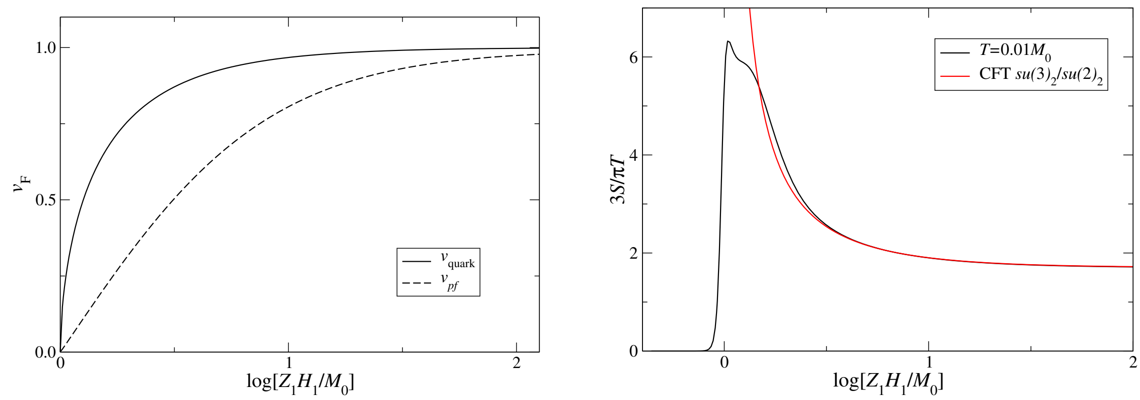

(a) **(b)**

Figure 13: (a) Fermi velocities of the quarks and first level $SU(3)$ parafermion modes as a function of the field $Z_1H_1 > M_0$ for $p_0 = 2 + 1/3$, $H_2 \equiv 0$ at zero temperature. For large fields, $H_1 > H_{1,\delta}$, both Fermi velocities approach 1 leading to the asymptotic result for the low-temperature entropy (II.55). (b) Entropy obtained from the numerical solution of the TBA equations (II.46) for $p_0 = 2 + 1/3$ and $H_2 \equiv 0$ as a function of the field $(Z_1H_1/M_0$ for $T = 0.01M_0$. For fields large compared to the soliton mass, $Z_1H_1 \gg M_0$, the entropy approaches the expected analytical value (II.55) for a field theory with a free bosonic sector and a $Z_{\mathfrak{su}(3)_{N_f=2}}/Z_{\mathfrak{su}(2)_{N_f=2}}$ parafermion sector propagating with velocities $v^{(1)}_{\text{quark}}$ and $v^{(1)}_{pf}$, respectively (full red line). For magnetic fields $Z_1H_1 < M_0$ and temperature $T \ll M_0$ the entropy is that of a dilute gas of non-interacting quasi-particles with degenerate internal degree of freedom due to the anyons.

conclude from Eqs. (II.46), (II.47) that

$$
\begin{aligned}
f(\phi^{(m)}_{j_0}(\lambda_\delta)) &= \begin{cases} 1 & m=1, \\ 1 & m=2 \end{cases}, \qquad & f(\phi^{(m)}_{j_0}(\infty)) &= 0, \\
f(\phi^{(m)}_{j_1}(\lambda_\delta)) &= 0, & f(\phi^{(m)}_{j_1}(\infty)) &= 0, \\
f(\phi^{(m)}_{j_2}(\lambda_\delta)) &= \begin{cases} 0 & m=1, \\ 0 & m=2 \end{cases}, & f(\phi^{(m)}_{j_2}(\infty)) &= \frac{\sin(\frac{\pi}{N_f+3})\sin(\frac{2\pi}{N_f+3})}{\sin(\frac{j_2\pi}{N_f+3})\sin(\frac{(j_2+1)\pi}{N_f+3})},
\end{aligned}
$$

and therefore

$$\rho^{h(m)}_{j_0}(\lambda) = \rho^{(m)}_{j_1}(\lambda) = \rho^{(m)}_{j_2} = 0, \quad \text{for } |\lambda| < \lambda_\delta\,,$$

giving $\mathcal{S}^{(m)}_j(\lambda_\delta) = 0$ for all j, m. Using the relation (II.54) the low-temperature behavior of the entropy is found to be

$$\mathcal{S} = \frac{\pi}{3}\left(2 + \frac{6(N_f-1)}{N_f+3}\right)T = \frac{\pi}{3}\frac{8N_f}{N_f+3}T \tag{II.59}$$

in the phase with finite soliton density on both levels. The low-energy excitations near the Fermi points $\epsilon^{(m)}_{j_0}(\pm\Lambda_m) = 0$ of the soliton dispersion propagate with velocities $v^{(m)}_{\text{quark/antiquark}} = (\partial_\lambda\epsilon^{(1/2)}_{j_0})/(2\pi\rho^{(1/2)}_{j_0})\Big|_{\Lambda_{1/2}} \to 1$ for fields $H_m > H_{m,\delta}$ such that $\Lambda_m(H_{m,\delta}) > \lambda_\delta$. From this we conclude that the conformal field theory (CFT) describing the collective low-energy modes is the $\mathfrak{su}(3)$ WZNW model at level N_f or, by conformal embedding [54], a product of two free

$\mathfrak{u}(1)$ bosons (contributing $c = 2$ to the central charge) and the $SU(3)$ parafermionic coset $\mathfrak{su}(3)_{N_f}/\mathfrak{u}(1)^2$ with central charge ((I.81) with $N = 3$)

$$c = \frac{6(N_f - 1)}{N_f + 3}\,. \tag{II.60}$$

For the transition between this regime and the phases where the antiquarks are gapped, see Section 2.2.2, one has to resort to a numerical analysis of the TBA equations (II.46) again: in the case of equal fields, $H_1 \equiv H_2$, where the corresponding modes on the two levels are degenerate it is found that the solitons $\epsilon^{(m)}_{j_0}$ propagate with Fermi velocity v_{quark} while the auxiliary modes $\epsilon^{(m)}_{j_2}$ propagate with velocity v_{pf} (independent of $j_2 = 1, \ldots, N_f - 1$), see Figure 14 (a).

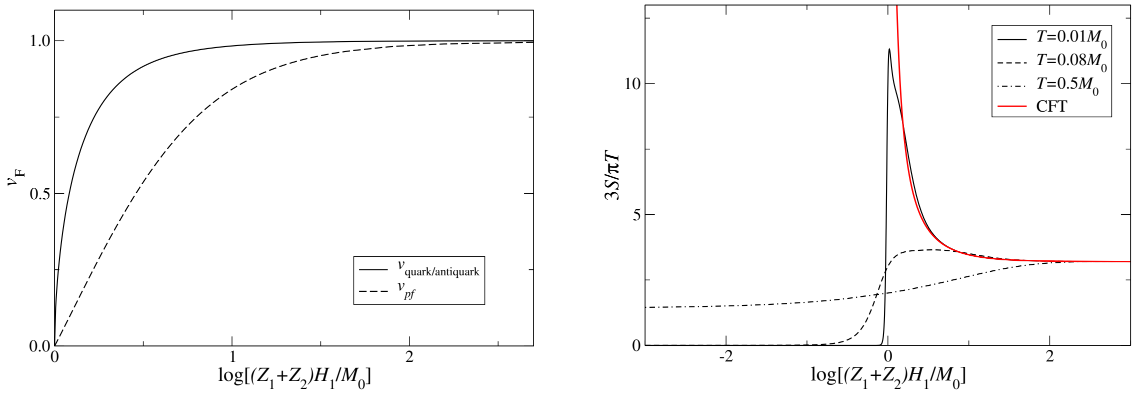

(a) **(b)**

Figure 14: (a) Fermi velocities of solitons and $\mathfrak{su}(3)$ parafermion modes as a function of the magnetic field $H_1 \equiv H_2 > M_0(Z_1 + Z_2)$ for $p_0 = 2 + 1/3$ at zero temperature. For large fields, $H_m > H_{m,\delta}$, both Fermi velocities converge to 1. (b) Same as Figure 13 (b) but for $H_1 \equiv H_2$. For fields large compared to the soliton mass, $(Z_1 + Z_2)H_1 \gg M_0$, the entropy approaches the expected analytical value (II.59) for a field theory with two free bosonic sectors and a $\mathfrak{su}(3)$ parafermion sector propagating with velocities $v_{\text{quark}} = v_{\text{antiquark}}$ and v_{pf}, respectively (full red line). For magnetic fields $zH < M_0$ and temperature $T \ll M_0$ the entropy is that of a dilute gas of non-interacting quasi-particles with degenerate internal degree of freedom due to the $\mathfrak{su}(3)_{N_f=2}$ anyons bound to the solitons.

As a consequence the contribution of the bosonic (quark/antiquark) and parafermionic degrees of freedom to the low-temperature entropy separate into

$$\mathcal{S} = \frac{\pi}{3}\left(\frac{2}{v_{\text{quark}}} + \frac{1}{v_{pf}}\frac{6(N_f - 1)}{N_f + 3}\right) T\,. \tag{II.61}$$

In Figure 14 (b) the computed entropy (II.57) for the $\mathfrak{su}(3)_{N_f=2}$ model with $\nu = 3$ is shown for various temperatures as a function of the fields $H_1 \equiv H_2$ together with the $T \to 0$ behavior (II.59) expected from conformal field theory.

Finally, in the regime $H_1 \geq H_2 \gtrsim M_0/(Z_1 + Z_2)$ the remaining degeneracy between the two levels is lifted. Quarks, antiquarks, and auxiliary modes are propagating with (generically) different Fermi velocities v_{quark}, $v_{\text{antiquark}}$, $v^{(1)}_{pf}$, and $v^{(2)}_{pf}$. The resulting low-temperature entropy behavior is found to be

$$\mathcal{S} = \frac{\pi}{3}\left(\frac{1}{v_{\text{quark}}} + \frac{1}{v_{\text{antiquark}}} + \frac{c_1}{v_{pf}^{(1)}} + \frac{c_2}{v_{pf}^{(2)}}\right)T,$$
$$c_1 = \frac{6(N_f-1)}{N_f+3} - \frac{2(N_f-1)}{N_f+2}\,, \quad c_2 = \frac{2(N_f-1)}{N_f+2}\,,$$

consistent with the conformal embedding [111]

$$\mathfrak{su}(3)_{N_f} = \mathfrak{u}(1)^2 + Z_{\mathfrak{su}(2)_{N_f}} + \frac{Z_{\mathfrak{su}(3)_{N_f}}}{Z_{\mathfrak{su}(2)_{N_f}}}\,.$$

Figure 15 shows the transition between the different regimes described above.

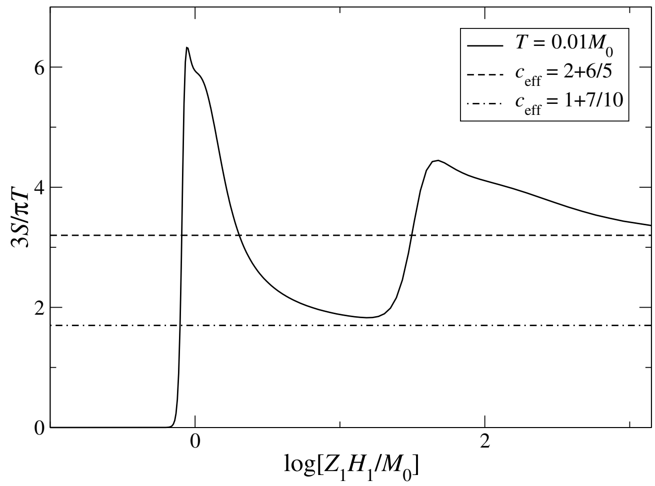

Figure 15: Same as Figure 13, but for fields along the line $\log(Z_2H_2/M_0) \equiv 0.4\log(Z_1H_1/M_0) - 2.58$. Transitions are observed at fields where the quarks and antiquarks condense, i.e. from the low-density phase of non-interacting anyons into the collective state described by the $\mathfrak{su}(3)_{N_f=2}/\mathfrak{su}(2)_{N_f=2}$ coset CFT and later into a phase whose low-energy description is in terms of the $\mathfrak{su}(3)_{N_f=2}$ WZNW model. The dashed-dotted lines indicate the corresponding central charges.

2.3. Phase diagram

The findings are summarized in a phase diagram based on the numerical analysis of the TBA equations (II.46), see Figure 16. For sufficiently small fields there is a dilute gas of anyons bound to the solitons in the system (regions I,II of Figure 16). By varying the magnetic fields the condensation of anyons can be driven into various collective states described by parafermionic cosets: the collective state describing the condensation of $[1,0]$ or $[1,1]$ $\mathfrak{su}(3)_{N_f}$ anyons is identified as the $Z_{\mathfrak{su}(3)_{N_f}}/Z_{\mathfrak{su}(2)_{N_f}}$ parafermion coset, while the condensation of a mixture of $[1,0]$ and $[1,1]$ $\mathfrak{su}(3)_{N_f}$ anyons results in a $Z_{\mathfrak{su}(3)_{N_f}}$ parafermionic theory. Other theories describing the condensation of $\mathfrak{su}(3)_{N_f}$ anyons are based on conformal embeddings, see Figure 16.

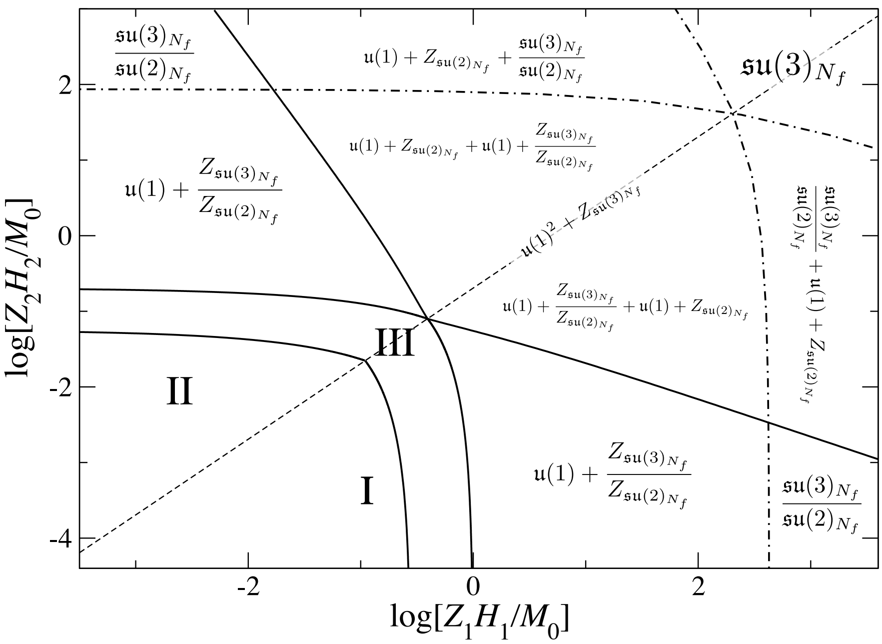

Figure 16: Contribution of the $\mathfrak{su}(3)_{N_f}$ anyons to the low-temperature properties of the model (II.35): using the criteria described in the main text the parameter regions are identified using analytical arguments for $T \to 0$ (the actual location of the boundaries is based on numerical data for $p_0 = 2+1/3$ and $T = 0.05/M_0$). For small fields (regions I,II) a gas of non-interacting quasi-particles with the anyon as an internal zero-energy degree of freedom bound to them is realized. Here the dashed line ($H_1 \equiv H_2$ or $\epsilon_j^{(1)} \equiv \epsilon_j^{(2)}$) indicates the crossover between regions where the quarks (region I) or antiquarks (region II) dominate the free energy. In region III the presence of thermally activated solitons with a small but finite density lift the degeneracy of the zero modes. The collective phases formed by condensed solitons are labelled by the corresponding CFT's providing the effective description of the low-energy excitations.

3. Perturbed $\mathfrak{so}(5)_{N_f}$ WZNW model

Following the ideas of the previous section an outlook is given for studying the condensation of $\mathfrak{so}(5)_{N_f}$ anyons in the framework of a perturbed $\mathfrak{so}(5)_{N_f}$ WZNW model. In Sec. II 3.1 the string solutions of the $SO(5)$ Bethe equations are discussed in the thermodynamic limit. The corresponding quasi-particles are found to carry quantum numbers in the fundamental representations with Young diagrams $[1,0]$ and $[1,1]$, which motivates calling them $[1,0]$- and $[1,1]$-solitons. By studying the thermodynamic Bethe ansatz for low-temperatures signatures of $\mathfrak{so}(5)_{N_f}$ anyons bound to the $[1,0]$- and $[1,1]$-solitons are observed. The density of them is varied by changing the external fields h_1, h_2 that couple to the currents of the Cartan subalgebra of $\mathfrak{so}(5)$. The findings, including the conformal field theories describing the interacting regimes, are summarized in a phase diagram in Sec. II 3.3.

3.1. Integrability study of perturbed $\mathfrak{so}(5)_{N_f}$ WZNW model

Fermionic models with $SO(5)$ symmetry have been investigated before using electronic-ladder models [113–116] and relativistic fermions [117]. Here an anisotropic generalization of the model discussed in [117] is studied at finite temperature, which is described by the massive sector of (II.5). The Hamiltonian density describing the free part can equivalently be written in terms of left- and right-moving fermion fields:

$$\mathcal{H}_{\text{free}} = -\mathrm{i}\sum_{j=1}^{N_f}\sum_{\alpha=1}^{5}(R^\dagger_{f\alpha}\partial_x R_{f\alpha} - L^\dagger_{f\alpha}\partial_x L_{f\alpha})\,.$$

Following [118] the interaction part of (II.5) in the isotropic case results in a current-current interaction. In the anisotropic case an integrable generalization of this is expected, which is referred to as $\mathcal{H}_{\text{int}}$. Together with the fields h_1 and h_2 coupling to the currents of the $\mathfrak{so}(5)$ Cartan-subalgebra the remaining terms of the Hamiltonian density become

$$\begin{aligned}\mathcal{H}_{\text{pert.}} &= \mathcal{H}_{\text{int}} + \mathcal{H}_{\text{fields}}\,,\\ \mathcal{H}_{\text{fields}} &= -\sum_{i=1}^{2} h_i(J^i + \bar{J}^i)\,,\end{aligned} \tag{II.62}$$

where J^i and $\bar{J}^i$ belong to the $\mathfrak{so}(5)_{N_f}$ Kac-Moody currents given by

$$\begin{aligned}J^i &= R^\dagger_{ak}(H^i_c)_{ab}R_{bk}\,, &\qquad J^\alpha &= R^\dagger_{ak}(E^\alpha)_{ab}R_{bk}\,,\\ \bar{J}^i &= L^\dagger_{ak}(H^i_c)_{ab}L_{bk}\,, &\qquad \bar{J}^\alpha &= L^\dagger_{ak}(E^\alpha)_{ab}L_{bk}\,,\end{aligned} \tag{II.63}$$

where H^i_c $(i = 1,2)$ are the generators of the $\mathfrak{so}(5)$ Cartan subalgebra and E^α denotes the ladder operator for the root α in the Cartan-Weyl basis ($1 \le a,b \le 5$ and $1 \le k \le N_f$ are the $SO(5)$ multiplet and flavor indices, respectively). In the previous sections non-Abelian bosonization was used to obtain the massive sector of the Hamiltonian density

$$\mathcal{H} = \mathcal{H}_{\text{free}} + \mathcal{H}_{\text{int}} + \mathcal{H}_{\text{fields}}\,. \tag{II.64}$$

Unfortunately, similar results are not known for $\mathcal{H}_{\text{free}}$ with $SO(5)\otimes SU(N_f)$ symmetry. Still it is conjectured that the effective Hamiltonian describing the massive sector of (II.64) is the

$\mathfrak{so}(5)_{N_f}$ WZNW model with a perturbation given by (II.62):

$$\begin{aligned} \mathcal{H}_{\text{massive}} &= \mathcal{H}[\mathfrak{so}(5)_{N_f}] + \mathcal{H}_{\text{int}} + \mathcal{H}_{\text{fields}}\,, \\ \mathcal{H}[\mathfrak{so}(5)_{N_f}] &= \frac{2\pi}{N_f+3}\left(:\mathbf{J}\cdot\mathbf{J}: + :\bar{\mathbf{J}}\cdot\bar{\mathbf{J}}:\right)\,, \end{aligned} \tag{II.65}$$

where $\mathbf{J}$, $\bar{\mathbf{J}}$ are currents with the components given by (II.63).

The spectrum of (II.65) can be obtained using Bethe ansatz methods under the assumption that the underlying structures coincide with those of an integrable anisotropic $SO(5)$ magnet with Dynkin label $(N_f,0)$ (cf. [118] for the isotropic case). Specifically, placing $\mathcal{N}$ fermions into a box of length L with periodic boundary conditions the energy eigenvalues in a particular sector of the Hilbert space specified by N_1, N_2 are

$$E = \sum_{j=1}^{\mathcal{N}/2} k_j^{(+)} - \sum_{j=1}^{\mathcal{N}/2} k_j^{(-)} + N_1 H_1 + N_2 H_2 - \mathcal{N}(H_1+H_2)\,, \tag{II.66}$$

where $k_j^{(\pm)}$ are the momenta of the fermions with $\pm$ chirality. The fields H_1, H_2 are linear combinations of the previous fields $H_1 \equiv \vec{\alpha}_1\cdot\vec{h}$, $H_2 \equiv \vec{\alpha}_2\cdot\vec{h}$, where $\vec{\alpha}_1$, $\vec{\alpha}_2$ are the simple roots of $\mathfrak{so}(5)$. The relativistic invariance of the fermion model is broken by the choice of boundary conditions but will be restored later by considering observables in the scaling limit $L,\mathcal{N}\to\infty$ and $g \ll 1$ such that the mass of the elementary excitations is small compared to the particle density $\mathcal{N}/L$.

The momenta of the energy eigenvalues (II.66) are parametrized by complex parameters $\lambda_\alpha^{(m)}$ with $\alpha = 1,\dots,N_m$ and $m = 1,2$ solving the hierarchy of Bethe equations (cf. Refs. [117, 119] for the isotropic case)

$$\begin{aligned} e^{\mathrm{i}k_j^{(\tau)}L} &= \prod_{\alpha=1}^{N_1} \frac{\sinh(\frac{\pi}{2p_0}(\lambda_\alpha - \tau/g + N_f\mathrm{i}))}{\sinh(\frac{\pi}{2p_0}(\lambda_\alpha - \tau/g - N_f\mathrm{i}))}\,, \\ \prod_{\tau=\pm1} e_{N_f}(\lambda_\alpha^{(1)}+\tau/g)^{\mathcal{N}/2} &= \prod_{\beta\neq\alpha}^{N_1} e_2(\lambda_\alpha^{(1)}-\lambda_\beta^{(1)}) \prod_{\beta=1}^{N_2} e_{-1}(\lambda_\alpha^{(1)}-\lambda_\beta^{(2)})\,,\quad \alpha = 1,\dots N_1\,, \\ \prod_{\beta=1}^{N_1} e_1(\lambda_\alpha^{(2)}-\lambda_\beta^{(1)}) &= \prod_{\beta\neq\alpha}^{N_2} e_1(\lambda_\alpha^{(2)}-\lambda_\beta^{(2)})\,,\quad \alpha = 1,\dots,N_2\,, \end{aligned} \tag{II.67}$$

where $e_k(x) = \sinh\left(\frac{\pi}{2p_0}(x+\mathrm{i}k)\right)/\sinh\left(\frac{\pi}{2p_0}(x-\mathrm{i}k)\right)$ and g, p_0 are functions of the coupling constants of $\mathcal{H}_{\text{int}}$. Written in terms of the Bethe roots the energy eigenvalues (II.66) become

$$E = \frac{\mathcal{N}}{L}\sum_{\alpha=1}^{N_1}\sum_{\tau=\pm1}\frac{\tau}{2\mathrm{i}}\ln\left(\frac{\sinh(\frac{\pi}{2p_0}(\lambda_\alpha^{(1)}+\tau/g-N_f\mathrm{i}))}{\sinh(\frac{\pi}{2p_0}(\lambda_\alpha^{(1)}+\tau/g+N_f\mathrm{i}))}\right) + N_1H_1 + N_2H_2 - \mathcal{N}\left(H_1+H_2\right)\,. \tag{II.68}$$

Based on equations (II.67), (II.68) the thermodynamics of the model can be studied provided that the solutions to the Bethe equations describing the eigenstates in the limit $\mathcal{N}\to\infty$ are known. Here it is argued that the root configurations corresponding to the ground state and excitations relevant for the low-temperature behavior of (II.65) can be built based on the string hypothesis for the $U_q(sl(2))$ models [74], i.e. that in the thermodynamic limit the

Bethe roots $\lambda_\alpha^{(m)}$ on both levels $m = 1, 2$ can be grouped into *j-strings* of length n_j and with parity $v_{n_j} \in \{\pm 1\}$

$$\lambda_{\alpha,j}^{(1)n} = \lambda_\alpha^{(1)n} + i\,(n + 1 - 2j) + \frac{p_0}{2}(1 - v_{N_f}^{(1)} v_n^{(1)}), \qquad j = 1, \ldots, n\,, \tag{II.69}$$

$$\lambda_{\alpha,j}^{(2)n} = \lambda_\alpha^{(2)n} + \frac{i}{2}\,(n + 1 - 2j) + \frac{p_0}{2}(1 - v_{2N_f}^{(2)} v_n^{(2)}), \qquad j = 1, \ldots, n \tag{II.70}$$

with real centers $\lambda_{j,\alpha}^{(m)} \in \mathbb{R}$. The allowed lengths and parities depend on the parameter p_0. Below the discussion is further simplified by assuming that $p_0 = N_f + 1/\nu$ with integer $\nu > 2$ where only a few string configurations are relevant for the low-temperature thermodynamics

$$\begin{aligned}
&n_{j_{2,1}}^{(1)} = j_{2,1}\,, && v_{j_{2,1}}^{(1)} = 1\,, && 1 \le j_{2,1} \le N_f - 1\,,\\
&n_{j_{2,2}}^{(2)} = j_{2,2}\,, && v_{j_{2,2}}^{(2)} = 1\,, && 1 \le j_{2,2} \le 2N_f - 1\,,\\
&n_{\tilde{j}_{0,1}}^{(1)} = N_f(\nu - 1) + 1\,, && v_{\tilde{j}_{0,1}}^{(1)} = (-1)^\nu\,, && \tilde{j}_{0,1} = N_f\,,\\
&n_{j_{0,1}}^{(1)} = N_f\,, && v_{j_{0,1}}^{(1)} = 1\,, && j_{0,1} = N_f + 1\,,\\
&n_{j_{0,2}}^{(2)} = 2N_f\,, && v_{j_{0,2}}^{(2)} = 1\,, && j_{0,2} = 2N_f + 1\,,
\end{aligned}$$

together with the string configuration for even ν

$$n_{\tilde{j}_{0,2}}^{(2)} = 2N_f(\nu/2 - 1) + 1\,, \quad v_{\tilde{j}_{0,2}}^{(2)} = (-1)^{\nu/2}\,, \qquad \tilde{j}_{0,2} = 2N_f\,.$$

Within the root density approach the Bethe equations are rewritten as coupled integral equations for the densities of these strings [107]. For vanishing external fields one finds that the Bethe root configuration corresponding to the lowest energy state is described by finite densities of $j_{0,m}$-strings on the levels $m = 1, 2$. The elementary excitations above this ground state are of three types: similar as for the discussion of the perturbed $\mathfrak{su}(3)_{N_f}$ WZNW model the excitations corresponding to holes in the distributions of $j_{0,m}$-strings on level $m = 1, 2$ are solitons. From their coupling to the fields it is found that they carry quantum numbers of the fundamental representations of $\mathfrak{so}(5)$ with Young diagrams $[1, 0]$ and $[1, 1]$, respectively. Hence, it will be referred to solitons of the first level as $[1, 0]$-solitons and to solitons of the second level as $[1, 1]$-solitons. The excitations corresponding to $j_{2,m}$-strings are denoted by auxiliary modes, while the contributions of breather excitations are assumed to be negligible for low temperatures.

The densities $\rho_j^{(m)}(\lambda)$ of these excitations (and $\rho_j^{h(m)}(\lambda)$ for the corresponding holes) satisfy the integral equations

$$\rho_k^{h(m)}(\lambda) = \rho_{0,k}^{(m)}(\lambda) - \sum_{l=1}^{2} \sum_j B_{kj}^{(m,l)} * \rho_j^{(l)} \qquad m = 1, 2\,, \tag{II.71}$$

see Appendix D. As mentioned above relativistic invariance is restored in the scaling limit $g \ll 1$ where the solitons are massive particles with bare densities $\rho_{0,j_{0,m}}^{(m)}$ and bare energies $\epsilon_{0,j_{0,m}}^{(m)}$

$$\rho_{0,j_{0,m}}^{(m)}(\lambda) \overset{g \ll 1}{=} \begin{cases} \frac{2\sqrt{3}M_0}{6} \cosh(\pi\lambda/3) & \text{if } m = 1\,,\\ \frac{2M_0}{6} \cosh(\pi\lambda/3) & \text{if } m = 2\,, \end{cases} \tag{II.72}$$

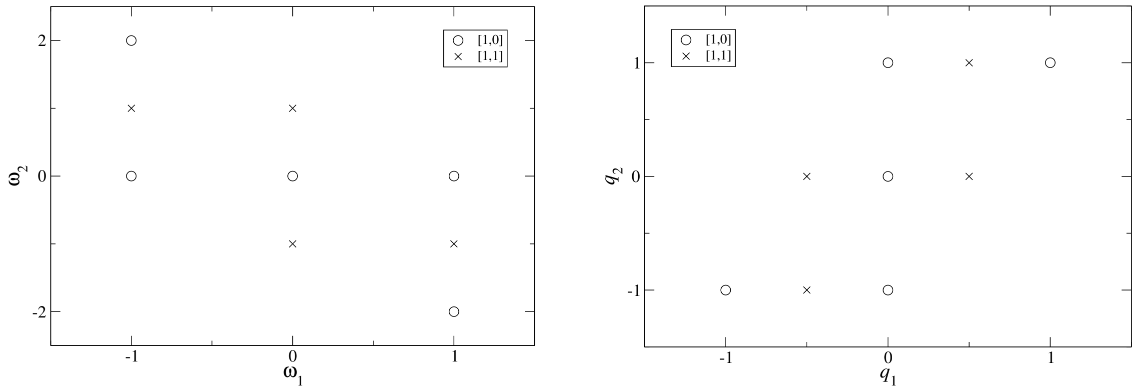

(a) weights

(b) charges

Figure 17: Relationship between the weights (a) of the $[1,0]$ (Dynkin labels $(1,0)$) and $[1,1]$ (Dynkin labels $(0,1)$) representation of $\mathfrak{so}(5)$ and the charges (b) determined by (II.74) with $H_1 = \vec{\alpha_1} \cdot \vec{h}$, $H_2 = \vec{\alpha_2} \cdot \vec{h}$.

$$\epsilon^{(m)}_{0,j_{0,m}}(\lambda) \overset{g \ll 1}{=} \begin{cases} 2\sqrt{3} M_0 \cosh(\pi\lambda/3) - zH_1 - zH_2 & \text{if } m = 1\,, \\ 2M_0 \cosh(\pi\lambda/3) - \frac{z}{2} H_1 - zH_2 & \text{if } m = 2\,, \end{cases} \tag{II.73}$$

where $z = (1 + N_f \nu)$. The prefactors $2\sqrt{3}M_0$ and $2M_0$ with $M_0 \equiv e^{-\pi/3g}$ are the masses of the $[1,0]$- and $[1,1]$-solitons, respectively. Furthermore, the corresponding charges can be read off from (II.73): for a general excitation with mass M and bare energy $\epsilon_0(\lambda)$ its charges (q_1, q_2) are defined by

$$\epsilon_0(\lambda) = M \cosh\left(\frac{\pi\lambda}{3}\right) - z \begin{pmatrix}\omega_1 \\ \omega_2\end{pmatrix} \cdot \begin{pmatrix} h_1 \\ h_2 \end{pmatrix} = M \cosh\left(\frac{\pi\lambda}{3}\right) - z \begin{pmatrix} q_1 \\ q_2 \end{pmatrix} \cdot \begin{pmatrix} H_1 \\ H_2 \end{pmatrix}\,, \tag{II.74}$$

where ω_1, ω_2 are the components of a weight in a $\mathfrak{so}(5)$ representation. Consequently, $[1,0]$-solitons of type $j_{0,1}$ carry the charge $(q_1, q_2) = (1, 1)$, while $[1,1]$-solitons of type $j_{0,2}$ carry the charge $(q_1, q_2) = (1/2, 1)$. These charges correspond to the highest weight states of the $[1,0]$ and $[1,1]$ representation of $\mathfrak{so}(5)$. All possible charges of $[1,0]$- and $[1,1]$-solitons are shown in Figure 17.

Similarly, the bare densities and energies of the $\tilde{j}_{0,m}$-strings are

$$\rho^{(m)}_{0,\tilde{j}_{0,m}}(\lambda) \overset{g \ll 1}{=} \begin{cases} \frac{2\sqrt{3}M_0}{6} \cosh(\pi\lambda/3) & \text{if } m = 1\,, \\ \frac{2M_0}{6} \cosh(\pi\lambda/3) & \text{if } m = 2\,, \end{cases} \tag{II.75}$$

$$\epsilon^{(m)}_{0,\tilde{j}_{0,m}}(\lambda) \overset{g \ll 1}{=} \begin{cases} 2\sqrt{3}M_0 \cosh(\pi\lambda/3) - zH_2 & \text{if } m = 1\,, \\ 2M_0 \cosh(\pi\lambda/3) - \frac{z}{2} H_1 & \text{if } m = 2\,. \end{cases} \tag{II.76}$$

The corresponding masses of these excitations coincide with the masses of the $[1,0]$- and $[1,1]$-solitons, respectively. However, they couple to these modes in a different way, i.e. $\tilde{j}_{0,1}$-strings carry the charge $(0,1)$ and $\tilde{j}_{0,2}$-strings the charge $(1/2, 0)$. Therefore, the excitations of type $\tilde{j}_{0,1}$ and $\tilde{j}_{0,2}$ are descendant states of the highest weight states in the $[1,0]$ and $[1,1]$ representation. From now on excitations of type $\{j_{0,1}, \tilde{j}_{0,1}\}$ are labeled as $[1,0]$-solitons while excitations of type $\{j_{0,2}, \tilde{j}_{0,2}\}$ are labeled as $[1,1]$-solitons. The masses and $\mathfrak{so}(5)$ charges of the auxiliary modes vanish, i.e. $\rho^{(m)}_{0,j_2}(\lambda) = 0 = \epsilon^{(m)}_{0,j_2}(\lambda)$.

The energy density of a macro-state with densities given by (II.71) is

$$\Delta\mathcal{E} = \sum_{m=1}^{2}\sum_{j}\int_{-\infty}^{\infty} \mathrm{d}\lambda\, \epsilon_{0,j}^{(m)}(\lambda)\rho_j^{(m)}(\lambda)\,. \tag{II.77}$$

Furthermore, it is convenient to define the masses $M_k^{(m)}$ of the different solitons as

$$M_k^{(m)} \equiv \begin{cases} 2\sqrt{3}M_0 & \text{if } m=1,\, k\in\{j_{0,1},\tilde{j}_{0,1}\}\,, \\ 2M_0 & \text{if } m=2,\, k\in\{j_{0,2},\tilde{j}_{0,2}\} \end{cases}.$$

3.2. Low-temperature thermodynamics

To derive the physical properties of the different quasi-particles appearing in the Bethe ansatz solution of the model (II.65) its low-temperature thermodynamics is studied. The equilibrium state at finite temperature is obtained by minimizing the free energy, $F/\mathcal{N} = \mathcal{E} - T\mathcal{S}$, with the combinatorial entropy [76]

$$\mathcal{S} = \sum_{j\geq 1}\int_{-\infty}^{+\infty} \mathrm{d}\lambda\, \left[(\rho_j+\rho_j^h)\ln(\rho_j+\rho_j^h) - \rho_j\ln\rho_j - \rho_j^h\ln\rho_j^h\right]\,. \tag{II.78}$$

The resulting thermodynamic Bethe ansatz (TBA) equations read

$$T\ln(1+e^{\epsilon_k^{(m)}/T}) = \epsilon_{0,k}^{(m)}(\lambda) + \sum_{l=1}^{2}\sum_{j\geq 1} B_{jk}^{(l,m)} * T\ln(1+e^{-\epsilon_j^{(l)}/T})\,, \tag{II.79}$$

where the dressed energies $\epsilon_j^{(m)}(\lambda)$ have been introduced through $e^{-\epsilon_j^{(m)}/T} = \rho_j^{(m)}/\rho_j^{h(m)}$. For studying the properties of free and interacting solitons it is convenient to rewrite the integral equations of the auxiliary modes: the auxiliary modes become independent of λ for $\epsilon_{j_{0,m}}^{(m)}(0)/T \to \infty$ as well as for finite λ with $\epsilon_{j_{0,m}}^{(m)}(0)/T \to \pm\infty$. In these cases the effective equations describing the auxiliary modes are

$$\begin{aligned} \epsilon_{j_{2,1}}^{(1)} =&\delta_{j_{2,1},N_f-1}T\ln\left(1+e^{-\epsilon_{j_{0,1}}^{(1)}/T}\right)^{\frac{1}{2}} + T\ln\left(1+e^{\epsilon_{j_{2,1}-1}^{(1)}/T}\right)^{\frac{1}{2}}\left(1+e^{\epsilon_{j_{2,1}+1}^{(1)}/T}\right)^{\frac{1}{2}} \\ &- T\ln\left(1+e^{-\epsilon_{2j_{2,1}-1}^{(2)}/T}\right)^{\frac{1}{2}}\left(1+e^{-\epsilon_{2j_{2,1}}^{(2)}/T}\right)\left(1+e^{-\epsilon_{2j_{2,1}+1}^{(2)}/T}\right)^{\frac{1}{2}}\,, \\ \epsilon_{j_{2,2}}^{(2)} =&\delta_{j_{2,2},2N_f-1}T\ln\left(1+e^{-\epsilon_{j_{0,2}}^{(2)}/T}\right)^{\frac{1}{2}} + T\ln\left(1+e^{\epsilon_{j_{2,2}-1}^{(2)}/T}\right)^{\frac{1}{2}}\left(1+e^{\epsilon_{j_{2,2}+1}^{(2)}/T}\right)^{\frac{1}{2}} \\ &- T\ln\left(1+e^{-\epsilon_{j_{2,2}/2}^{(1)}/T}\right)^{\frac{1}{2}}\,, \end{aligned} \tag{II.80}$$

where $\epsilon_0^{(1)} = \epsilon_0^{(2)} = -\infty$ and $\epsilon_{j_{2,2}/2}^{(1)} = \infty$ for odd $j_{2,2}$. In terms of the dressed energies the free energy per particle is

$$\begin{aligned} \frac{F}{\mathcal{N}} &= -T\sum_{m=1}^{2}\sum_{j\notin\{j_{2,m}\}}\int_{-\infty}^{\infty}\mathrm{d}\lambda\,\rho_{0,j}^{(m)}(\lambda)\ln(1+e^{-\epsilon_j^{(m)}(\lambda)/T}) \\ &\overset{g\ll 1}{=} -\frac{T}{6}\sum_{m=1}^{2}\sum_{j\notin\{j_{2,m}\}} M_j^{(m)}\int_{-\infty}^{\infty}\mathrm{d}\lambda\,\cosh(\pi\lambda/3)\ln(1+e^{-\epsilon_j^{(m)}(\lambda)/T})\,. \end{aligned} \tag{II.81}$$

Solving the equations (II.79) the spectrum of the model (II.65) for a given temperature T and fields H_1, H_2 is obtained. From the expressions (II.73) and (II.76) for the bare energies of the elementary excitations the qualitative behavior of these modes at low temperatures can be deduced: as long as $zH_2 < \min\left(2\sqrt{3}M_0 - zH_1,\, 2M_0 - zH_1/2\right)$ solitons remain gapped. By increasing the field H_1 (above $zH_1 \geq 2\sqrt{3}M_0 - zH_2$) for sufficiently small H_2 ($zH_2 < (4-2\sqrt{3})M_0$) the gap of the $[1,0]$-solitons closes and they condense into a phase with finite density. The gap of the $[1,1]$-solitons, on the other hand, remains open until $zH_1 \gg M_0$, see Figure 18 (a) for the $T=0$ spectrum with $H_2 \equiv 0$.

Similarly, for sufficiently small H_1 ($zH_1 < 4(\sqrt{3}-1)M_0$) increasing the field H_2 (above $zH_2 \geq 2M_0 - zH_1/2$) closes the gap of the $[1,1]$-solitons, while the gap of the $[1,0]$-solitons remains open until $zH_2 \gg M_0$, see Figure 18 (b) for the $T=0$ spectrum with $H_1 \equiv 0$. Figure 19 shows the case, where the gap of $[1,0]$- and $[1,1]$-solitons closes simultaneously.

Notice that the string hypothesis (II.69) does not capture all solitons of the $[1,0]$ and $[1,1]$ multiplet that may occur. However, from their coupling to the field the energy gaps of all $[1,0]$- and $[1,1]$-solitons can be predicted in the non-interacting regime, see Figures 18,19. Below the temperature is chosen sufficiently small such that only the solitons corresponding to the highest weight states of the $[1,0]$ and $[1,1]$ multiplet, i.e. excitations of type $j_{0,m}$, contribute to the thermodynamics.

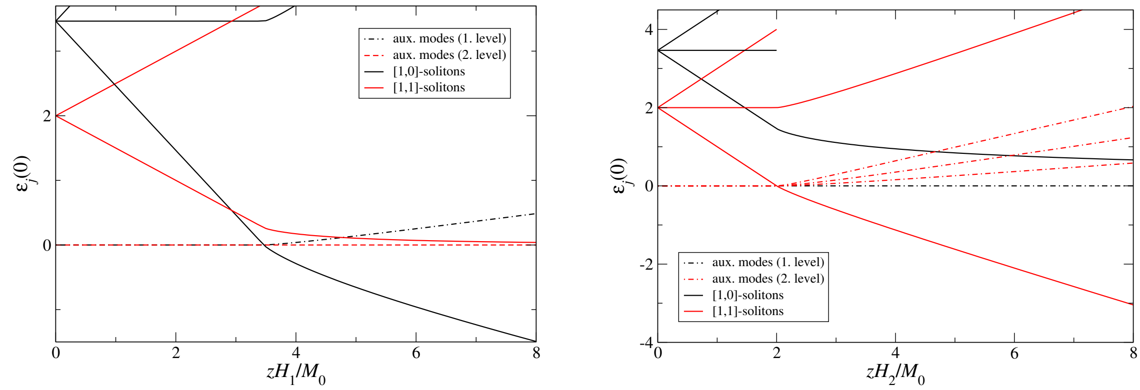

Figure 18: The zero temperature spectrum of elementary excitations (and Fermi energy of solitons in the condensed phase) $\epsilon_j^{(m)}(0)$ obtained from the numerical solution of (II.79) for $p_0 = 2 + 1/3$ as a function of the field H_1 with fixed $H_2 = 0$ (a) or as a function of H_2 with $H_1 = 0$ (b). Once the gap of $[1,0]$-solitons in (a) or $[1,1]$-solitons in (b) closes the system forms a collective state of these objects. In this phase the degeneracy of the auxiliary modes is lifted. In the limit $zH_1 \gg M_0$ the gap of $[1,1]$-solitons (with charges $(1/2,1)$ and $(1/2,0)$) closes as well in (a). Similarly, for $zH_2 \gg M_0$ the gap of $[1,0]$-solitons (with charges $(1/2,1)$ and $(1/2,0)$) closes in (b).

3.2.1. Non-interacting solitons

For fields $zH_2 < \min\left(2\sqrt{3}M_0 - zH_1, 2M_0 - zH_1/2\right)$ temperatures below the gaps of the solitons are considered, i.e. $T \ll \min\left(\epsilon^{(1)}_{0,j_{0,1}}(0),\, \epsilon^{(2)}_{0,j_{0,2}}(0)\right)$. Analogously to [39, 52, 53] the nonlinear integral equations (II.79) can be solved iteratively in this regime: the energies $\epsilon_k^{(m)}$ of solitons are well described by their first order approximation while those of the auxiliary modes can be replaced by the asymptotic solution for $|\lambda| \to \infty$, see Table 2 for $2 \leq N_f \leq 5$.

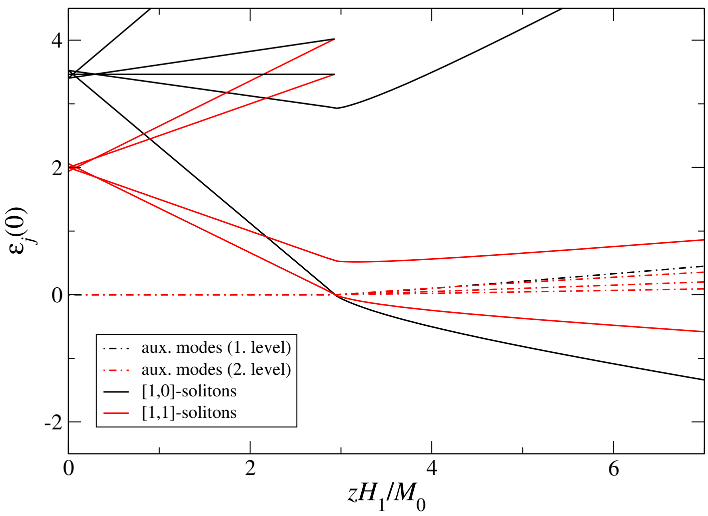

Figure 19: The zero temperature spectrum of excitations (and Fermi energy of $[1,0]$- and $[1,1]$-solitons for $zH_1 > \left(4\sqrt{3}-4\right) M_0 \approx 2.93 M_0$, respectively) $\epsilon_j^{(m)}(0)$ obtained from the numerical solution of (II.79) as a function of the field H_1 for $p_0 = 2 + 1/3$ and fixed $zH_2/M_0 = -0.06 + 0.21 zH_1/M_0$. For $zH_1 = \left(4\sqrt{3}-4\right) M_0$ the gaps of the $[1,0]$- and $[1,1]$-solitons ($\epsilon_{j_{0,m}}^{(m)}(0)$) close and the degeneracy of the auxiliary modes is lifted.

N_f	$\left\{\exp\left(-\epsilon_{j_{2,1}}^{(1)}/T\right)\right\}_{j_{2,1}=1}^{N_f-1}$	$\left\{\exp\left(-\epsilon_{j_{2,2}}^{(2)}/T\right)\right\}_{j_{2,2}=1}^{2N_f-1}$
2	3	$\frac{2}{3}$, $\frac{4}{5}$, $\frac{2}{3}$
3	$\sqrt{3}$, $\sqrt{3}$	$\frac{1}{\sqrt{3}}$, $\frac{1}{2}$, $\frac{1}{3}$, $\frac{1}{2}$, $\frac{1}{\sqrt{3}}$
4	1.34601, 0.91557, 1.34601	0.53679, 0.40477, 0.24991, 0.27673, 0.24991, 0.40477, 0.53679
5	1.16591, 0.66818, 0.66818, 1.16591	0.51415, 0.35935, 0.21297, 0.20711, 0.17157, 0.20711, 0.21297, 0.35935, 0.51415

Table 2: Asymptotic solution ($|\lambda| \to \infty$) of auxiliary modes ($\epsilon_{j_{2,m}}^{(m)}/T \equiv \epsilon_{j_{2,m}}^{(m)}(\lambda \to \infty)/T$) for $2 \leq N_f \leq 5$ derived numerically from the equations II.80 with $\epsilon_{j_{0,m}}^{(m)}/T = \infty$.

For the other modes

$$\epsilon_j^{(m)}(\lambda) = \epsilon_{0,j}^{(m)}(\lambda) - T \ln Q_j^{(m)}$$

is obtained for $m = 1$, $j \in \{j_{0,1}, \tilde{j}_{0,1}\}$ and $m = 2$, $j \in \{j_{0,2}, \tilde{j}_{0,2}\}$ resulting in the free energy

$$\frac{F}{\mathcal{N}} = -\sum_{m=1}^{2} \sum_{j \notin \{j_{2,m}\}} T Q_j^{(m)} \int \frac{\mathrm{d}p}{2\pi} e^{-\epsilon_{0,j}^{(m)}(0)/T - p^2/2M_j^{(m)}T}, \tag{II.82}$$

where $Q_k^{(m)}$ ($k \neq j_{2,m}$) depends on the asymptotic solution of the auxiliary modes

$$Q_k^{(m)} = \prod_{i=1}^{2} \prod_{j_{2,i}} \left(1 + e^{-\epsilon_{j_{2,i}}^{(i)}/T}\right)^{-B_{j_{2,m}k}^{(i,m)}(0)}. \tag{II.83}$$

See Table 3 for explicit values of $Q_k^{(m)}$ for $2 \leq N_f \leq 5$.

N_f	$Q^{(1)}$	$Q^{(2)}$
2	2	$\sqrt{5}$
3	$1+\sqrt{3}$	$1+\sqrt{3}$
4	$2+\sin\left(\frac{3\pi}{14}\right)$	$\frac{1}{2\sin\left(\frac{3\pi}{14}\right)-1}$
5	$1+\sqrt{4+2\sqrt{2}}$	$\sqrt{2}+\sqrt{2+\sqrt{2}}$

Table 3: Internal degrees of freedom of $[1,0]$-solitons ($Q^{(1)} \equiv Q^{(1)}_{j_{0,1}}$) and $[1,1]$-solitons ($Q^{(2)} \equiv Q^{(2)}_{j_{0,2}}$) derived from (II.83) using the asymptotic solutions of the auxiliary modes (see Table 2).

Following [39, 52] each of the terms appearing in II.82 is the free energy of an ideal gas of particles with the corresponding mass carrying an internal degree of freedom with possibly non-integer quantum dimension $Q_k^{(m)}$ for the solitons. It is found that solitons of the same multiplet carry the same quantum dimension, i.e. $Q^{(m)} \equiv Q^{(m)}_{j_{0,m}} = Q^{(m)}_{\tilde{j}_{0,m}}$. The densities of the solitons

$$n_j^{(m)} = Q^{(m)} \sqrt{\frac{M_j^{(m)} T}{2\pi}} e^{-\epsilon_{0,j}^{(m)}(0)/T}\,, \tag{II.84}$$

derived from the free energy (II.82) for $j \in \{j_{0,m}, \tilde{j}_{0,m}\}$, can be controlled by variation of the temperature and the fields.

In order to identify the quantum dimensions $Q_k^{(m)}$ with the quantum dimensions of $\mathfrak{so}(5)_{N_f}$ anyons the topological charges are written in terms of Young diagrams: given the $\mathfrak{so}(5)$ Cartan-Matrix

$$A_{ij} = \begin{pmatrix} 2 & -2 \\ -1 & 2 \end{pmatrix}$$

and the condition (I.56) it can be shown that irreducible representations of the affine Lie algebra $\mathfrak{so}(5)_{N_f}$, and therefore also the topological charges, can be labeled by Dynkin labels m_1, m_2 satisfying

$$m_1 + m_2 \leq N_f\,.$$

In terms of Young diagrams this results in the following allowed set of topological charges for $N_f = 2$

$$\text{labels} = \{[0,0],\ [1,1],\ [1,0],\ [2,1],\ [2,0],\ [2,2]\}\,.$$

The corresponding fusion rules can be found in [120] using the identification

$$\psi_1 = [0,0],\ \psi_2 = [1,1],\ \psi_3 = [1,0],\ \psi_4 = [2,1],\ \psi_5 = [2,0],\ \psi = [2,2]\,.$$

Notice that these fusion rules are consistent with the tensor product reductions of $\mathfrak{so}(5)$ irreducible representations with reasonable modifications due to the level $N_f = 2$ [8]. The

[8] An elegant graphical method for deriving tensor product reductions for Lie algebras with rank $r \leq 2$ can be found in [121].

quantum dimensions extracted from the fusion rules for $N_f = 2$ are given by

$$d([0,0]) = d([2,2]) = 1,\ d([1,1]) = d([2,0]) = 2,\ d([1,0]) = d([2,1]) = \sqrt{5}\,.$$

Therefore, the appearance of the internal degrees of freedom, $Q^{(1)}$ and $Q^{(2)}$, can be interpreted as $[1,1]$ or $[2,0]$ anyons being bound to the $[1,0]$-solitons and $[1,0]$ or $[2,1]$ anyons being bound to the $[1,1]$-solitons.

For $N_f > 2$ this identification cannot be done, since the fusion rules and quantum dimensions of $\mathfrak{so}(5)_{N_f>2}$ anyons have not yet been derived. However, following the results from the perturbed $\mathfrak{su}(3)_{N_f}$ WZNW model it is conjectured that the internal degrees of freedom, $Q^{(1)}$ and $Q^{(2)}$, coincide with the quantum dimensions of $[1,1]$ and $[1,0]$ anyons for arbitrary $N_f \geq 2$, respectively.

The densities of $[1,1]$ and $[1,0]$ anyons appearing in the one-dimensional model are determined by the densities of the corresponding solitons (II.84). For fields satisfying

$$zH_1 > (4\sqrt{3}-4)M_0 - 2T\log\left(3^{1/4}\frac{Q^{(1)}}{Q^{(2)}}\right)$$

the dominant contribution to F is that of the $[1,0]$-solitons with $[1,1]$ anyons being bound to them. In the remaining region of non-interacting solitons the $[1,1]$-solitons with $[1,0]$ anyons bound to them are the dominant excitations.

3.2.2. Condensate of $[1,0]$-solitons

For fields $zH_2 < (4-2\sqrt{3})M_0$, $zH_1 > 2\sqrt{3}M_0 - zH_2$ and temperatures $T \ll zH_1 + zH_2 - 2\sqrt{3}M_0$ the $[1,0]$-solitons (of type $j_{0,1}$) form a condensate, while the contribution to the free energy of the other quasi-particles can be neglected. Following [71] we observe that the dressed energies and densities can be related as

$$\begin{aligned}
\rho_j^{(m)}(\lambda) &= (-1)^{\delta_{j\in\{j_{2,m}\}}}\frac{1}{2\pi}\frac{\mathrm{d}\epsilon_j^{(m)}(\lambda)}{\mathrm{d}\lambda} f\left(\frac{\epsilon_j^{(m)}(\lambda)}{T}\right),\\
\rho_j^{h(m)}(\lambda) &= (-1)^{\delta_{j\in\{j_{2,m}\}}}\frac{1}{2\pi}\frac{\mathrm{d}\epsilon_j^{(m)}(\lambda)}{\mathrm{d}\lambda}\left(1 - f\left(\frac{\epsilon_j^{(m)}(\lambda)}{T}\right)\right),
\end{aligned} \tag{II.85}$$

for $\lambda > \lambda_\delta$ with $\exp(\pi\lambda_\delta/3) \gg 1$, where $f(\epsilon) = (1+e^\epsilon)^{-1}$ is the Fermi function. Inserting this into (II.78) we get ($\phi_j^{(m)} = \epsilon_j^{(m)}/T$)

$$\begin{aligned}
\mathcal{S} = &-\frac{T}{\pi}\sum_{m,j}(-1)^{\delta_{j\in\{j_{2,m}\}}}\int_{\phi_j^{(m)}(\lambda_\delta)}^{\phi_j^{(m)}(\infty)}\mathrm{d}\phi_j^{(m)}\,\left[f(\phi_j^{(m)})\ln f(\phi_j^{(m)}) + (1-f(\phi_j^{(m)}))\ln(1-f(\phi_j^{(m)}))\right]\\
&+\sum_{m,j}\mathcal{S}_j^{(m)}(\lambda_\delta)\,,\\
\mathcal{S}_j^{(m)}(\lambda_\delta) \equiv &\int_{-\lambda_\delta}^{\lambda_\delta}\mathrm{d}\lambda\,\left[(\rho_j^{(m)}+\rho_j^{h(m)})\ln(\rho_j^{(m)}+\rho_j^{h(m)}) - \rho_j^{(m)}\ln\rho_j^{(m)} - \rho_j^{h(m)}\ln\rho_j^{h(m)}\right]\,.
\end{aligned} \tag{II.86}$$

The integrals over $\phi_j^{(m)}$ can be performed giving

$$\mathcal{S} = \sum_{m,j}\mathcal{S}_j^{(m)}(\lambda_\delta) - \frac{2T}{\pi}\sum_{m,j}(-1)^{\delta_{j\in\{j_{2,m}\}}}[L(f(\phi_j^{(m)}(\infty)) - L(f(\phi_j^{(m)}(\lambda_\delta)))] \tag{II.87}$$

in terms of the Rogers dilogarithm $L(x)$

$$L(x) = -\frac{1}{2}\int_0^x \mathrm{d}y \left(\frac{\ln y}{1-y} + \frac{\ln(1-y)}{y}\right) .$$

For large fields $zH_1 \gg 2\sqrt{3}M_0 - zH_2 \log((zH_1 + zH_2)/2\sqrt{3}M_0) > \lambda_\delta \gg 1$ holds, which implies using (II.79), (II.80)

$$\begin{aligned}
&f(\phi^{(m)}_{j_{0,m}}(\lambda_\delta)) = \begin{cases} 1 & m=1\,, \\ 0 & m=2 \end{cases} , && f(\phi^{(m)}_{j_{0,m}}(\infty)) = 0\,, \\
&f(\phi^{(m)}_{\tilde{j}_{0,m}}(\lambda_\delta)) = 0\,, && f(\phi^{(m)}_{\tilde{j}_{0,m}}(\infty)) = 0\,, \\
&f(\phi^{(m)}_{j_{2,m}}(\lambda_\delta)) = \begin{cases} 0 & m=1 \\ \left(\frac{\sin\left(\frac{\pi}{2N_f+2}\right)}{\sin\left(\frac{\pi(j_{2,2}+1)}{2N_f+2}\right)}\right)^2 & m=2 \end{cases} .
\end{aligned} \tag{II.88}$$

For the remaining term, $f(\phi^{(m)}_{j_{2,m}}(\infty))$, an analytical expression is not known. However, it can be computed numerically using the results for the asymptotic behavior of the auxiliary modes from Table 2. From (II.88) one can further conclude that the densities for $|\lambda| < \lambda_\delta$ are given by

$$\rho^{h(1)}_{j_{0,1}}(\lambda) = \rho^{(2)}_{j_{0,2}}(\lambda) = \rho^{(m)}_{\tilde{j}_{0,m}}(\lambda) = \rho^{(1)}_{j_{2,1}} = 0, \quad \rho^{(2)}_{j_{2,2}}(\lambda) = e^{-\epsilon^{(2)}_{j_{2,2}}/T}\rho^{h(2)}_{j_{2,2}}(\lambda)\,,$$

where $e^{-\epsilon^{(2)}_{j_{2,2}}/T} = \text{const.}$ for $|\lambda| < \lambda_\delta$. Since the integral equations (II.71) for $\rho^{h(2)}_{j_{2,2}}$ simplify in this regime to

$$\rho^{h(2)}_{j_{2,2}} = -\sum_{k_{2,2}} B^{(2,2)}_{j_{2,2}k_{2,2}} * e^{-\epsilon^{(2)}_{k_{2,2}}/T}\rho^{h(2)}_{k_{2,2}} \qquad \text{for } |\lambda| < \lambda_\delta,$$

one can conclude that $\rho^{h(2)}_{j_{2,2}} \to 0$, $\rho^{(2)}_{j_{2,2}} \to 0$ such that $\rho^{(2)}_{j_{2,2}}/\rho^{h(2)}_{j_{2,2}} = e^{-\epsilon^{(2)}_{j_{2,2}}/T} = \text{const.}$ Consequently, $\mathcal{S}^{(m)}_j(\lambda_\delta) = 0$ for all j, m is obtained. Using $L(1) = \pi^2/6$ and the Rogers dilogarithm identity (II.30) it is found that

$$\sum_{j_{2,2}} L\left(f(\phi^{(2)}_{j_{2,2}}(\lambda_\delta))\right) = \frac{\pi^2}{6}\left(\frac{3N_f}{N_f+1} - 1\right) .$$

In general Rogers dilogarithm identities giving the relationship between Lie algebras and central charges of parafermion conformal field theories have only been proven for the simply laced case [122]. However, for the non-simply laced Lie algebra $\mathfrak{so}(5)$ similar relations can be verified numerically

$$\sum_{m=1}^{2}\sum_{j_{2,m}} L\left(f(\phi^{(m)}_{j_{2,m}}(\infty))\right) = \frac{\pi^2}{6}\left(\frac{10N_f}{N_f+3} - 2\right) . \tag{II.89}$$

Hence, the following low-temperature behavior of the entropy

$$\mathcal{S} = \frac{\pi}{3}\left(\frac{10N_f}{N_f+3} - \frac{3N_f}{N_f+1}\right) T \tag{II.90}$$

is obtained, which is consistent with a conformal field theory describing the collective modes given by the coset $\mathfrak{so}(5)_{N_f}/\mathfrak{so}(3)_{N_f}$ with central charge

$$c = \frac{10N_f}{N_f+3} - \frac{3N_f}{N_f+1} \,.$$

Using the conformal embedding

$$\frac{\mathfrak{so}(5)_{N_f}}{\mathfrak{so}(3)_{N_f}} = \mathfrak{u}(1) + \frac{Z_{\mathfrak{so}(5)_{N_f}}}{Z_{\mathfrak{so}(3)_{N_f}}}, \tag{II.91}$$

where $Z_{\mathfrak{so}(2p+1)_{N_f}} = \mathfrak{so}(2p+1)_{N_f}/\mathfrak{u}(1)^p$ denotes generalized parafermions [54], the collective modes can equivalently be described by a product of a free $\mathfrak{u}(1)$ boson and a parafermion coset $Z_{\mathfrak{so}(5)_{N_f}}/Z_{\mathfrak{so}(3)_{N_f}}$ contributing $c=1$ and

$$c = \frac{8N_f-6}{N_f+3} - \frac{2N_f-1}{N_f+1} \,.$$

Notice that for $N_f = 2$ the central charge of the coset $Z_{\mathfrak{so}(5)_{N_f}}/Z_{\mathfrak{so}(3)_{N_f}}$ is $c=1$, which is consistent with the results for interacting chains of $[1,1]$ $\mathfrak{so}(5)_{N_f}$ anyons [120].

Following [52] the entropy $\mathcal{S} = -\frac{\mathrm{d}}{\mathrm{d}T}\frac{F}{N}$ is computed numerically to study the transition from free anyons to a condensate of anyons. In the region $2\sqrt{3}M_0 - zH_2 \lesssim zH_1$ the entropy deviates from the asymptotic expression (II.90): in this range of H_1 the auxiliary modes of the first level propagate with a velocity (independent of $j_{2,1}$) differing from that of the $[1,0]$-solitons, $v_{[1,0]}$, namely

$$v_{[1,0]} = \left.\frac{\partial_\lambda \epsilon^{(1)}_{j_{0,1}}(\lambda)}{2\pi\rho^{(1)}_{j_{0,1}}(\lambda)}\right|_{\Lambda_1}, \quad v^{(1)}_{pf} = -\left.\frac{\partial_\lambda \epsilon^{(1)}_{j_{2,1}}(\lambda)}{2\pi\rho^{h(1)}_{j_{2,1}}(\lambda)}\right|_{\lambda\to\infty},$$

where Λ_1 denotes the Fermi point of $[1,0]$-solitons defined by $\epsilon^{(1)}_{j_{0,1}}(\pm\Lambda_1) = 0$. Also notice that Fermi velocities of the second level do not exist in this regime. As a consequence the bosonic (spinon) and parafermionic degrees of freedom in the first level separate and the low-temperature entropy is

$$\mathcal{S} = \frac{\pi}{3}\left(\frac{1}{v_{[1,0]}} + \frac{1}{v^{(1)}_{pf}}\left(\frac{8N_f-6}{N_f+3} - \frac{2N_f-1}{N_f+1}\right)\right) T \,. \tag{II.92}$$

This behavior can be explained by the conformal embedding (II.91). Note that both Fermi velocities depend on the field H_1 and approach 1 as $H_1 \gtrsim H_{1,\delta}$ such that $\Lambda_1(H_{1,\delta}) > \lambda_\delta$, see Figure 20 (a), giving the entropy (II.90) of the coset $\mathfrak{so}(5)_{N_f}/\mathfrak{so}(3)_{N_f}$. In Figure 20 the computed entropy is shown for $T = 0.02M_0$ as a function of the field H_1 together with the $T \to 0$ behavior (II.92) expected from conformal field theory.[9]

[9] Actually, this behavior can only be seen for temperatures $T < 0.02M_0$, which was not accessible by available numerical methods. To overcome this problem the entropy for $T = 0.02M_0$ was computed, while already neglecting the contribution of $\epsilon^{(2)}_{j_{0,2}}$ in the integral equations (II.79).

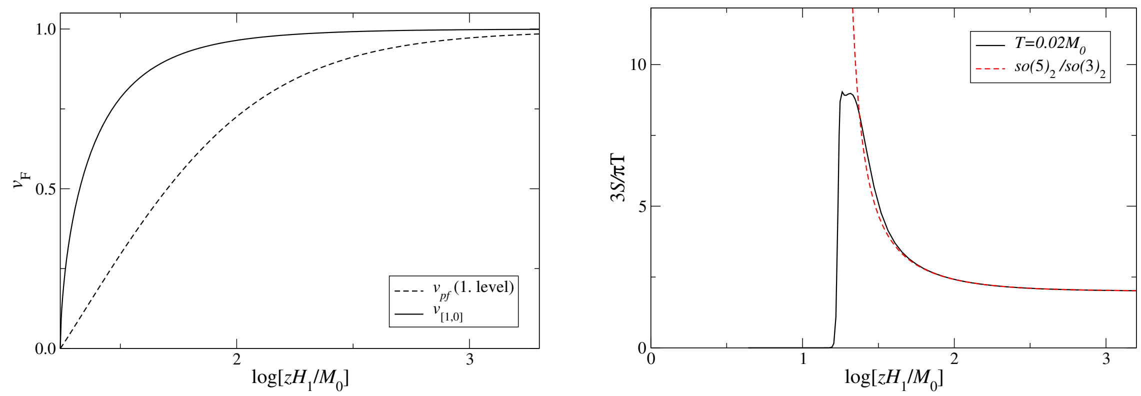

(a) **(b)**

Figure 20: (a) Fermi velocities of the $[1,0]$-solitons and first level parafermion modes as a function of the field zH_1/M_0 for $p_0 = 2+1/3$, $H_2 \equiv 0$ at zero temperature. For large field, $H_1 > H_{1,\delta}$, both Fermi velocities approach 1 leading to the asymptotic result for the low-temperature entropy (II.90). (b) Entropy obtained from numerical solution of the TBA equations (II.79) for $p_0 = 2+1/3$ and $H_2 \equiv 0$ as a function of the field zH_1/M_0 for $T = 0.02M_0$. For fields large compared to the $[1,0]$-soliton mass, $zH_1 \gg 2\sqrt{3}M_0$, the entropy approaches the expected analytical value (II.90) for a field theory with a free bosonic sector and a $Z_{\mathfrak{so}(5)_{N_f}}/Z_{\mathfrak{so}(3)_{N_f}}$ parafermion sector propagating with velocities $v_{[1,0]}$ and $v_{pf}^{(1)}$, respectively (full red line). For magnetic fields $zH_1 < 2\sqrt{3}M_0$ and temperature $T \ll 2\sqrt{3}M_0$ the entropy is that of a dilute gas of non-interacting quasi-particles with degenerate internal degree of freedom due to the anyons.

3.2.3. Condensate of $[1,1]$-solitons

For fields $zH_1 < (4\sqrt{3}-4)M_0$, $zH_2 > 2M_0 - zH_1/2$ and temperatures $T \ll zH_1/2 + zH_2 - 2M_0$ the $[1,1]$-solitons (of type $j_{0,2}$) form a condensate, while the contribution to the free energy of the other quasi-particles can be neglected. For large fields $zH_2 \gg 2M_0 - zH_1/2 \ll zH_2$ $\log((zH_1/2 + zH_2)/2M_0)) > \lambda_\delta \gg 1$ holds, which implies using (II.79)

$$
\begin{aligned}
f(\phi^{(m)}_{j_{0,m}}(\lambda_\delta)) &= \begin{cases} 0 & m = 1\,, \\ 1 & m = 2 \end{cases}, \qquad & f(\phi^{(m)}_{j_{0,m}}(\infty)) &= 0\,, \\
f(\phi^{(m)}_{\tilde{j}_{0,m}}(\lambda_\delta)) &= 0\,, & f(\phi^{(m)}_{\tilde{j}_{0,m}}(\infty)) &= 0\,, \\
f(\phi^{(m)}_{j_{2,m}}(\lambda_\delta)) &= \begin{cases} \left(\dfrac{\sin\left(\frac{\pi}{N_f+2}\right)}{\sin\left(\frac{\pi(j_{2,1}+1)}{N_f+2}\right)}\right)^2 & m = 1 \\ 0 & m = 2 \end{cases}
\end{aligned}
\tag{II.93}
$$

together with the numerical expressions for $f(\phi^{(m)}_{j_{2,m}}(\infty))$ using the asymptotic behavior of the auxiliary modes from Table 2. The densities for $|\lambda| < \lambda_\delta$ following from (II.93) are

$$
\rho^{h(2)}_{j_{0,2}}(\lambda) = \rho^{(1)}_{j_{0,1}}(\lambda) = \rho^{(m)}_{\tilde{j}_{0,m}}(\lambda) = \rho^{(2)}_{j_{2,2}} = 0, \quad \rho^{(1)}_{j_{2,1}}(\lambda) = e^{-\epsilon^{(1)}_{j_{2,1}}/T}\rho^{h(1)}_{j_{2,1}}(\lambda)\,,
$$

where $e^{-\epsilon^{(1)}_{j_{2,1}}/T} = \text{const.}$ for $|\lambda| < \lambda_\delta$. Since the integral equations (II.71) for $\rho^{h(1)}_{j_{2,1}}$ simplify in this regime to

$$
\rho^{h(1)}_{j_{2,1}} = -\sum_{k_{2,1}} B^{(1,1)}_{j_{2,1}k_{2,1}} * e^{-\epsilon^{(1)}_{k_{2,1}}/T}\rho^{h(1)}_{k_{2,1}} \qquad \text{for } |\lambda| < \lambda_\delta,
$$

one can conclude that $\rho^{h(1)}_{j_{2,1}} \to 0$, $\rho^{(1)}_{j_{2,1}} \to 0$ such that $\rho^{(1)}_{j_{2,1}}/\rho^{h(1)}_{j_{2,1}} = e^{-\epsilon^{(1)}_{j_{2,1}}/T} = \text{const}$. Consequently, $\mathcal{S}^{(m)}_j(\lambda_\delta) = 0$ for all j, m is obtained. Using $L(1) = \pi^2/6$ and the Rogers dilogarithm identity (II.30) the relation for $Z_{\mathfrak{su}(2)_{N_f}}$ parafermions is found:

$$\sum_{j_{2,1}} L\left(f(\phi^{(1)}_{j_{2,1}}(\lambda_\delta))\right) = \frac{\pi^2}{6}\left(\frac{3N_f}{N_f+2} - 1\right)$$

Hence, the following low-temperature behavior of the entropy is obtained using (II.89)

$$\mathcal{S} = \frac{\pi}{3}\left(\frac{10N_f}{N_f+3} - \frac{3N_f}{N_f+2}\right)T, \tag{II.94}$$

which is consistent with a conformal field theory describing the collective modes given by the coset $\mathfrak{so}(5)_{N_f}/\mathfrak{su}(2)_{N_f}$ with central charge

$$c = \frac{10N_f}{N_f+3} - \frac{3N_f}{N_f+2}.$$

Using the conformal embedding

$$\frac{\mathfrak{so}(5)_{N_f}}{\mathfrak{su}(2)_{N_f}} = \mathfrak{u}(1) + \frac{Z_{\mathfrak{so}(5)_{N_f}}}{Z_{\mathfrak{su}(2)_{N_f}}},$$

where $Z_{\mathfrak{su}(N)_{N_f}} = \mathfrak{su}(N)_{N_f}/\mathfrak{u}(1)^N$ denotes generalized $\mathfrak{su}(N)_{N_f}$ parafermions [54], the collective modes can equivalently be described by a product of a free $\mathfrak{u}(1)$ boson and a parafermion coset $Z_{\mathfrak{so}(5)_{N_f}}/Z_{\mathfrak{su}(2)_{N_f}}$ contributing $c = 1$ and

$$c = \frac{8N_f - 6}{N_f+3} - \frac{2(N_f-1)}{N_f+2}.$$

Notice that for $N_f = 2$ the central charge of the coset $Z_{\mathfrak{so}(5)_{N_f}}/Z_{\mathfrak{su}(2)_{N_f}}$ is $c = 3/2$, which is consistent with the results for interacting chains of $[1,0]$ $\mathfrak{so}(5)_{N_f}$ anyons [55].

Analogously to the regime discussed in 3.2.2, the entropy deviates from the asymptotic expression in the region $2M_0 - zH_1 \lesssim zH_2$, since the auxiliary modes of the second level propagate with a velocity differing from that of the $[1,1]$-solitons, $v_{[1,1]}$, namely

$$v_{[1,1]} = \left.\frac{\partial_\lambda \epsilon^{(2)}_{j_{0,2}}(\lambda)}{2\pi\rho^{(2)}_{j_{0,2}}(\lambda)}\right|_{\Lambda_2}, \quad v^{(2)}_{pf} = -\left.\frac{\partial_\lambda \epsilon^{(2)}_{j_{2,2}}(\lambda)}{2\pi\rho^{h(2)}_{j_{2,2}}(\lambda)}\right|_{\lambda\to\infty},$$

where Λ_2 denotes the Fermi point of $[1,1]$-solitons defined by $\epsilon^{(2)}_{j_{0,2}}(\pm\Lambda_2) = 0$. Also notice that Fermi velocities of the first level do not exist in this regime. As a consequence the bosonic (spinon) and parafermionic degrees of freedom in the first level separate and the low-temperature entropy is

$$\mathcal{S} = \frac{\pi}{3}\left(\frac{1}{v_{[1,1]}} + \frac{1}{v^{(2)}_{pf}}\left(\frac{8N_f-6}{N_f+3} - \frac{2(N_f-1)}{N_f+2}\right)\right)T\,. \tag{II.95}$$

Figure 21 (a) shows how both Fermi velocities depend on the field H_2 and approach 1 as $H_2 \geq H_{2,\delta}$ such that $\Lambda_2(H_{2,\delta}) > \lambda_\delta$. In Figure 21 (b) the computed entropy is shown as a function of the field H_2 together with the $T \to 0$ behavior expected from conformal field theory.

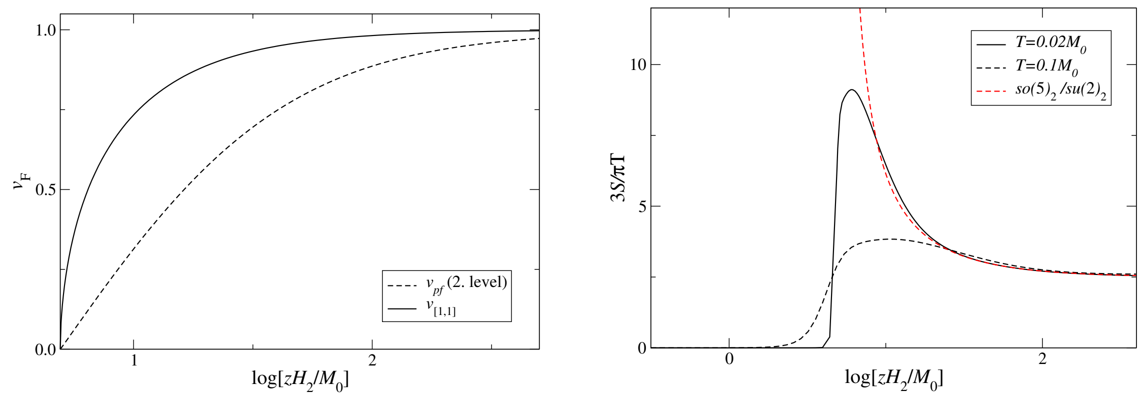

(a) **(b)**

Figure 21: (a) Fermi velocities of the $[1,1]$-solitons and second level parafermion modes as a function of the field zH_2/M_0 for $p_0 = 2 + 1/3$, $H_1 \equiv 0$ at zero temperature. For large fields, $H_2 > H_{2,\delta}$, both Fermi velocities approach 1 leading to the asymptotic result for the low-temperature entropy (II.94). (b) Entropy obtained from numerical solution of the TBA equations (II.79) for $p_0 = 2 + 1/3$ and $H_1 \equiv 0$ as a function of the field zH_2/M_0 for $T = 0.02M_0$. For fields large compared to the $[1,1]$-soliton mass, $zH_2 \gg 2M_0$, the entropy approaches the expected analytical value (II.94) for a field theory with a free bosonic sector and a $Z_{\mathfrak{so}(5)_{N_f}}/Z_{\mathfrak{su}(2)_{N_f}}$ parafermion sector propagating with velocities $v_{[1,1]}$ and $v_{pf}^{(2)}$, respectively (full red line). For magnetic fields $zH_2 < 2M_0$ and temperature $T \ll 2M_0$ the entropy is that of a dilute gas of non-interacting quasi-particles with degenerate internal degree of freedom due to the anyons.

3.2.4. Condensate of $[1,0]$- and $[1,1]$-solitons

For fields H_1, H_2 satisfying $zH_2 > \max(2\sqrt{3}M_0 - zH_1,\, 2M_0 - zH_1/2)$ and temperatures $T \ll -\min\left(\epsilon^{(1)}_{0,j_{0,1}}(0),\, \epsilon^{(2)}_{0,j_{0,2}}(0)\right)$ the $[1,0]$- and $[1,1]$-solitons condense. This results in non-zero Fermi velocities $v_{[1,0]}$, $v_{[1,1]}$, $v_{pf}^{(m)}$ $(m = 1, 2)$ for the solitons and the auxiliary modes. For large fields $zH_1 \gg M_0$, $zH_2 \gg M_0$ the following relations are found using (II.79)

$$
\begin{aligned}
f(\phi^{(m)}_{j_{0,m}}(\lambda_\delta)) &= 1, & f(\phi^{(m)}_{j_{0,m}}(\infty)) &= 0,\\
f(\phi^{(m)}_{\bar{j}_{0,m}}(\lambda_\delta)) &= 0, & f(\phi^{(m)}_{\bar{j}_{0,m}}(\infty)) &= 0,\\
f(\phi^{(m)}_{j_{2,m}}(\lambda_\delta)) &= 0 & &
\end{aligned}
$$

and therefore

$$
\rho^{h(m)}_{j_{0,m}}(\lambda) = \rho^{(m)}_{j_{1,m}}(\lambda) = \rho^{(m)}_{j_{2,m}} = 0, \quad \text{for } |\lambda| < \lambda_\delta\,,
$$

giving $\mathcal{S}^{(m)}_j(\lambda_\delta) = 0$ for all j, m. Using the relation (II.89) the low-temperature behavior of the entropy becomes

$$
\mathcal{S} = \frac{\pi}{3}\frac{10N_f}{N_f+3}T \tag{II.96}
$$

in the phase with finite $[1,0]$- and $[1,1]$-soliton density. The low-energy excitations near the Fermi points $\epsilon^{(m)}_{j_{0,m}}(\pm\Lambda_m) = 0$ of the soliton dispersion propagate with velocity $v_{[1,0]} = v_{[1,1]} \to 1$ for fields $H_m > H_{m,\delta}$ such that $\Lambda_m(H_{m,\delta}) > \lambda_\delta$. Hence, the conformal field theory describing the collective low-energy modes is the $\mathfrak{so}(5)$ WZNW model at level N_f or, by conformal embedding [54], a product of two free $\mathfrak{u}(1)$ bosons and a $\mathfrak{so}(5)$ parafermionic coset $\mathfrak{so}(5)_{N_f}/\mathfrak{u}(1)^2$ contributing $c = 2$ and

$$c = \frac{10N_f}{N_f + 3} - 2 = \frac{8N_f - 6}{N_f + 3} \tag{II.97}$$

to the central charge, respectively.

For fields H_1, H_2 such that $v_{[1,0]} = v_{[1,1]} < 1$ and $v_{pf}^{(1)} = v_{pf}^{(2)} < 1$ the degeneracy between the solitons and the parafermions is lifted resulting in the low-temperature behavior of the entropy given by

$$\mathcal{S} = \frac{\pi}{3}\left(\frac{2}{v_{[1,0]}} + \frac{1}{v_{pf}^{(m)}}\frac{8N_f - 6}{N_f + 3}\right) T\,.$$

Additionally, the fields can be chosen such that the remaining degeneracies are lifted, i.e. $v_{[1,0]} < v_{[1,1]}$ and $v_{pf}^{(1)} < v_{pf}^{(2)}$. In this case the entropy becomes

$$\mathcal{S} = \frac{\pi}{3}\left(\frac{1}{v_{[1,0]}} + \frac{1}{v_{pf}^{(1)}}\frac{2(N_f-1)}{N_f+2} + \frac{1}{v_{[1,1]}} + \frac{1}{v_{pf}^{(2)}}\left(\frac{8N_f - 6}{N_f + 3} - \frac{2(N_f-1)}{N_f+2}\right)\right) T\,,$$

which is consistent with the conformal embedding

$$\mathfrak{so}(5)_{N_f} = \mathfrak{u}(1) + Z_{\mathfrak{su}(2)_{N_f}} + \mathfrak{u}(1) + \frac{Z_{\mathfrak{so}(5)_{N_f}}}{Z_{\mathfrak{su}(2)_{N_f}}}\,,$$

see Figure 22 (a) for the Fermi velocities and Figure 22 (b) for the entropy in this regime.

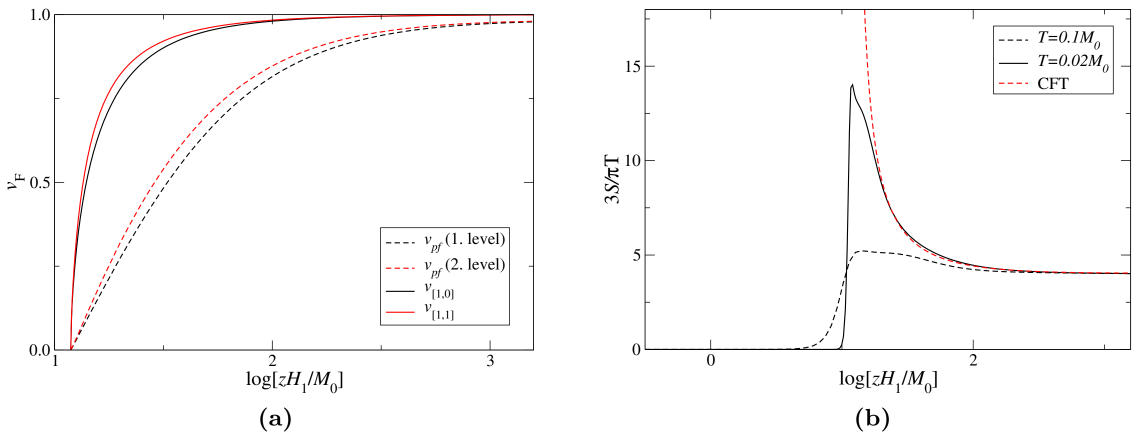

Figure 22: (a) Fermi velocities as a function of the field zH_1/M_0 for $p_0 = 2+1/3$, $zH_2 = -0.06M_0 + 0.21zH_1$ at zero temperature. For large fields, $H_1 > H_{1,\delta}$, all Fermi velocities approach 1 leading to the asymptotic result for the low-temperature entropy (II.96). (b) Entropy obtained from numerical solution of the TBA equations (II.79) as a function of the field zH_2/M_0 for $p_0 = 2 + 1/3$, fixed $zH_2 = -0.06M_0 + 0.21zH_1$ and different temperatures. For fields large compared to the kink mass, $zH_1 \gg M_0$, the entropy approaches the expected analytical value (II.96) (full red line). For magnetic fields $zH_1 < 2(M_{j_{0,1}}^{(1)} - M_{j_{0,2}}^{(2)})$ and temperature $T \ll M_0$ the entropy is that of a dilute gas of non-interacting quasi-particles with degenerate internal degree of freedom due to the anyons.

At last, for Fermi velocities $v_{[1,1]} < v_{[1,0]}$ and $v_{pf}^{(2)} < v_{pf}^{(1)}$ the entropy results in

$$\mathcal{S} = \frac{\pi}{3}\left(\frac{1}{v_{[1,1]}} + \frac{1}{v_{pf}^{(2)}}\frac{2N_f-1}{N_f+1} + \frac{1}{v_{[1,0]}} + \frac{1}{v_{pf}^{(1)}}\left(\frac{8N_f-6}{N_f+3} - \frac{2N_f-1}{N_f+1}\right)\right)T\,,$$

which is consistent with the conformal embedding

$$\mathfrak{so}(5)_{N_f} = \mathfrak{u}(1) + Z_{\mathfrak{so}(3)_{N_f}} + \mathfrak{u}(1) + \frac{Z_{\mathfrak{so}(5)_{N_f}}}{Z_{\mathfrak{so}(3)_{N_f}}}\,.$$

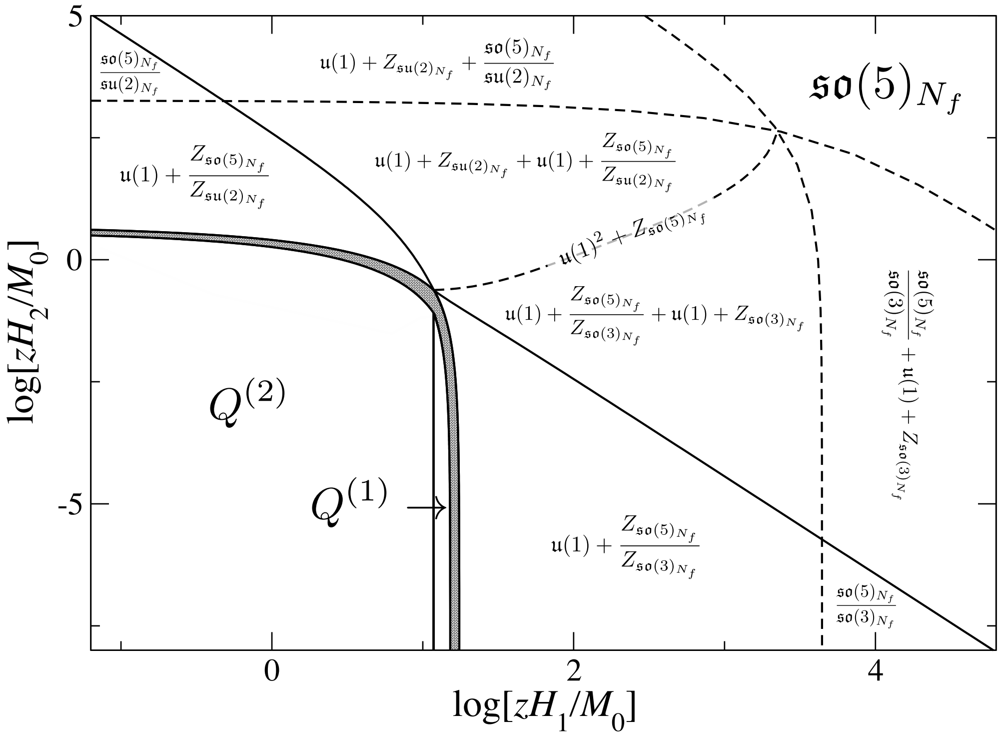

Figure 23: Contribution of the $\mathfrak{so}(5)_{N_f}$ anyons to the low-temperature properties of the model (II.65): using the criteria described in the main text the parameter regions are identified using analytical arguments for $T \to 0$ (the actual location of the boundaries is based on numerical data for $p_0 = 2+1/3$ and $T = 0.035M_0$). For small fields (regions $Q^{(1)}$, $Q^{(2)}$) a gas of non-interacting quasi-particles which have anyons with quantum dimension $Q^{(1)}$ or $Q^{(2)}$ as an internal zero-energy degree of freedom bound to them is realized. In the shaded region the presence of thermally activated solitons with a small but finite density lifts the degeneracy of the zero modes. All the other phases are labelled by the corresponding CFT describing it.

3.3. Phase diagram

The findings are summarized in a phase diagram based on the numerical analysis of the TBA equations (II.79), see Figure 23. For sufficiently small fields a dilute gas of anyons with quantum dimension $Q^{(1)}$ or $Q^{(2)}$ is dominating the contribution to the free energy. By varying the magnetic fields the condensation of anyons can be driven into various collective states described by parafermionic cosets: the collective state describing the condensation of $[1,1]$ $\mathfrak{so}(5)_{N_f}$ anyons is identified as the $Z_{\mathfrak{so}(5)_{N_f}}/Z_{\mathfrak{so}(3)_{N_f}}$ parafermion coset, while the condensation of $[1,0]$ $\mathfrak{so}(5)_{N_f}$ anyons results in the $Z_{\mathfrak{so}(5)_{N_f}}/Z_{\mathfrak{su}(2)_{N_f}}$ parafermionic theory. Moreover, the condensation of a mixture of $[1,0]$ and $[1,1]$ anyons is studied resulting in the $Z_{\mathfrak{so}(5)_{N_f}}$ parafermion theory describing the collective state. Other theories describing the condensation of $\mathfrak{so}(5)_{N_f}$ anyons are based on conformal embeddings, see Figure 23.

Conclusion

Zero-energy modes with non-Abelian statistics are the fundamental objects needed to be realized and controlled in a laboratory to implement decoherence-free quantum computing. While the emergence of Z_2 parafermionic zero-energy modes (also called Majorana anyons) has possibly been observed in experiments [30–32, 40, 41], $Z_{n>2}$ parafermionic zero-energy modes, that are universal for quantum computing, are still limited to theoretical studies. To demonstrate that $Z_{n>2}$ parafermions also emerge on the boundary between ground states of different topology, Tsvelik studied an integrable perturbed $\mathfrak{su}(2)_{N_f}$ WZNW model based on fermions with spin and orbital degrees of freedom [39]. A striking feature of this model is that the density of anyon zero-energy modes, that are located on solitons, can be varied continuously to study the transition from free to interacting anyons. Prior to this, interactions between anyons were investigated using lattices of anyons with effective short-range interactions based on their fusion rules [20–24]. However, changing the density or average distance between the anyons using a control parameter was not possible in this approach. Therefore, perturbed WZNW models in general are useful candidates to obtain a better understanding of interactions between anyons, which not only limit the working of topological quantum computing but also may be useful for stabilizing quantum memories [15–17].

In this thesis Tsvelik's research of the perturbed $\mathfrak{su}(2)_{N_f}$ WZNW model was extended and generalized to the $SU(3)$ and $SO(5)$ symmetry groups, while focusing on studying the transition from free to interacting anyons. On that account the TBA equations of the perturbed $\mathfrak{su}(2)_{N_f}$ WZNW model were derived and the low-temperature anyonic modes with respect to the magnetic field were identified. For magnetic fields below the energy scale of the solitonic 'kink' gap also bound states, called breathers, contribute to the free energy. Their degeneracy was found to coincide with the quantum dimension of two spin-1/2 $\mathfrak{su}(2)_{N_f}$ anyons. For larger magnetic fields the kink gap closes and interactions from the spin-1/2 $\mathfrak{su}(2)_{N_f}$ anyons, that are bound to the kinks, lift the degeneracy. It was found by Tsvelik [39] that the TBA equations in this regime resemble those of critical RSOS models, which describe a Z_{N_f} parafermion CFT in the low-energy limit. To further understand this relationship the TBA equations for magnetic fields $zH > M_0$ were studied: in this regime the excitations become massless resulting in an effective field theory of a free boson describing the kinks and a Z_{N_f} parafermion CFT describing the collective state of the anyons with ferromagnetic pair interaction. The transition from free anyons to a condensate of anyons forming a collective state is clearly visible in the behavior of the entropy with respect to the magnetic field, that was computed numerically. At the point, where interactions become significant stronger magnetic fields only increase the Fermi velocities of the kinks and parafermions, which degenerate in the limit $zH \gg M_0$. The resulting central charge in this regime coincides with that of the $\mathfrak{su}(2)_{N_f}$ WZNW model. To summarize the anyonic modes contributing to the low-temperature phases of the perturbed $\mathfrak{su}(2)_{N_f}$ WZNW model a phase diagram was proposed, see Sec. II 1.4.

To generalize Tsvelik's approach to other symmetry groups we started with a fermionic model with color $SU(3)$ and flavor $SU(N_f)$ degrees of freedom. In the low-temperature limit non-Abelian bosonization is used to obtain the perturbed $\mathfrak{su}(3)_{N_f}$ WZNW model describing the non-Abelian fractional degrees of freedom of the fermionic model. Similar to the $SU(2)$ case the thermodynamic Bethe ansatz is used to study the emergence and condensation of

$\mathfrak{su}(3)_{N_f}$ anyons in the perturbed $\mathfrak{su}(3)_{N_f}$ WZNW model. Using the string hypothesis the low-energy excitations were identified as quark and antiquark solitons with $[1,0]$ and $[1,1]$ $\mathfrak{su}(3)_{N_f}$ anyons beeing bound to them.

In the non-interacting regime external fields can be used to transition continuously between the phase dominated by free anyons of type $[1,0]$ and $[1,1]$. Breather excitations also appear as bound states of quarks and antiquarks, however, their contribution to the low-temperature phases can be neglected for sufficiently small temperatures.

Another feature of the perturbed $\mathfrak{su}(3)_{N_f}$ WZNW model is that anyon condensation of $[1,0]$ anyons, $[1,1]$ anyons as well as of a mixture of $[1,0]$, $[1,1]$ anyons can be studied. The $[1,0]$ anyons or $[1,1]$ anyons form a condensate as soon as the gap of quarks or antiquarks is closed, respectively. In both cases the excitations become massless resulting in an effective field theory of a free boson describing the quarks or antiquarks and a parafermion coset $Z_{\mathfrak{su}(3)_{N_f}}/Z_{\mathfrak{su}(2)_{N_f}}$ describing the collective state of $[1,0]$ or $[1,1]$ anyons. For sufficiently large fields the Fermi velocities of both sectors degenerate and the resulting central charge coincides with that of the $\mathfrak{su}(3)_{N_f}/\mathfrak{su}(2)_{N_f}$ coset of WZNW models.

For equal fields $H_1 \equiv H_2$ there is an equal density of quarks and antiquarks in the system. The effective field theory specifying the massless phase of this mixture involves a product of two free bosons describing the quarks and antiquarks and a $Z_{\mathfrak{su}(3)_{N_f}}$ parafermion conformal field theory describing the collective state of the anyons. Again the Fermi velocities degenerate for sufficiently large fields and the resulting central charge coincides with that of the $\mathfrak{su}(3)_{N_f}$ WZNW model.

The identification of the conformal field theories describing the interacting anyons is, however, not sufficient to determine the underlying interaction type of the anyons based on its fusion rules. One possibility to answer this question would be to directly rewrite the Hamiltonian of the corresponding RSOS model [123] such that the energetically favored fusion outcome of two neighboring anyons becomes apparent. With respect to the quantum Hall effect the identification of the conformal field theories describing the interacting $\mathfrak{su}(3)_{N_f}$ anyons may be important to further understand the condensation of $\mathfrak{su}(3)_2$ anyons at the boundary of the quantum Hall liquid with filling factor $\nu = 4/7$ [34].

At last, relativistic fermions with $SO(5)$ and $SU(N_f)$ symmetry were studied. As before it is argued that in the low-temperature limit the massive sector of this model results in a perturbed $\mathfrak{so}(5)_{N_f}$ WZNW model. The analysis of this model is mathematically similar to the analysis of the perturbed $\mathfrak{su}(3)_{N_f}$ WZNW model since both $\mathfrak{so}(5)$ and $\mathfrak{su}(3)$ Lie algebras have rank two. However, the effect of low-energy excitations that are not governed by the string hypothesis is less clear. Still by studying the spectrum of solitons with charges corresponding to the fundamental $\mathfrak{so}(5)$ multiplets with $[1,0]$ and $[1,1]$ Young diagrams, evidence was given that the low-energy behavior of the model is governed by a few string solutions. The corresponding low-energy excitations are in agreement with the highest weight states of the $\mathfrak{so}(5)$ multiplets with Young diagrams $[1,0]$ and $[1,1]$, while their degeneracy for $N_f = 2$ coincides with the quantum dimension of $[1,1]$ and $[1,0]$ $\mathfrak{so}(5)_2$ anyons, respectively. For $N_f > 2$ this identification cannot be done, since the fusion rules and therefore also the quantum dimensions of $\mathfrak{so}(5)_{N_f}$ anyons have not been classified so far.

By studying the condensation of $[1,0]$-solitonic excitations it was found that the resulting effective field theory involves a free boson describing the solitons and a parafermion coset $Z_{\mathfrak{so}(5)_{N_f}}/Z_{\mathfrak{so}(3)_{N_f}}$ describing the collective state of the $[1,1]$ anyons. Similarly, the collective state specifying the interacting $[1,0]$ anyons was identified as the parafermion coset

$Z_{\mathfrak{so}(5)_{N_f}}/Z_{\mathfrak{su}(2)_{N_f}}$, while a mixture of interacting $[1,0]$ and $[1,1]$ anyons resulted in the $Z_{\mathfrak{so}(5)_{N_f}}$ parafermion conformal field theory. For $N_f = 2$ the results for interacting $[1,0]$ anyons or $[1,1]$ anyons are in agreement with results of corresponding anyonic chains [55, 120]. Interacting chains of alternating $[1,0]$ and $[1,1]$ $\mathfrak{so}(5)_{N_f}$ anyons, however, have not been studied before.

A limitation of studying the condensation of anyons using perturbed WZNW models is that only the condensation of anyons with a particular topological charge and coupling can be studied. In future works possibilities to adjust the interactions of the underlying fermions to study the condensation of anyons with different interaction types should therefore be investigated. Apart from that interacting anyonic lattice models need to be further studied to obtain a general understanding of interacting anyons.

From a practical point of view, it was argued that each perturbed WZNW models studied in this thesis could be realized as a sector in the low-energy limit in a system of cold atoms trapped in a periodic potential. However, as discussed in Sec. II 1, a mechanism to single out the non-Abelian anyons of the perturbed WZNW model from excitations of the other sectors is currently missing [87, 124]. Nonetheless, there are similar models with $Z_{n>2}$ parafermionic zero-energy modes proposed by Tsvelik that may be experimentally feasible [50].

In general, this thesis as well as related developments [39, 50, 87] unveiled new insights about the rich structure of non-Abelian anyons and demonstrated that fermionic systems with spin and orbital degrees of freedom are a possible alternative for realizing non-Abelian quasi-particles in electronic systems.

A. Kernels of the perturbed $\mathfrak{su}(2)_{N_f}$ WZNW model

Following [70] the Fourier transformed kernels $A_{jk}(\omega)$ of the XXZ model are expressed in terms of the functions $a_j(\omega)$, $S_j(\omega)$ and $\zeta_j(\omega)$

$$
\begin{aligned}
a_j(\omega) &= \frac{\sinh(q_j\omega)}{\sinh(p_0\omega)}\,, \qquad S_j(\omega) = \frac{1}{2\cosh(p_j\omega)}\,,\\
\zeta_j(\omega) &= \cosh\left[\left(\left\{\frac{n_j}{p_0}\right\} - \frac{1-(-1)^{r(j)}}{2}\right)p_0\omega\right] + \sum_{\ell=1}^{n_j-1}\cosh\left[\left(\left\{\frac{n_j-\ell}{p_0}\right\}\left\{\frac{\ell}{p_0}\right\}\right)p_0\omega\right]
\end{aligned}
\tag{A.1}
$$

where $\{x\}$ denotes the fractional part of x. This yields the Fourier-transformed kernels $A_{jk}(\omega)$ and the Fourier transformed functions $a_{j,N_f}(\omega)$

$$
\begin{aligned}
&A_{kj}(\omega) = A_{jk}(\omega) = 2a_k(\omega)\,\zeta_j(\omega) - \delta_{k,j_0}\delta_{j,j_0-1}\\
&a_{j,N_f}(\omega) = A_{j,\sigma-1}(\omega)S_{r+1}(\omega) + 2\cosh(q_\sigma\omega)\sum_{\ell=1}^{r} A_{j,m_\ell-1}(\omega)S_\ell(\omega)S_{\ell+1}(\omega).
\end{aligned}
\tag{A.2}
$$

The Fourier transformed kernels $B_{jk}(\omega)$ used for the integral equations (II.13), (II.20) are defined by

$$
\begin{aligned}
B_{j_0j_0} &= \frac{1}{A_{j_0j_0}}, & B_{j_0j_1} &= \frac{A_{j_0j_1}}{A_{j_0j_0}}, & B_{j_0j_2} &= \frac{A_{j_0j_2}}{A_{j_0j_0}},\\
B_{j_1k_1} &= \frac{A_{j_0j_1}A_{j_0k_1}}{A_{j_0j_0}} - A_{j_1k_1}, & B_{j_1j_2} &= \frac{A_{j_0j_1}A_{j_0j_2}}{A_{j_0j_0}} - A_{j_1j_2}, & B_{j_2k_2} &= A_{j_2k_2} - \frac{A_{j_0j_2}A_{j_0k_2}}{A_{j_0j_0}}
\end{aligned}
$$

and the relations

$$
\begin{aligned}
B_{j_kj_0} &= -(-1)^{r(j_k)}B_{j_0,j_k}, \qquad k = 1, 2\,,\\
B_{j_2j_1} &= -B_{j_1j_2}.
\end{aligned}
$$

B. Scaling limit

To give an example of how to perform the scaling limit for perturbed WZNW models in general the scaling limit $g \ll 1$ of $\rho^{(0)}_{j_0}(\lambda)$ (II.16) is computed. First the expression is simplified in Fourier space

$$
\begin{aligned}
\rho^{(0)}_{j_0}(\omega) &= \cos(\omega/g)\frac{a_{j_0,N_f}(\omega)}{A_{j_0j_0}(\omega)}\\
&= \cos(\omega/g)\frac{\cosh((p_0-1)\omega) + \frac{\cosh(q_\sigma\omega)}{\cosh\omega}\sum_{l=0}^{N_f-2}\cosh((N_f-2l-1)\omega)}{2\sum_{\ell=0}^{N_f-1}\cosh((N_f-2\ell)\omega)\cosh(\omega/\nu)}\\
&= \cos(\omega/g)\frac{1}{2\cosh\omega}\,,
\end{aligned}
$$

where the expressions (A.2) and the sequences for $p_0 = N_f + 1/\nu$ given in Sec. I 1.2 have been used. After applying the inverse Fourier transformation to $\rho^{(0)}_{j_0}(\omega)$ this results in

$$
\begin{aligned}
\rho^{(0)}_{j_0}(\lambda) &= \frac{1}{8\cosh\left(\frac{\pi}{2}(\lambda+1/g)\right)} + \frac{1}{8\cosh\left(\frac{\pi}{2}(\lambda-1/g)\right)}\\
&\overset{g\ll 1}{=} \frac{M_0}{4}\cosh\left(\frac{\pi\lambda}{2}\right), \qquad M_0 = 2e^{-\frac{\pi}{2g}}.
\end{aligned}
$$

The scaling limit $g \ll 1$ for other bare densities and bare energies of the perturbed WZNW models can be performed in a similar way.

C. TBA of the perturbed $\mathfrak{su}(3)_{N_f}$ WZNW model

In order to obtain the integral equations (II.40) one can consider a root configuration consisting of $\nu_j^{(m)}$ strings of type (n_j, v_{n_j}) on the m-th level and rewrite the Bethe equations (II.37) in terms of the real string-centers $\lambda_\alpha^{(m,j)} \equiv \lambda_\alpha^{(m)n_j}$ using (II.39). In their logarithmic form they read

$$\begin{aligned} \sum_{\tau=\pm 1} \frac{\mathcal{N}}{2} t_{k,N_f}(\lambda_\alpha^{(1,k)} + \tau/g) &= 2\pi I_\alpha^{(1,k)} + \sum_{m=1}^{2} \sum_j \sum_{\beta=1}^{\nu_j^{(m)}} (-1)^{m+1} \theta_{kj}^{(m)}(\lambda_\alpha^{(1,k)} - \lambda_\beta^{(m,j)}) \,, \\ 0 &= 2\pi I_\alpha^{(2,k)} + \sum_{m=1}^{2} \sum_j \sum_{\beta=1}^{\nu_j^{(m)}} (-1)^{m} \theta_{kj}^{(3-m)}(\lambda_\alpha^{(2,k)} - \lambda_\beta^{(m,j)}) \,, \end{aligned} \tag{C.3}$$

where $I_\alpha^{(m,k)}$ are integers (or half-integers) and the functions

$$\begin{aligned} t_{k,N_f}(\lambda) &= \sum_{l=1}^{\min(n_k,N_f)} f(\lambda, |n_k - N_f| + 2l - 1, v_k v_{N_f}) \,, \\ \theta_{kj}^{(1)}(\lambda) &= f(\lambda, |n_k - n_j|, v_k v_j) + f(\lambda, n_k + n_j, v_k v_j) + \\ &\quad 2 \sum_{\ell=1}^{\min(n_k,n_j)-1} f(\lambda, |n_k - n_j| + 2\ell, v_k v_j) \,, \\ \theta_{kj}^{(2)}(\lambda) &= \sum_{l=1}^{\min(n_k,n_j)} f(\lambda, |n_k - n_j| + 2l - 1, v_k v_j) \end{aligned} \tag{C.4}$$

have been introduced with

$$f(\lambda, n, v) = \begin{cases} 2\arctan\left(\tan((\frac{1+v}{4} - \frac{n}{2p_0})\pi)\tanh(\frac{\pi\lambda}{2p_0})\right) & \text{if } \frac{n}{p_0} \neq \text{integer} \\ 0 & \text{if } \frac{n}{p_0} = \text{integer} \end{cases} .$$

In the thermodynamic limit, $N_m, \mathcal{N} \to \infty$ with $N_m/\mathcal{N}$ fixed, the centers $\lambda_\alpha^{(m,k)}$ are distributed continuously with densities $\rho_k^{(m)}(\lambda)$ and hole densities $\rho_k^{h(m)}(\lambda)$. Following [76] the densities are defined through the following integral equations

$$\begin{aligned} \tilde{\rho}_{0,k}^{(1)}(\lambda) &= (-1)^{r(k)} \rho_k^{h(1)}(\lambda) + \sum_j A_{kj}^{(1)} * \rho_j^{(1)}(\lambda) - \sum_j A_{kj}^{(2)} * \rho_j^{(2)}(\lambda) \,, \\ 0 &= (-1)^{r(k)} \rho_k^{h(2)}(\lambda) + \sum_j A_{kj}^{(1)} * \rho_j^{(2)}(\lambda) - \sum_j A_{kj}^{(2)} * \rho_j^{(1)}(\lambda) \,, \end{aligned} \tag{C.5}$$

where $a*b$ denotes a convolution and $r(j)$ is defined in Appendix A of [52]. The bare densities $\tilde{\rho}_{0,j}^{(1)}(\lambda)$ and the kernels $A_{jk}^{(m)}(\lambda)$ of the integral equations are defined by

$$\begin{aligned} \tilde{\rho}_{0,j}^{(1)}(\lambda) &= \frac{1}{2}\left(a_{j,N_f}(\lambda + 1/g) + a_{j,N_f}(\lambda - 1/g)\right) , \quad a_{j,N_f}(\lambda) = \frac{1}{2\pi}\frac{d}{d\lambda} t_{j,N_f}(\lambda) \\ A_{kj}^{(m)}(\lambda) &= \frac{1}{2\pi}\frac{d}{d\lambda}\theta_{kj}^{(m)}(\lambda) + (-1)^{r(k)} \delta_{m1}\delta_{jk}\delta(\lambda) \,. \end{aligned} \tag{C.6}$$

The energy density $\mathcal{E} = E/\mathcal{N}$ is rewritten using (II.38) and the solutions $\rho_k^{(m)}$ of (C.5) as

$$\begin{aligned}\mathcal{E} &= \frac{1}{\mathcal{N}}\sum_j\sum_{\alpha=1}^{\nu_j^{(1)}}\left(\sum_{\tau=\pm1}\frac{\tau}{2}t_{j,N_f}(\lambda_\alpha^{(j,1)}+\tau/g)+n_jH_1\right)+\frac{1}{\mathcal{N}}\sum_j\sum_{\alpha=1}^{\nu_j^{(2)}}n_jH_2-\frac{2}{3}H_1-\frac{1}{3}H_2\\ &\overset{\mathcal{N}\to\infty}{=}\sum_{m=1}^{2}\sum_{j\geq1}\int_{-\infty}^{+\infty}\mathrm{d}\lambda\,\tilde{\epsilon}_{0,j}^{(m)}(\lambda)\rho_j^{(m)}(\lambda)-\frac{2}{3}H_1-\frac{1}{3}H_2\,,\end{aligned} \tag{C.7}$$

where the bare energies were introduced:

$$\tilde{\epsilon}_{0,j}^{(1)}(\lambda)=\sum_{\tau=\pm1}\frac{\tau}{2}t_{j,N_f}(\lambda+\tau/g)+n_jH_1,\quad \tilde{\epsilon}_{0,j}^{(2)}(\lambda)=n_jH_2$$

It turns out that the energy (C.7) is minimized by a configuration, where only the strings of length N_f have a finite density. After inverting the kernels $A_{j_0j_0}^{(1)}$ on both levels in equation (C.5) and inserting the resulting expression for $\rho_{j_0}^{(m)}(\lambda)$ into the other equations for $k\neq j_0$ the integral equations (II.40) are obtained, where the densities $\rho_{j_0}^{h(m)}\leftrightarrow\rho_{j_0}^{(m)}$ are redefined and the kernels $B_{jk}^{(1,1)}=B_{jk}^{(2,2)}\equiv B_{jk}^{(1)}$, $B_{jk}^{(1,2)}=B_{jk}^{(2,1)}\equiv B_{jk}^{(2)}$ are introduced. The Fourier-transformed kernels $B_{jk}^{(1)}(\omega)$, $B_{jk}^{(2)}(\omega)$ are given by

$$\begin{aligned}B_{j_0j_0}^{(m)}&=\frac{A_{j_0j_0}^{(m)}}{(A_{j_0j_0}^{(1)})^2-(A_{j_0j_0}^{(2)})^2},\\ B_{kj_0}^{(m)}&=(-1)^{r(k)}\frac{A_{kj_0}^{(2)}A_{j_0j_0}^{((m\bmod 2)+1)}-A_{kj_0}^{(1)}A_{j_0j_0}^{(m)}}{(A_{j_0j_0}^{(1)})^2-(A_{j_0j_0}^{(2)})^2}\,,\qquad k\neq j_0\,,\\ B_{j_0k}^{(m)}&=-(-1)^{r(k)}B_{kj_0}^{(m)}\,,\qquad k\neq j_0\,,\\ B_{kj}^{(m)}&=(-1)^{r(k)}\left(A_{kj_0}^{(2)}B_{j_0j}^{((m\bmod 2)+1)}-A_{kj_0}^{(1)}B_{j_0j}^{(m)}+(-1)^{m+1}A_{kj}^{(m)}\right),\qquad k,j\neq j_0\,.\end{aligned}$$

The inverse of the Fourier transformed kernel $B_{j_2k_2}^{(1)}(\omega)$ is given by (see for e.g. [94])

$$C_{j_2k_2}=\delta_{j_2k_2}-s(\delta_{j_2k_2+1}+\delta_{j_2k_2-1})\,.$$

Hence, the Fourier transformed kernels $C_j^{(m)}(\omega)$ of equation (II.47) are determined by

$$\sum_{j_2}C_{kj_2}B_{jj_2}^{(1)}=\delta_{k,N_f-1}C_j^{(m)}\,.$$

D. TBA of the perturbed $\mathfrak{so}(5)_{N_f}$ WZNW model

In order to obtain the integral equations (II.71) a root configuration consisting of $\nu_j^{(m)}$ strings of type $(n_j^{(m)}, v_{n_j}^{(m)})$ on the m-th level is considered and the Bethe equations (II.67) are rewritten in terms of the real string-centers $\lambda_\alpha^{(m,j)} \equiv \lambda_\alpha^{(m)n_j}$ using (II.69). In their logarithmic form they read

$$\begin{aligned}\sum_{\tau=\pm1} \frac{N}{2} t_{k,N_f}(\lambda_\alpha^{(1,k)} + \tau/g) &= 2\pi I_\alpha^{(1,k)} + \sum_{m=1}^{2} \sum_j \sum_{\beta=1}^{\nu_j^{(m)}} (-1)^{m+1} \theta_{kj}^{(1,m)}(\lambda_\alpha^{(1,k)} - \lambda_\beta^{(m,j)})\,, \\ 0 &= 2\pi I_\alpha^{(2,k)} + \sum_{m=1}^{2} \sum_j \sum_{\beta=1}^{\nu_j^{(m)}} (-1)^{m} \theta_{kj}^{(2,m)}(\lambda_\alpha^{(2,k)} - \lambda_\beta^{(m,j)})\,,\end{aligned} \tag{D.8}$$

where $I_\alpha^{(m,k)}$ are integers (or half-integers) and the functions

$$\begin{aligned} t_{k,N_f}(\lambda) &= \sum_{l=1}^{\min(n_k,N_f)} f(\lambda, |n_k - N_f| + 2l - 1, v_k v_{N_f})\,, \\ \theta_{kj}^{(m,m)}(\lambda) &= f(\lambda, |n_k^{(m)} - n_j^{(m)}|, v_k^{(m)} v_j^{(m)}) + f(\lambda, n_k^{(m)} + n_j^{(m)}, v_k^{(m)} v_j^{(m)}) \\ &\quad + 2 \sum_{\ell=1}^{\min(n_k^{(m)}, n_j^{(m)})-1} f(\lambda, |n_k^{(m)} - n_j^{(m)}| + 2\ell, v_k^{(m)} v_j^{(m)}) \qquad \text{with } m = 1,2\,, \\ \theta_{kj}^{(1,2)}(\lambda) &= \sum_{l=1}^{\min(2n_k^{(1)}, n_j^{(2)})} f(\lambda, |n_j^{(2)}/2 - n_k^{(1)}| + 2l - 1, v_k^{(1)} v_j^{(2)})\,, \\ \theta_{kj}^{(2,1)}(\lambda) &\equiv \theta_{jk}^{(1,2)}(\lambda) \end{aligned} \tag{D.9}$$

were introduced with

$$f(\lambda, n, v) = \begin{cases} 2\arctan\left(\tan((\frac{1+v}{4} - \frac{n}{2p_0})\pi)\tanh(\frac{\pi\lambda}{2p_0})\right) & \text{if } \frac{n}{p_0} \neq \text{integer} \\ 0 & \text{if } \frac{n}{p_0} = \text{integer} \end{cases}.$$

In the thermodynamic limit, $N_m, \mathcal{N} \to \infty$ with $N_m/\mathcal{N}$ fixed, the centers $\lambda_\alpha^{(m,k)}$ are distributed continuously with densities $\rho_k^{(m)}(\lambda)$ and hole densities $\rho_k^{h(m)}(\lambda)$. Following [125] the densities are defined through the following integral equations

$$\begin{aligned} \tilde{\rho}_{0,k}^{(1)}(\lambda) &= (-1)^{r^{(1)}(k)} \rho_k^{h(1)}(\lambda) + \sum_{m=1}^{2} \sum_j (-1)^{m+1} A_{kj}^{(1,m)} * \rho_j^{(m)}(\lambda) \quad \text{with } k = 1, \ldots, j_{0,1}\,, \\ 0 &= (-1)^{r^{(2)}(k)} \rho_k^{h(2)}(\lambda) + \sum_{m=1}^{2} \sum_j (-1)^{m} A_{kj}^{(2,m)} * \rho_j^{(m)}(\lambda) \quad \text{with } k = 1, \ldots, j_{0,2}\,, \end{aligned} \tag{D.10}$$

where $a * b$ denotes a convolution and $r^{(m)}(j)$ is given by

$$r^{(m)}(j_{2,m}) = 0\,, \qquad r^{(m)}(\tilde{j}_{0,m}) = 1\,, \qquad r^{(m)}(j_{0,m}) = 2\,.$$

The bare densities $\tilde\rho^{(1)}_{0,j}(\lambda)$ and the kernels $A^{(m)}_{jk}(\lambda)$ of the integral equations are defined by

$$\begin{aligned}\tilde\rho^{(1)}_{0,j}(\lambda) &= \frac{1}{2}\left(a_{j,N_f}(\lambda+1/g)+a_{j,N_f}(\lambda-1/g)\right)\,, \quad a_{j,N_f}(\lambda)=\frac{1}{2\pi}\frac{d}{d\lambda}t_{j,N_f}(\lambda)\,,\\ A^{(m,l)}_{kj}(\lambda) &= \frac{1}{2\pi}\frac{d}{d\lambda}\theta^{(m,l)}_{kj}(\lambda)+(-1)^{r^{(m)}(k)}\delta_{m,l}\delta_{jk}\delta(\lambda)\,.\end{aligned} \tag{D.11}$$

Using (II.68) and the solutions $\rho^{(m)}_k$ of (D.10) the energy density $\mathcal{E}=E/\mathcal{N}$ is rewritten as

$$\begin{aligned}\mathcal{E} &= \frac{1}{\mathcal{N}}\sum_j\sum_{\alpha=1}^{\nu_j^{(1)}}\left(\sum_{\tau=\pm1}\frac{\tau}{2}t_{j,N_f}(\lambda_\alpha^{(j,1)}+\tau/g)+n_jH_1\right)+\frac{1}{\mathcal{N}}\sum_j\sum_{\alpha=1}^{\nu_j^{(2)}}n_jH_2-H_1-H_2\\ &\overset{\mathcal{N}\to\infty}{=}\sum_{m=1}^{2}\sum_{j\geq1}\int_{-\infty}^{+\infty}\mathrm{d}\lambda\,\tilde\epsilon^{(m)}_{0,j}(\lambda)\rho^{(m)}_j(\lambda)-H_1-H_2\,,\end{aligned} \tag{D.12}$$

where the bare energies

$$\tilde\epsilon^{(1)}_{0,j}(\lambda)=\sum_{\tau=\pm1}\frac{\tau}{2}t_{j,N_f}(\lambda+\tau/g)+n_jH_1,\quad \tilde\epsilon^{(2)}_{0,j}(\lambda)=n_jH_2$$

were introduced. It turns out that the energy (D.12) is minimized by a configuration, where only the strings of length N_f on the first level and strings of length $2N_f$ on the second level have a finite density (cf. Ref. [117] for the isotropic case). After inverting the kernels $A^{(1,1)}_{j_{0,1}j_{0,1}}$ and $A^{(2,2)}_{j_{0,2}j_{0,2}}$ in equation (D.10) and inserting the resulting expression for $\rho^{(1)}_{j_{0,1}}(\lambda)$ and $\rho^{(2)}_{j_{0,2}}(\lambda)$ into the other equations for $k\neq j_{0,1}$ on the first level and $k\neq j_{0,2}$ on the second level the integral equations (II.71) are found, where the densities $\rho^{h(m)}_{j_{0,m}}\leftrightarrow\rho^{(m)}_{j_{0,m}}$ were redefined and the Fourier-transformed kernels $B^{(l,m)}_{kj}(\omega)$ were introduced:

$$\begin{aligned}B^{(m,m)}_{j_{0,m}j_{0,m}} &= (-1)^{r^{(m)}_{j_{0,m}}}A^{(\tilde m,\tilde m)}_{j_{0,\tilde m},j_{0,\tilde m}}/K\,,\\ B^{(m,l)}_{j_{0,m}j_{0,l}} &= (-1)^{r^{(l)}_{j_{0,l}}}A^{(m,l)}_{j_{0,m}j_{0,l}}/K \qquad m\neq l\,,\\ B^{(l,m)}_{j_{0,l}j} &= (-1)^{l+m}\left(A^{(l,m)}_{j_{0,l}j}A^{(\tilde l,\tilde l)}_{j_{0,\tilde l}j_{0,\tilde l}}-A^{(l,\tilde l)}_{j_{0,l}j_{0,\tilde l}}A^{(\tilde l,m)}_{j_{0,\tilde l}j}\right)/K \qquad j\neq j_{0,l}\text{ if } l=m\,,\\ B^{(l,m)}_{kj_{0,m}} &= (-1)^{r^{(l)}_k}\left(A^{(l,\tilde l)}_{kj_{0,\tilde l}}B^{(\tilde l,m)}_{j_{0,\tilde l}j_{0,m}}-A^{(l,l)}_{kj_{0,l}}B^{(l,m)}_{j_{0,l}j_{0,m}}\right) \qquad k\neq j_{0,m}\text{ if } l=m\,,\\ B^{(l,m)}_{kj} &= (-1)^{r^{(l)}_k}\left(A^{(l,\tilde l)}_{kj_{0,\tilde l}}B^{(\tilde l,m)}_{j_{0,\tilde l}j}-A^{(l,l)}_{kj_{0,l}}B^{(l,m)}_{j_{0,l}j}+(-1)^{l+m}A^{(l,m)}_{kj}\right) \qquad k\neq j_{0,l}\,,\ j\neq j_{0,m}\,,\end{aligned}$$

where $\tilde m=m \mod 2+1$, $\tilde l=l \mod 2+1$ and

$$K(\omega)=A^{(1,1)}_{j_{0,1}j_{0,1}}(\omega)A^{(2,2)}_{j_{0,2}j_{0,2}}(\omega)-A^{(2,1)}_{j_{0,2}j_{0,1}}(\omega)A^{(1,2)}_{j_{0,1}j_{0,2}}(\omega)\,.$$

The Fourier-transformed kernels $A^{(m,l)}_{jk}(\omega)$ $(m,l\in\{1,2\})$ can be derived using (D.9), (D.11), while $A^{(1,1)}_{jk}$ corresponds to A_{jk} in [52].

The expressions determining the bare densities $\rho_{0,k}^{(m)}(\lambda)$ of (II.72), (II.75) and the bare energies $\epsilon_{0,k}^{(m)}(\lambda)$ of (II.73), (II.76) are

$$
\begin{aligned}
&\rho_{0,k}^{(m)}(\lambda) = B_{kj_{0,1}}^{(m,1)} * \tilde{\rho}_{0,j_{0,1}}^{(1)}(\lambda) \quad \text{for } k = j_{0,m}, \\
&\rho_{0,k}^{(m)}(\lambda) = \delta_{m,1}\tilde{\rho}_{0,k}^{(1)}(\lambda) + B_{kj_{0,1}}^{(m,1)} * \tilde{\rho}_{0,j_{0,1}}^{(1)}(\lambda) \quad \text{for } k \neq j_{0,m}\,, \\
&\epsilon_{0,k}^{(m)}(\lambda) = -B_{j_{0,1}k}^{(1,m)} * \tilde{\epsilon}_{0,j_{0,1}}^{(1)}(\lambda) - B_{j_{0,2}k}^{(2,m)} * \tilde{\epsilon}_{0,j_{0,2}}^{(2)}(\lambda) \quad \text{for } k = j_{0,m}\,, \\
&\epsilon_{0,k}^{(m)}(\lambda) = \tilde{\epsilon}_{0,k}^{(m)} - B_{j_{0,1}k}^{(1,m)} * \tilde{\epsilon}_{0,j_{0,1}}^{(1)}(\lambda) - B_{j_{0,2}k}^{(2,m)} * \tilde{\epsilon}_{0,j_{0,2}}^{(2)}(\lambda) \quad \text{for } k \neq j_{0,m}\,.
\end{aligned}
$$

References

[1] M. Fierz. "Über die relativistische Theorie kräftefreier Teilchen mit beliebigem Spin." PhD thesis. Birkhäuser, 1939.

[2] W. Pauli. "The connection between spin and statistics." *Phys. Rev.* 58.8 (1940), p. 716.

[3] J. M. Leinaas and J. Myrheim. "On the theory of identical particles." *Nuovo Cim. B* 37.1 (1977), pp. 1–23.

[4] F. Wilczek. "Quantum mechanics of fractional-spin particles." *Phys. Rev. Lett.* 49.14 (1982), p. 957.

[5] K. v. Klitzing, G. Dorda, and M. Pepper. "New method for high-accuracy determination of the fine-structure constant based on quantized Hall resistance." *Phys. Rev. Lett.* 45.6 (1980), p. 494.

[6] D. C. Tsui, H. L. Stormer, and A. C. Gossard. "Two-dimensional magnetotransport in the extreme quantum limit." *Phys. Rev. Lett.* 48.22 (1982), p. 1559.

[7] R. B. Laughlin. "Anomalous quantum Hall effect: an incompressible quantum fluid with fractionally charged excitations." *Phys. Rev. Lett.* 50.18 (1983), p. 1395.

[8] D. J. Thouless et al. "Quantized Hall conductance in a two-dimensional periodic potential." *Phys. Rev. Lett.* 49.6 (1982), p. 405.

[9] X.-G. Wen and Q. Niu. "Ground-state degeneracy of the fractional quantum Hall states in the presence of a random potential and on high-genus Riemann surfaces." *Phys. Rev. B* 41.13 (1990), p. 9377.

[10] R. P. Feynman. "Simulating physics with computers." *Int. J. Theor. Phys.* 21.6-7 (1982), pp. 467–488.

[11] D. Deutsch. "Quantum theory, the Church–Turing principle and the universal quantum computer." *Proc. R. Soc. Lond. A* 400.1818 (1985), pp. 97–117.

[12] P. W. Shor. "Polynomial-time algorithms for prime factorization and discrete logarithms on a quantum computer." *SIAM Rev.* 41.2 (1999), pp. 303–332.

[13] J. Preskill. "Quantum Computing in the NISQ era and beyond." *arXiv:1801.00862* (2018).

[14] A. Y. Kitaev. "Fault-tolerant quantum computation by anyons." *Ann. Phys.* 303.1 (2003), pp. 2–30.

[15] A. Hamma, C. Castelnovo, and C. Chamon. "Toric-boson model: Toward a topological quantum memory at finite temperature." *Phys. Rev. B* 79.24 (2009), p. 245122.

[16] S. Chesi, B. Röthlisberger, and D. Loss. "Self-correcting quantum memory in a thermal environment." *Phys. Rev. A* 82.2 (2010), p. 22305.

[17] B. J. Brown et al. "Quantum memories at finite temperature." *Rev. Mod. Phys.* 88.4 (2016), p. 45005.

[18] M. H. Freedman, M. Larsen, and Z. Wang. "A Modular Functor Which is Universal for Quantum Computation." *Commun. Math. Phys.* 227.3 (2002), pp. 605–622.

[19] L. H. Kauffman and S. J. Lomonaco Jr. "Braiding operators are universal quantum gates." *New J. Phys.* 6.1 (2004), p. 134.

[20] A. Feiguin et al. “Interacting anyons in topological quantum liquids: The golden chain.” *Phys. Rev. Lett.* 98.16 (2007), p. 160409.

[21] C. Gils et al. “Anyonic quantum spin chains: Spin-1 generalizations and topological stability.” *Phys. Rev. B* 87.23 (2013), p. 235120.

[22] P. E. Finch et al. “Quantum phases of a chain of strongly interacting anyons.” *Phys. Rev. B* 90.8 (2014), p. 81111.

[23] N. Braylovskaya, P. E. Finch, and H. Frahm. “Exact solution of the D_3 non-Abelian anyon chain.” *Phys. Rev. B* 94.8 (2016), p. 85138.

[24] E. Vernier, J. Jacobsen, and H. Saleur. “Elaborating the phase diagram of spin-1 anyonic chains.” *SciPost Phys.* 2.1 (2017), p. 4.

[25] C. Gils et al. “Collective states of interacting anyons, edge states, and the nucleation of topological liquids.” *Phys. Rev. Lett.* 103.7 (2009), p. 70401.

[26] E. Grosfeld and K. Schoutens. “Non-abelian anyons: when Ising meets Fibonacci.” *Phys. Rev. Lett.* 103.7 (2009), p. 76803.

[27] F. A. Bais, J. K. Slingerland, and S. M. Haaker. “Theory of topological edges and domain walls.” *Phys. Rev. Lett.* 102.22 (2009), p. 220403.

[28] R. S. K. Mong et al. “Universal topological quantum computation from a superconductor-abelian quantum hall heterostructure.” *Phys. Rev. X* 4.1 (2014), p. 11036.

[29] G. Moore and N. Read. “Nonabelions in the fractional quantum Hall effect.” *Nucl. Phys. B* 360.2-3 (1991), pp. 362–396.

[30] M. Banerjee et al. “Observation of half-integer thermal Hall conductance.” *Nature* (2018), p. 1.

[31] C. Wang, A. Vishwanath, and B. I. Halperin. “Topological order from disorder and the quantized Hall thermal metal: possible applications to the $\nu = 5/2$ state.” *Phys. Rev. B* 98.4 (2018), p. 45112.

[32] D. F. Mross et al. “Theory of disorder-induced half-integer thermal Hall conductance.” *Phys. Rev. Lett.* 121.2 (2018), p. 26801.

[33] N. Read and E. Rezayi. “Beyond paired quantum Hall states: Parafermions and incompressible states in the first excited Landau level.” *Phys. Rev. B* 59.12 (1999), p. 8084.

[34] E. Ardonne and K. Schoutens. “New class of non-Abelian spin-singlet quantum Hall states.” *Phys. Rev. Lett.* 82.25 (1999), p. 5096.

[35] S. D. Sarma, M. Freedman, and C. Nayak. “Topologically protected qubits from a possible non-Abelian fractional quantum Hall state.” *Phys. Rev. Lett.* 94.16 (2005), p. 166802.

[36] N. Read and D. Green. “Paired states of fermions in two dimensions with breaking of parity and time-reversal symmetries and the fractional quantum Hall effect.” *Phys. Rev. B* 61.15 (2000), p. 10267.

[37] A. Y. Kitaev. “Unpaired Majorana fermions in quantum wires.” *Physics-Uspekhi* 44.10S (2001), p. 131.

[38] D. Asahi and N. Nagaosa. “Topological indices, defects, and Majorana fermions in chiral superconductors.” *Phys. Rev. B* 86.10 (2012), p. 100504.

[39] A. M. Tsvelik. "Integrable Model with Parafermion Zero Energy Modes." *Phys. Rev. Lett.* 113.6 (2014), p. 66401.

[40] V. Mourik et al. "Signatures of Majorana fermions in hybrid superconductor-semiconductor nanowire devices." *Science (80-.).* 336.6084 (2012), pp. 1003–1007.

[41] M. T. Deng et al. "Anomalous zero-bias conductance peak in a Nb–InSb nanowire–Nb hybrid device." *Nano Lett.* 12.12 (2012), pp. 6414–6419.

[42] S. D. Sarma, M. Freedman, and C. Nayak. "Majorana zero modes and topological quantum computation." *npj Quantum Inf.* 1 (2015), p. 15001.

[43] J. Alicea et al. "Non-Abelian statistics and topological quantum information processing in 1D wire networks." *Nat. Phys.* 7.5 (2011), p. 412.

[44] P. Fendley. "Parafermionic edge zero modes in Zn-invariant spin chains." *J. Stat. Mech. Theory Exp.* 2012.11 (2012), P11020.

[45] A. S. Jermyn et al. "Stability of zero modes in parafermion chains." *Phys. Rev. B* 90.16 (2014), p. 165106.

[46] Y. Zhuang et al. "Phase diagram of the Z_3 parafermionic chain with chiral interactions." *Phys. Rev. B* 92.3 (2015), p. 35154.

[47] A. Alexandradinata et al. "Parafermionic phases with symmetry breaking and topological order." *Phys. Rev. B* 94.12 (2016), p. 125103.

[48] F. Iemini, C. Mora, and L. Mazza. "Topological Phases of Parafermions: A Model with Exactly Solvable Ground States." *Phys. Rev. Lett.* 118.17 (2017), p. 170402.

[49] N. Moran et al. "Parafermionic clock models and quantum resonance." *Phys. Rev. B* 95.23 (2017), p. 235127.

[50] A. M. Tsvelik. "Z_N parafermion zero modes without Fractional Quantum Hall effect." *arXiv:1407.4002* (2014).

[51] R. J. Baxter. *Exactly solved models in statistical mechanics.* Elsevier, 2016.

[52] D. Borcherding and H. Frahm. "Signatures of non-Abelian anyons in the thermodynamics of an interacting fermion model." *J. Phys. A Math. Theor.* 51.19 (2018), p. 195001.

[53] D. Borcherding and H. Frahm. "Condensation of non-Abelian $SU(3)_{N_f}$ anyons in a one-dimensional fermion model." *J. Phys. A Math. Theor.* 51.49 (2018), p. 495002.

[54] D. Gepner. "New conformal field theories associated with lie algebras and their partition functions." *Nucl. Phys. B* 290 (Jan. 1987), pp. 10–24.

[55] P. E. Finch, M. Flohr, and H. Frahm. "Z_n clock models and chains of $so(n)_2$ non-Abelian anyons: symmetries, integrable points and low energy properties." *J. Stat. Mech. Theory Exp.* 2018.2 (2018), p. 23103.

[56] P. Francesco, P. Mathieu, and D. Sénéchal. *Conformal field theory.* Springer Science & Business Media, 2012.

[57] I. Affleck. "Exact critical exponents for quantum spin chains, non-linear σ-models at $\theta = \pi$ and the quantum hall effect." *Nucl. Phys. B* 265.3 (1986), pp. 409–447.

[58] L. Faddeev. *Integrable models in* $1 + 1$ *dimensional quantum field theory.* Tech. rep. CEA Centre d'Etudes Nucleaires de Saclay, 1982.

[59] A. G. Izergin and V. E. Korepin. "The most general L operator for the R-matrix of the XXX model." *Lett. Math. Phys.* 8.4 (1984), pp. 259–265.

[60] L. D. Faddeev. "How the algebraic Bethe ansatz works for integrable models." *Fifty Years Math. Phys. Sel. Work. Ludwig Faddeev.* World Scientific, 2016, pp. 370–439.

[61] F. Franchini. *An introduction to integrable techniques for one-dimensional quantum systems.* Vol. 940. Springer, 2017.

[62] J.-S. Caux and J. Mossel. "Remarks on the notion of quantum integrability." *J. Stat. Mech. Theory Exp.* 2011.02 (2011), P02023.

[63] L. Šamaj and Z. Bajnok. *Introduction to the statistical physics of integrable many-body systems.* Cambridge University Press, 2013.

[64] V. E. Korepin, N. M. Bogoliubov, and A. G. Izergin. *Quantum inverse scattering method and correlation functions.* Vol. 3. Cambridge university press, 1997.

[65] H. Bethe. "Zur theorie der metalle." *Zeitschrift für Phys.* 71.3-4 (1931), pp. 205–226.

[66] L. A. Takhtajan. "The picture of low-lying excitations in the isotropic Heisenberg chain of arbitrary spins." *Phys. Lett. A* 87.9 (1982), pp. 479–482.

[67] H. M. Babujian. "Exact solution of the one-dimensional isotropic Heisenberg chain with arbitrary spins S." *Phys. Lett. A* 90.9 (1982), pp. 479–482.

[68] H. M. Babujian. "Exact solution of the isotropic Heisenberg chain with arbitrary spins: thermodynamics of the model." *Nucl. Phys. B* 215.3 (1983), pp. 317–336.

[69] K. Sogo. "Ground state and low-lying excitations in the Heisenberg XXZ chain of arbitrary spin S." *Phys. Lett. A* 104.1 (1984), pp. 51–54.

[70] A. N. Kirillov and N. Y. Reshetikhin. "Exact solution of the integrable XXZ Heisenberg model with arbitrary spin. I. The ground state and the excitation spectrum." *J. Phys. A: Math. Gen.* 20 (1987), p. 1565.

[71] A. N. Kirillov and N. Y. Reshetikhin. "Exact solution of the integrable XXZ Heisenberg model with arbitrary spin. II. Thermodynamics of the system." *J. Phys. A: Math. Gen.* 20 (1987), p. 1587.

[72] P. P. Kulish, N. Y. Reshetikhin, and E. K. Sklyanin. "Yang-Baxter equation and representation theory: I." *Lett. Math. Phys.* 5.5 (Sept. 1981), pp. 393–403.

[73] P. P. Kulish and N. Y. Reshetikhin. "Quantum linear problem for the sine-Gordon equation and higher representations." *J. Sov. Math.* 23.4 (Nov. 1983), pp. 2435–2441.

[74] M. Takahashi and M. Suzuki. "One-dimensional anisotropic Heisenberg model at finite temperatures." *Prog. Theor. Phys.* 48.6 (1972), pp. 2187–2209.

[75] H. Frahm, N.-C. Yu, and M. Fowler. "The integrable XXZ Heisenberg model with arbitrary spin: construction of the Hamiltonian, the ground-state configuration and conformal properties." *Nucl. Phys. B* 336.3 (1990), pp. 396–434.

[76] C.-N. Yang and C. P. Yang. "Thermodynamics of a One-Dimensional System of Bosons with Repulsive Delta-Function Interaction." *J. Math. Phys.* 10.7 (1969), pp. 1115–1122.

[77] J. Preskill. "Lecture notes for Physics 219: Quantum computation." *Caltech Lect. Notes* (1999).

[78] A. Kitaev. "Anyons in an exactly solved model and beyond." *Ann. Phys.* 321.1 (2006), pp. 2–111.

[79] E. C. Rowell and Z. Wang. "Degeneracy and non-Abelian statistics." *Phys. Rev. A* 93.3 (2016), p. 30102.

[80] S. MacLane. "Natural associativity and commutativity." *Rice Inst. Pam. Univ. Stud.* 49.4 (1963).

[81] B. Field and T. Simula. "Introduction to topological quantum computation with non-Abelian anyons." *Quantum Sci. Technol.* (2018).

[82] P. H. Bonderson. "Non-Abelian anyons and interferometry." PhD thesis. California Institute of Technology, 2007.

[83] Y. Nakayama. "Scale invariance vs conformal invariance." *Phys. Rep.* 569 (2015), pp. 1–93.

[84] E. Ardonne and K. Schoutens. "Wavefunctions for topological quantum registers." *Ann. Phys.* 322.1 (2007), pp. 201–235.

[85] P. Lecheminant. "Massless renormalization group flow in $SU(N)_k$ perturbed conformal field theory." *Nucl. Phys. B* 901 (2015), pp. 510–525.

[86] A. M. Tsvelik. "Exact solution of a model of one-dimensional fermions with $SU(N) \times SU(M)$ symmetry." *Sov. Phys. JETP* 66 (1987), p. 754.

[87] A. J. A. James et al. "Non-perturbative methodologies for low-dimensional strongly-correlated systems: From non-abelian bosonization to truncated spectrum methods." *Rep. Prog. Phys.* 81.4 (2018), p. 46002.

[88] V. Bois et al. "Phase diagrams of one-dimensional half-filled two-orbital $SU(N)$ cold fermion systems." *Phys. Rev. B* 91.7 (2015), p. 075121.

[89] S. Capponi, P. Lecheminant, and K. Totsuka. "Phases of one-dimensional $SU(N)$ cold atomic Fermi gases—From molecular Luttinger liquids to topological phases." *Ann. Phys.* 367 (2016), pp. 50–95.

[90] F. H. L. Essler et al. *The one-dimensional Hubbard model.* Cambridge University Press, 2005.

[91] H. M. Babujian and A. M. Tsvelick. "Heisenberg magnet with an arbitrary spin and anisotropic chiral field." *Nucl. Phys. B* 265.1 (1986), pp. 24–44.

[92] A. M. Polyakov. "Theory of nonabelian Goldstone bosons in two dimensions." *Phys. Lett.* 131 (1983), p. 121.

[93] L. D. Faddeev and N. Y. Reshetikhin. "Integrability of the principal chiral field model in 1+ 1 dimension." *Ann. Phys.* 167.2 (1986), pp. 227–256.

[94] A. M. Tsvelik. "1 + 1-dimensional sigma model at finite temperatures." *Sov. Phys. JETP* 66 (1987), p. 221.

[95] P. B. Wiegmann. "Exact solution of the $O(3)$ nonlinear sigma-model." *Phys. Lett. B* 152 (1985), pp. 209–214.

[96] A. N. Kirillov and N. Y. Reshetikhin. "Exact solution of the Heisenberg XXZ model of spin s." *J. Sov. Math.* 35 (1986), p. 2627.

[97] V. V. Bazhanov and N. Y. Reshetikhin. "Critical RSOS models and conformal field theory." *Int. J. Mod. Phys.* 4.01 (1989), pp. 115–142.

[98] P. P. Kulish and N. Y. Reshetikhin. “Generalized Heisenberg ferromagnet and the Gross-Neveu model.” *Sov. Phys. JETP* 53.1 (1981), pp. 108–114.

[99] J. H. H. Perk and C. L. Schultz. “New families of commuting transfer matrices in q-state vertex models.” *Phys. Lett. A* 84.8 (1981), pp. 407–410.

[100] P. P. Kulish, N. Y. Reshetikhin, and E. K. Sklyanin. “Yang–Baxter equation and representation theory: I.” *Yang-Baxter Equ. Integr. Syst.* World Scientific, 1990, pp. 498–508.

[101] O. Babelon, H. J. De Vega, and C. M. Viallet. “Exact solution of the $Z_{n+1} \times Z_{n+1}$ symmetric generalization of the XXZ model.” *Nucl. Phys. B* 200.2 (1982), pp. 266–280.

[102] P. P. Kulish and N. Y. Reshetikhin. “Diagonalisation of $GL(N)$ invariant transfer matrices and quantum N-wave system (Lee model).” *J. Phys. A. Math. Gen.* 16.16 (1983), p. L591.

[103] N. Andrei and H. Johannesson. “Higher dimensional representations of the $SU(N)$ Heisenberg model.” *Phys. Lett. A* 104.6-7 (1984), pp. 370–374.

[104] C. L. Schultz. “Eigenvectors of the multi-component generalization of the six-vertex model.” *Phys. A Stat. Mech. its Appl.* 122.1-2 (1983), pp. 71–88.

[105] H. J. De Vega and E. Lopes. “Exact solution of the Perk-Schultz model.” *Phys. Rev. Lett.* 67.4 (1991), p. 489.

[106] E. Lopes. “Exact solution of the multi-component generalized six-vertex model.” *Nucl. Phys. B* 370.3 (1992), pp. 636–658.

[107] C.-N. Yang and C.-P. Yang. “One-dimensional chain of anisotropic spin-spin interactions. II. Properties of the ground-state energy per lattice site for an infinite system.” *Phys. Rev.* 150.1 (1966), p. 327.

[108] H. Johannesson. “The structure of low-lying excitations in a new integrable quantum chain model.” *Nucl. Phys. B* 270 (1986), pp. 235–272.

[109] A. N. Kirillov. “Identities for the Rogers dilogarithm function connected with simple Lie algebras.” *J. Math. Sci.* 47.2 (1989), pp. 2450–2459.

[110] K. Schoutens and X.-G. Wen. “Simple-current algebra constructions of $2 + 1$-dimensional topological orders.” *Phys. Rev. B* 93.4 (2016), p. 45109.

[111] O. A. Castro-Alvaredo et al. “Thermodynamic Bethe ansatz of the homogeneous sine-Gordon models.” *Nucl. Phys. B* 575.3 (2000), pp. 535–560.

[112] K. Huitu, D. Nemeschansky, and S. Yankielowicz. “$N = 2$ supersymmetry, coset models and characters.” *Phys. Lett. B* 246.1-2 (1990), pp. 105–113.

[113] H.-H. Lin, L. Balents, and M. P. A. Fisher. “Exact $SO(8)$ symmetry in the weakly-interacting two-leg ladder.” *Phys. Rev. B* 58.4 (1998), p. 1794.

[114] D. G. Shelton and D. Sénéchal. “$SO(5)$-symmetric description of the low-energy sector of a ladder system.” *Phys. Rev. B* 58.11 (1998), p. 6818.

[115] D. Scalapino, S.-C. Zhang, and W. Hanke. “$SO(5)$ symmetric ladder.” *Phys. Rev. B* 58.1 (1998), p. 443.

[116] H. Frahm and M. Stahlsmeier. “Electronic ladders with $SO(5)$ symmetry: Phase diagrams and correlations at half filling.” *Phys. Rev. B* 63.12 (2001), p. 125109.

[117] M. Nakagawara. "Magnetic Properties of Two-Dimensional $SO(5) \times SO(5)$ Chiral Model." *Prog. Theor. Phys.* 76.1 (July 1986), pp. 216–237.

[118] E. Ogievetsky, N. Reshetikhin, and P. Wiegmann. "The principal chiral field in two dimensions on classical lie algebras: the Bethe-ansatz solution and factorized theory of scattering." *Nucl. Phys. B* 280 (1987), pp. 45–96.

[119] N. Y. Reshetikhin. "Integrable models of quantum one-dimensional magnets with $O(N)$ and $Sp(2K)$ symmetry." *Theor. Math. Phys.* 63.3 (1985), pp. 555–569.

[120] P. E. Finch, M. Flohr, and H. Frahm. "Integrable anyon chains: From fusion rules to face models to effective field theories." *Nucl. Phys. B* 889 (2014), pp. 299–332.

[121] N. D. Vlasii, F. von Rütte, and U.-J. Wiese. "Graphical tensor product reduction scheme for the Lie algebras $so(5) = sp(2)$, $su(3)$, and $g(2)$." *Ann. Phys.* 371 (2016), pp. 199–227.

[122] T. Nakanishi. "Dilogarithm identities for conformal field theories and cluster algebras: simply laced case." *Nagoya Math. J* 202 (2011), pp. 23–43.

[123] V. V. Bazhanov and N. Reshetikhin. "Restricted solid-on-solid models connected with simply laced algebras and conformal field theory." *J. Phys. A. Math. Gen.* 23.9 (1990), p. 1477.

[124] R. M. Konik et al. "Studying the perturbed Wess–Zumino–Novikov–Witten $SU(2)_k$ theory using the truncated conformal spectrum approach." *Nucl. Phys. B* 899 (2015), pp. 547–569.

[125] C.-N. Yang and C.-P. Yang. "One-dimensional chain of anisotropic spin-spin interactions. I. Proof of Bethe's hypothesis for ground state in a finite system." *Phys. Rev.* 150.1 (1966), p. 321.

Acknowledgements

This work would not have been possible without the continuous support of my supervisor Prof. Dr. Holger Frahm. I am very grateful for every discussion with him and especially for every idea that helped me overcome technical hurdles throughout the last three years. Along with him I want to thank all the present and former members of his research group for always having time for any question I might have.

I also want to thank Prof. Dr. Patrik Recher and Prof. Dr. Andreas Klümper for agreeing to review this thesis as well as Prof. Dr. Rolf Haug for chairing the PhD organization committee.

On top of that, I enjoyed the scientific exchange at various workshops. Most prominent among them are the workshops of the research unit *Correlations in Integrable Quantum Many-Body Systems* (FOR2316) and the *School for Contacts in Nanosystems*. Apart from that I really appreciated the kind hospitality during my visit of Prof. Dr. Klümper's group this year in June. Also, I want to thank him for his advice on solving integral equations numerically.

At last, I would like to thank my family and all of my friends for their tremendous support and necessary distractions from work during the last years.

Daniel Borcherding

Curriculum Vitae

Personal

Name	Daniel Borcherding
Date of birth	06.04.1991
Place of birth	Hameln

Education

11/2015 - 12/2018	Research associate, Leibniz University Hannover, Doctoral thesis: Non-Abelian quasi-particles in electronic systems
10/2013 - 11/2015	M.Sc. Physics, Leibniz University Hannover, Master's thesis: Self-correcting quantum memories with two-body interactions
10/2010 - 9/2013	B.Sc. Physics, Leibniz University Hannover, Bachelor's thesis: Upper bounds on electromagnetic field strengths in the exterior region of black holes
6/2010	Allgemeine Hochschulreife, Otto-Hahn-Gymnasium Springe